Repair by basic excision at the mitochondrial level in Drosophila. Analysis of a potential actor in this process : the PARP protein

Luis Cruz-Rodriguez

UNIVERSITÉ BLAISE PASCAL **UNIVERSITÉ D'AUVERGNE**

N° D.U. 2423 ANNEE 2013

ÉCOLE DOCTORALE DES SCIENCES DE LA VIE, SANTÉ, AGRONOMIE, ENVIRONNMENT

N° d'ordre 622

Thèse

Soutenance à l'Université Blaise Pascal

Pour l'obtention du grade de

DOCTEUR D'UNIVERSITÉ

Spécialité

Physiologie et Génétique Moléculaires

Présentée par

Luis CRUZ-RODRIGUEZ

"Réparation par Excision de Base au niveau mitochondrial chez la Drosophile. Analyse d'un acteur potentiel de ce processus : la protéine PARP"

Soutenue le 17 Décembre 2013

Devant le jury composé de

Dr. Etienne LEFAI	Rapporteur
Dr. Ludovic PELOSI	Rapporteur
Pr. Michel RIGOULET	Rapporteur
Pr. Jean-Marc LOBACCARO	Président
Pr. Patrick VERNET	Directeur de thèse

Laboratoire d'accueil : Réparation du Génome Mitochondrial (RGM) EA 4645

Beaucoup d'entre nous qui espèrent devenir docteur, ignorons son origine

Ceux qui luttaient à mort dans les arènes du Colisée de Rome afin de survivre, malgré de graves blessures, devaient se rétablir rapidement pour affronter le prochain combat .Survivre à chaque combat grâce à l'expérience du précédent était la stratégie du gladiateur. La résistance physique et mentale étaient ses véritables armes, mais plus encore, celui qui réussissait à intégrer une équipe de combat était appelé Docteur.

Il est plus difficile, de réussir l'intégration d'une équipe, que la notre au sein d'une existante. S'intégrer est la mission de gladiateur, intégrer est le résultat d'un Docteur....

Remercier est un acte de gratitude en réponse aux résultats positifs obtenus grâce à la participation de tierces personnes. L'être humain, en tant qu'entité sociale, est constamment soumis à une grande interaction avec des personnes qui permettent le développement ou la frustration de ses projets.

Généralement celui qui réalise une thèse remercie ceux qui ont rendu possible celle-ci.

Néanmoins, Aujourd'hui je remercie ceux qui n'ont pas rendu possible la fin de l'étudiant.

... et durant toute cette nouvelle vie qui commence aujourd'hui, de par mes résultats positifs,

je dirai merci à l'équipe d'accueil qui représenta l'arène ou j'ai livré tous mes combats ;

je dirai merci à l'Université Blaise Pascal d'être le Colisée de chaque de mes batailles ;

je dirai merci à la FRANCE d'être le César qui, dirigeant toujours son pouce vers le ciel, permit ma survie bien que je n'ais pas triomphé à chaque combat.

J'exprime mes sincères remerciements aux membres du jury

Aux Dr. Etienne LEFAI, Dr. Ludovic PELOSI, Pr. Michel RIGOULET et Pr. Jean-Marc LOBACCARO

Au Merci au Professeur VERNET qui soigna ce gladiateur de ses blessures mortelles et lui apprit à marcher dans l'arène. Trois ans ne suffisent pas pour apprendre tout ce que tu peux enseigner ! (Ni tampoco suficiente tres meses para escribir un manuscrito de tres años de trabajo junto a ti...)

Merci Isabelle, Fréderic, Stéphanie, Mathilde, Marie-Jo, Angel, ...

Merci Professeur JULIEN, gracias Maria GALLEGO, gracias José Yelamos,...

Merci Eriel, Anaïs, Guy, Zulimar, José-Luis, Hervé, Virginie, Hugo, Ludo, Layal...

Gracias madrecita linda por tu apoyo, eres tu mi faro, una Estrella Marina caída del cielo...

Thank you Reiner for your moral support what was my energy and inspiration, thanks for trust me, I want to become in greater due to I want to be like you my father...

Merci beaucoup Philippe de m'avoir écouté à chaque fois que j'ai eu besoin de parler. Grace à toi, plus de trouver PARP dans la mito, j'ai trouvé un ami dans le labo...

Merci BEAUCOUP Saily de m'avoir supporté durant cette dernière étape de la thèse et d'avoir affronté seule toutes les responsabilités du foyer et de notre famille.

Merci Pascal d'être la personne et le maître que tu es.

Avant il n'existait dans mon arc en ciel que le blanc et le noir comme couleur, mais depuis que je l'observe comme tu le fais, il existe plus que les sept couleurs habituelles.... Plus que merci pardonne-moi...

MERCI BEAUCOUP Serge et Patrick !!!

Si aujourd'hui je sens que je peux toucher les étoiles, ce n'est pas grand-chose puisque

J'étais assis sur les épaules des géants.....

Attention !

C'est mieux ne pas se hisser sur les épaules des grands hommes, tâcher de se glisser entre leurs jambes

Jean Rostand

A mes enfants

Marie-Élisabeth

et

Luis-Daniel

Abstract

Mitochondria are key organelles mainly devoted to energy production through ATP synthesis. Such a function is permitted by oxidative phosphorylation (OXPHOS) within mitochondria inner membrane. Key components of the OXPHOS processes are encoded by mitochondrial DNA (mtDNA) that is particularly sensitive to exogenous or endogenous insults. As a result, mtDNA mutations are often correlated with OXPHOS dysfunction leading to diseases. ROS production in mitochondria is the main source of mtDNA damage. Such DNA damages are mainly taken over by BER systems within mitochondria. In this study, we focused on this peculiar mitochondrial DNA repair system in Drosophila. In a first step, we analysed in a comprehensive manner through microarray, most glycosylases and endonucleases involved in mitochondrial BER and compared their evolution during aging. Using mutant flies for specific BER enzymes, we started to decipher some of the transcriptional interactions between key BER actors. In a second step, Parp molecule was further studied due its changes in all mutant contexts and for its importance in several cellular processes. We described its nuclear but also its mitochondrial location in S2 cells. Interestingly, two Parp mRNA variants were observed showing distinct regulations following stress induction. However, PARP protein isoforms observed in this study were different compared to what was described in literature. This discrepancy is discussed.
Key words: Mitochondrial DNA, DNA repair, BER, microarrays, Poly(ADP-ribosyl)ation, PARP, PARG

Résumé

Les mitochondries sont des organites essentiels pour la production d'énergie cellulaire grâce à la synthèse d'ATP au cours des étapes de phosphorylations oxydatives (OXPHOS). Les complexes de la chaine respiratoire sont en partie codés par le génome mitochondrial (ADNmt), dont la structure est très sensible aux facteurs exogènes ou endogènes De nombreuses mutations de l'ADNmt sont associés à des dysfonctionnements de la chaine respiratoire conduisant à des pathologies. La production d'Espèces Oxygénées Réactives (EOR) mitochondriale est la principale source de dommages à l'ADNmt. Une voie de réparation particulière, le système de réparation par excision de bases (BER) est mis en œuvre dans ce cas. Nous avons, au cours de notre étude, analysé le système BER mitochondrial chez la drosophile. Dans une première approche, nous avons caractérisé de manière globale par une technologie de puces à ADN un ensemble de glycosylases et endonucléases impliquées dans la voie BER mitochondriale et comparé leur variation au cours du vieillissement. Cette étude a été complétée par une analyse transcriptionnelle sur des modèles de drosophiles mutantes pour des enzymes spécifiques de la voie BER, ceci afin de déterminer les éventuelles interactions transcriptionnelles entre les acteurs de cette voie. L'ARNm de Parp présentait de fortes variations dans les différents contextes mutants testés. C'est une molécule essentielle de la réparation BER. Elle a fait l'objet dans un deuxième temps, d'une étude plus approfondie. Dans le modèle des cellules S2, PARP bien que majoritairement nucléaire est également présent dans la mitochondrie. Le comportement différentiel des deux variants ARNm de Parp a pu être mis en évidence lors de stress cellulaires. Les isoformes protéiques de PARP observées dans nos études apparaissent différentes de celles habituellement décrites dans la littérature. Cet aspect a été discuté.

Mots-clés : ADN mitochondrial, Réparation, BER, puces ADN, Poly(ADP-ribosyl)ation, PARP, PARG

Sommaire

Abstract **6**

Sommaire **7**

Abreviations **11**

INTRODUCTION *14*

I.→Mitochondria *14*

I.1.1. Main features 15

I.1.2. The inner compartments 15

I.1.2.1. The intermembrane space 15

I.1.2.2. The mitochondrial matrix 16

I.1.3. The Outer mitochondrial Membrane 17

I.1.4. The Inner mitochondrial Membrane 18

I.1.5.1. Organization 19

I.1.5.3. mtDNA transcription 22

I.1.5.3.1. Mitochondrial RNA polymerase (POLRMT) 25

I.1.5.3.2. Transcription regulation in human mitochondria 27

I.2. Mitochondria Distribution *29*

I.3. Mitochondrial fusion and fission *31*

I.4. Mitochondrial Functions *33*

I.5. Mitochondrial diseases *35*

I.5.1. Mendelian: associated with genes of the nuclear genome 36

I.5.2. not Mendelian: associated with maternal inheritance 36

II. DNA maintenance *38*

II.2. DNA repair mechanisms 40

II.2.1. Base Excision Repair (BER) 40

II.2.1.1. BER in mitochondria 44

II.3.2. Single or double strand breaks repair 47

II.3.2.1. Non-homologous end-joining (NHEJ) 48

II.3.2.2. Homologous recombination (HR) 50

II. 4. DNA repair in mitochondria 51

II.5. DNA repair and pathologies 56

II.5.1. BER and cancer 56

II.5.2. HR, NHEJ and cancer 57

II.5.3. NHEJ and immunity 57

III.1. Poly(ADP-ribose) metabolism 59

III.2. The structure-function of human PARP-1 62

III.2.1. PARP-1 structure 62

III.2.2. The structure-function of PARP-3 66

III.3. Tankyrases *66*

III.4. Other PARPs *67*

III.5. PARPs inhibitors *67*

III.6. PARP in mitochondria *69*
IV.→. DNA repair mechanisms in Drosophila *69*

THESIS PROJECT **72**
a) Analysis of key BER enzymes activities during aging. *72*
b) Is PARP protein involved in mtDNA repair in Drosophila melanogaster? *72*
c) How is PARP regulated at a transcriptional level in different Drosophila mutants for key BER enzymes? *73*
MATERIAL AND METHODS 74
I.→.Animals *74*
II.→.Sub-cellular fractionation *75*
II.1. Sub-cellular fractions purification (nucleus and mitochondria) 75
II.2. Mitochondrial fractions validation 76
II.2.1. Western blot analysis 76
II.2.2. Enzyme assays 77
III.→Comprehensive BER repair analysis through microarray technology *77*
IV. →Molecular Analysis *79*
IV.1. Expression analyses 79
IV.1.1. mRNA extraction 79
IV.1.2. cDNA production 79
IV.1.3. RT-q-PCR 79
IV.2. PCR prior to cloning 80
IV.3. PARP-B-target construction 82
IV.4. DNA electrophoresis 86
IV.5. Bacteria transformation 86
IV.5.1. Competent cells preparation 86
IV.5.2. Transformation 86
IV.5.3. Cloning control 87
V.→ In silico analyses *87*
V.1. Mitochondrial targeting analysis *87*
V.2. Protein sequences homology *88*
V.3. Caspase cleavage sites determination *88*
V.4. Physico-chemical properties *88*
VI.→.PARP sub-cellular localization *88*
VI.1. S2 cells culture 88
VI.2. Cells transfection 88
VI.3. Validation of stable cells lines 89
VI.4. Stress conditions 90
VI.4.1. Copper stress 90
VI.4.2. Oxidative stress 90
VI.4.3. Copper /oxidative stress 90
VII.→.Microscopy *90*
VIII.→.Proteins analyses from Drosophila *91*
VIII.1. Protein extraction 91
VIII.2. Electrophoresis and blotting 91
VIII.3. Parp-B protein detection 92

VIII.4. Mass spectrometry 92
IX. Recombinant protein production *94*
IX.1. Protein expression 94
IX.2. Protein purification 94
RESULTS *95*
I.→ Global analysis of BER system in Drosophila melanogaster 95
I.1. BER activities 95
I.1.1. Validation of mitochondrial fractions 95
I.1.1.1. Purity analysis 95
I.1.1.2. Functionality analysis 96
I.1.2. Nuclear BER activities 97
I.1.3. Mitochondrial BER activities 97
II.→ Mitochondrial addressing predictions *99*
III.→.Base excision repair genes expression in Drosophila *100*
III.1 Relative mRNA expression in wild-type context 100
III.2. Relative mRNA expression in ogg1^{-} mutant flies 101
III.3. Relative mRNA expression in Rrp1-$^{-}$ mutant flies 102
III.4. Relative mRNA expression in Xrcc1^{-} mutant flies 103
III.5. ogg1^{-}/xrcc1^{-} double knockout generation 104
III.6. Relative mRNA expression in ogg1-/xrcc1^{-} double knockout flies 104
IV.→.PARP AS A CANDIDATE FOR MITOCHONDRIAL DNA REPAIR IN DROSOPHILA? *105*
IV.1 PARP isoforms relative expression *105*
IV.1.1 In whole Drosophila organism 105
IV.1.2. In S2 cells 106
IV.2. PARP isoforms relative expression in stress conditions *106*
IV.2.1. Copper stress 106
IV.2.2. Oxidative stress 107
IV.2.3 Combination of copper and oxidative stress 108
IV.3. PARP isoforms relative expression after stress and recovery *109*
IV.4. Subcellular PARP localization in Drosophila melanogaster model *110*
IV.4.1. Expression vectors and transfection in S2 cells 110
IV.4.2. PARP subcellular localization 111
IV.4.2.1. PARP PB in basal conditions 111
IV.4.2.2. PARP PB-V5 under copper induction 112
IV.4.2.3. Parp PB-GFP under copper induction 113
IV.4.3. PARP subcellular localization under oxidative stress 114
IV.4.3.1. PARP PB 114
IV.4.3.2. PARP PB-V5 115
IV.5. Sub-cellular fractionation and PARP detection *116*
IV.6. Mass spectrometry analysis *117*
IV.7. Potential caspase cleavage sites in PARP *118*
IV.7.1. Human Parp-1 118
IV.7.2. Recombinant protein Parp-B-V5-$(Hist)_6$ 119
V.→.Production of recombinant PARP protein *120*
DISCUSION 122
I.→.BER activities in mitochondria *122*

II.→.Mitochondrial addressing predictions *124*
III.→.Base excision repair genes expression in Drosophila *125*
IV.→.PARP isoforms relative expression *126*
V.→ Subcellular PARP localization in Drosophila melanogaster *128*
CONCLUSIONS 130
PERSPECTIVES 131
REFERENCES AND ANNEXES 132
ANNEXES 156

Abreviations

2D-PAGE: Two-dimensional gel electrophoresis
ADP: Adenosine diphosphate
AER: Alternative Excision Pathway
AIF: Apoptotic inducing factor
AP: Apurinic/apyrimidinic
APE1: AP Endonuclease 1
APTX: Aprataxin
ARD: ankyrin repeat domains
ARH3: ADP ribosyl-acceptor hydrolase
ARTs: ADP-ribosyltransferases
ATM: Ataxia telangiectasia mutated
ATP : Adenosine triphosphate
BER : Base Excision Repair
BRCA1: Breast Cancer gene 1
BRCT : BRCA1 C Terminus
BrdU : 5-Bromo-2´-Deoxyuridine
CAC : Krebs cycle
Casp : Caspase
CL : Cardiolipin
CoQ : Coenzyme Q
COX : Cytochrome Oxidase
CPEO: Chronic progressive external ophthalmoplegia
Cyt c : Cytochrome c
DNA : Deoxyribonucleic acid
DNA-PKcs : Protein kinase DNA-dependent
DSBs : Double-strand breaks
e.g : Exempli gratia
ER : Expression ratio
FAD : Flavin adenine dinucleotide
FEN1: Flap structure-specific endonuclease 1
HMG : High Mobility Group
HR : Homologous recombination
HSP : Heavy-strand promoter
IMM : Mitochondrial Inner Membrane
IUPAC: International Union of Pure and Applied Chemistry
KSS : Kearns-Sayre syndrome
LSP : Light-strand promoter
MCU : Calcium uniporter
MELAS: Syndromes of mitochondrial encephalopathy, myopathy, lactic acidosis, and stroke-like episodes
MERRF: Myoclonic epilepsy with ragged red fibers
Mfn : Mitofusin
MIA : Mitochondrial intermembrane space import and assembly

MMEJ: Microhomology Mediated End Joining
MMM : Mitochondrial Morphology and Maintenance
MMR : Missmatch repair
mRNA : Messenger RNA
mtDNA : Mitochondrial DNA
mTERF : Mitochondrial transcription termination factor
MTS : Mitochondrial Targeting Sequence
MW : Molecular Weight
NAD : Nicotinamide adenine dinucleotide
NADP : Nicotinamide adenine dinucleotide phosphate
NARP: Neurogenic muscle weakness, Ataxia, and Retinitis Pigmentosa
NER : Nucleotide Excision Repair
NHEJ : Non-Homologous End Joining
NLS : Nuclear localization signal
NoLS : Nucleolar localization signal
OGG1 : 8-Oxoguanine DNA Glycosylase 1
OMM : Mitochondrial outer membrane
OXPHOS : Oxidative phosphorylation system
p53 : Protein 53
PALF: Polynucleotide Kinaseand Aprataxin-like Forkhead-associated
PAR : Poly-(ADP-ribosylation)
PARG : poly(ADP-ribose) glycohydrolase
PARP: Poly ADP ribose polymerase
PCNA: Proliferating cell nuclear antigen
PCR : Polymerase Chain Reaction
PDAC : Pancreatic ductal adenocarcinoma
pI : Isoelectric Point
PNK : Polynucleotide kinase
POLRMT : Mitochondrial RNA polymerase
PRD : PARP regulatory domain
RITOLS: Ribonucleotide incorporation throughout the lagging strand
RNA : Ribonucleic Acid
ROS : Reactive Oxygen Species
rRNA : Ribosomal RNA
RSS : Recombination Signal Sequence
SAM: Sorting and assembly machinery

SCID : Severe combined immunodeficiency

SD : Standard Deviation
siRNA : Small interfering RNA
SSBs : Single-strand breaks
ssDNA : Single Stranded DNA
TAE : Tris Acetate EDTA
TFAM : Mitochondrial transcription factor A
TIM: Translocase of inner membrane
Tm : Melting Temperature
TM : Transmembrane domain
TOM : Translocase outer membrane
TpT : Terminal phosphoTransferase
tRNA : Transfer RNA
TRX : Thioredoxin
UCP : Uncoupling proteins
UV : Ultra Violet
VDAC : Protein voltage-dependent anion-selective channel
VDJ: Variable, Diverse, and Joining
vWA: von Willebrand type A
XLF : XRCCA-like factor
XRCC1: X-ray repair cross-complementing protein 1

INTRODUCTION

I.→Mitochondria

According to the endosymbiosis theory, mitochondria origin is from α-proteobacteria, which after the internalization by an anaerobic cell, (***Figure 1***), carried out an endosymbiotic relationship with them, based in exchanges of metabolites, energetic sources such as ATP and complex mechanism of signaling (**Kutschera U et Niklas KJ., 2005**).

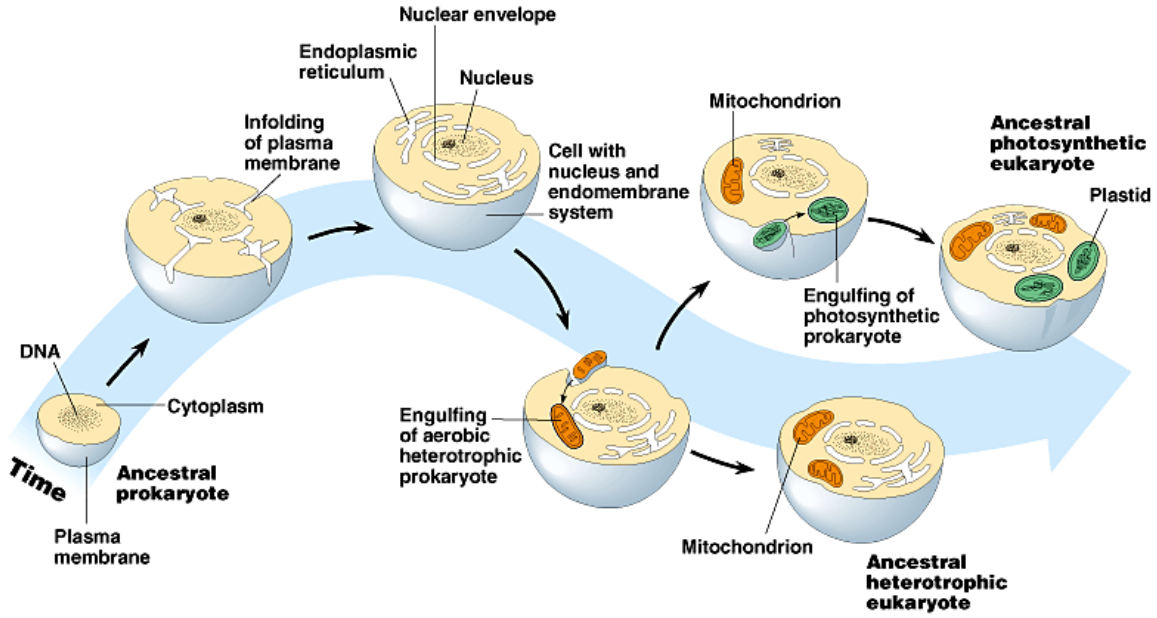

Figure 1*: Endosymbiosis theory: The first eukaryote may have originated from an ancestral prokaryote that had undergone membrane proliferation, compartmentalization of cellular function (into a nucleus, lysosomes, and an endoplasmic reticulum), and the establishment of endosymbiotic relationships with an aerobic prokaryote, and, in some cases, a photosynthetic prokaryote, to form mitochondria and chloroplasts, respectively. (modified from http://mrkingbiochemistry.files.wordpress.com/2013/02/theory-of-endosymbiosis.gif?w=300&h=166)*

In mammalian the number of mitochondria per cell differs widely from cell type to cell type. Robin et al. calculated the virtual mitochondrial number/cell range. They estimated the virtual number of mitochondria per cell measuring a plasmid probe developed that represent DNA/mitochondrion. They propose a range from 83 ± 17 mitochondria per cell (**Robin ED, et R Wong., 1988**).

I.1. Structure

I.1.1. Main features

Mitochondria contain two membranes (outer and inner) composed of phospholipid bilayers and proteins. The two membranes have different properties and they delimit three compartments such as: cytosol, intermembrane space and mitochondrial matrix.

The structure of mitochondria is represented in ***Figure 2*** and shows:

a) outer membrane
b) inner membrane
c) cristae
d) intermembrane space (zone between outer and inner membrane)
e) mitochondrial matrix

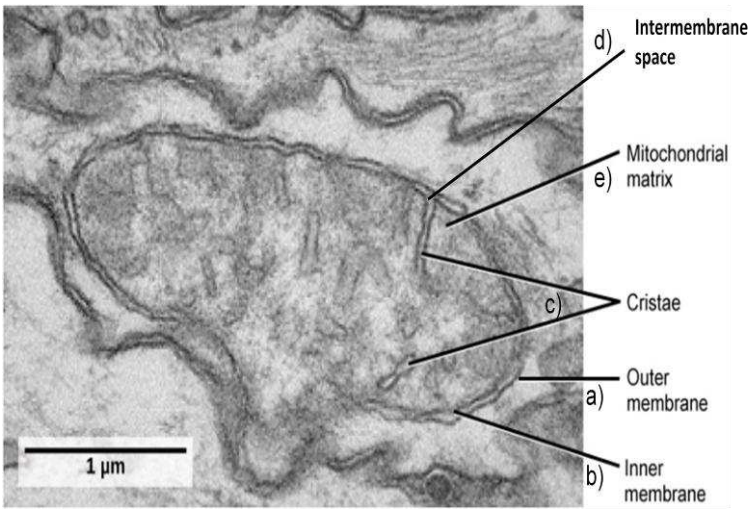

Figure 2*: Electron microscopy of mitochondrial structure (modified from* ***Herrmann JM. et Riemer J., 2010****).*

I.1.2. The inner compartments

I.1.2.1. The intermembrane space

The intermembrane space is the space between the outer and the inner membrane. Its nature is very similar to cytoplasm; it became clear very recently that the intermembrane space plays a pivotal role in the coordination of mitochondrial activities with other cellular processes. In human, these activities include the exchange of proteins, lipids, or metal ions between the matrix and the cytosol, the regulated initiation of apoptotic cascades, signalling

pathways that regulate respiration and metabolic functions, the prevention of reactive oxygen species produced by the respiratory chain, or the control of mitochondrial morphogenesis[1].

In Yeast mitochondria, several proteins were localized in the intermembrane space such as: Ups1p, Ups2p, Cytochrome *bz* and Cytochrome c (Cyt c) and peroxidase (**Maccecchini ML., 1981 ; Tamura Y et al., 2012**).

In normal functioning of mitochondria, Cyt c remains attached (electrostatic interactions) with proteins (complex II and IV) inserted in inner mitochondrial membrane. A disorder in electrostatic potential of inner membrane leads to the traffic of Cyt c to cytosol where it is involved in apoptosis pathway (**Liu X. et al., 1996**).

I.1.2.2. The mitochondrial matrix

The mitochondrial matrix is the scenario of metabolic pathways implicated in ATP production, such as: fatty acid oxidation, amino acid catabolism and Krebs cycle (also named the citric acid cycle CAC). (***Figure 3***) The machinery enzymes of the CAC is represented in different sub-compartments (metabolic canalization) in the mitochondrial matrix, with the exception of succinate dehydrogenase, which is bound to the inner mitochondrial membrane as part of Complex II.

The mitochondrial matrix can integrate cytosolic and mitochondrial pathways where metabolites such as, amino acids, fatty acid and glucose become in ATP. Recently, thanks to microscopy and mass spectrometry techniques, 495 proteins inside the human mitochondrial matrix were identified. The method was based on a genetically targetable peroxidase enzyme that biotinylated nearby proteins, which were subsequently purified and identified by mass spectrometry. Also it was identified 31 proteins not previously involved in mitochondria (**Rhee HW. et al., 2013**).

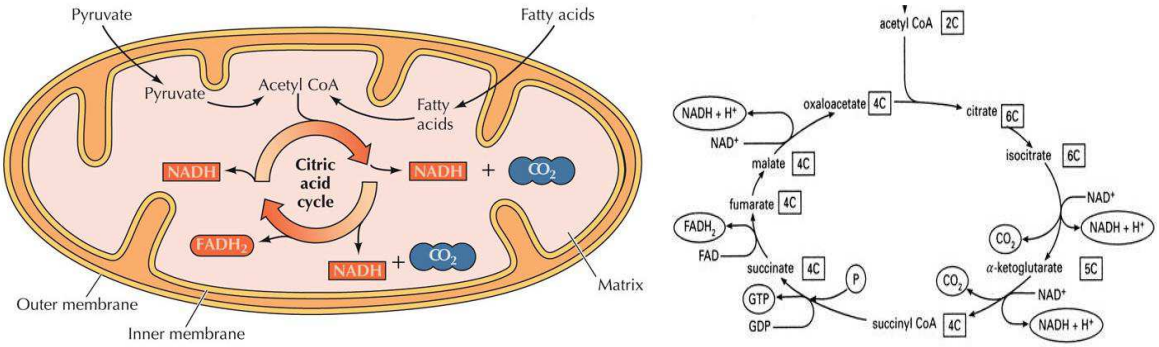

***Figure 3**: Schematic representations of acetyl-CoA integration to CAC (left) and the different reaction of CAC implicating acetyl-CoA integration (right) http://oregonstate.edu/instruction/bi314/summer09/Fig-11-02-0.jpg and http://content.answcdn.com/main/content/img/oxford/Oxford_Chemistry/0192801015.krebs-cycle.1.jpg (left)*

I.1.3. The Outer mitochondrial Membrane

The mitochondrial outer membrane (OMM) separates the intermembrane space from the cytosol, which encloses totally the organelle. OMM lipid composition is near 40% of phospholipids permitting the whole exchange of metabolites between mitochondrial internal compartments and the cytosol in eukaryote cell. OMM creates a diffusion barrier for small molecules such as adenine nucleotides, creatine phosphate and creatine, causing rate-dependent concentration gradients as a prerequisite for the action of ADP shuttles *via* creatine kinases or adenylate kinases. If the OMM becomes leaky, Cyt c and apoptosis-inducing factor can be released (**Gellerich FN. et al., 2000 ; Horvath SE. et Daum G., 2013**).

The protein voltage-dependent anion-selective channel (VDAC) (Rostovtseva TK., 2012) constitutes the main pathway for ATP, ADP, and other mitochondrial metabolic substrates in OMM. Recent findings suggest that regulation of VDAC by cytosolic proteins, such as kinases, and cytoskeletal proteins, dynamically and globally controls mitochondrial metabolism in normal cells and might play a role in aerobic glycolysis in cancer cells (the Warburg effect). Bigger molecules can only cross the OMM by active transport through mitochondrial membrane transport proteins, and mitochondrial pre-proteins are imported through specialized translocase complexes (***Figure 4***) as translocase outer membrane (TOM). The OMM also contains enzymes involved in: fatty acids elongation, hormones oxidation and tryptophan catabolism.

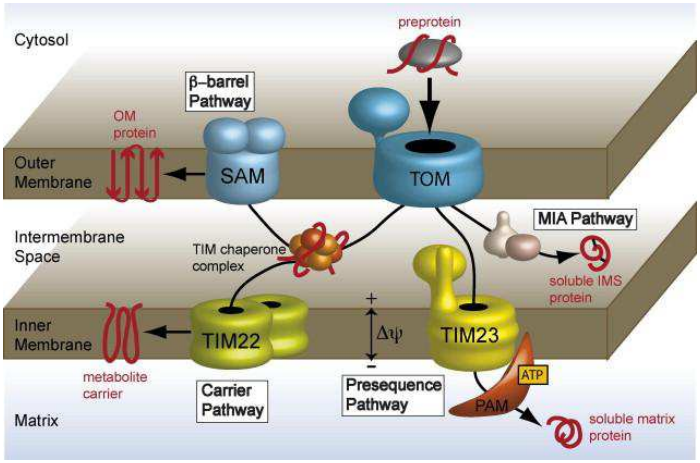

***Figure 4**: The pre-protein import machinery of mitochondria. Abbreviations: MIA, mitochondrial intermembrane space import and assembly; SAM, sorting and assembly machinery; TIM, translocase of inner membrane; TOM, translocase of outer membrane (**Bohnert M, et al., 2007**).*

I.1.4. The Inner mitochondrial Membrane

The Inner mitochondrial Membrane (IMM) is composed about 80 % protein and only 20% of phospholipids.

a) According to phospholipid composition: Mitochondria are capable of synthesizing several lipids autonomously such as phosphatidylglycerol, cardiolipin and in part phosphatidylethanolamine, phosphatidic acid and CDP-diacylglycerol.

b) According to proteins composition, the IMM doesn't contain porins, the metabolic traffic is due to: protein import machinery and specific protein transportation, such as: TIM22 and TIM23. The oxidative phosphorylation (OXPHOS) carried out in IMM involved the complexes of electron transport and ATP synthetase (**Dimroth P, Kaim G, et Matthey U., 2000 ; Hunte C et al., 1993**).

In Eukaryotes, the IMM presents different receptors involved in diverse pathways such as: Ca^{2+} internalization (**Hajnóczky G et al., 2002**) or in mtDNA maintenance (**Rossi MN et al., 2009**).

Other mitochondrial membrane lipids such as phosphatidylcholine, phosphatidylserine, phosphatidylinositol, sterols and sphingolipids have to be imported (**Becker T, et al., 2013**). The more important phospholipid from IMM is the cardiolipin (CL), which provides essential structural (***Figure 5***) and functional support to several proteins involved in mitochondrial bioenergetics. Thus, CL leads to IMM freely permeable only to oxygen, carbon dioxide, and

water, but slightly permeable to the passage of ions and molecules across the membrane without carriers. CL mediates the cooperativity between cytochrome-c-binding sites in the dimeric enzyme complex (**Arnold S. et Kadenbach B., 1997**).

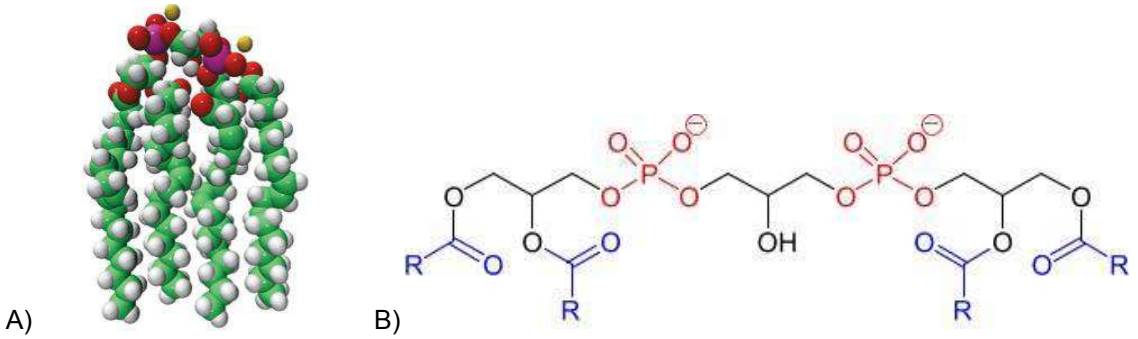

***Figure 5**: (A) 3D conformation of CL* http://classconnection.s3.amazonaws.com/737/flashcards/1944737/jpg/cardiolipin1349112348119.jpg*; and (B) formula IUPAC:* http://www.chemgapedia.de/vsengine/media/width/433/height/128/vsc/de/ch/16/im/divpic/cardiolipin.svg.jpg

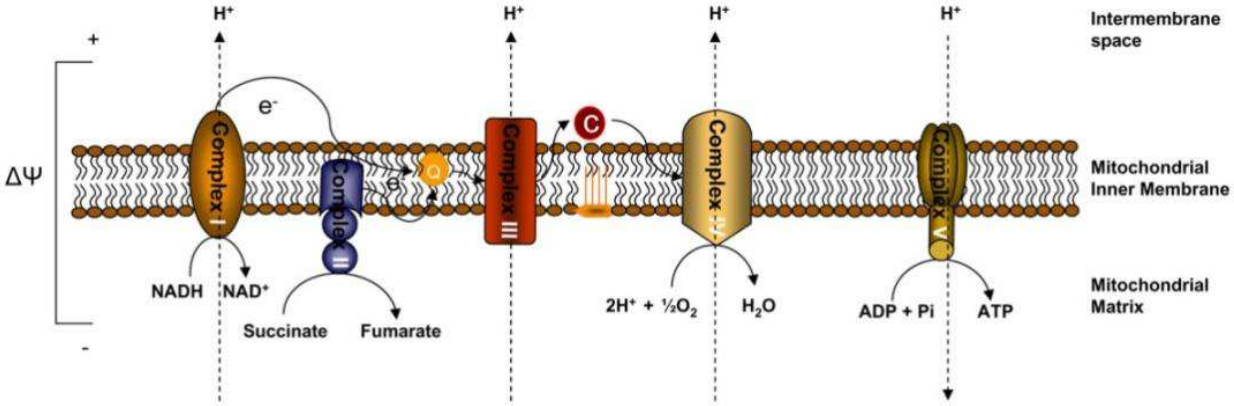

Figure 6: Schematic representation of ATP synthesis. Three H^+ pumping sites create variation in the inner membrane potential (ψ).(modified from *http://ccforum.com/content/figures/cc6779-2-l.jpg*)

I.1.5. Mitochondrial DNA

In humans, the mitochondrial genome (circular double-stranded DNA) is about 1% of genomic DNA and it is composed of 16 569 base pairs (***Figure 7***). This DNA is devoid of introns and histones (**Anderson S. et al., 1981**).

I.1.5.1. Organization

According to ***Figure 7***, the mtDNA contains 37 genes (**Adams KL, Palmer JD., 2003**), which represent the 95% of total mitochondrial genome, coding for: 22 transfer RNA, 2

ribosomal RNA genes (in yellow) (**Montoya J et al., 1982 ; Christianson TW et Clayton DA., 1986 ; Montoya J, Gaines GL, et Attardi G., 1983**) and 13 polypeptides: 7 subunits - ND1, ND2, ND3, ND4, ND4L, ND5, and ND6 (all in green) - of Complex I (NADH-Coenzyme Q oxidoreductase); 1 subunit - cytochrome b (in red) - of Complex III (CoQ-cyt *c* oxidoreductase), 3 subunits - COX I, COX II, and COX III(all in blue) - of Complex IV (cyt *c* oxidase, or COX), and 2 subunits - ATPase 6 and ATPase 8 (both in gray) - of Complex V (ATP synthase) (**Popot JL. et C de Vitry., 1990**).

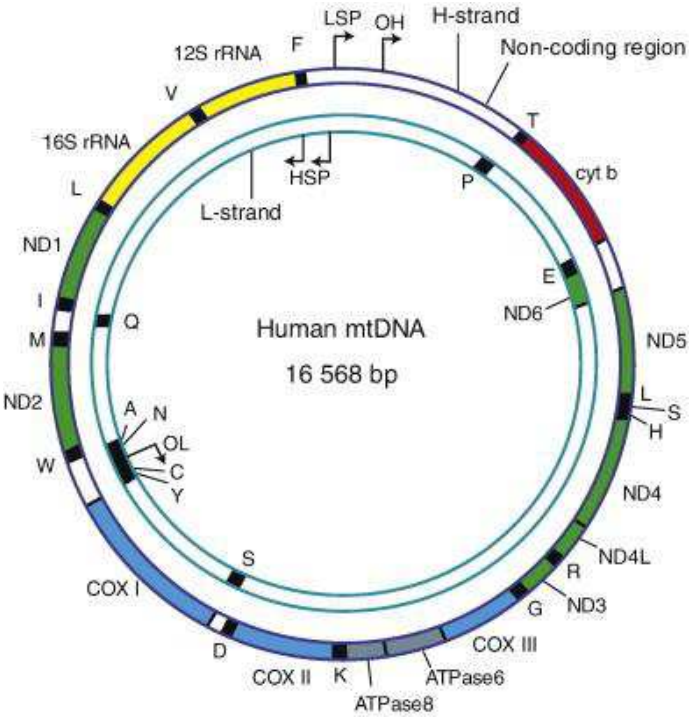

***Figure 7**: Schematic representation of the human mtDNA (**Wanrooij S et Falkenberg M., 2010**).*

The genes organization is strongly conserved in every completely sequenced mitochondrial genome. The remaining 5% of mitochondrial genome is a non-coding region named D-loop (or zone A-T rich) (in white). The D-loop presents an origin of DNA synthesis in each strand named O_L the origin of light (lagging) strand synthesis and O_H the origin of heavy strand.

I.1.5.2. mtDNA replication

The ***Figure 8*** shows different replication modes of mammalian mtDNA.

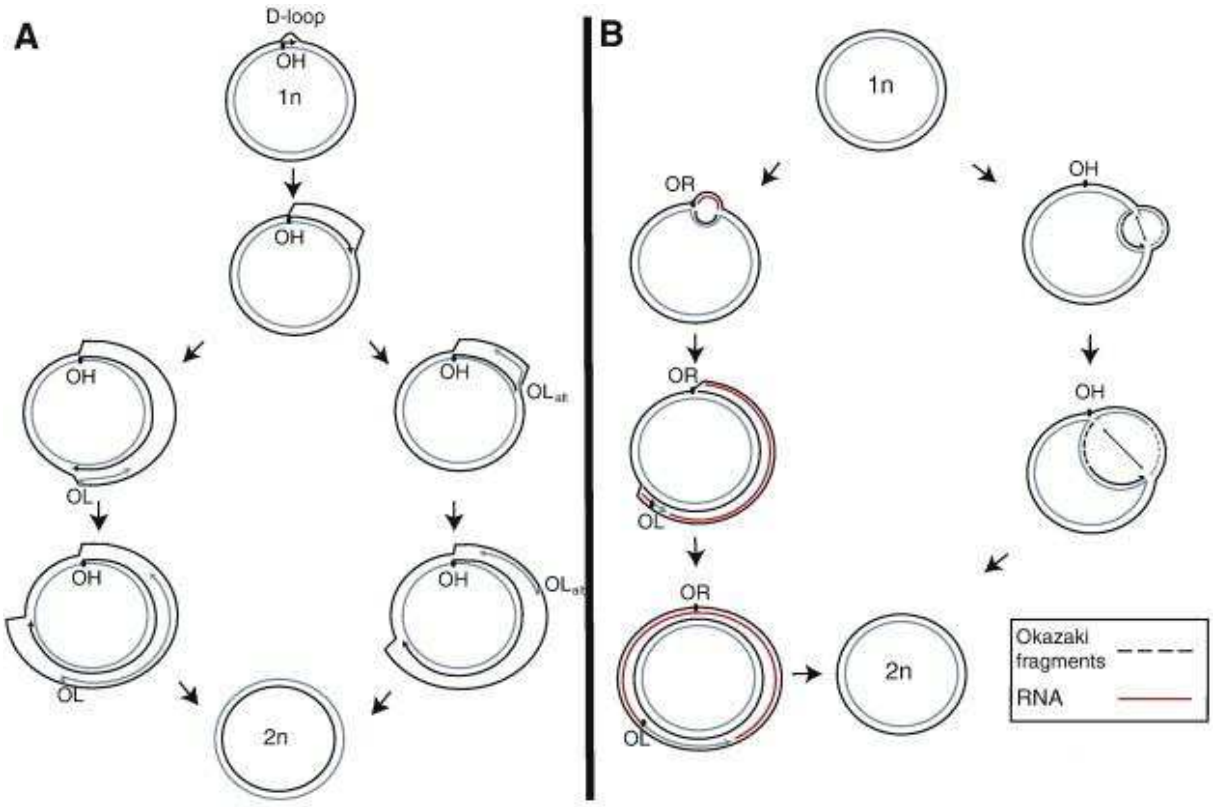

Figure 8*: Schematic representations mtDNA replication modes. (A) Strand-displacement replication mode. (B) RITOLS (left pathway) and strand coupled (right pathway) mode of mtDNA replication (**Antoshechkin I, et al., 1997**).*

Replication of leading strand (H-strand) initiates at OH and proceeds unidirectionally (black arrow), displaying the parental H-strand as ssDNA. When OL (or OLalt) is exposed, the lagging strand (L-strand) synthesis initiates in the opposite direction (gray arrow).

In the ribonucleotide incorporation throughout the lagging strand (RITOLS) model, replication of leading strand (H-strand) initiates at a discrete origin (OR) and proceeds unidirectionally (black arrow), displaying the parental H-strand. The lagging strand (L-strand) is initially laid down as RNA (red line) using the displayed H-strand as template. The RNA is subsequently replaced by DNA (gray arrow), which probably starts as soon as OL is exposed by a yet unclear mechanism. In the strand-coupled mode (right pathway) initiation of both leading- (H-strand) and lagging strand (L-strand) synthesis occurs bidirectionally from multiple origins across a broad zone downstream of OH. This is followed by progression of both forks until the forks arrest at OH (**Antoshechkin I, et al., 1997**).

I.1.5.3. mtDNA transcription

In human cells, each strand contains promoter for transcriptional initiation, one on the light-strand promoter (LSP) and two on the heavy-strand promoter (HSP), (***Figure 7***). Transcription from the mitochondrial promoters produces polycistronic precursor RNA encompassing all the genetic information encoded in each of the specific strands, and the primary transcripts are processed to produce the individual tRNA and mRNA molecules (**Clayton DA., 1991**). T he transcription of mtDNA operates in each promoter independently and it is carrying out oriented in opposite direction. The heavy strand has two sites of transcription initiation such as HSP1 and HSP2 Besides, the strand-coupled and the RITOLS models coexisting as interconnected events leading as multiple priming sites of the new lagging strand for the DNA synthesis.

More recently, Reyes and collaborators observed that long tracts of RNA are associated with replicating molecules of mtDNA and they suggested that the mitochondrial genome of mammals is copied by a non classical mechanism (synthesis in parallel of each strand with 5'-3' orientation)

Finally using DNA synthesis in organelle, they demonstrated that isolated mitochondria incorporate radiolabeled RNA precursors, as well as DNA precursors, into replicating DNA molecules. They indicate that RITOLS is a physiological mechanism of mtDNA replication, and that it involves a 'bootlace' mechanism, illustrated in (***Figure 9***) in which processed transcripts are successively hybridized to the lagging-strand template, as the replication fork advances (**Reyes A et al., 2013**).

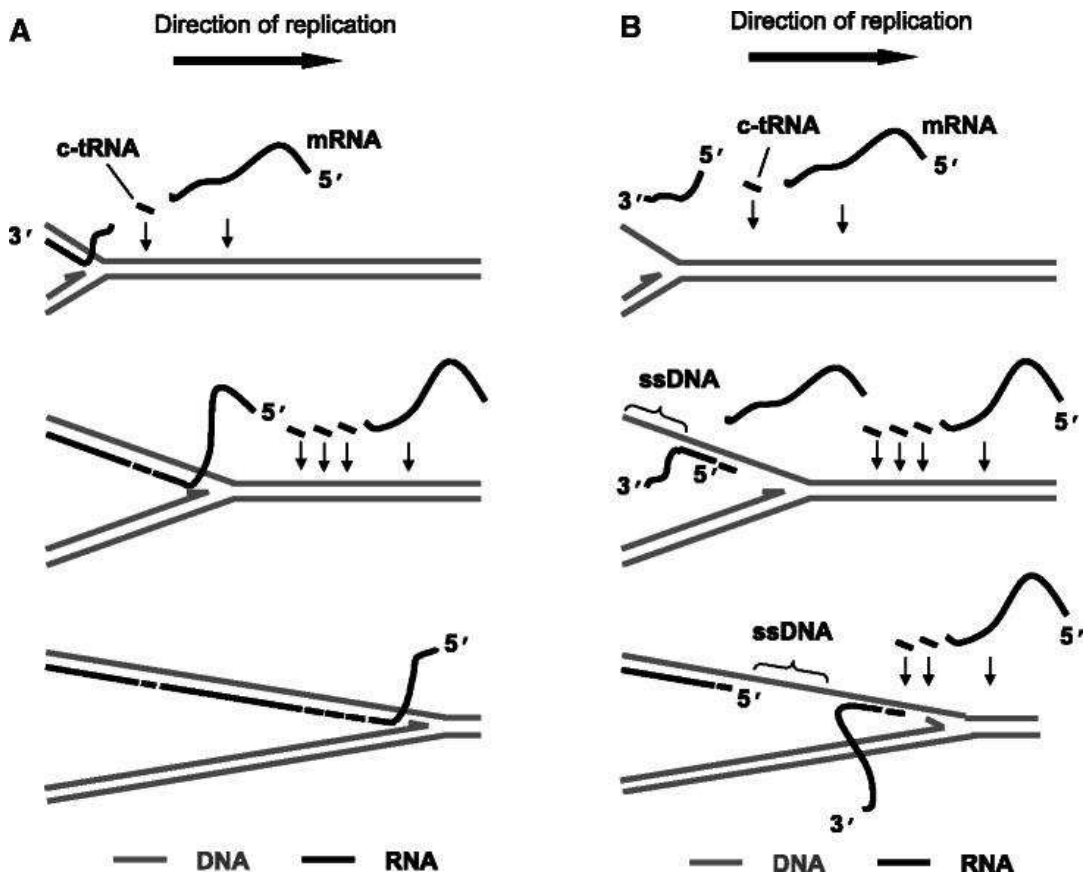

***Figure 9**: The bootlace model of mtDNA replication. Preformed (L-strand) transcripts, including complementary tRNA and mRNA hybridize to the template lagging strand of mammalian mtDNA as leading strand DNA synthesis proceeds. RNA recruitment is an ongoing process*

The transcription machinery in budding yeast appears less complicated, since it only contains one single TFB1M/TFB2M homologue, which is denoted mt-TFB or Mtf1. The *S. cerevisiae* mitochondrial RNA polymerase (Rpo41) and mt-TFB form a heterodimer that recognizes mitochondrial promoters and initiate transcription (**Cliften PF. et al., 1997 ; Mangus DA, et al., 1994**). TFAM (from human mitochondria) and its homologue from yeast, Abf2, are not required for transcription of mtDNA (**Diffley JF et Stillman B., 1991 ; Parisi MA, et al., 1993 ; Dairaghi DJ, et al., 1995**) but rather have a role in mtDNA maintenance and packaging. Recently, by overexpressing human TFAM in P1 artificial chromosome (PAC) transgenic mice, it was reported that also mammalian TFAM may serve as a key regulator of mtDNA copy number. This results that the human TFAM protein is a poor activator of mouse mtDNA transcription, despites its high capacity for unspecific DNA binding (**Campbell CT, et al., 2012**). Now, therefore it would be possible to dissociate the role of TFAM in mtDNA copy number regulation from mtDNA expression and mitochondrial biogenesis in mammals *in vivo*.

The yeast POLRMT contains a unique amino-terminal extension, which is absent in homologous bacteriophage RNA polymerases. The function of the amino-terminal extension is separable from the known RNA polymerization activity of the enzyme (**Wang Y et Shadel GS., 1999**)

In support of this notion, the domain interacts specifically with Nam1, a protein originally identified as a high copy suppressor of mtDNA point mutations that affect splicing of introns in budding yeast. The N-terminal domain may therefore provide the means to couple factors involved in additional aspects of RNA metabolism directly to the transcription machinery (**Rodeheffer MS. et al., 2001**).

According with *S. cerevisiae* transcription model, it will be of interest to analyze human mitochondrial transcription. It was demonstrated in human that the levels of TFAM directly regulate the activity of both TFB1M/POLRMT - and TFB2M/POLRMT -dependent mtDNA transcription both *in vivo* and *in vitro* (**Falkenberg M.et al., 2002**).

The TFAM protein contains two tandem HMG box domains separated by a 27-amino-acid residue linker region and followed by a 25-residue carboxy-terminal tail. Mutational analysis of TFAM has revealed that the tail region is important for specific DNA recognition and essential for transcriptional activation (**Shadel GS, et Clayton., 1995**).

TFAM can bind, unwind and bend DNA without sequence specificity, similar to other proteins of the HMG domain family (**Fisher RP. et al., 1992**).

The sequence-specific binding of a TFAM tetramer (**Antoshechkin I, et al., 1997**), upstream of HSP and LSP, may allow the protein to introduce these structural alterations at a precise position in the promoter region and perhaps partially unwind the start site for transcription.

This model may explain why the exact distance between the TFAM binding site and the start site for LSP transcription is of critical importance (**Dairaghi DJ, et al., 1995**).

The POLRMT (with proof-reading ability) can collaborate with Twinkle protein (with 5’ to 3’ DNA helicase) in DNA replication (**McKinney EA, Oliveira MT 2013**).

Also, the ***Figure 10*** shows POL γ A , POL γ B and POLRMT action .

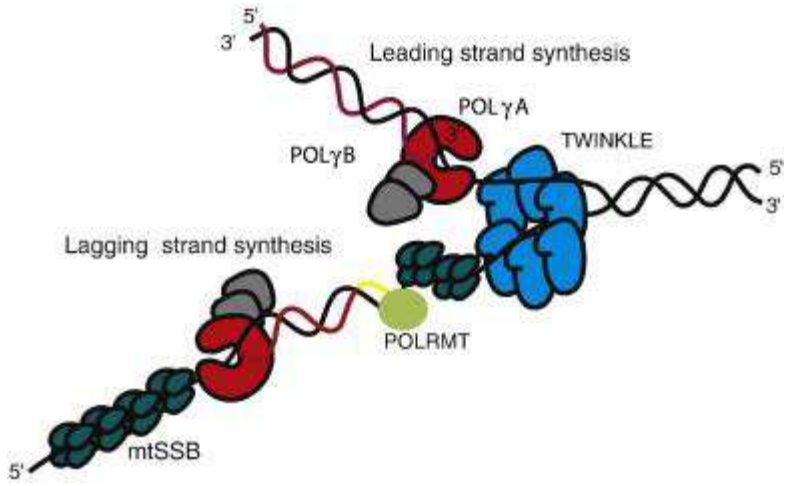

***Figure 10**: Proteins at the human mtDNA replication for (**Wanrooij S et Falkenberg M., 2010**).*

The mtDNA replication machinery exposes OL in its single-stranded conformation. Strand displacement causes the origin sequence to adopt a stem–loop structure, which is recognized by an origin-specific primase (**Wong TW et Clayton DA., 1985 A ; Wong TW et Clayton DA., 1985 B ; Wong TW et Clayton DA., 1986)**.

I.1.5.3.1. Mitochondrial RNA polymerase (POLRMT)

The POLRMT was initially identified in *Saccharomyces cerevisiae*. This enzyme is a unique mitochondrial RNA polymerase that is distinct from the nuclear RNA polymerases (**Greenleaf AL, et al., 1986 ; Kelly JL, et al., 1986**).

In human cells POLRMT was later identified and sequence analysis demonstrated that it was structurally related to the bacteriophage T7 RNA polymerase (**Tiranti V, et al., 1997**). The POLRMT as the T7 homologue cannot initiate transcription on its own (**Fuchs E, et al., 1971**), but requires the simultaneous presence of a high mobility group-box protein (mitochondrial transcription factor A; TFAM), and either transcription factor B1 (TFB1M) or B2 (TFB2M) (**Fernández-Silva P., 2003).**

Both TFB1M and TFB2M can form a heterodimeric complex with POLRMT. The four proteins of the basal mitochondrial transcription machinery have been purified in recombinant form and used to reconstitute transcription *in vitro* with a promoter-containing DNA fragment (**Falkenberg M, et al., 2002**).

The POLRMT is not only required for transcription, besides, at the origin of heavy strand DNA replication (OH), it generates the RNA primers used to initiate leading-strand mtDNA synthesis (**Wanrooij S. et al., 2008 ; Chang DD et Clayton DA., 1985 ; Chang DD, Hauswirth WW, et Clayton DA., 1985**). About 100 nucleotides are primed in LSP region leading strand DNA synthesis (***Figure 11***).

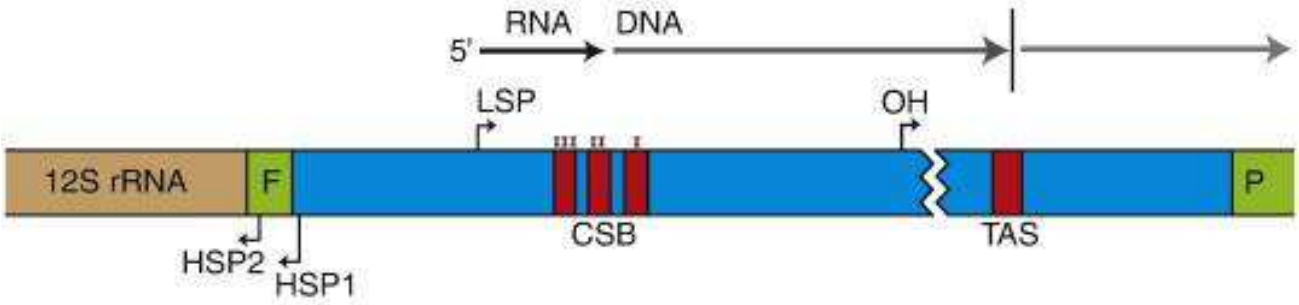

Figure 11*: Schematic representation of the D-loop regulatory region. The three conserved sequence blocks (CSBI, CSBII and CSBIII) are located just downstream of light-strand promoter (LSP). Transition from RNA primer to the newly synthesized DNA has been mapped to sequence within or near CSB II (**Kang D et al., 1997**). The conserved termination-associated sequence (**Pham XH. et al., 2006**) (TAS) elements are located at the 3' of the nascent D-loop strand and are proposed to be a major regulation point of mtDNA replication. Abbreviations: HSP, heavy-strand promoter; LSP, light-strand promoter; OH, origin of H-strand; F, tRNA phenylalanine; P, tRNA prolin (**Wanrooij S. et al., 2008**).*

The ***Figure 12*** shows in three steps the different proteins involved in mtDNA transcription. The POLRMT has the capacity to specifically initiate RNA primer synthesis at the OL stem–loop structure. At this point, POLγ replaces POLRMT and lagging strand DNA synthesis is initiated. Interestingly, unlike in H-strand replication, the primer hand-off between POLRMT and POLγ could be reconstituted in vitro, suggesting that this event in OL dependent initiation is not a regulated event (**Wanrooij S. et al., 2008**).

The proposed model is mainly based on *in vitro* data, but receives support from two-dimensional gel electrophoresis (2D-PAGE) analysis in combination with siRNA knockdown of POLRMT. In human cells, depletion of POLRMT generates replication intermediates with delayed lagging strand synthesis, thereby providing evidence for POLRMT acting as a lagging-strand primase also *in vivo* (**Fusté JM. et al., 2010**).

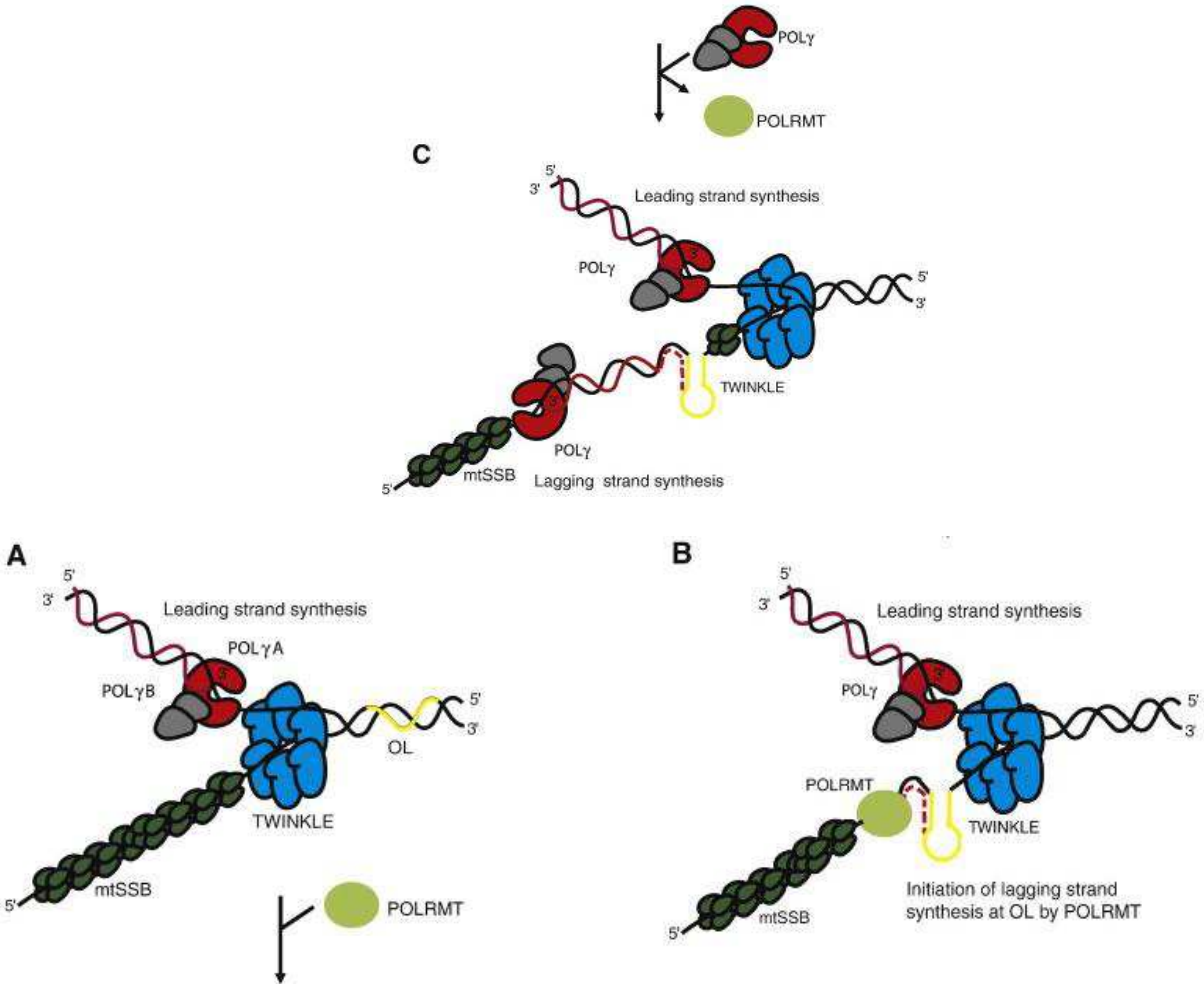

***Figure 12**: Schematic model of DNA strands synthesized: (A) the leading strand (H-strand) DNA replication machinery approaches the OL sequence (yellow). (B) the upon passage, single-stranded OL is exposed and adopts a stem–loop structure. MtSSB is unable to bind to the stem–loop and POLRMT can initiate primers from the poly-dT stretch in the single-stranded region of OL (C). After about 25 nucleotides (dotted red), POLRMT is replaced by POLγ, and lagging-strand DNA (L-strand) synthesis(**Fusté JM. et al., 2010**).*

I.1.5.3.2. Transcription regulation in human mitochondria

Transcription of mitochondrial genes is carried out by POLRMT, together with several nuclear-encoded transcription factors. Mitochondrial transcription (and as a consequence oxidative phosphorylation) may be regulated by transcription initiation and termination factors, and by changes in ATP levels in response to alterations of the cell metabolic demands (**Sologub MIu, et al., 2009**).

Recently, it has been suggested that transcription in mitochondria is also coordinated with other crucial processes such as DNA replication and translation, indicating the importance of studies of molecular mechanisms of mitochondrial gene expression in these organelles (**Sologub MIu, et al., 2009**).

It was reported different levels among the steady-state of the promoter-proximal transcripts and steady-state of promoter-distal from mRNA transcripts (**Gelfand R et Attardi G., 1981**).

The second heavy-strand promoter dedicated to rRNA gene transcription justifies this difference in transcript levels (**Montoya et al., 1982 ; Montoya., 1983**).

Besides, the existence of a tridecamer template sequence downstream of the 16S rRNA 3′-end, which serves as a binding site for the mitochondrial transcription termination factor mTERF (**Christianson TW et Clayton DA., 1988 ; Kruse B, et al., 1989 ; Fernandez-Silva P. et al., 1997)**.

Although mTERF binding to the termination sequence blocks transcription bidirectionally in a partially purified human mitochondrial system, it only blocks heterologous RNA polymerases in the direction opposite that of mitochondrial rRNA synthesis (**Shang J. et Clayton DA., 1994**).

The number of mitochondrial proteins is estimated 10 % of the total cellular proteome. But only a few polypeptides of OXPHOS are translated in mitochondria (due to mtDNA coding limitation).

Certainly, the mitochondrial translation system is very similar to the bacterial system. It is inhibited by chloramphenicol and initiation is carried out by a formyl-methionine. Another feature of this system is the use of a genetic code that differs from the universal genetic code for several codons (**Osawa S et al., 1992**).

The ***Table 1*** shows mitochondrial genetic code use. The universal arginine codons AGG and AGA became in STOP, nevertheless UAG (universal STOP) became in Trp. Further, AUA has been reassigned to Met rather than serving as an Ile codon (**Smits P. et al., 2010**).

Codon	Universal code	Human mitochondrial code
UGA	**STOP**	**Trp**
AGA	**Arg**	**STOP**
AGG	**Arg**	**STOP**
AUA	**IIe**	**Met**

***Table 1**: Comparison of mitochondrial genetic code to universal code (**Osawa S et al., 1992**)*

I.2. Mitochondria Distribution

Mitochondria exist in two interconverting forms; as organelle isolated or/and as extended filaments, networks or clusters connected with intermitochondrial junctions (**Skulachev VP., 2001**). Mitochondria distribution is very variable in human cell. The ***Figure 13*** shows primary skin fibroblasts labeled with antibodies against DNA, COX2 and/or BrdU under normal conditions. The merge DNA/COX2 illustrated the co-localization mtDNA and IMM. Besides, the merge DNA/BrdU shows that mitochondria fission and mtDNA replication are not depending mechanisms. Thus, mitochondria can replicate its genome without mitochondrial division or mitochondrial fission takes place without mtDNA replication.

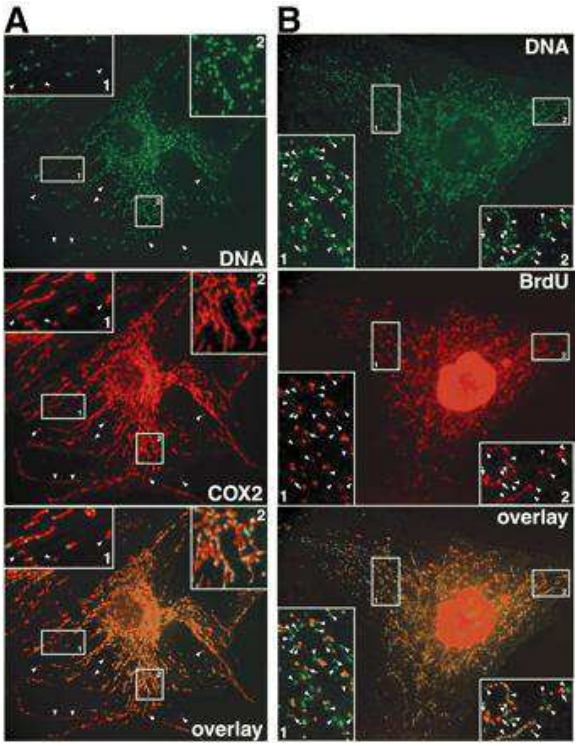

***Figure 13**: CoQ10 partially preserves mitochondrial structure of ONH astrocytes against oxidative stress-induced mitochondrial fission. (**Noh YH, et al., 2013**).*

The ***Figure 14*** shows the mitochondria of ONH astrocytes were stained with MitoTracker Red. Control ONH astrocytes exposed to vehicle contained classic elongated tubular mitochondria. In contrast, ONH astrocytes exposed to H_2O_2 contained small rounded mitochondria.

However, ONH astrocytes pretreated with CoQ10 showed a partial preservation of mitochondrial morphology compared with the ONH astrocytes exposed to H_2O_2.

Furthermore, the mitochondria appearance as network-like regrouped organelles with the same functionally is supports by fission and fusion mitochondrial cycles. Also these organelles can be morphologically and functionally independent within cells (**Noh YH, et al., 2013**).

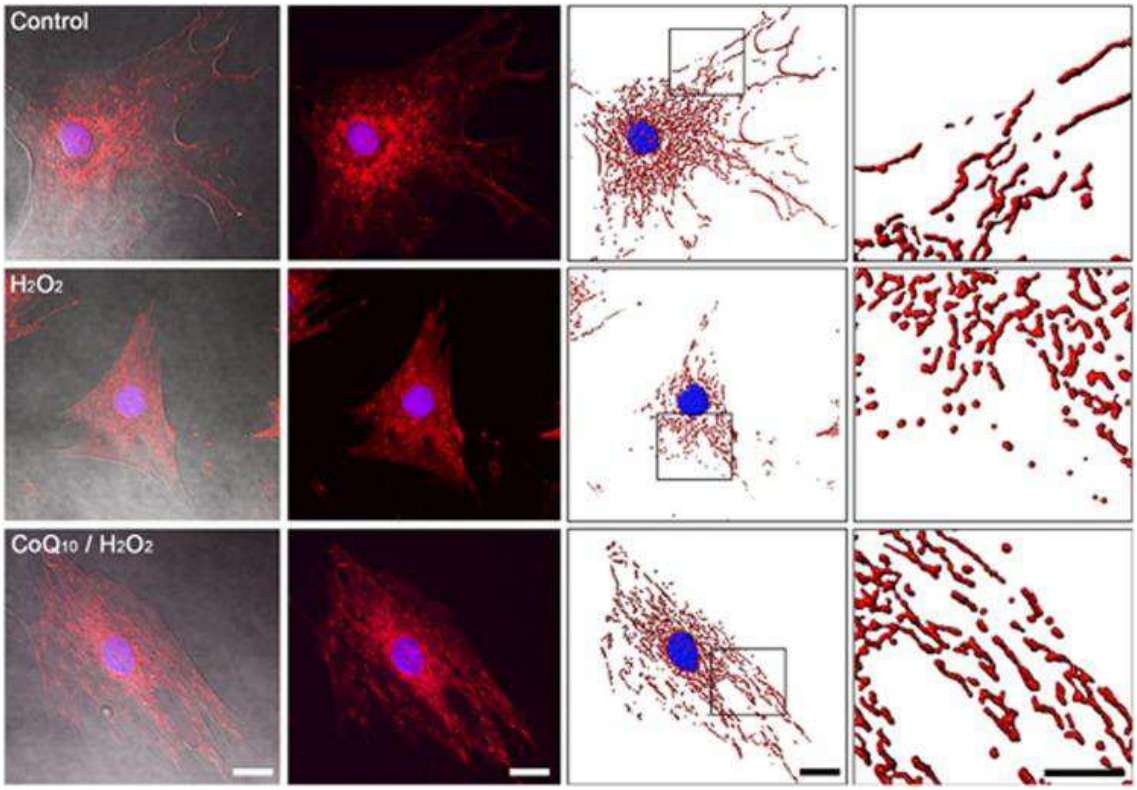

Figure 14*: Mitochondrial DNA localizes to punctuate structures that are distributed throughout the mitochondrial compartment. (A) or after a 20 hour pulse with BrdU (B). Insets 1 and 2 depict enlargements of the boxed areas. (A) Monoclonal antibodies against DNA label punctuate structures that are distributed throughout mitochondria labeled with antibodies against the inner membrane protein COX2. Only a few mitochondria appear devoid of DNA-labeling (arrowheads). (B) Antibodies against the thymidine analogue BrdU label the nucleus as well as punctuate mitochondrial structures labeled with DNA-antibodies. Some of the mitochondrial DNA-positive structures are devoid of BrdU (arrowheads) and very few BrdU-positive structures escape detection with DNA-antibodies (arrows). CoQ10, coenzyme Q10; H_2O_2, hydrogen peroxide. Scale bars, 10 μm*

Mitochondria are organized into a big network in perinuclear zone where ATP is highly required (**Collins TJ et al., 2002**). (***Figure 15***)

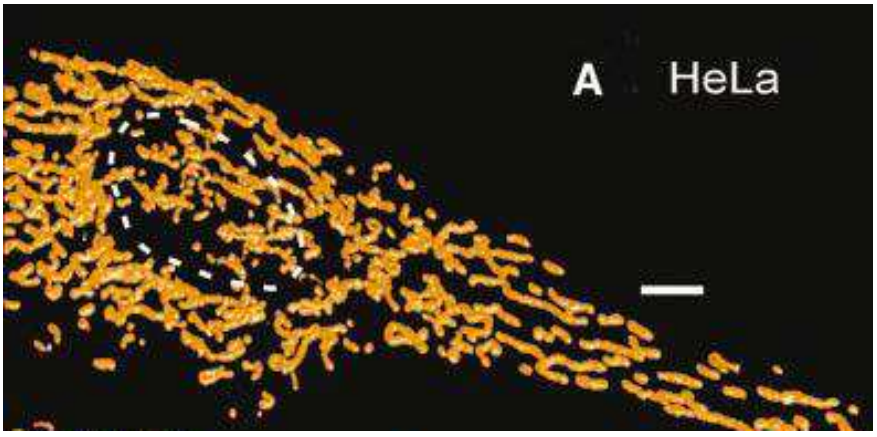

Figure 15*: Surface-rendered three-dimensional reconstructions of HeLa cell expressing mito-DsRed1. The dashed circle indicates the position of nuclear zone. Scale bars, 5 μm* ***(CollinsTJ et al., 2002****)*

I.3. Mitochondrial fusion and fission

Mitochondrial fusion and fission cycles are opposing processes involved in the division and the morphology of the mitochondrial population dynamic (**Chen H. et al., 2004**). Mitochondrial fusion is regulated by proteins localized in OMM named mitofusin (Mfn) family (**Mozdy AD et Shaw, 2003**). Mitofusin 2 is involved in ER and mitochondria exchange of $Ca2^{+}$. Mitochondria are in constant remodeling in the cell with half-life between 6 to 10 days and this variation is because of fusion and fission regulation (**Jakobs S., 2006**).

Fusion and fission events were originally studied in the yeast *Saccharomyces cerevisiae* and allowed the identification of many protein actors as MMM (Mitochondrial Morphology and Maintenance). Most of the MMM genes are highly conserved through of species evolution and highly implicated in the mitochondrial morphology changes by coordinated fusion and fission.

These results were confirmed in human mitochondria where it has been shown that fusion and fission reactions are involved in matrix exchanges (**Legros F et al., 2002 ; Santel A et al., 2003**) . These studies confirm that alterations in mitochondrial energy generation, ROS production, and apoptosis can all contribute to the pathophysiology of mitochondrial disease (**Wallace DC., 2002**).

Studies in the yeast *Saccharomyces cerevisiae* have shown that in two mitochondria synchronized in fusion and fission events, the fission between external membranes leads to the very slow exchange of mtDNA and very rapid exchange of mitochondrial matrixes, several cycles of outer and inner membrane fusion and fission are required for the exchange of mtDNA damaged (**Okamoto K et al., 2005**) (***Figure 16***).

Recently, it has been demonstrated that mitochondrial network mobility is associated with the cytoskeleton proteins as actin and involved in cytosqueleton dynamic (**Kremneva K et al., 2013**).

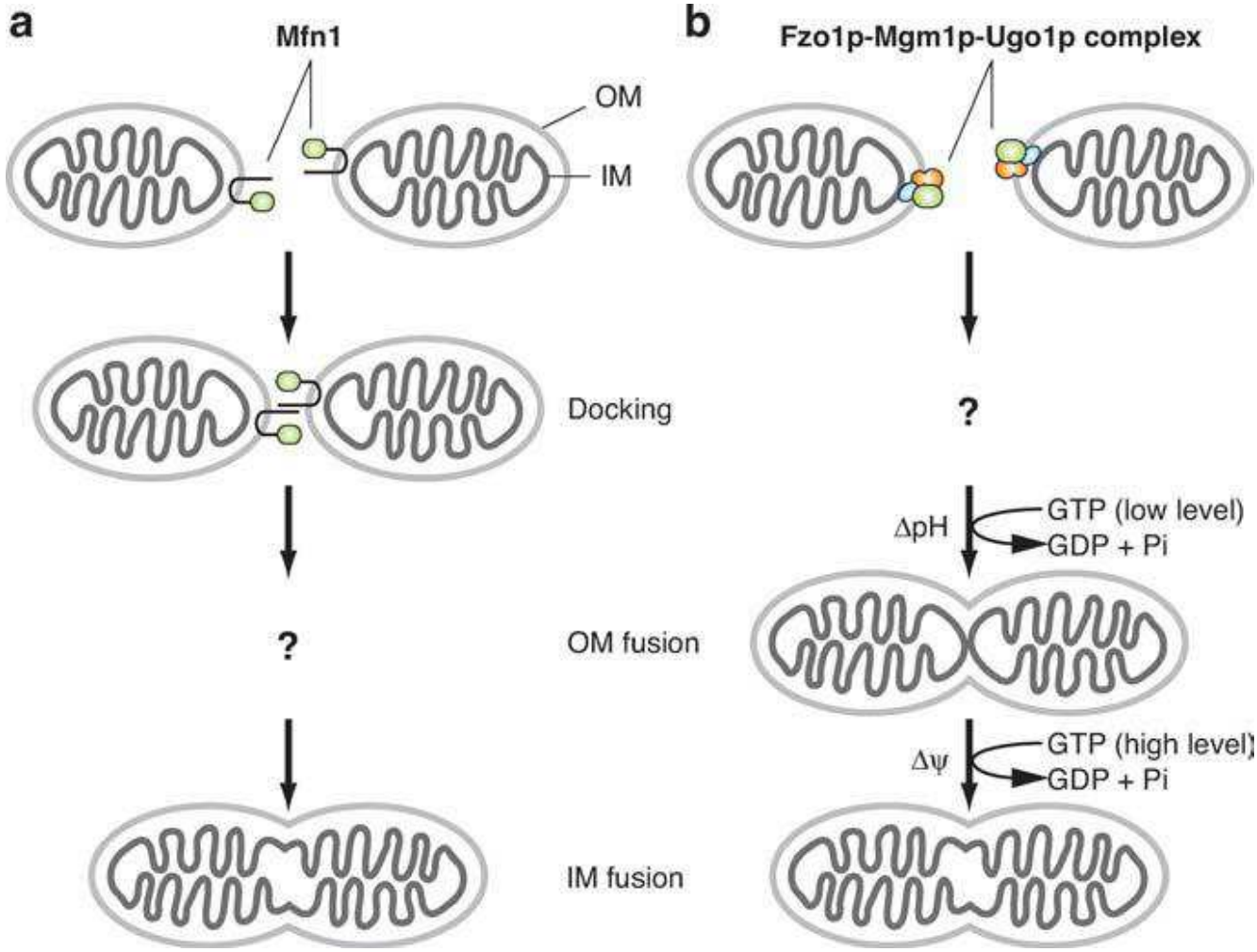

Figure 16*: Models for mitochondrial fusion in yeast Saccharomyces cerevisiae a) Mfn1 single protein interaction and b) Fzo1p-Mgm1p-Ugo1p complex protein interaction (**OkamotoK et al., 2005**).*

Nevertheless, proteins involved in DNA repair present in matrix can be exchanged very fast (**Kaufman BA. et al., 2000 ; Nunnari J et al., 1997 ; Otera H, et al., 2013**).

Mutations in MMM lead to modify the mitochondrial profile of subcellular localization and mitochondrial morphology.

The ***Figure 17*** shows different interactions of MMM complex with proteins that plays important role in the cell (**Millau JF. et al., 2008**).

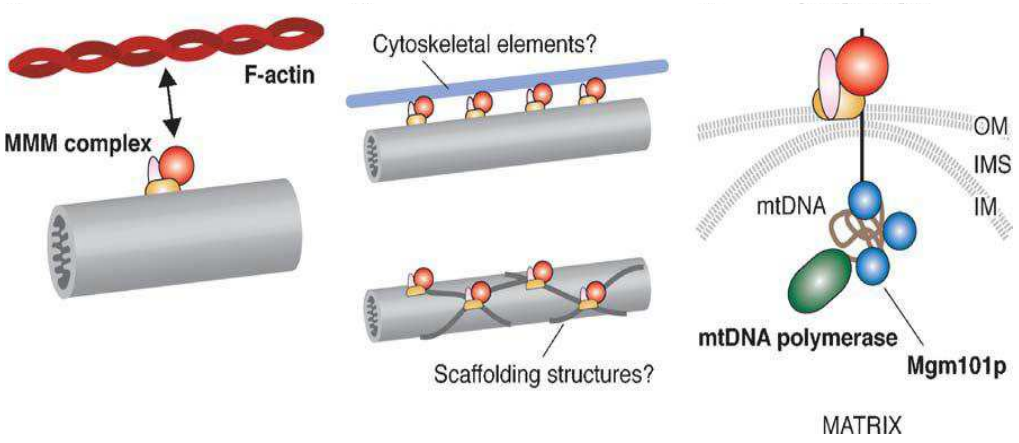

***Figure 17**: The MMM complex may mediate at least three processes: actin-mitochondria attachment (left), formation of tubular mitochondria (middle), and anchoring of mtDNA nucleoids (right) (**Okamoto K et al, 2005**)*

I.4. Mitochondrial Functions

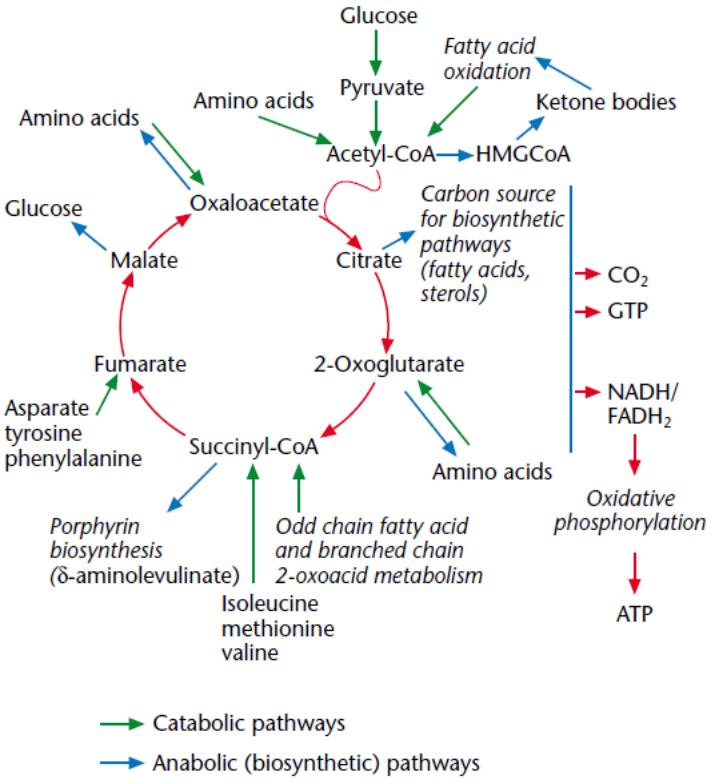

***Figure 18**: The CAC has integrative functions between mitochondrial matrix and cytosolic pathways in ATP production. The 3 main sources for ATP production are: carbohydrates, lipids and proteins(**Krauss S., 2001**).*

In the eukaryotic cell mitochondria is involved in several mechanisms such as: Ca^{2+} storage (**Leanza L. et al., 2013**), thermogenesis (**Tine M et al., 2012**)) and ATP production. The more important mitochondrial function in eukaryotic cell is the ATP production. The ***Figure 18*** shows the different pathways for ATP synthesis from various sources such as: amino acids, fatty acids and glucose. The protein catabolism is involved directly with CAC in the formation of oxaloacetate and 2-oxoglutarate. On the other hand, glucose and fatty acids became in acetyl-CoA by glycolysis and ß-oxidation respectively.

Finally, the ATP production depends of OXPHOS capacity. The ATP production (***Figure 19)*** is generated from a gradient of protons (H^+) which is used by the ATP synthase to convert ADP and phosphate ions in ATP.

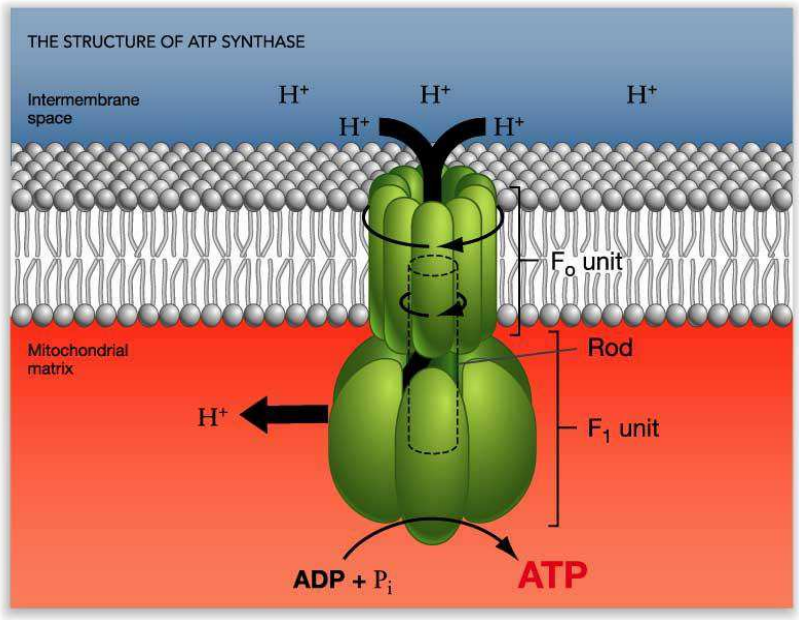

Figure 19*: Representation of ATP synthase structure. The F1 unit was localized in mitochondrial matrix and the Fo unit in IMM. The synthesis of ATP is depending on the H^+ gradient.* *http://www.jpboseret.eu/uploads/images/ATPase.jpg*

This gradient of protons is the result of several oxidation-reduction reactions and depends of three important coenzymes such as: nicotinamide adenine dinucleotide (NAD); nicotinamide adenine dinucleotide phosphate (NADP); and flavin adenine dinucleotide (FAD). OXPHOS is carried out in IMM involving the electrons traffic through respiratory chains complexes.

During cellular respiration, ATP production is controlled by product excess, ATP being an allosteric inhibitor of Cyt-C oxidase (**Arnold S. et Kadenbach B., 1997**).

I.5. Mitochondrial diseases

The ***Table 2*** shows mitochondrial diseases due to mitochondrial (mt) tDNA and nuclear (n) DNA (nDNA) damage

Genetic and biochemical classification of the mitochondrial diseases				
Genome	Gene	[mtDNA]	Biochemistry	Clinical phenotype
mtDNA		single Δ	x prot. synth.	KSS; ocular myopathy; PS
	tRNA $^{Leu(UUR)}$		↓ prot. synth	MELAS
	tRNA^{Lys}		↓ prot. synth	MERRF
	other ^{tRNAs}		↓ prot synth.	multiple phenotypes
	ATPase6		↓ATP synth.	NARP/MILS
	ND1, ND4, ND6		↓complex I	LHON
	ND1, ND4		↓ complex I	myopathya
	Cyt b		↓ complex III	myopathya
	COX III		↓ complex IV	myopathya
nDNA				
	NDUF		↓ complex I	LS
	SDHA		↓complex II	LS
	BCS1L		↓ complex III	GRACILE
	SURF1		↓ complex IV	LS
	SCO1		↓ complex IV	hepatoencephalomyopathy
	SCO2		↓ complex IV	cardioencephalomyopathy
	COX10		↓ complex IV	nephroencephalomyopathy
	COX 15		↓complex IV	cardioencephalomyopathy
	ATP 12		↓ complex V	fatal infantile multisystemic
	TP	multiple Δ	↓ _	MNGIE
	ANT1	multiple Δ	↓ prot. synth.	adPEO-plus[b]
	Twinkle	multiple Δ	↓ prot. synth	adPEO-plus[b]
	POLG	multiple Δ	↓ prot. synth.	ad/arPEO-plus[b]
	dGK	depletion	↓ prot. synth.	hepatocerebral syndrome
	TK2	depletion	↓prot. synth	myopathy; SMA
	TAZ		↓ cardiolipin	Barth syndrome
	OPA1		↓ mit. Motility	ad optic atrophy

Table 2*: Representation of mitochondrial diseases due to mtDNA and nuclear DNA (nDNA) damage. Abbreviations and symbols: Δ, deletion; ↓, decrease, KSS, Kearns-Sayre syndrome; PS, Pearson syndrome;*

MELAS, Mitochondrial encephalomyopathy, lactic acidosis and stroke-like episodes; LS, Leigh syndrome; MILS, maternally inherited LS; GRACILE, growth retardation, aminoaciduria, cholestasis, lactacidosis, early death; adPEO, autosomal dominant progressive external ophthalmoplegia arPEO, autosomal recessive PEO; SMA, spinal muscular atrophy. [mtDNA] indicates changes of mtDNA secondary to nDNA mutations (defects of intergenomic signaling).

a Mutations in cyt b and COX genes can also cause multisystemic diseases.
*b Plus refers to proximal weakness, neuropathy, psychiatric disorders, parkinsonism (**DiMauro S., 2004**).*

I.5.1. Mendelian: associated with genes of the nuclear genome

When DNA disorders concern OXPHOS system, hereditary mitochondrial diseases usually affect tissues with high energy needs, like neuromuscular or central nervous system. Frequently the deleterious mitochondrial mutations are heteroplasmic, thus wild type and mutated forms of mtDNA coexist in the same cell. The mitochondria functions start to shut down when a threshold of mtDNA mutation was exceeded. This threshold is variable and differs from mutation to mutation: for example 60 to 70% in chronic progressive external ophthalmoplegia (CPEO) and probably 95% in the syndromes of mitochondrial encephalopathy, myopathy, lactic acidosis, and stroke-like episodes (MELAS), and myoclonic epilepsy with ragged red fibers (MERRF) (**Tonin Y et al.**, **2013**). The threshold effect may explain the tissue-specific patterns of clinical expression (**Nonaka I., 1992**). Consequently, a shift in the proportion between mutant and wild type molecules could restore mitochondrial functions (**Tonin Y et al., 2013**).

Mutations in mtDNA that encoded OXPHOS system are related to damage effect in respiratory function increasing electron leak and ROS production and therefore mtDNA damage. This result guides to vicious cycle that leads to the differential accumulation of mutation in mtDNA during aging (**Wei YH. et al., 1998**). It was show the relationship among damages in mtDNA and illnesses apparition such as: MELAS, MERRF, KSS, LHON and NARP (**Thorburn DR et Rahman S., 1993**), where this last one is the consequence of ATPase 6 mutation.

I.5.2. not Mendelian: associated with maternal inheritance

The strictly maternal inheritance of mitochondria is the result of the removal of sperm tail containing mitochondria prior to egg entry, and the destruction of the sperm mitochondria in very little time after fertilization (**Sutovsky P, et al., 2000**). Thus, this mechanism proposed to promote the strictly inheritance of mtDNA in humans and animals (**Thompson WE, et al.,**

2003). As well, pedigree schematized by ***Figure 20*** represents a typical maternal mode of inheritance of diseases caused by mtDNA mutations (***Figure 21***).

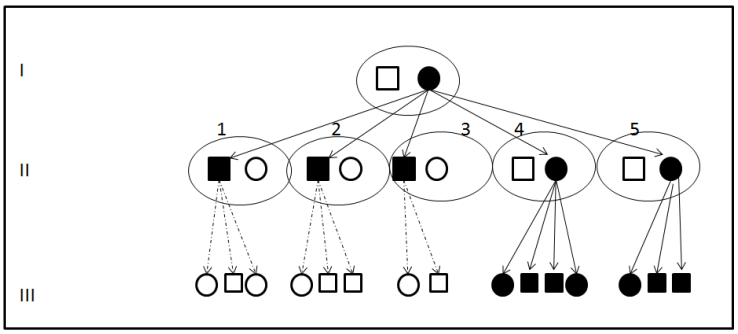

Figure 20*: Typical pedigree of three filial generations. The black color was used in order to illustrate the illness phenotype. The maternal inheritance was shown in the third filial generation where all illness phenotype was the maternal origin. Nevertheless, the males (II: 1, 2 and 3) did not transmit the illness phenotype to generation III.* *http://t3.gstatic.com/images?q=tbn:ANd9GcSGVALk3oCWEGsz3rEj0bsWt40YOiWjnonukMHFi_3MonfWDeuhAgc18lJIvg*

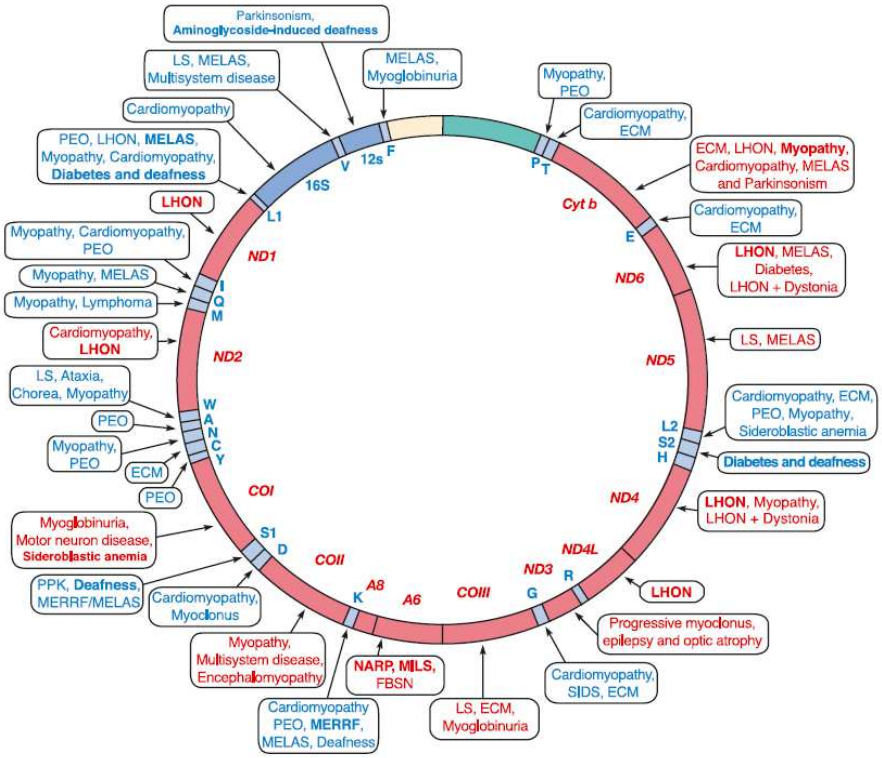

Figure 21*: Schematic representation of mtDNA representing the protein-coding genes for the seven subunits of complex I (ND), the three subunits of cytochrome oxidase (COX), cytochrome b (Cyt b), and the two subunits of ATP synthetase (A8/6), the 12S and 16S ribosomal RNAs (12S, 16S), and the 22 transfer RNAs (tRNA) identified by one-letter codes for the corresponding amino acids. Abbreviations: FBSN, familial bilateral striatal necrosis; KSS, Kearns–Sayre syndrome; LHON, Leber's hereditary optic neuropathy; MELAS, mitochondrial encephalomyopathy, lactic acidosis, and stroke-like episodes; MILS, maternally inherited Leigh syndrome; NARP, neuropathy, ataxia, retinitis pigmentosa. In blue the diseases due to mutations that impair mitochondrial protein synthesis; and in red diseases because of mutations in protein coding genes (**DiMauro S., 2004**).*

II. DNA maintenance

Evolution and natural selection have used DNA sequence to store and protect the ¨life information¨ to formulate our bodies. The DNA molecules are long complementary chains, consisting of 4 bases and referred to as A, G, C and T. The entire information content of a human is stored in a long sequence packed into the nucleus and several copies of few circular genomes into the mitochondria. Mitochondria genome size represents about 1% of nuclear genome size. Mammalian cells stored the genetic information in nucleus with maternal and paternal contribution and in mitochondria strictly with maternal contribution (**Trafton A., 2012**).

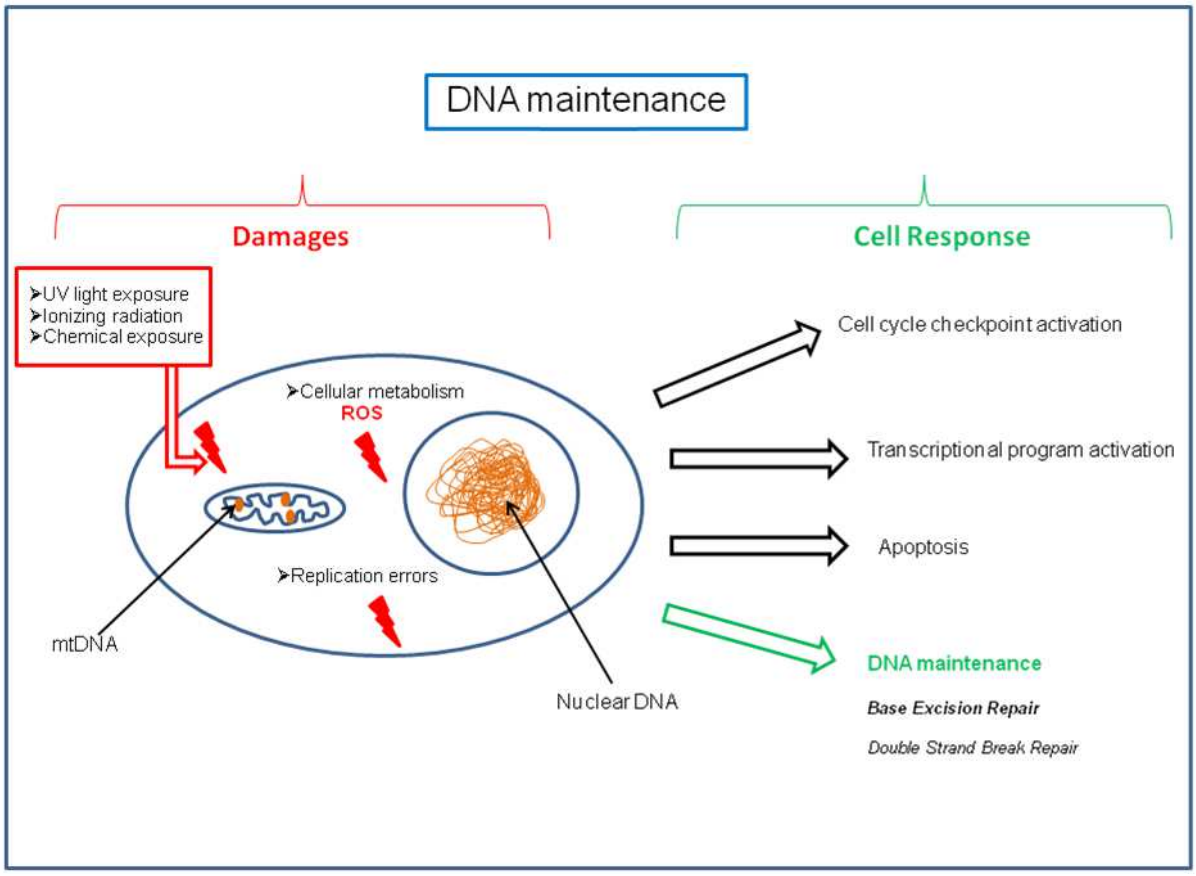

***Figure 22**: Schematic representation of exogenous and endogenous sources of mitochondrial and nuclear DNA damages involving different cell responses.*

In humans, DNA damage has been shown to be involved in a variety of genetically inherited disorders, in aging (**Finkel T et N J Holbrook NJ., 2000**) and in carcinogenesis (**Hoeijmakers NJ., 2001**).

The more often sources of DNA damages such as UV exposure, ionizing radiation, chemical exposure, cellular metabolism and replication errors and different cell responses (***Figure 22***).

II.1. DNA damage

From a structural definition, DNA damage can be divided in 3 main categories: base modifications, single or double strand breaks. The amount of lesions that we face is enormous with estimates suggesting that each of our 10^{13} cells has to deal with around 10.000 lesions per day (**Lopez-Contreras AJ, et Fernandez-Capetillo O., 2012**).

The more representative quantities of mutations in human cells are from endogenous sources (**De Bont R. et van Larebeke N., 2004**).

They are because of oxidative damages (**Ames BN, et al., 1993**), depurinations (**Lindahl T et Nyberg B., 1972**), depyrimidinations, single-strand breaks, double-strand breaks, O6-methylguanines and cytosine deamination.

The oxidative damage 8-oxoG is a consequence of reactive oxygen species (ROS) generated during oxidative metabolism and its mechanism of DNA repair is highly studied by the Base Excision Repair (BER). Analytical measurements of the oxidative DNA adduct 8-oxo-deoxyguanosine (oxo8dG) show that mtDNA suffers greater endogenous oxidative damage than nuclear DNA. The subsequent discovery demonstrated that somatic deletions of mtDNA occur in humans. One hypothesis born: ¨The mitochondrial genome is particularly more susceptible to ROS damage¨ (**Beckman KB. et Ames BN., 1999**). This hypothesis opened doors in investigations concerning mtDNA ¨protection¨ in 1999.

Recently thanks to advances in analytical chemistry it was validated that the major sources of DNA damage in human is resulting from endogenous sources such as ROS that not only produces 8-OHdG in mtDNA, but also more extensive damages altering DNA chemical structure (i.e. strand break) (**Wang Z et al., 2013 ; Muralidharan S. et Mandrekar P., 2013**).DSB can be formed because of SSB accumulation, ionizing radiation or clastogenic drugs; endogenously, during DNA replication, or as a consequence of ROS generated during oxidative metabolism. In addition, DSB are involved in the lost of DNA sequence frequently associated with certain pathologies (**Lopez-Contreras AJ, et Fernandez-Capetillo O., 2012**).

II.2. DNA repair mechanisms

II.2.1. Base Excision Repair (BER)

The BER system is a multi-step process that repair damage to modified bases following oxidation, methylation, deamination, or spontaneous loss of the DNA base itself (**A Memisoglu A et Samson L., 2000**).

The ***Table 3*** shows the more studied human DNA glycosylases

Human DNA glycosylases			
	Localization		
Enzyme	**Chromosomal**	**Cellular**	**Mayor sustrates**
UNG	12q23-24.1	N and M	U in single or double strand DNA, 5-OH-meU
SMUG1	12q13.3-11	N	U in single or double strand DNA
TDG	12q23-24.1	N	T, U or ethenoC opposite G (preferably CpG sites)
MBD4	3q21-22	N	T or U opposite G at CpG sites T opposite O6-meG
MYH	1p32.1-34.3	N and M	A opposite 8-oxoG, 2-OH-A opposite G
OGG1	3p26.2	N and M	8-oxoG, 2-OH-A opposite C, fapyG
NTH1	16p13.3	N and M	Tg, DHU, fapyG, 5-OHU, 5-OHC
NEIL1	15q22-24	N	As NTH1; also fapyA, 5S,6R Tg isomer, 8-oxoG
NEIL2	8p23	N	Overlap and some differences with NTH1/NEIL1
NEIL3	4q34.2	N	to be determinated
MPG	16p13.3	N	3-meA, hypoxanthine, ethenoA

***Table 3**: List of certain enzymes DNA glycosylases present in nucleus and mitochondria from human cells. Chromosomal location, cellular localization and major substrates are represented (**Barnes DE et Lindahl T., 2004**).*

Endogenous DNA damages were largely as a consequence of unavoidable hydrolysis and oxidation. The endogenous ROS production is one main source of damage to DNA present in eukaryotes, particularly in aerobic organisms responsible of certain human disease.

Most of the single-base damages are repaired through the base excision repair (BER) pathway that is initiated by members of the DNA glycosylase family (**Barnes DE et Lindahl T., 2004**).

The DNA glycosylases are responsible for initial recognition of the lesion. They flip the damaged base out of the double helix, and cleave the N-glycosidic bond of the damaged base, leaving an apurinic/apyrimidinic (AP) site. (***Figure 23***) There are two categories of glycosylases: monofunctional glycosylases have only glycosylase activity, whereas bifunctional glycosylases also possess AP lyase activity.

Therefore, bifunctional glycosylases can convert a base lesion into a single-strand break without the need for an AP endonuclease. In human cells, oxidative pyrimidine lesions are generally removed by hNTH1, hNEIL1, or hNEIL2, whereas oxidative purine lesions are removed by hOGG1. At least 11 distinct mammalian DNA glycosylases are known.

One example of DNA bifunctional glycosylases is OGG1 that recognizes 8-oxoG paired with cytosine in DNA. Similar fonction was identified in *Escherichia coli* as MutM (Fpg) (**van der Kemp PA. et al., 1996**).

BER initiated by a DNA glycosylase leaves an abasic site. Depending on the numbers of nucleotides eliminated (short or long excision), BER will progress either by short-patch repair or long-patch repair using different proteins in each mechanism (**Krokan HE et al., 2013**).

After glycosylase intervention, the protein AP endonuclease (APE1) cleaves the AP site to yield a 3' hydroxyl adjacent to a 5' deoxyribosephosphate. This excision can be carried out by bifunctional glycosylases like OGG1.

In order to facilitate ligation 3'-5' ends, the empty DNA zone is completed by the DNA Polymerase. The Pol β is the main human polymerase involved in short and long-patch BER. In short-patch pathway, BER ligation is permitted by DNA ligase III that catalyzes, in presence of two partners XRCC1 and Poly ADP ribose polymerase 1 (PARP1), the nick-sealing step.

For the long-patch pathway, DNA ligase III is replaced by DNA ligase I (**Rice PA., 1999** ; **Braithwaite EK et al., 2005**).

. Also the ***Figure 23*** illustrates short-patch and long-patch BER pathways in the nucleus and mitochondria.

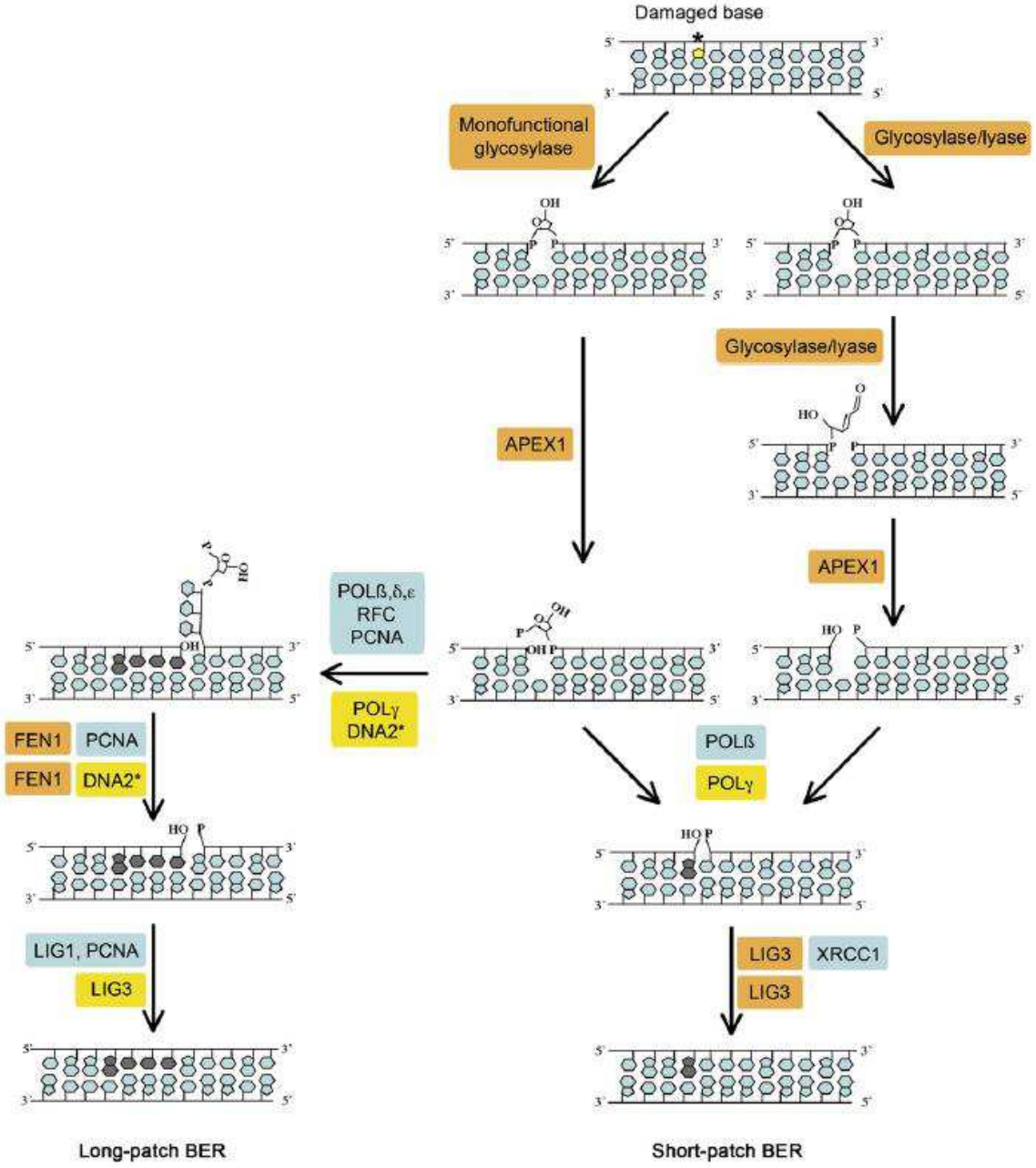

Figure 23*: Short-patch and long-patch BER pathways in the nucleus and mitochondria of mammalian cells. The major factors involved are highlighted. Factors common to both compartments are displayed with an orange background, factors specific for the nucleus are on a blue background and factors specific for mitochondria are on a yellow background. *DNA2 is present in the nucleus but its putative role in nuclear BER is not clear so far. APEX1, AP endonuclease; POL* β, δ, ε, γ, *DNA polymerase* β, δ, ε, γ; *RFC, replication factor C; PCNA, proliferating cell nuclear antigen; DNA2, endonuclease/helicase; FEN1, flap endonuclease 1; LIG1, LIG3, DNA ligase 1, 3; XRCC1, X-ray crosscomplementing protein-1(****Boesch P. et al., 2011****).*

As guanine oxidized (8-oxoG (GO)) ***Figure 24*** appears structurally close to thymine, DNA polymerase introduces adenine in complementary DNA strand. This Adenine: 8-oxo-G mispair is proficiently recognized by the MutY glycosylase homologue (MUTYH). If Adenine is removed by MUTYH, the BER will proceed, the DNA will be repaired. If unrepaired, a new mutation is created.

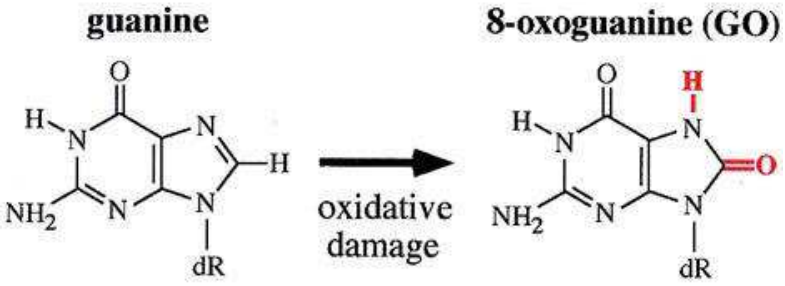

Figure 24*: Schematic representation oxidative damage of guanine.* *http://mol-biol4masters.masters.grkraj.org/html/DNA_Damage_And_Repair2-Types_of_Damages_and_Effects_files/image030.jpg*

The ***Figure 25*** shows the various repair mechanisms observed for 8-oxo-G following ROS attack leading to the formation of C: 8-oxo-G base pairs:

Left column: These can be recognized by OGG1, which excises the 8-oxo-G and incises there sulting AP-site by β-elimination, giving rise to a 3'ddR 5P and a 5'P residue. This 3' sugar phosphate is then removed by APE1, yielding in a 1 nucleotide gap with a 3'OH and a 5' P. Subsequently, pol β catalyzes the insertion of a G opposite the templating C in this SP-BER pathway, and ligation by XRCC1/DNA ligase I leads to restoration of an intact, correctly base-paired double-stranded DNA again. Middle column: If the C: 8-oxo-G base pairs are not recognized before S-phase by OGG1, or they arise through oxidation in S-phase, the replicative pols will often incorporate a wrong A opposite8-oxo-G, giving rise to A: 8-oxo-G mispairs. If these are not corrected, another round of replication will lead to a CG→AT transversion mutation. Right column: The A: 8-oxo-G base pairs can be recognized by MUTYH, which catalyzes the excision of the wrong A from opposite 8-oxo-G, leading to the formation of an AP site. This AP site is further processed by APE1, which results in a 1nucleotide gap with 3' OH and 5' dRP moieties. The incorporation of the correct C opposite

8-oxo-G and one more nucleotide is performed by pol λ in collaboration with the cofactors PCNA and RP-A, thus performing strand displacement of the downstream DNA strand. FEN1 cleaves the 5' flap, leading to a 5'P moiety, which can be ligated by DNA ligase I to yield an intact C: 8-oxo-G containing double-stranded DNA. This C: 8-oxo-G is then again substrate for OGG1-mediated removal of 8-oxo-G (left column) (**Markkanen E, et al., 2013**).

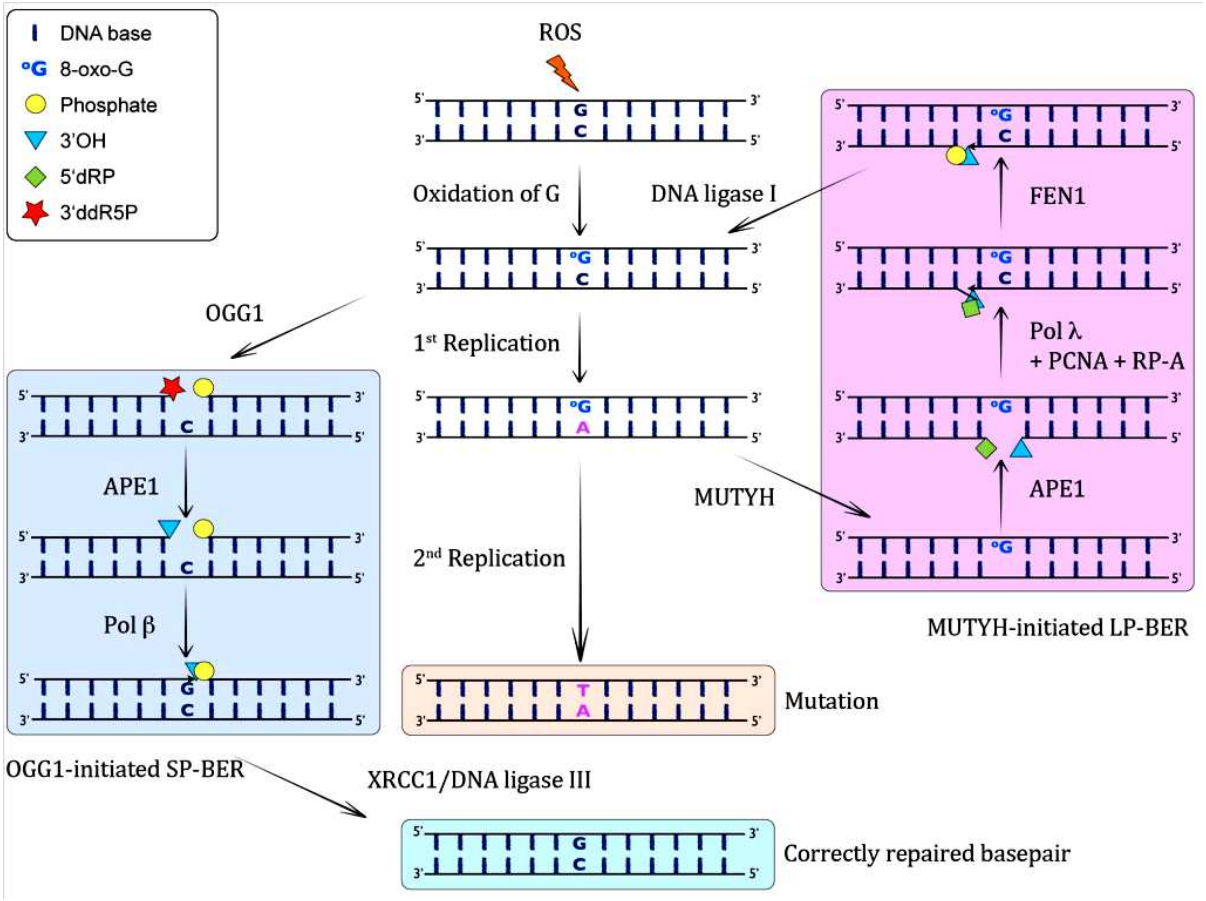

***Figure 25**: MUTYH-initiated BER of A:8-oxo-G lesions(**Markkanen E, et al., 2013**).*

II.2.1.1. BER in mitochondria

In ***Figure 26***, Boesch and collaborators summarized the dialogue between nucleus and mitochondria in mtDNA repair under mitochondrial oxidative stress in human and plants cells.

They schematized how probably post-translational modifications in DNA repair proteins can be involved in mitochondrial damage signals.

One of the more important function of mitochondria is ATP production involved ROS generation and damage of mtDNA repair mechanisms are unclear until nowadays. Due to ROS level in mitochondria BER mechanism remains like one of the more often studied mechanism (**Lopez-Contreras AJ, et Fernandez-Capetillo O., 2012**).

They demonstrated ***Figure 27*** that mitochondrial damage signaling may compete with nuclear damage signaling for the recruitment of monofunctional and bifunctional glycosylases such as UNG1, MUTYH, OGG1, NTHL1, NEIL1 and NEIL2 where most of the BER proteins are also membrane-bound.

The Short-patch BER, by example, is mediated by OGG1 for 8-oxoG repair in coordination with APEX1, the DNA polymerase POL γ and the DNA ligase (LIG3).

Besides, CSB recruits the BER proteins to the membrane; CSA and CSB interact with the single-stranded DNA-binding protein SSB and the glycosylase; the tumor suppressor p53 stimulates the glycosylase and POL γ; PARP-1 modulates BER.

Long patch BER pathway is carried out in addition the endonuclease/helicase DNA2 and the endonuclease FEN1.

The transcription factor and packaging protein TFAM binds with high affinity to damaged DNA; TFAM binding is modulated by p53 and the thioredoxin TRX2 and p53 itself can hydrolyse oxidized nucleotides at DNA $3'$ -ends and the reaction is enhanced by SSB (**Lopez-Contreras AJ, et Fernandez-Capetillo O., 2012**).

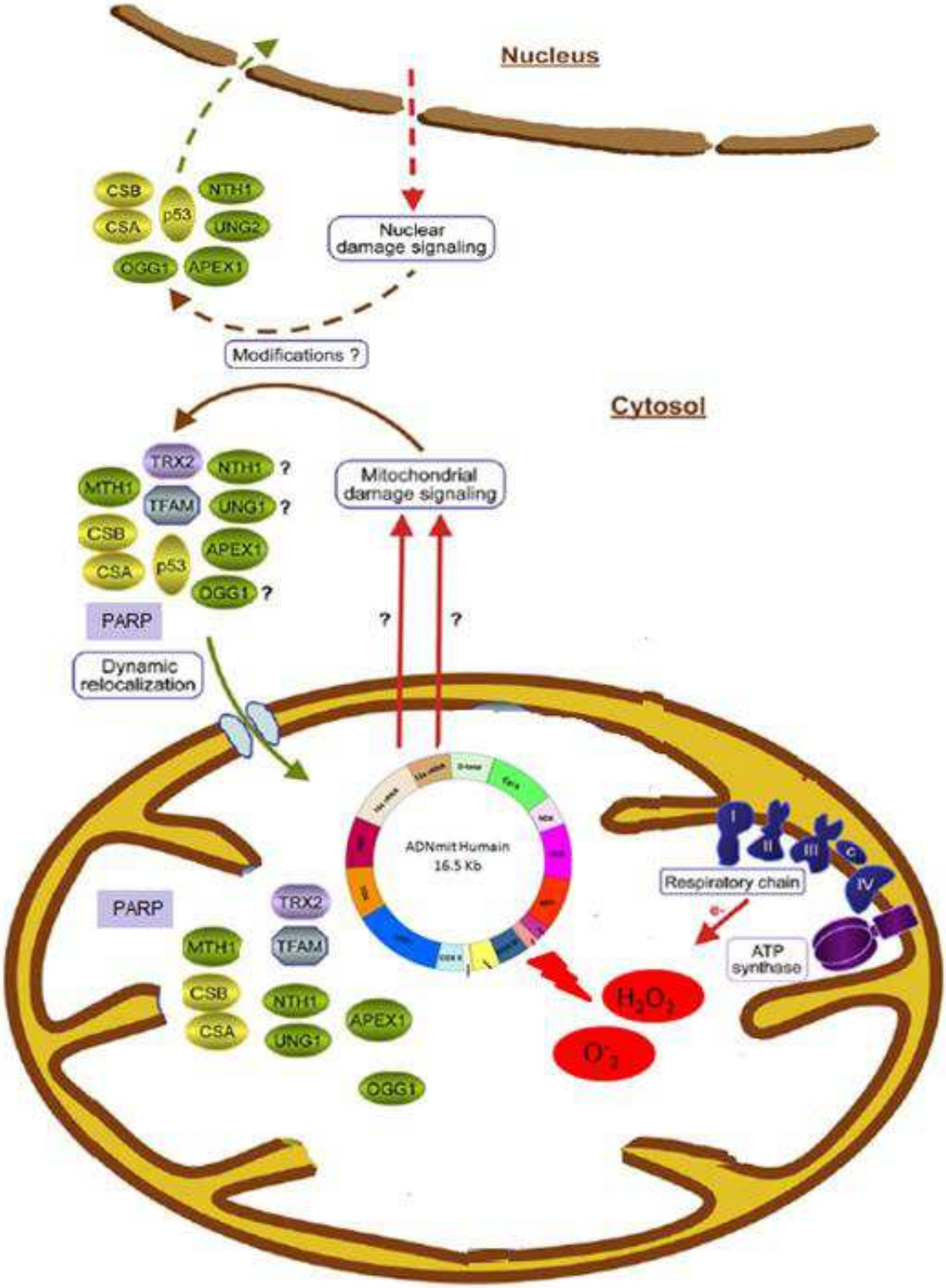

***Figure 26**: Organization of oxidative DNA damage repair processes and factors in mammalian mitochondria, Main repair enzymes are in green; further factors are in yellow or purple; core DNA-interacting proteins are in blue. Modified from (**Boesch P. et al., 2011**).*

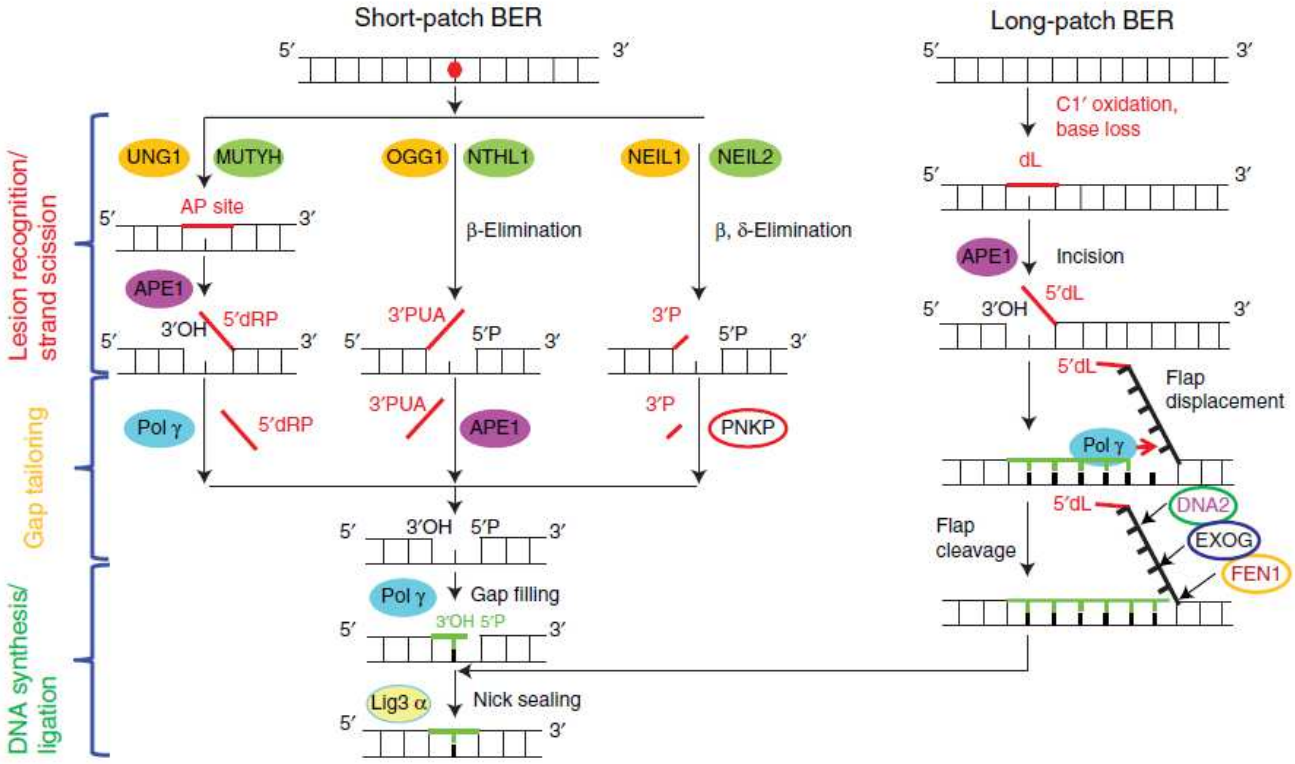

***Figure 27**: Mitochondrial BER in mammalian cells. Three different sub-pathways of SP-BER converge at the gap filling step. SP-BER (left) and LP-BER (right) converge at the nick-sealing step. In addition to FEN1, DNA2 is required for efficient flap processing during LP-BER in mitochondria (**Lopez-Contreras AJ, et Fernandez-Capetillo O., 2012**).*

II.3.2. Single or double strand breaks repair

In mammalian cells single strand break can be repaired by BER mechanism and DSB by Non-Homologous End Joining (NHEJ), and Homologous Recombination (HR), (***Figure 28***) which is only available S and G2 phases when a sister chromatid can be used as a template for the repair reaction (**Lopez-Contreras AJ, et Fernandez-Capetillo O., 2012**).

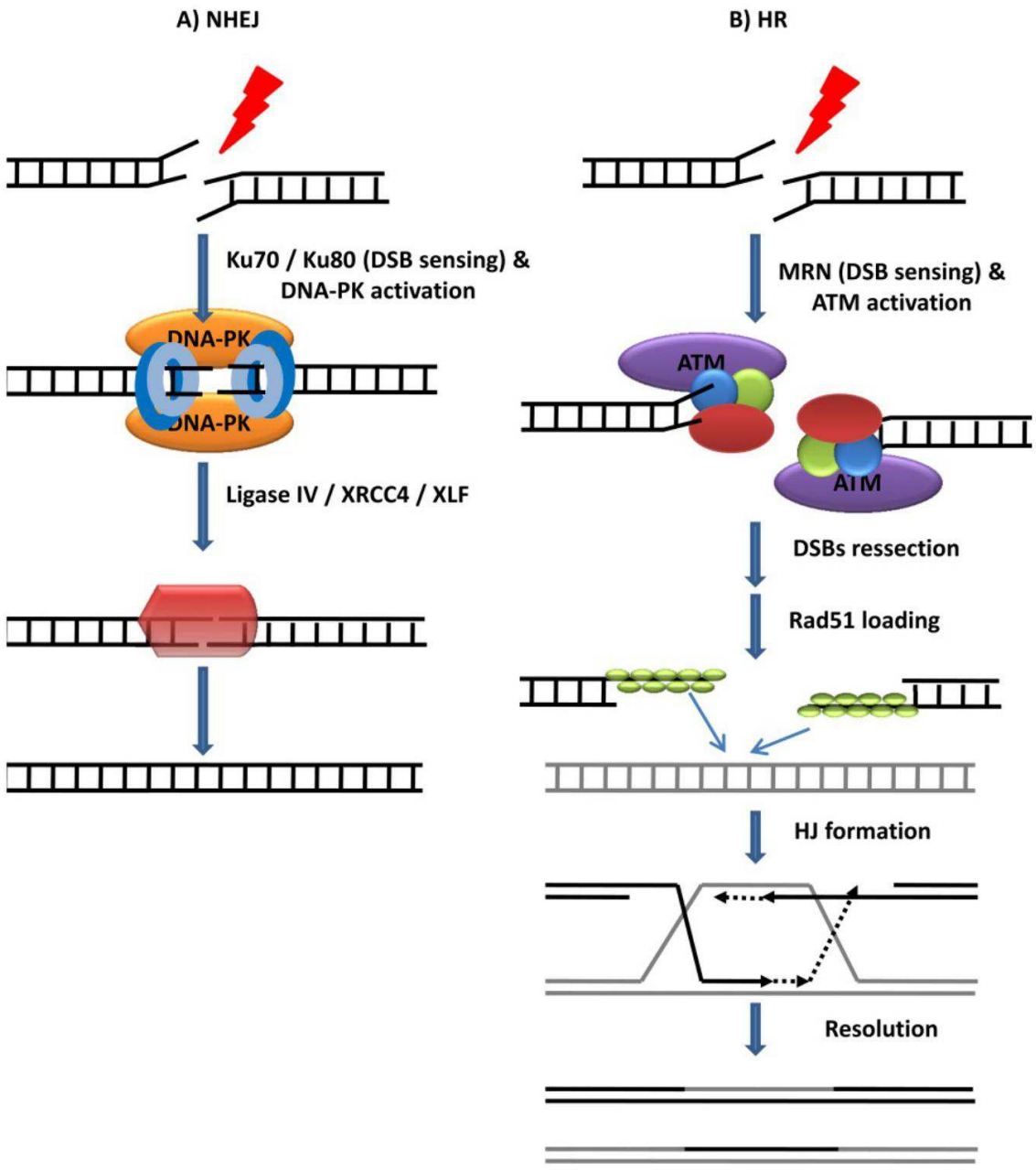

***Figure 28**: Schematic representation of DSBs repair mechanisms. A) NHEJ.and B) HR. Both mechanism are in response to ROS DNA damage. B) HR (**Lopez-Contreras AJ, et Fernandez-Capetillo O., 2012**).*

II.3.2.1. Non-homologous end-joining (NHEJ)

The NHEJ represents the major pathway (concerning HR limitation into cycle cell) for DSBs repair in multicellular eukaryotes involving at least six DNA repair proteins such as: Ku, DNA protein kinases, artemis, polymerase (mu and lambda), XLF: XRCC4 and DNA Ligase IV.

DNA damage as DSBs can be detected by heterodimer Ku70/Ku80 that keeps the right structure of the two DNA ends and guide to DNA-PK recruitment. Consequently, DNA-PK phosphorylates and activates the NHEJ effector complex (ligase IV/XRC44/XLF) that finally religates the broken DNA. The accessory factors are the mammalian polynucleotide kinase (PNK), aprataxin (APTX) and the Polynucleotide Kinaseand Aprataxin-like Forkhead-associated (PALF). (***Figure 29***). This flexibility permits NHEJ to function on the wide range of possible substrate configurations that can arise when double-strand breaks occur, particularly at sites of oxidative damage or ionizing radiations (**Weterings E et al., 2004 ; Lieber MR et al., 2008 ; Lieber MR., 2010**).

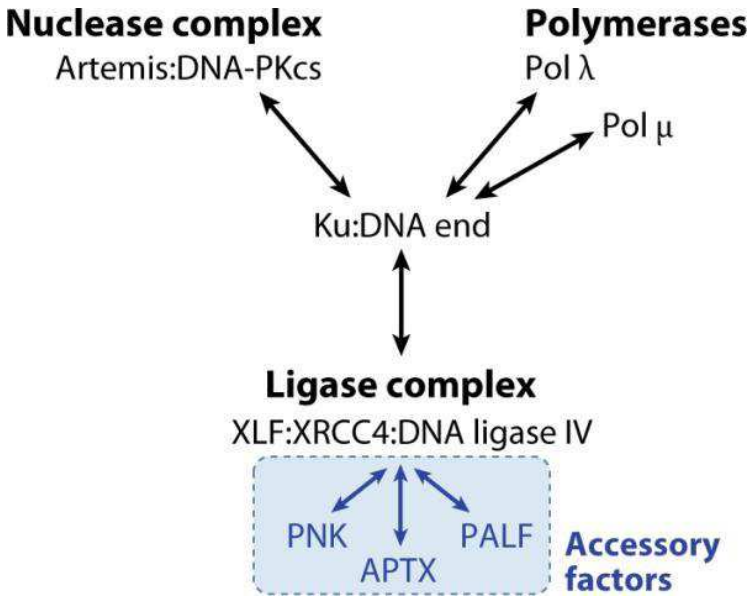

Figure 29*: Interactions between NHEJ proteins. Physical interactions between NHEJ components are summarized* (**Rooney S, et al., 2004**).

DSB repair by NHEJ is associated with limited or extensive additions or deletions of nucleotides at the generated junction, which alters the original DNA sequence at the damaged site. In addition, it is notable that vertebrates have extended their pool of end joining activities with the protein kinase DNA-dependent (DNA-PKcs), which play a role in this shift from HR to NHEJ (**Mladenov E et Iliakis G., 2011**).

Nevertheless DSB can be repaired throughout the cell cycle by non-homologous end joining (NHEJ) or microhomology mediated end joining (MMEJ), which repair breaks regardless of DNA sequence and therefore are error prone. In NHEJ DNA ends are ligated

directly, sometimes after trimming by nucleases or filling in by polymerases. NHEJ is initiated by the binding of Ku70/80, which recruits downstream factors including DNA-PKcs and Artemis. Ligation of ends is carried out by the XRCC4–LigaseIV complex. In some circumstances one or more of the broken ends is refractory to Ku mediated NHEJ. In this case repair can proceed by nucleolytic processing and resection of the 3-end until a short region of complimentary bases is revealed (in blue). Pairing of this microhomology stabilizes the broken ends, displaced flaps are removed (by Fen1 or Rad1/Rad10) and ligation can occur (**Hiom K., 2010**).

II.3.2.2. Homologous recombination (HR)

Homologous recombination is a universal process, conserved from bacteriophage to human, which is important for the repair of double-strand DNA breaks. The general process is as follow : the free ends of a DSB are first processed by an exonuclease. The ATM kinase is recruited to DSB via an interaction with the MRN (Mre11-Rad50-Nbs1) complex. Once at the break, ATM that becomes activated, phosphorylating multiple substrates. In a reaction that depends in multiple endo and exonuclease activities. The exposed 3' ssDNA tails are coated by single-strand DNA binding proteins (SSBs) to prevent the formation of secondary structures. The recombination mediator, (not show in figure) Rad52 then displaces SSB and recruits the Rad51/RecA-type recombinase to form presynaptic helical nucleoprotein filaments. These filaments then initiate homology search and catalyze ATP-dependent strand invasion within duplex DNA templates. The invading strand provides a free 3' end for priming DNA replication that allows the restoration of genetic information missing from the dsDNA breaks. The Rad52 protein has a second function in this pathway, which is to capture the second end through its single-strand annealing activity. After DNA synthesis and ligation, double Holliday junctions are formed.

The Holliday junctions can be resolved by different molecular strategies with or without DNA strand crossover. Without the capturing of the second end by Rad52, the invading strand may be dissociated from the D-loop and reannealed to the ssDNA on the second end, a process known as synthesis-dependent strand annealing (**Chen XJ., 2013**).

Recently studies reveal a recombination protein of likely bacteriophage origin in mitochondria and support the notion that recombination is indispensable for mtDNA integrity (**Mbantenkhu M, et al., 2011**).

II. 4. DNA repair in mitochondria

From 1974 Clayton and collaborators show that mitochondria are unable to repair pyrimidine dimers and some types of alkylation damage (**Miyaki, et al., 1977**). Several years took for discovery of mitochondrial BER (**Pettepher, et al., 1991**). Recently Gredilla 2010 and Boesch and collaborators in 2011 proved that DNA repair mechanisms are present in nucleus but are also in mitochondria illustrating different pathways which need further confirmation with a hatched background. Just the Nucleotide Excision Repair (NER) pathway was not detected in mitochondria. Nevertheless Homologous recombination (HR) and Non-homologous end-joining (NHEJ) were associated with Double Strand Break Repair (DSBR) of mtDNA. The ***Figure 30*** shows the DNA repair pathways highly conserved among nucleus and mitochondria (**Wilson S, et al., 2012**). The ***Figure 31*** shows a possible PARP action in strand break with blocking groups at one or both exposed ends is unable to be repaired by simple short patch-BER.

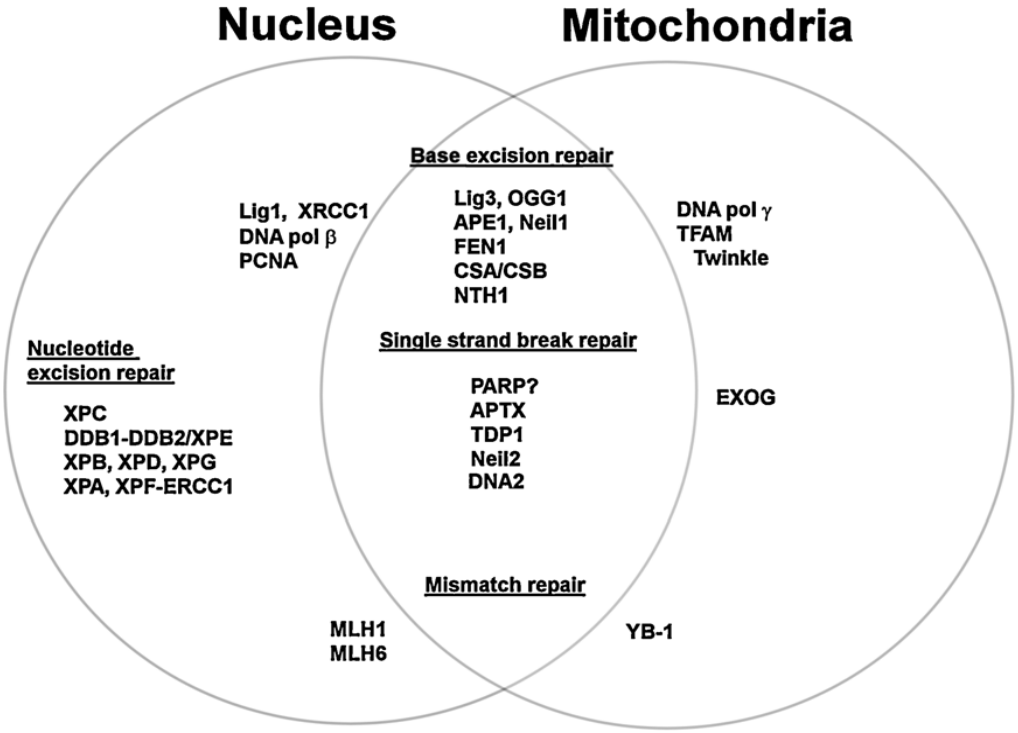

Figure 30*: Nuclear and mitochondrial DNA repair shares common proteins. However not all nuclear DNA repair pathways are present in the mitochondria. BER proteins, isoforms of nuclear relatives (**Wilson S, et al., 2012**).*

The detection method may influence the type of lesion processing, either damage reversal, if a specific enzyme such as APTX or TDP1 is able to resolve the lesion, or damage excision, a more generic pathway that excises the DNA damage using the long patch-BER pathway.

In the mitochondria long-patch BER dependant multi nucleotide excision appears to be driven by EXOG as part of an APE1 complex however the presence of FEN-1 and DNA2 in the mitochondria suggests a secondary long patch-BER pathway, potentially to excise lesions resistant to EXOG activity. After the lesion has been resolved nucleotides are inserted by polymerase γ □□□ □□□□□□□□**Wilson S, et al., 2012**).

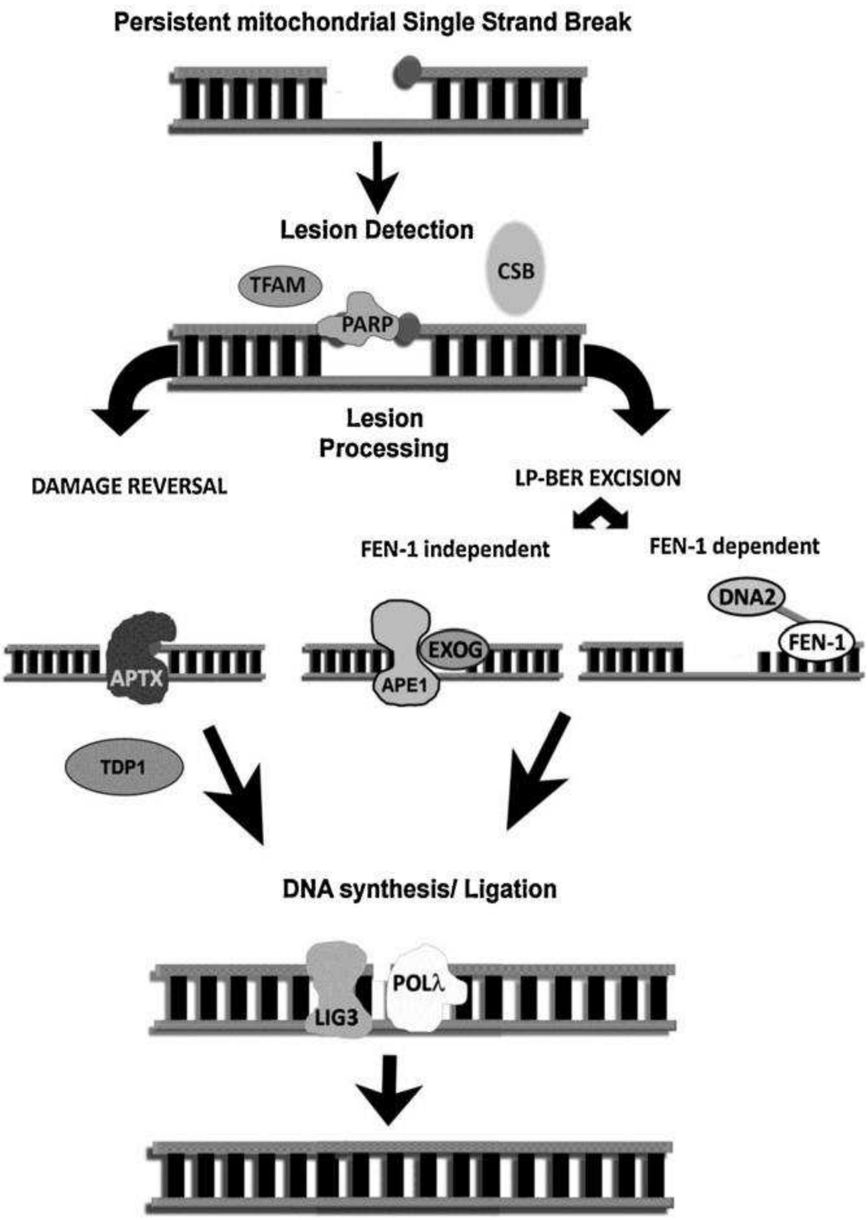

***Figure 31**: Resolution of persistent mitochondrial single strand breaks (**Wilson S, et al, 2012**).*

a). Proteins involved in mtDNA strands breaks repair

The ***Table 4*** illustrates some proteins involved in mtDNA recombination pathways in yeast, mammalian and plant. In 2008, our group demonstrated that bleomycin-induced DSB were efficiently repaired in *Drosophila* mitochondria using S2 cells, with a comparable rate to that was observed for nuclear repair (**Morel F et al., 2008**).

Organism and protein	Molecular function	Mutant phenotype on recombination
Yeast		
Abf2	high-mobility-group	Increases Holliday junctions,
	protein primarily for mtDNA packaging	reduces repeat-mediated recombination
Exo5	5'-3' exonuclease	Unknown
Hmi1	3'-5' DNA helicase	mtDNA fragmentation
Mgm101	Single-strand annealing protein	Decreases repeat-mediated recombination
Mhr1	Homologous pairing in vitro	Decrease gene conversion
MRX complex	5'-3' exonuclease	Decrease repeat-mediated recombination
Msh1	Mismatch repair-like protein	Increases repeat-mediated recombination
Nuc1	Endo/exonuclease	Decreases mtDNA recombination
Pif1	5'-3' DNA helicase	Reduce recombination in p+ x p- crosses
Rim1	Single-strand annealing	Suppresses pif1 mutation

Table 4*: Proteins known to affect DNA recombination in yeast, mammalian, and plant mitochondria (****Chen., 2013****)* .

Normally, the Yeast Mgm101 protein (***Figure 32***) is involved in single-strand annealing but in response to oxidative stress or to other signals which generate dsDNA breaks, Mgm101 can be involved in dsDNA breaks repair pathways in mitochondria (**Chen., 2013**).

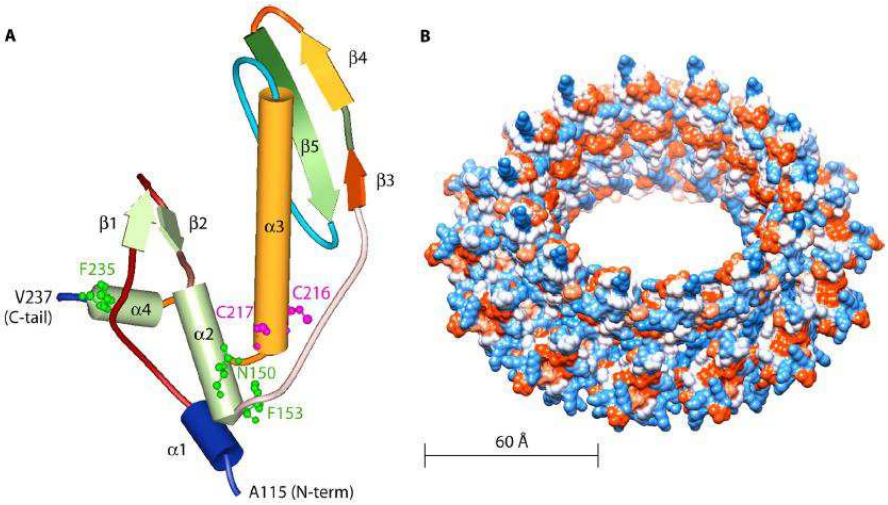

***Figure 32**: Molecular modeling of the Mgm101 core domain (from A115 to V237) based on the Rad52 structure (1H2I). (A) The positions of N150, F153, and F235, which are highly conserved in Rad52-related proteins, are highlighted. Also indicated are C216 and C217, which form a putative redox sensor for regulating Mgm101 function. (B) Surface representation model of a 14-mer ring formed by Mgm101115-237 (**Chen., 2013**).*

The ***Figure 33*** shows that Mgm101 can be activated by ROS and guide mitochondria to repair mtDNA by pathways such as HR and NHEJ (**Chen., 2013**).

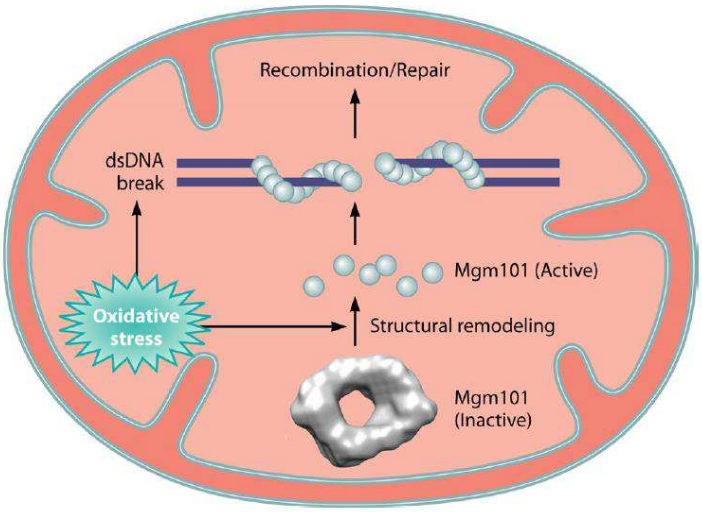

***Figure 33**: A model for activation of Mgm101 in mtDNA repair. The Mgm101 rings are proposed to be the storage form of the protein in mt-nucleoids. In response to oxidative stress or other signals, the C216/C217 cysteine pair is modified. This may induce structural remodeling in the rings, which stimulates ssDNA binding and the repair of dsDNA breaks (**Chen., 2013**).*

The ***Figure 34*** shows the gene duplication that occurred before the divergence of archaea and eukaryotes giving rise to two lineages, *RADα* and *RADβ*, *recA* has remained as a single-copy gene. In eukaryotes, both *RADA* and *RADB* genes experienced several duplication events, but, in *archaea*, they remained as single-copy genes.

Eukaryotic *recA* genes originated from proteobacteria (*recAmt*) and cyanobacteria (*recAcp*) *recA* genes after two separate endosymbiotic events. *recAmt*s were subsequently lost in the ancestors of animals and fungi (**Lin Z. et al., 2006**).

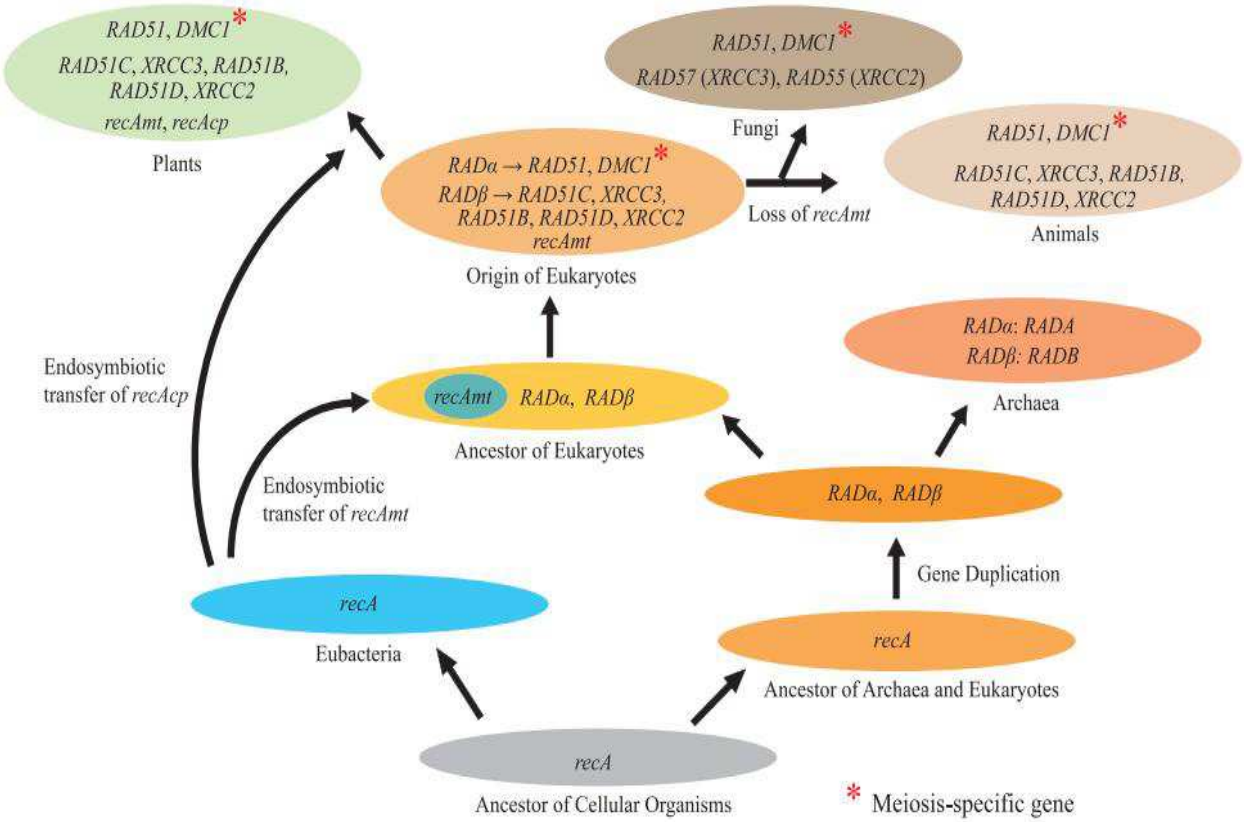

Figure 34*: A model of the evolutionary history of recA/RAD51 gene family (**Lin Z.et al., 2006**).*

II.5. DNA repair and pathologies

II.5.1. BER and cancer

Disorders in DNA repair pathways lead to cancer predisposition, predicting that shut of BER efficacy could contribute to the development cancer diseases. Indeed, somatic mutations

in Pol β have been found in 30% of human cancers (**Starcevic D, et al., 2004**). Mutations in the DNA glycosylase MYH are also highly implicated to colon cancer (**Gryfe R., 2009**).

Genetic variations of APE1 have been shown to influence an individual's susceptibility to carcinogenesis. Also, the genetic polymorphisms of APE1 are associated with the risk of renal cell carcinoma (**Cao Q, et al., 2011**) and with breast cancer progression (**Kang H. et al., 2013**).

Recently, it was published the genetic polymorphisms of OGG1 associated with pancreatic and colorectal cancer risks (**Chen H. et al., 2013 ; Su Y, et al., 2013**).

II.5.2. HR, NHEJ and cancer

Heat shock is an effective radiosensitizer. A combination of heat with ionizing radiation (IR) is one of the more frequent strategies in the treatment of human cancer. Heat exposure causes extensive death of irradiated cells. DNA double strand breaks (DSBs) are the main cause for IR-induced cell death. For this reason, inhibition of DSB processing has long been considered a major candidate for heat radiosensitization. However, it has been shown that radiosensitization of mutants with defects in DSB repair failed to find a relation between DSB repair pathway and radiosensitization (**Iliakis G., et al., 2008**).

Pancreatic ductal adenocarcinoma (PDAC) is one of the major causes of death in human's cancers. PDAC is extremely resistant to currently available therapeutics. PDAC harbors high levels of spontaneous DNA damage. Inhibition of NHEJ repair results in further accumulation of DNA damage, growth inhibition and apoptosis even without DNA damaging agents. In response to radiation, NHEJ pathway rapidly repairs DNA double strand breaks in PDAC cells. Because of that, inhibition of NHEJ has been considered into PDAC therapeutic approaches (**Li YH et al., 2012**).

II.5.3. NHEJ and immunity

XRCCA-like factor (XLF) plays a fundamental role nonomologous end joining DNA double-strand break repair (NHEJ). This system is required to repair DNA break occurring during lymphocyte development. Mutations in XLF cause a progressive lymphocytopenia. It has been reported that XLF-deficient murine cells show no detectable defects in Variable, Diverse, and Joining (V(D)J) recombination.

In contrast with the moderate role of ATM kinase and its H2AX substrate for V(D)J recombination in WT cells, it has been reported that both factors become essential in XLF-deficient lymphocytes. p53-binding protein 1 (53BP1) is also involved in ATM. 53BP1 deficiency causes a small reduction of peripheral lymphocyte number. The severe defects in end joining are carries out during chromosomal V(D)J recombination. V(D)J recombination which is required for lymphocyte development, is initiated by introduction of DNA double-strand breaks.

This is catalyzed by the RAG endonuclease and occurs between the conserved recombination signal sequences (RSS) and the participating germ-line V, D, or J gene segments. After, ubiquitously expressed NHEJ factors join the two 5′ -phosphorylated blunt signal ends forming a coding join (CJ) (**Rooney S.et al., 2004**). The heterodimer KU70-KU80 (KU86 in human) directly binds DSB ends, recruits and activates other NHEJ factors. DNA-KU complex activates the endonuclease function of Artemis for end process during V(D)J recombination (**Lieber., 2010**).

Finally a complex including ligase 4 and XRCC4 factor ligates the ends together. Although XLF binding to XRCC4 was known, its exact function needs to be elucidated (**Ahnesorg P, et al., 2006 ; Buck D et al., 2006 ; Andres SN. et al., 2007**).

As C-NHEJ is essential for V(D)J recombination, defects in previous characterized NHEJ factors completely block lymphocyte development at the progenitor stage and also cause T^- and B^- severe combined immunodeficiency (T^-B^-SCID) in both human and mouse models (**Rooney S. et al., 2004 ; Lieber., 2010 ; Li G. et al., 2008**). XLF mutations cause a less severe lymphocytopenia than SCID in human patients. In the case of XLF-deficient mice, the lymphocytes numbers are reduced with not stage-specify blockade. In agreement, chromosomal V(D)J recombination occur normally in XLF-deficient lymphocyte but not in XLF-deficient murine embryonic stem cells. This observation suggested that more than one repair pathway(s) might exist in developing lymphocytes to compensate XLF deficiency during V(D)J recombination (**Lieber., 2010**).

Recently, it has been reported that chromosomal V(D)J recombination in XLF-deficient lymphocytes requires ATM and its kinase activity (**Zha S. et al., 2011**) ATM kinase is a master regulator of the DNA damage response. Although ATM promotes efficient DNA repair during CJ formation (**Bredemeyer A L et al., 2006**), ATM is not required for V(D)J recombination and lymphocyte development (**Barlow C et al., 1996**).

Additionally, it was demonstrated that blockade of IgG in bladder cancer cell T24 resulted in up regulation of cleaved caspase-3 and cleaved poly(ADP-ribose) polymerase (PARP) (**Liang PY, et al., 2013**). The Poly(ADP-ribosyl)ation is considered a reversible post-translational protein modification and is involved in the regulation of a number of biological functions such as: maintenance of genomic stability, transcriptional regulation, energy metabolism, centromere function, telomere dynamics, mitotic spindle formation during cell division, concluding, poly(ADP-ribosyl)ation is involved in aging and cell death **(Aguilar-Quesada R. et al., 2007 ; Lee HH et al., 2013)**.

III.1. Poly(ADP-ribose) metabolism

The metabolism of Poly(ADP-ribose) is a dynamic process mediated by ARTs and poly(ADP-ribose) glycohydrolase (PARG) enzymes (**Bonicalzi ME et al., 2005**). Polymers with chain lengths about 200 ADP-ribose units are rapidly degraded by PARG poly(ADP-ribose) and / or ADP ribosyl-acceptor hydrolase (ARH3) (**Isabelle M et al., 2010**).

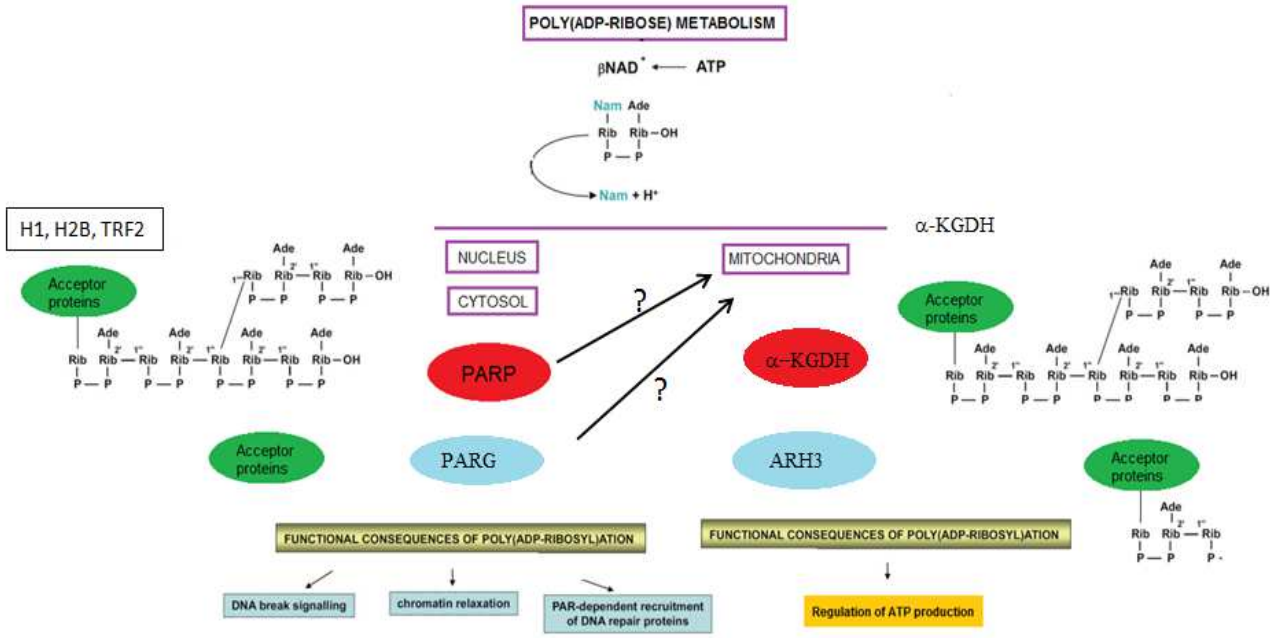

***Figure 35**: Poly(ADP-ribosyl)ation reaction activated by DNA strand breaks. PARP-1 and PARP-2, rapidly recognizes DNA-strand breaks generated by genotoxic agents leading to their activation (**Yelamos J et al., 2011**).*

The ***Figure 35*** shows the Poly(ADP-ribosyl)ation regulation reversed by the activities of poly(ADP-ribose)polymerase PARP and poly(ADP-ribose) glycohydrolase (PARG) in

nucleus and ADP ribosyl-acceptor hydrolase (ARH3) and □KGDH in mitochondria (**Pankotai E, et Lacza Z., 2009**).

In nucleus the proteins targeted such as H1, H2B and TRF2 are involved in numerous biological processes, including DNA repair, chromatin structure and transcription. Poly(ADP-ribosyl)ation of acceptor proteins has functional consequences such as DNA-break signaling, chromatin relaxation and recruitment of DNA repair proteins (**Yelamos J et al., 2011***)*.

Recently, in order to clarify the Poly(ADP-ribose) metabolism, using siRNA in PARG knock-down it was shown that the poly(ADP-ribosyl)ation of proteins in the cells was lost, revealing that PARP1 expression and activity is involved with PARG expression in knockdown cells. (**Uchiumi F, et al., 2013**)

Thus, poly(ADP-ribose) in a cell is regulated under the control of PARP1/PARG gene expression balance. Structural and enzymological evidences of PARP family lead to propose a new consensus nomenclature for all ADP-ribosyltransferases (ARTs) based on the catalyzed reaction and on structural features. ARTs members are classified in two big subfamilies such as: the DNA-dependent PARPs, (PARP1, PARP2 and PARP3) and the tankyrases (**Hottiger MO et al., 2010**).

From the 18 member of ARTs described (***Figure 36***), PARP-1 accounts for more than 90% of the poly(ADP-ribosyl)ating capacity of the cells The domains of each member are indicated: According to protein sequence from NH2 to COOH terminal in PARP1 The ART domain is the catalytic core required for basal ART activity. The WGR domain named after a conserved central motif (W-G-R) is also found in a variety of polyA

The PARP regulatory domain (PRD) might be involved in regulation of the PARP-branching activity. polymerases and in proteins of unknown function. The sterile alpha motif (SAM), a widespread domain found in signaling and nuclear proteins, can mediate homo- or heterodimerization. The ankyrin repeat domains (ARD) mediate protein–protein interactions in diverse families of proteins. The vault protein inter-alpha-trypsin (VIT) and von Willebrand type A (vWA) domains are conserved domains found in all inter-alpha-trypsin

inhibitor (ITI) family members. The WWE domain is named after three conserved residues (W-W-E), and is predicted to mediate specific protein–protein interactions in ubiquitin- and ADP-ribose conjugation systems. The Macro or A1pp domains are structurally related to the catalytic domain of enzymes that process ADP-ribose-1′-phosphate, a reaction product derived from ADP-ribose 1′-2′ cyclic phosphate generated by Terminal Phosphotransferase (TpT). The Macro domain can serve as ADPr or O-acetyl-ADP-ribose binding module The BRCT domain (BRCA1 carboxy-terminal domain) (**Amé JC, et al., 2004**).

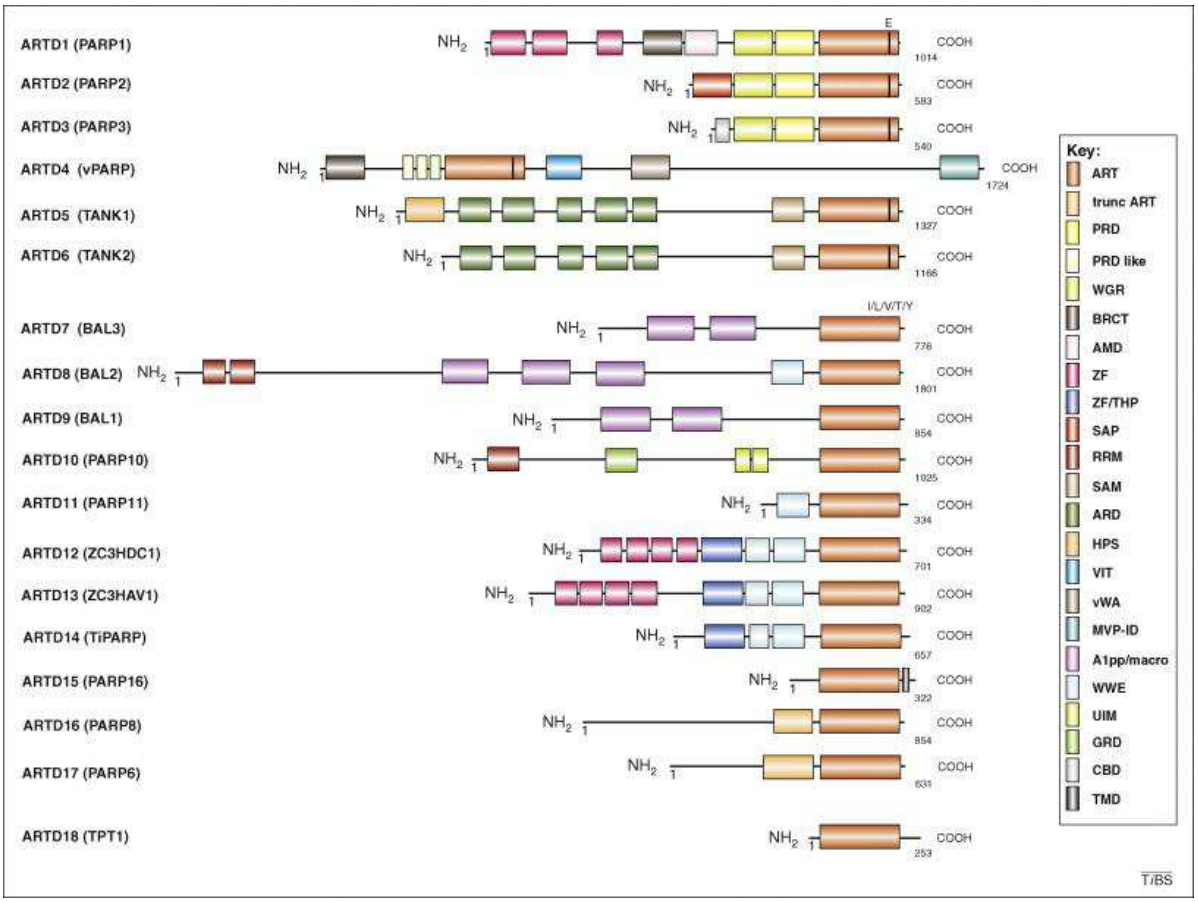

Figure 36*: Schematic comparison of the ARTD (PARP) family. ZF: zinc finger domains. SAP: SAF/Acinus/PIAS-DNA-binding domain, MVP-ID: Major-vault particle interaction domain, NLS: nuclear localization signal. CLS: centriole-localization signal. HPS: Histidine-proline-serine region. RRM is an RNA-binding/recognition motif. UIM: ubiquitin interaction motif. MVP-ID: M-vault particle interaction domain. TPH: Ti-PARP homologous domain. GRD: glycine-rich domain. Within each ART domain, the region that is homologous to the PARP signature (residues 859–908 of PARP1) as well as the equivalent of the PARP1 catalytic E988 is shaded. The WWE domain is a protein–protein interaction motif. TM: transmembrane domain (**HottigerMO et al., 2010**).*

III.2. The structure-function of human PARP-1

The member PARP-1 has been studied most extensively; it is a monomeric enzyme, of 116-kDa highly conserved (**Amé JC, et al., 2004**), (***Figure 37***). This molecule is involved in the polyADP-ribosylation carried out by poly(ADP-ribose)polymerase (PARP) enzymes, of which the first discovered and most important is PARP-1, a very highly abundant nuclear protein found in higher eukaryotes (**Amé JC, et al., 2004**). The main targets for addition of PAR by PARP-1 are histones and PARP-1 itself (**Adamietz P., 1987 ; Poirier GG et al., 1982**). although there are many other targets including HMG proteins (**Tanuma S, et al., 1983**), topoisomerase I (**Krupitza G et Cerutti P., 1989**) and p53 (**Kanai M et al., 2007**).

III.2.1. PARP-1 structure

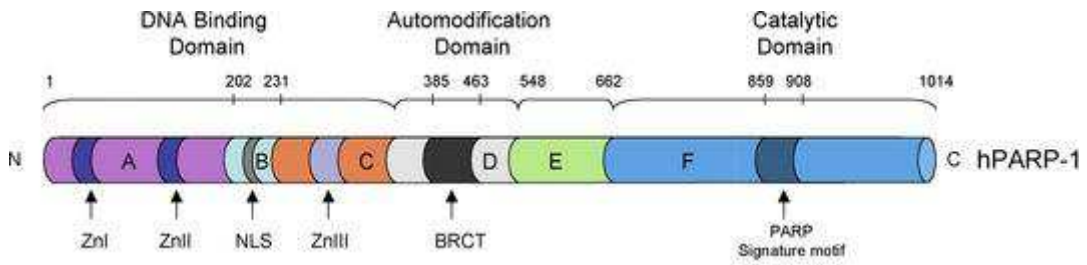

Figure 37*: The domain structure of PARP-1, showing the DNA-binding, the automodification and catalytic domains (domains A–F). The PARP signature sequence (in dark blue within the F catalytic domain) is the most conserved between the PARPs. Zn I and Zn II: Zinc-finger motifs. Zn III: Zinc ribbon domain. NLS nuclear localization signal; BRCT BRCA1 carboxy terminus (**Mégnin-Chanet F, et al., 2010**).*

According with ***Figure 37*** the DNA binding domain contains three zinc finger motifs, the two first enclosing the motif A showed in ***Figures 38 and 39*** by F1 and F2 domains (**Eustermann S et al., 2011**) and the third isolating zinc finger motifs is localized among the motifs B and C. The two first zinc finger domains are responsible for DNA interaction and genome screening, while the third zinc finger domain is involved in PARP-1 dimerisation (**Langelier MF et al., 2008**).

Motif B contains a bipartite nuclear localization signal (NLS) responsible for the nuclear addressing of PARP-1, and also, motif B enclose a caspase3/7 cleavage site (**Eustermann S. et al., 2011**), ***Figures 40 and 41***).

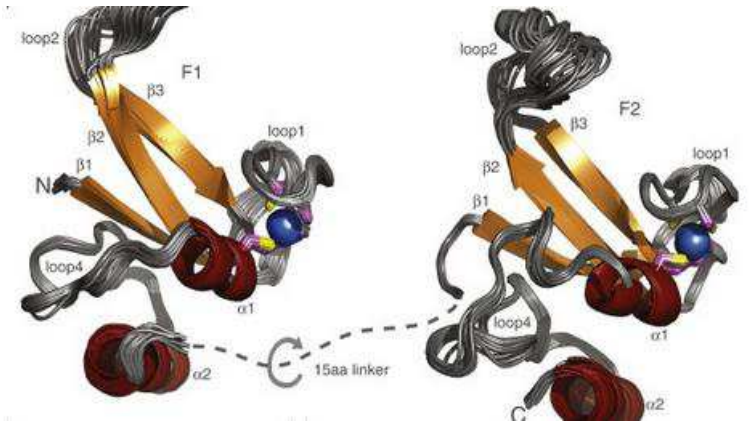

***Figure 38**: Schematic representation 3D of PARP-1 zinc fingers. F1 and F2 were structurally independent. (modified from (**Eustermann S. et al., 2011**)*

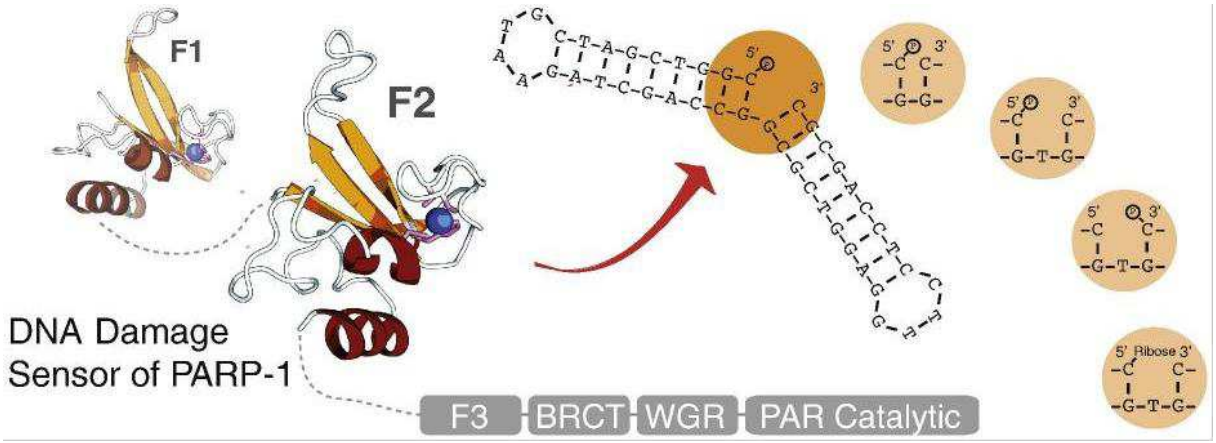

***Figure 39**: PARP-1 fingers F1 +F 2 form a 1:1 monomeric complex with DNA single-strand breaks modified from (**Eustermann S. et al., 2011**).*

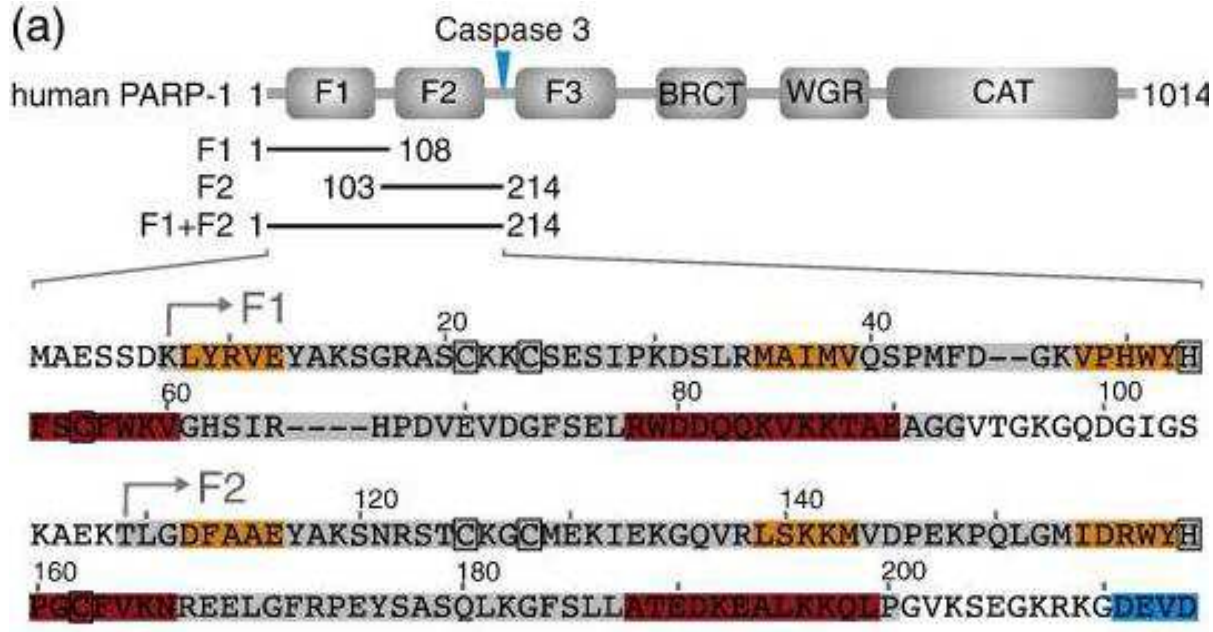

***Figure 40**: (a) Human PARP-1 clevage site. (a) During apoptosis, PARP-1 is cleaved by caspase-3 (common with caspase7) into a 24-kDa and an 89-kDa fragment. (Modified from **Eustermann S. et al., 2011**).*

The automodification domain contains a BRCT, D and E motifs. BRCT motif guides to PARP-1 interaction with similar motif in proteins such as: XRCC1, BRCA-1 and BRCA-2. The catalytic domain with motif F is the smallest PARP-1 fragment retaining catalytic activity. The NAD^+ acceptor sites is named PARP signature motif and it is a sequence of 49 amino acids highly conserved through the evolution (**Elkoreh G. et al.,2012**).

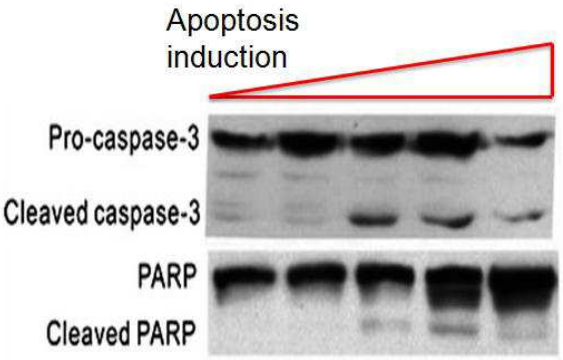

***Figure 41**: Relationship between caspase-3 activation and PARP cleavage during apoptosis (**Liang PY. et al., 2013**).*

III.2.2. PARP-1 in DNA repair

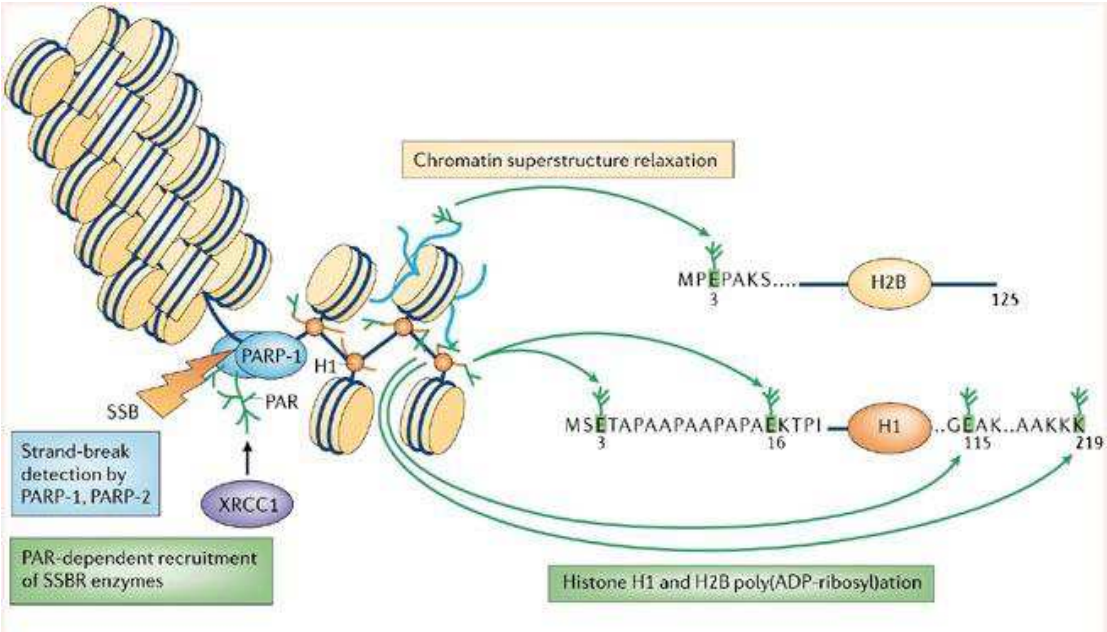

***Figure 42**: Schematic representation of chromatin superstructure relaxation due to PARP action: relationship between SSB and PARP-1 activation. The position of covalent histone-tail poly(ADP-ribosyl)ation is indicated below the sequences of rat histones (**Schreiber V et al., 2006**).*

PARP-1, with the N-terminal two first zinc finger motives, makes genome screening until DNA-nicks detection (**Eustermann S et al., 2011**). This results into auto-posttranslational modification (auto ADP-ribosilation) but also histones poly(ADP-ribosyl)ation.

The ***Figure 42*** shows poly(ADP-ribose) synthesis at the DNA-damage site triggers both the immediate recruitment of the SSB repair (SSBR) scaffold protein XRCC1, but also the relaxation of chromatin superstructure as mediated by poly(ADP-ribosyl)ation of histone H1 and H2. This modification facilitates repair enzymes access to the DNA lesion and interaction with XRCC1.

III.2.3. PARP-1 role in few DNA repair pathways

PARP-1 has a role in SSBs repair. PARP-1 knock down with siRNA or PARP-1 activity inhibition with small molecules reduce SSB repair and the absence of PARP1 increase the quantity of DSBs.

The SSB accumulated is transformed in DBSs as well, HR system can be modulated due to the new level of DBSs, thus PARP-1 can be involved in different mechanisms such as: BER, SSB, NHEJ and HR mechanisms (**Godon C, et al., 2008**).

III.3. The structure-function of PARP-2 ambiguity

PARP-2 was discovered as a result of the presence of residual DNA-dependent PARP activity in embryonic fibroblasts derived from PARP-1-deficient mice (**Shieh WM et al., 1998**).

The crystal structure of the murine PARP-2 is very similar to that of PARP-1, with the difference that PARP-2 hasnot Zinc-finger motifs, (***Figure 43***). This structural difference leads the acceptor site that reflects differences in terms of substrates (**Oliver AW et al., 2004**).

The catalytic domain has the strongest resemblance to that of PARP-1 with 69% similarity. PARP-2 carries out multiple modifications in histone H2B while PARP-1 preferentially makes only one modification in H1(**Poirier GG, et al., 1982**).

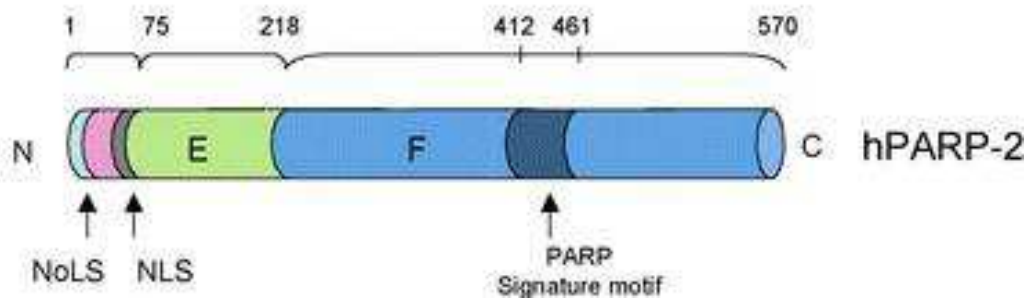

Figure 43*: The domain structure of PARP-2, showing the PARP signature sequence (in dark blue within the F catalytic domain). NLS nuclear localization signal; NoLS nucleolar localization signa (****Mégnin-Chanet F, et al., 2010****).*

PARP-2 whose function is still not clear, acts as a chromatin modifier as mentioned above. PARP-2 interacts with PARP-1 and shares common partners involved in SSBR and BER pathways: XRCC1, DNA polymerase β,□and DNA ligase III. PARP-1 and PARP-2 also interact with proteins involved in the kinetochore structure and in the mitotic spindle checkpoint. Also remodeling of chromatin by PARylating histones and relaxing chromatin structure, thus allowing transcription complex to genes access (**Bürkle A, et al., 2005**).

III.2.2. The structure-function of PARP-3

PARP-3 has been identified as a core component of the centrosome preferentially located at the daughter centriole and interferes with the G1/S cell cycle progression (**Augustin A, et al., 2003**).

Of all ARTs, PARP-3 displays the smallest N-terminal domain with only 54 residues responsible for the centrosomal localization. Besides, PARP-3 shares with PARP-1 two domains, E and F, which display a 61% similarity. Functionally, PARP-3 activity is annulated using the PARP-1 inhibitor (3-aminobenzamide), thus, PARP-3 shares with PARP-1 function in DNA damage surveillance (**Kanai M, et al., 2003**).

Recently, PARP-1, PARP-2 and PARP-3 are characterized as DNA-dependent PARPs with presence of special catalytic domain integrated by histidine–tyrosine–glutamate (H-Y-E) named ¨***catalytic triad***¨ of PARP (**Scarpa ES, et al., 2013**).

III.3. Tankyrases

Tankyrases (ART-5 and 6 in ***Figure 36***) contain large ankyrin domain repeats that mediate protein–protein interactions using a 33-residue sequence motif. This sequence was first

identified in yeast and Drosophila and was named for the cytoskeletal protein ankyrin, which contains 24 copies of this repeat. Subsequently, ankyrin repeats have been found in many proteins spanning a wide range of functions.which facilitate target selection and activation (**Mosavi LK. et al., 2004**).

Tankyrase1 (TRF1-interacting, ankyrin-related ADP-ribose polymerase), ART5 was identified as a partner of the human telomeric protein TRF1 in a two-hybrid screening (**Sbodio JI. et Chi NW., 2002**). Thus, its functions are involved in telomere length regulation in mitotic division (**Hsiao SJ et al., 2008**). Accordingly, Tankyrase-1 (ART-5) and Tankyrase-2 (ART-6) show multiple subcellular localizations such as: telomeres, nuclear pores, pericentriolar material during mitosis, and Golgi complexes. It was hypothesized that tankyrases are involved in energy homeostasis in mammals, thus present in mitochondria (**Yeh TY, et al., 2009**).

III.4. Other PARPs

The TIPARP: containing the TPH domain (Cys-Cys-Cys-His) and Trp-Trp-Glu domain, (***Figure 36***) which can exhibit PAR-binding activity (**Katoh M, et Katoh M., 2003**).

The macroPARPs: containing macrodomain folds, which are ADP-ribose-binding modules that can facilitate the localization of these ARTs to sites of poly and mono(ADP-ribosyl)ation (**Gibson BA et Kraus WL., 2012**).

III.5. PARPs inhibitors

PARP-1 has been the target for design of PARP inhibitors. These have been claimed to have applications in the treatment of many disease including cancer, inflammations and retroviral infection. It must made some questions concerning to PARP-1 inhibitors before their use in treating of human diseases.

These questions are related to chemical properties of the inhibitors, specificity, including isoforme-selectivity. Another question concerns the fact that different diseases may require therapeutic PARP-1 inhibition to be either short-term or chronic. The answers to these questions could determine the future of disease therapy through inhibition of PARP (**Woon EC et al., 2005**).

The ***Figure 44*** shows different DNA repair pathways involving PARP inhibitor action. The PARP inhibition can perturb highly the HR mechanism.

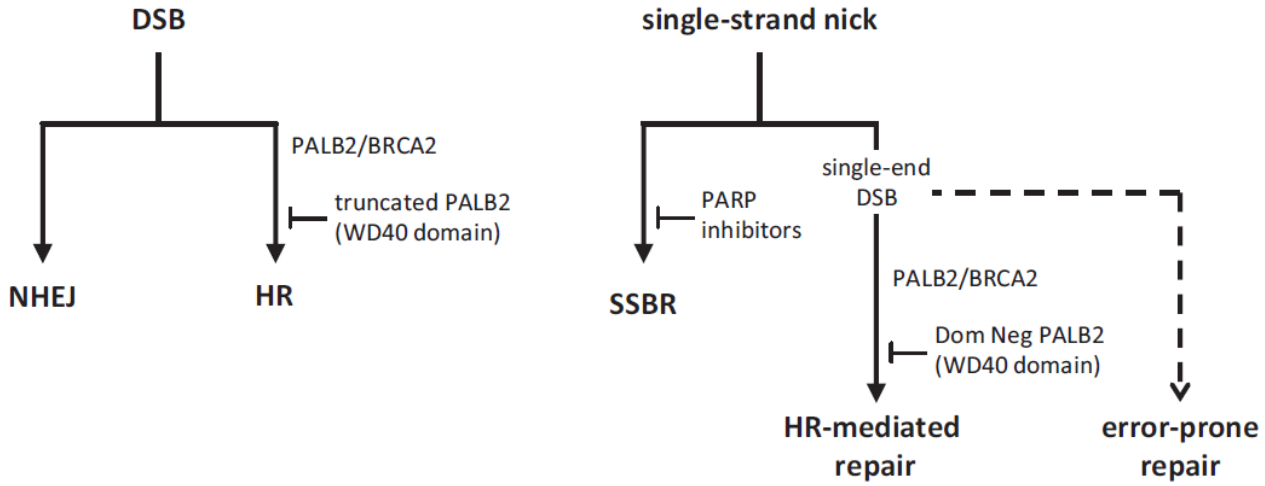

Figure 44*: Model of PARP inhibitors action in single strand nick. PARP inhibitors and truncated PALB2 pathway leads to error prone repair of DNA.(**Metzger MJ, et al., 2013**).*

PARP inhibitors increased the rate of nick-induced HR. Additionally, expression of the PALB2 (partner and localizer of BRCA2 with synergistically function with a BRCA2) revealed an alternative mutagenic repair pathway for nicks. When PARP inhibitors were added both DNA damages (SSBs and DSBs) are using in a common pathway NHEJ when PALB2 mechanism is truncated and/or.(**Metzger MJ, et al., 2013**).

The use of ABT-888 (platinum drugs for cancer therapy) associated with PARP inhibitors in the same treatment can increase mutation risk and cancer rate in murine model. In this model, it was demonstrated that pharmacological inhibition of PARP-1 led to NHEJ driven repair mechanisms (**Southan GJ et al., 2003**).

Recently, PARP inhibitors combined with cytotoxic chemotherapeutic agents in the treatment of BRCA-1/2 deficient cancers are in the clinical development. PARP inhibitors can be applied with other anticancer agents in clinical trials since them maybe playing anti-inflammatory role (**He YJ et al., 2013**).

III.6. PARP in mitochondria

Of all ARTs only PARP-1 was detected into mitochondria in HeLa cells thanks to internalization by mitofilin receptor present in IMM (**Rossi et al., 2009**). Knockdown of mitofilin in HeLa cells with siRNA led to disorganization IMM and Cyt c redistribution linked with intrinsic apoptotic induction. Thus, mitofilin plays important functions in cristae remodeling and controls Cyt c release during apoptosis (**Rui-Feng Yang et al., 2012**).

IV.→. DNA repair mechanisms in *Drosophila*

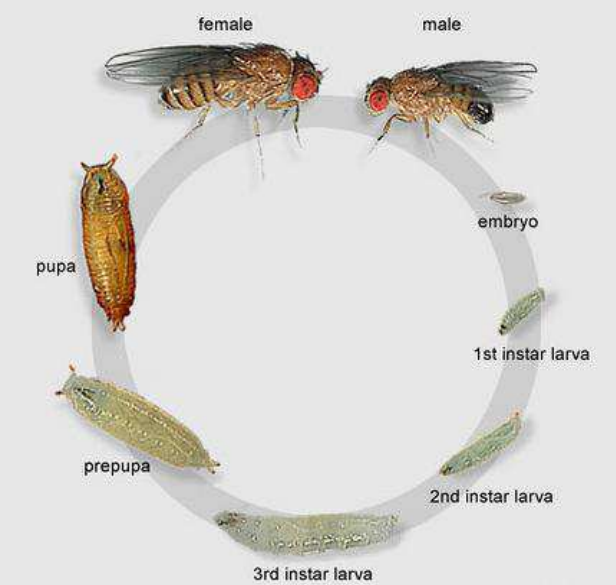

Figure 45*: Schematic representation of Drosophila melanogaster life cycle.*
http://www.flickr.com/photos/11304375@N07/2993342324/

Drosophila melanogaster genome is very well known and some genetic mutation can be visibly manifest as morphological changes in the adult animal as eyes color. It is easily cultured population of the wild, (***Figure 45)***, has a short generation time, and also large number of mutant animals are readily obtainable.

The Poly(ADP-ribose) metabolism

In *D. melanogaster*, PARP gene is localized in chromosome 3 (**Miwa M, et al., 1995**), determined by in situ hybridization (**Hanai S. et al., 1998**) and cytology confirmed by PCR and finally classified as essential gene for fly development. The PARP gene consisted of six translatable exons and spanned more than 50 kb.

There are two PARP RNAs populations in *D. melanogaster*, the first encodes the full length PARP protein (PARP-B), while the other is a truncated RNA which could encode a partial-length PARP protein (PARP-C), the second RNA was produced by alternative splicing (loss of exon 5) and the resulting protein lacks the automodification domain (**Uchida M et al., 2001**). (***Figure 46***).

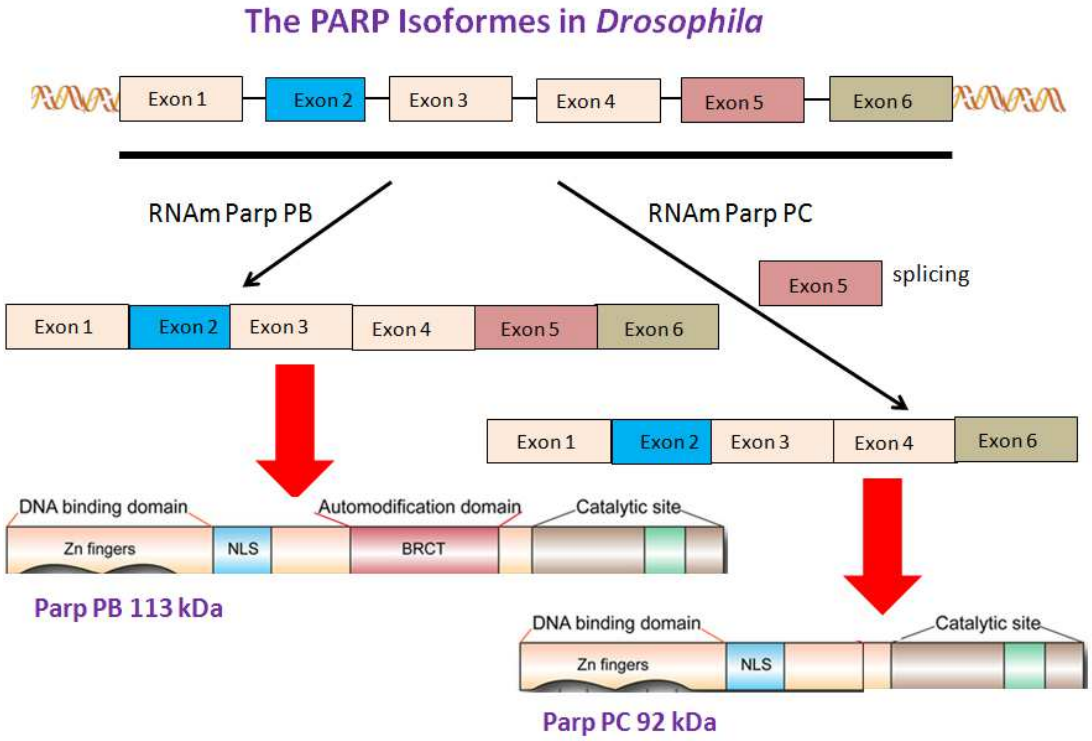

Figure 46*: Schematic representation of PARP isoformes in Drosophila. ParpPB (113 kDa) is encoded by the full transcript and ParpPC (92 kDa) by the truncated transcript.*

Two main actors of the Poly(ADP-ribose) metabolism were shown in nucleus from *Drosophila melanogaster cells.* Boamah and collaborators showed the presence of PARP-B and PARG in nucleus. PARP-B is essential for fly development. Deletion or disruption of PARP-B protein functions disintegrates nucleolus structure (***Figure 47***). Thus, PARP-B controls nucleolar structural integrity (**Boamah EK, et al., 2012**).DNA repair pathways in *Drosophila melanogaster* can be associate with larval diet.

Recently studies show a repair reporter construct system (**Preston CR., 2006**) that allows us to induce DSBs in the germ-line cells of adult male *D. melanogaster* and compare the relative frequencies of HR, SSA, and NHEJ across the two condition groups these males bear gene constructs that serve as the site of DSB creation as well as a homologous repair template. They also carry an endonuclease construct and continuous expression of this gene results in DSBs being created at the same recognition site in individual germ-line cells.

Successful repair by each of these three different pathways leaves behind a unique repair product whose genetic signature can be traced in the progeny of the males. Unfortunately, BER system was not studied in order to demonstrate glycosylases actions after oxidative DNA damages.

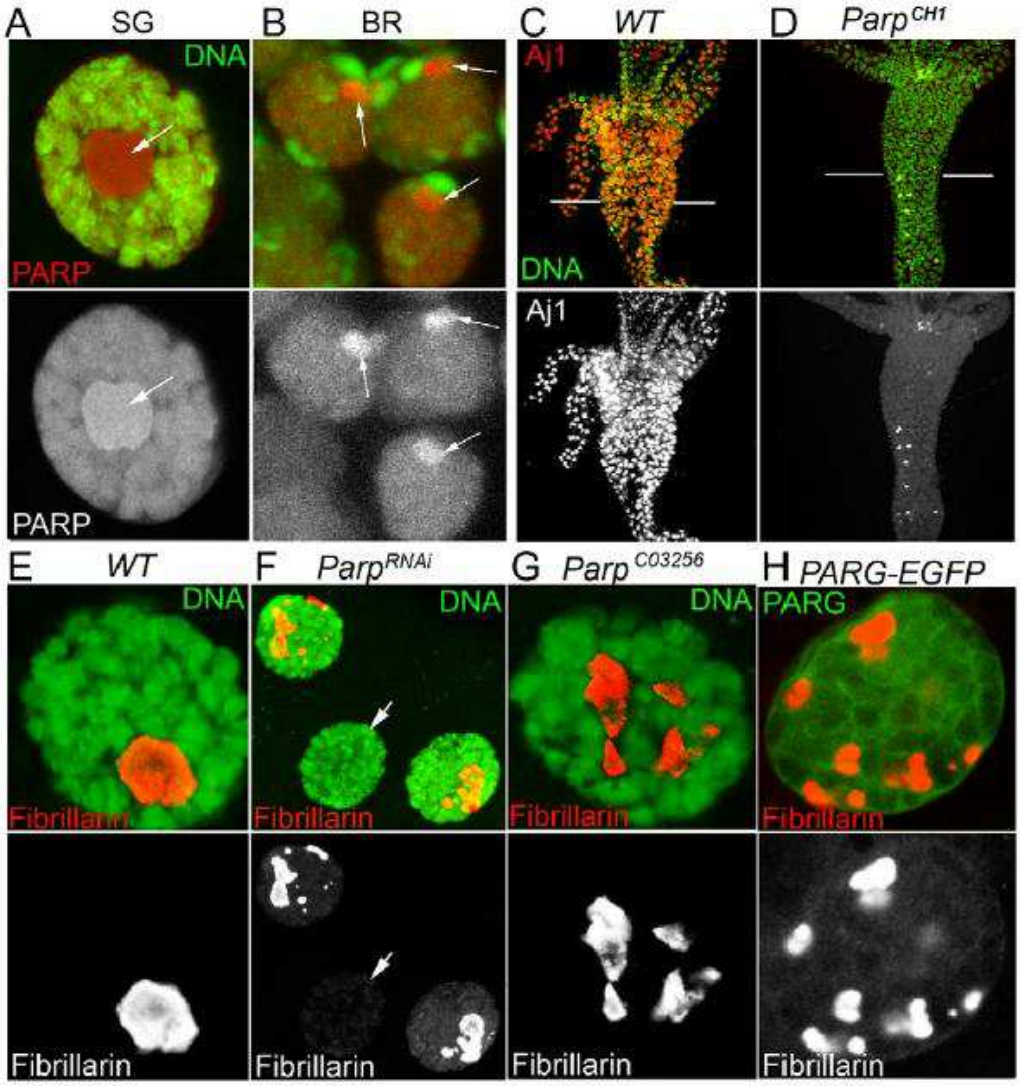

***Figure 47**: A–B: PARP-B protein localizes to nucleoli in all Drosophila tissues, including polytene chromosomes of larval salivary glands (A) and diploid nuclei of larval brain (B). The dissected larval salivary glands and brains expressing PARP1-DsRed (red) were stained with the DNA binding dye Draq5 (green). Positions of nucleoli are indicated with arrows. SG – larval salivary gland; BR – larval brain. C–D. PARP-B deletion displaces nucleoli protein as detected by nucleoli-specific antibody AJ1 (red). AJ1 detects nucleoli in every cell of Drosophila mid-intestine in wild-type second-instar larvae (C), but only in a few cells in ParpCH1 mutants (D). DNA is detected with OliGreen dye (green). E–H. Deletion or disruption of PARP-B protein functions disintegrates nucleolus structure. Salivary glands from wild-type (E), ParpRNAi expressing (F), hypomorphic Parp mutant, ParpC03256 (G), and overexpressing antagonist of PARP-B, PARG (H) 3rd instar larvae were stained for the nucleolar specific protein Fibrillarin (red) (**Boamah EK et al., 2012**).*

THESIS PROJECT

Previous experiences of my training team concerning DNA repair (**Morel., 2008**) and aging (**Dubessay P., 2007)** in *Drosophila melanogaster* as biological model led that my thesis project was focused on three main aspects of mtDNA repair.

a) Analysis of key BER enzymes activities during aging.

ROS production is strongly correlated with aging. Drosophila mitochondria function is very similar to mammalian mitochondria thus experimental Drosophila model for biochemical studies can be associate related to aging (**Sanz A, Stefanatos R, McIlroy G., 2010**).

This analysis will be performed through a comprehensive approach using a microarray carrying various oligonucleotides of DNA modified. Each DNA modification represents a specific DNA damage what is susceptible of glycosylases and endonuclease enzymatic action. The biological potential of certains enzymes BER can be quantify during aging in *Drosophila melanogaster* model.

b) Is PARP protein involved in mtDNA repair in *Drosophila melanogaster?*

Miwa and collaborators showed the PARP expression in *Drosophila melanogaster*, they also identified the PARP-B and PARP-C isoforms demonstrating that only PARP-B has catalytic action (Miwa prénom et al., 1999). Ten years after PARP-1 was identified in human mitochondria by Rossi and al 2009.

¨*in silico*¨ analysis shows 61% homologies between orthologs proteins. All these points put together with the essential role in DNA repair processes stimulated the questioning about PARP involvement into mtDNA repair in fly model. This question will be sequentially answered:

Is PARP-B present in Drosophila mitochondria?

Is PARP-B isoform involved in mtDNA repair?

Does PARP-B isoforms expression profile change under oxidative stress conditions?

c) How is PARP regulated at a transcriptional level in different Drosophila mutants for key BER enzymes?

PARP-1 is involved in BER mechanism at different levels with different roles. It interacts with protein such as OGG1 (**Hooten N, et al., 2011**) in first steps of BER as well with DNA strands after abasic site excision by endonuclease in order to stabilize DNA damage. This question will be answered with a RT-QPCR analysis of mRNA PARP accumulation in various mutants such as ogg1-/-, rrp1-/-, xrcc1-/- and ogg1-/xrcc1-.

MATERIAL AND METHODS

All chemicals were obtained from Sigma unless otherwise stated

I.→.Animals

All flies used in this study were from *D. melanogaster* strain either generated in our laboratory (Wild type flies) or obtained from Bloomington Stock collections for mutants (University of Indiana, USA), (***Table 5***).

They were reared on axenic medium (**Alziari S, et al., 1985**) at 19°C.

D. melanogaster	**Phenotype (eyes color)**	**Origin**
Wild Type (WT)	white	Laboratory
ogg1- (FlyBase code) 19122	orange	Bloomington Stock
rrp1- (FlyBase code) 10213	orange	Bloomington Stock
xrcc1- (FlyBase code) 18682	orange	Bloomington Stock
ogg1^{-}/xrcc1^{-}	red	This study

Table 5*: Different D. melanogaster strains used in this study. Number beside the mutant name indicates the FlyBase code.*

Only ogg1^{-}/xrcc1^{-} mutant strain was generated using classical genetic crossings illustrated in ***Figure 48***.

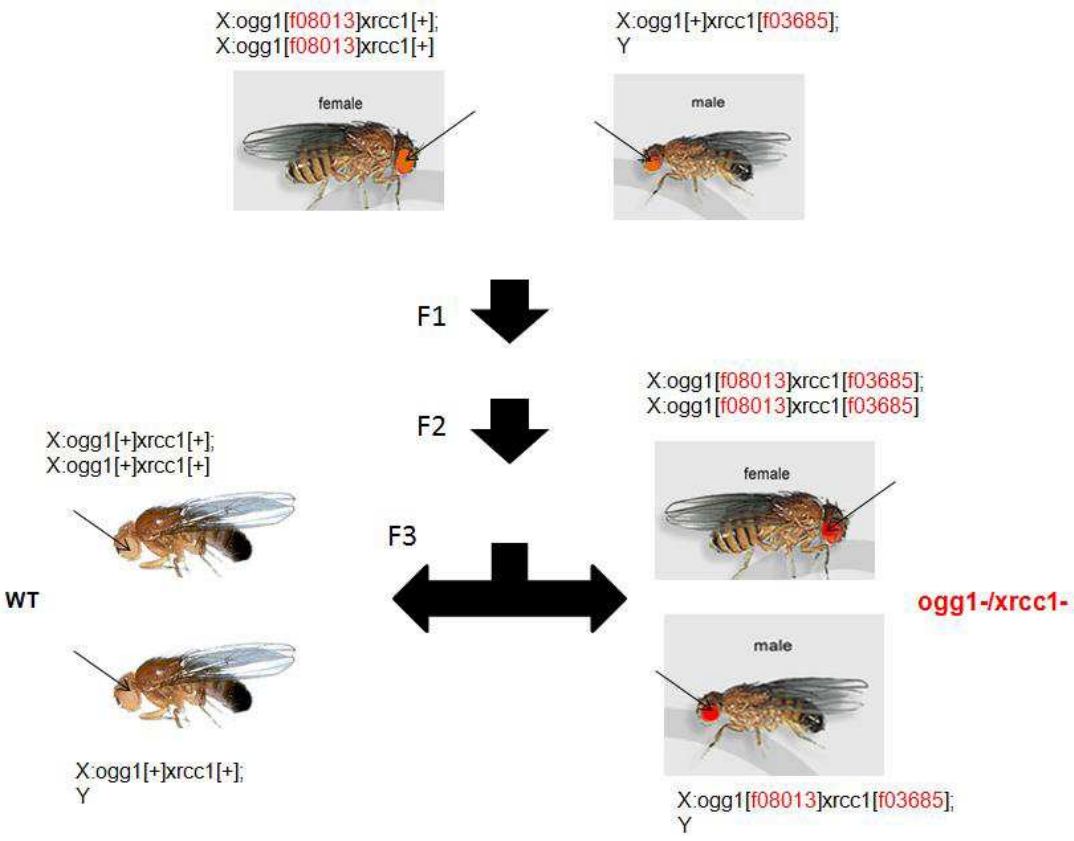

***Figure 48**: Representation of double mutant production strategy. The pBac DNA insertion ogg1[f08013] and xrcc1[f03685] were represented in red color. Eyes colors were indicated with thin arrows in all fruitflies.*

II.→.Sub-cellular fractionation

II.1. Sub-cellular fractions purification (nucleus and mitochondria)

Mitochondria were prepared according to protocols previously described in *Alziari and collaborators* briefly (**Alziari S, et al., 1985**), 300-400 males fruitflies were used for each mitochondria preparation. They were immobilized on ice and ground into small aliquots (50 individuals) with a mortar and pestle in 2 mL of isolation buffer. The resulting suspension was filtered on Sefar Nitex membrane, and centrifuged (240*g*, 10 min.). The pellet was kept for further nuclear purification and the supernatant (lysate) was centrifuged (3000*g*, 10 min). The resulting pellet was suspended in 2 mL of isolation buffer, and centrifuged twice for 10 min at 7000*g*. The final pellet was the “crude mitochondrial fraction”.

The following steps were conducted according to Alziari and collaborators Preformed Percoll gradient was prepared by a 55,000*g* centrifugation of 55% Percoll solution for 1 h. The crude mitochondrial fraction was gently layered onto this preformed Percoll gradient. After further centrifugation (55,000*g*, 1 h), purified mitochondria could be detected as discrete bands in the middle part of the gradient. Bands were collected from the tube with a needle, pooled, and diluted volume to volume with isolation buffer. This solution was centrifuged twice for 10 min at 7000*g*. The resulting pellet was the "pure mitochondrial fraction".

The next step for mitochondria purification was mitoplast preparation. Pure mitochondrial fraction was incubated for 15 min at 4 °C with 0.1 mg of digitonin per mg protein with frequent stirring. After dilution with two volumes of isolation buffer, the solution was centrifuged (10,000g, 5 min). The pellet was washed twice (10,000*g*, 5 min), and finally suspended in 200-400 µL of isolation buffer. This fraction was "purified mitoplasts".

The first pellet obtained after the first centrifugation of the crushed fruitfly suspension was suspended in isolation buffer, filtered on Sefar Nitex membrane, and centrifuged for 10 min at 240*g*. The pellet was suspended in 2 mL of isolation buffer and centrifuged for 10 min at 650*g*, giving the "*crude nuclear fraction*".

The purified nuclear fraction was obtained using a subsequent purification step on a sucrose cushion. Briefly, a 2 mL solution of 2M sucrose was prepared in 3.5 mM $MgCl_2$, 3 mM DTT and loaded onto a polyallomer tube. The crude nuclear fraction was gently layered on the sucrose cushion top, and centrifuged at 124,000*g* for 1 h. The pellet was washed twice at 10,000*g* for 10 min in 1 mL of isolation buffer, and suspended in 500 µL.

II.2. Mitochondrial fractions validation

II.2.1. Western blot analysis

Equivalent protein amounts (15 µg) from mitochondrial or nuclear fractions were run on 10% or 15% SDS-PAGE, and blotted on nitrocellulose membrane (*GeHealthcare*). Western blot analyses were performed with the following dilutions using antibodies raised against lamin 1:750 (DSBH), histone H3 1:2,000, Rieske 1:13,500 (gift from Dr C. Godinot, Lyon), PDH 1:2,000 (*Mitosciences*). Various incubations and detection were as previously described by Dubessay and collaborators (**Dubessay P, et al., 2007**).

II.2.2. Enzyme assays

All the enzymatic measurements were made with a heat-controlled spectrophotometer (Shimadzu) at 28 °C. Both activities were assayed using a previously described protocol.

a. Cytochrome oxidase assay

The activity of Cyt c oxidase was measured as the decrease in absorbance due to the oxidation of Cyt c at 550 nm (ε = 18,500 M^{-1}. cm^{-1}). The addition of 10 μg of protein from mitochondrial or nuclear fractions to the reaction mixture (50 mM KH_2 PO_4, mM EDTA, 100 μM cytochrome c, pH 7.4) initiated the reaction.

b. Citrate synthase assay

Citrate synthase activity was measured as the increase in absorbance due to the reduction of 5,5'-dithiobis-2-nitrobenzoic acid (DTNB) at 412 nm, coupled to the reduction of coenzyme A by citrate synthase in the presence of oxaloacetate (ε = 13,600 M^{-1}. cm^{-1}). The assay was performed with 10 μg of proteins added to the reaction mixture (100 mM Tris HCl, pH 8, 2.5 mM EDTA, 37 μM acetyl-CoA, 75 μM DTNB, 320 μM oxaloacetate).

III.→Comprehensive BER repair analysis through microarray technology

The excision reactions were conducted using the modified oligonucleotide arrays already described elsewhere (**Pons B et al., 2010**).

Briefly, each well of a 24-well slide was functionalized by a series of lesion-containing oligonucleotide duplexes (lesion ODNs) and a control duplex (control ODN, with no lesion). The duplexes were tethered to the slide surface by one end, and labeled with a Cy3 at the other end. All the duplexes were attached in duplicate.

Eight lesion substrates were present: ethenoadenine (EthA) paired with T, hypoxanthine (Hx) paired with T, 8oxoguanine (8oxoG) paired with C, A paired with 8oxoG, thymine glycol (Tg) paired with A, tetrahydrofuran (THF), as abasic site (AP site) analog, paired with A, uracil (U) with G and U paired with A.

Excision reactions were conducted with 10 μg of protein per well at room temperature (23 °C) for 1 h in 80 μL of excision buffer (10 mM Hepes/KOH pH 7.8, 80 mM KCl, 1 mM

EGTA, 0.1 mM $ZnCl_2$, 1 mM DTT, 0.5 mg/mL BSA). The slides were subsequently rinsed at room temperature for 3 x 5 min with 80 µL of washing buffer (PBS containing 0.2 M NaCl and 0.1% Tween 20). On each slide, two wells were incubated with the excision buffer only (control wells) to serve as a reference, arbitrarily set at a fluorescence level of 100% for the calculation of the excision rates (***Figure* 49**)

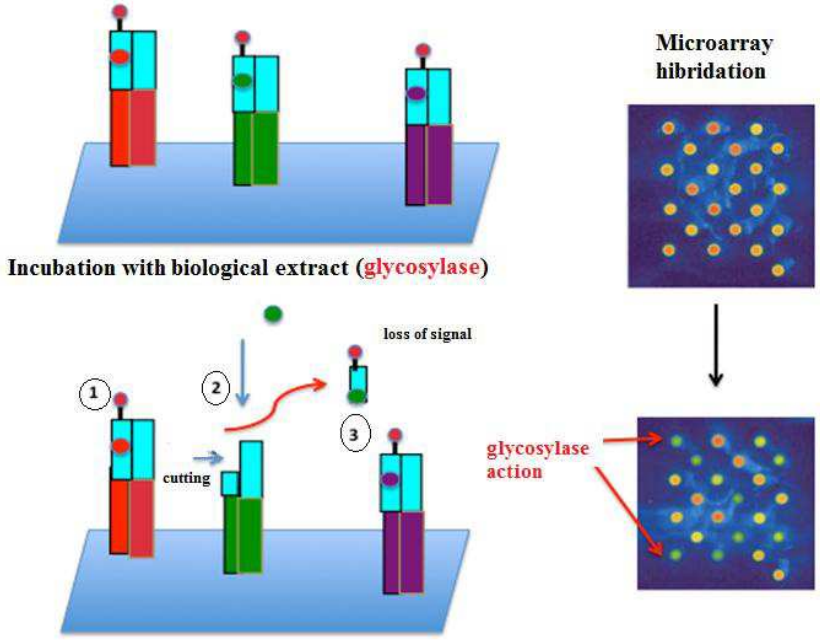

Figure 49*: Schematic representation of glycosylase action detection on microarray. Step 1 represents incubation of oligonucleotides modified with biological extract; step 2 represents the glycosylase and endonuclease actions enzyme and the step 3 washing . Microarray analyses show in green color the glycosylase action dot.*

The spot fluorescence was quantified using a GenePix 4200A scanner (*Axon Instrument, Molecular Devices, Sunnyvale, CA, USA*). Total spot fluorescence intensity was determined using the GenePix Pro5.1 software (*Axon Instrument*).

Each extract was tested twice. The results between replicates (four spots) were normalized using the NormalizeIt software as described by Millau and collaborators. A first operation calculated the excision rate of each of the lesion ODNs in the extract-containing wells compared with the lesion ODNs of the control wells. A correction was then applied that took into account the possible degradation of the control ODN (no lesion). Final results for each lesion ODN, expressed as percentage of cleavage, were calculated using the formula: (100-(1-percentage of fluorescence of lesion ODN/percentage of fluorescence of control ODN)).

IV. →Molecular Analysis

IV.1. Expression analyses

These analyses were performed either with S2 cells lines from *Drosophila melanogaster* or with fruitfly stock

IV.1.1. mRNA extraction

50 flies or S2 cells (10^6 cells) were disrupted in 1 ml TRIZOL. The total RNA was purified according to the manufacturer's protocol (Invitrogen). The samples were solubilised in 50 µl distilled water and immediately stored at -80°C.

IV.1.2. cDNA production

Reverse transcriptase reactions were made using random primers (2.5 mM) and reverse transcriptase enzyme RT M-MLV (1 U) (PROMEGA) at 37°C during 60 minutes. All Reverse transcriptase reactions were made including no-template, no-RT enzyme as controls of genomic DNA contamination. After cDNA amplification the PCR products were incubated with RNAse (4µg/µL) at 37°C during 30 min and quantified in *Nanodrop1000 spectrophotometer*. cDNA aliquots were stored at -80°C.

IV.1.3. RT-q-PCR

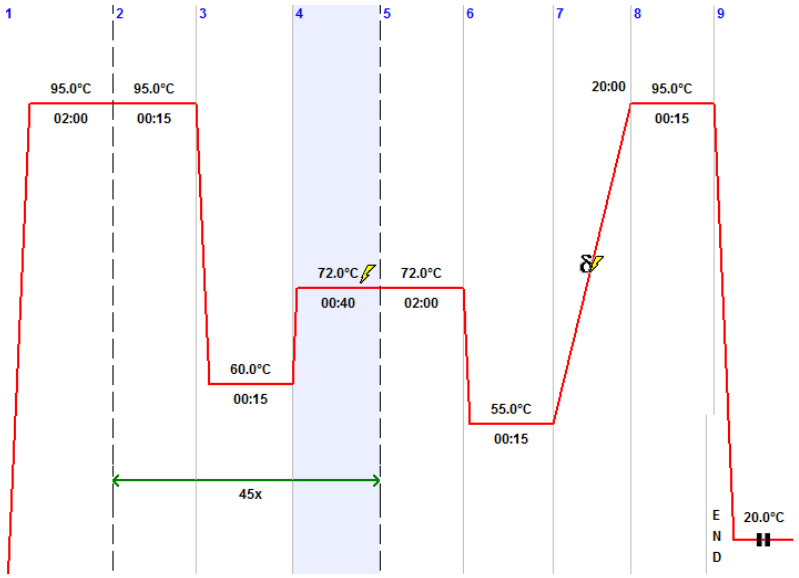

***Figure 50**: Schematic representation of the Real Time quantity PCR amplification conditions.*

All amplifications were made according to the manufacturer's protocol using kit MESA GREEN *qPCR MasterMix Plus*; *SYBR PCR*, (*Eurogentec*). The specific oligonucleotides are described in ***Table 6***. The Rp49 gene was used as a reference and all cDNA amplifications were made in Mastercycler-Pros PCR machine (BioRad) at Tm 60°C and 45 cycles (***Figure 50***).

cDNA	Primers	Sequence 5'-3'	Tm (°C)	Product size (pb)
ogg1	Forward (Exon1-Exon2)	GGACAGAGTTTCCGATGGC	61	199
	Reverse (Exon2)	CGCACAGGCTTACTCAAGAA	60	
rrp1	Forward (Exon1-Exon2)	TTGGTTTCCTGCAGGCAG	61	213
	Reverse Exon2	CTTTTGTTTTCCAGCCACCA	61	
xrcc1	Forward (Exon2-Exon3)	GTGGCATACAGAATCCCGAT	60	210
	Reverse (Exon3)	GCCATGGCAGGTACTTCTTC	60	
parpB/C	Forward (Exon1-Exon2)	TTGCTGTCATGGTTCAATCTG	60	198
	Reverse Exon2	TTTTTCCTAATTGTGCGCTTAT	60	
parp-B	Forward (Exon5-Exon6)	GCGGATAAAAAGGAGAAATATTG	58	199
	Reverse Exon6	CGATTGGGTACATTCGACCT	60	
parp-C	Forward (Exon4-Exon6)	ACAATGATGTTTTGGTTAGATATTGG	58	201
	Reverse Exon6	Parp-B reverse		
parg	Forward (Exon2-Exon3)	GTCGATTGGTAAAGCCTGTTAAA	60	269
	Reverse (Exon3)	GAACTGGACGAGAGCGAAAC	60	
rp49	Forward	GCTAAGCTGTCGCACAAATG	57	190
	Reverse	TCTGCATGAGCAGGACCTC	58	

Table 6*: Primers used for Rt-qPCR experiments. Characteristics are as follow (Gene name, Primers names, Sequence, Tm and amplified product length)*

IV.2. PCR prior to cloning

All amplifications were made at 60°C Tm during 30 cycles using Pfu polymerase (Promega). Amplifications were performed with specific primers (***Table 7***) and protocol presented in ***Figure 51***.

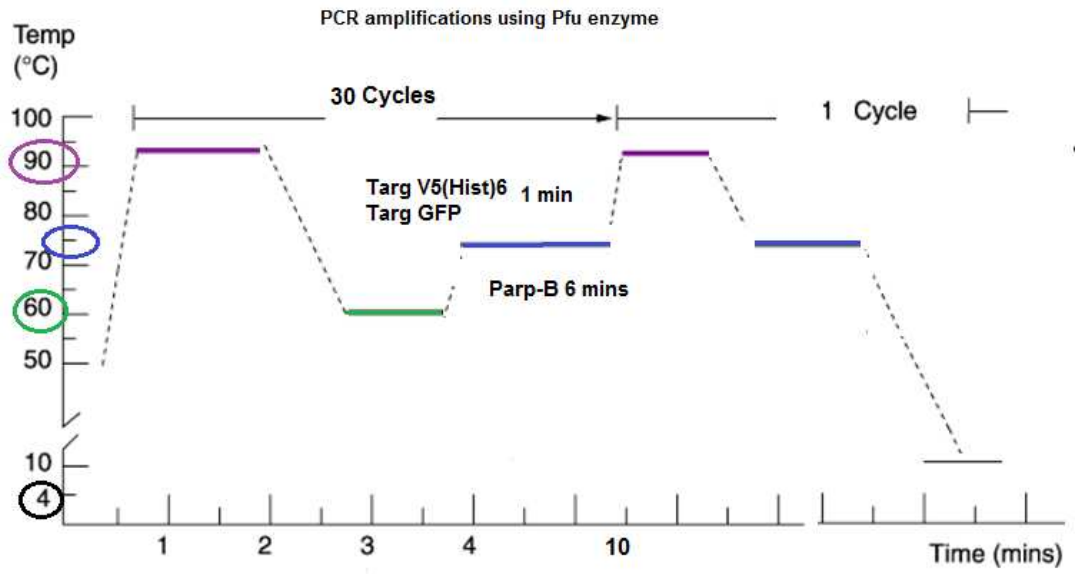

***Figure 51**: Schematic representation of PCR amplification conditions of Parp-B, GFP-targ and $(Hist)_6$-V5-targ using Pfu enzyme during 30 cycles. Denaturation at 90°C, annealing at 60°C and DNA synthesis at 72°C were represented in purple, green and blue colors respectively.*

cDNA	Primers	Sequence 5'-3'	Product size (pb)
Parp-B	Forward KpnI-parp	ccgatatcGTGTAATATGGATATTGAATTACCTTATCTTG	2982
	Resverse SmaI-parp	ggCCCGGGATAAGAATACTTGAATTCCATAC	
GFP	Forward SmaI-GFP	ggcccgggGGTGGTAAAGGAGAAGAACTTTTC	733
	Reverse BamHI-GFP	ggggatccgatatcTTACTTGTATAGTTCATCCATGC	
$(Hist)_6$-V5	Forward	GGTAAGCCTATCCCTAACCCTCTCC	115
	Reverse	TAGAAGGCACAGTCGAGG	

***Table 7**: Primers used for Parp-B, GFP and (Hist)6-V5 PCR amplification. Parp-B and GFP primers contained restriction site (small letters). (Hist)6-V5 Tag was amplified without restriction site.*

IV.3. PARP-B-target construction

DNA	Enzyme for DNA digestion	Cloning vector
GFP PCR product	**SmaI/ BamHI**	**pGEM7z(+) (SmaI/ BamHI)**
PARP-B PCR product	**KpnI/ SmaI**	**clon-19 (KpnI/ SmaI)**
$(Hist)_6$-V5 PCR product	**not**	**clon-1 (SmaI)**
clon-7	**KpnI/ PmeI**	**pMT puro (KpnI/ EV)**
clon-1	**BamHI (klenow) /KpnI**	**pMT puro (KpnI/ EV)**

Table 8*:Summary of clones for PARP-B construct: clon-19 J-2 represents GFP cloned in pGEM7z(+) vector in SmaI/BamHI positions; clon-1 represents Parp-B cloned in clon-19 in KpnI/SmaI positions; clon-7 represent clon-1 inserted with targ (Hist)6-V5 PCR product in SmaI position; J2 plasmid represents Parp-B-(Hist)6-V5 cloned in pMT puro vector in KpnI/EV positions; C-4 plasmid represent Parp-B-GFP cloned in pMT puro vector in KpnI/EV position and the plasmid A-8 represents Parp-B-(Hist)6-V5 cloned in pBAD24 vector in HindIII (treatment with klenow)/KpnI positions.*

Tables 8 and 9 show the PARP-B-target construct and vector source. All DNA digests were made according to the manufacturer's protocol from PROMEGA.

The DNA product purification was made using NucleoSpin Gel and PCR Clean-Up from MACHEREY NAGEL and the ligation reactions were performed with T4 ligase (2.5 U) from PROMEGA at 4°C overnight.

Plasmid	Source	Description
pGEM7z(+) vector	PROMEGA	***annexes 1***
pMT puro	PROMEGA	***annexes 2***
pBAD24	Gift from Dr. MARTINEZ E, CNRS Paris	***annexes 3***
J2 plasmid	In this study	***Figure 52***
C4 plasmid	In this study	***Figure 53***
A8 plasmid	In this study	***Figure 54***

Table 9*: List of plasmids used in this study.*

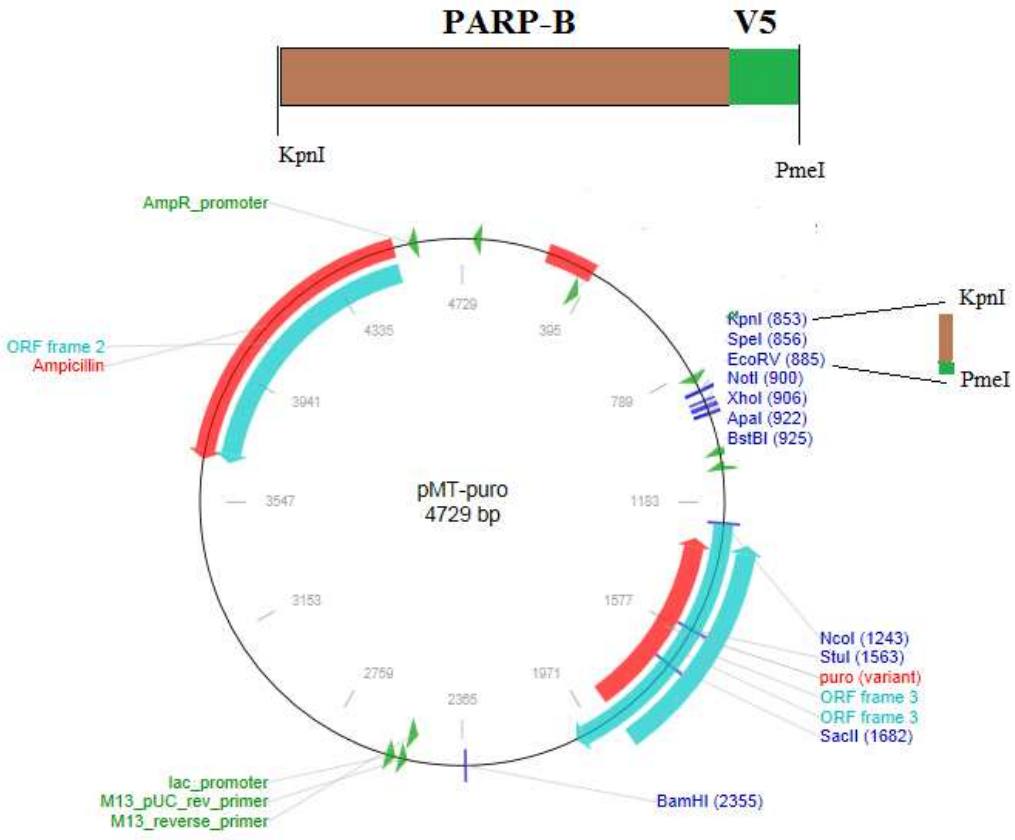

Figure 52*: J2 plasmid: PARP-B-V5 cloned in pMT-puro vector*

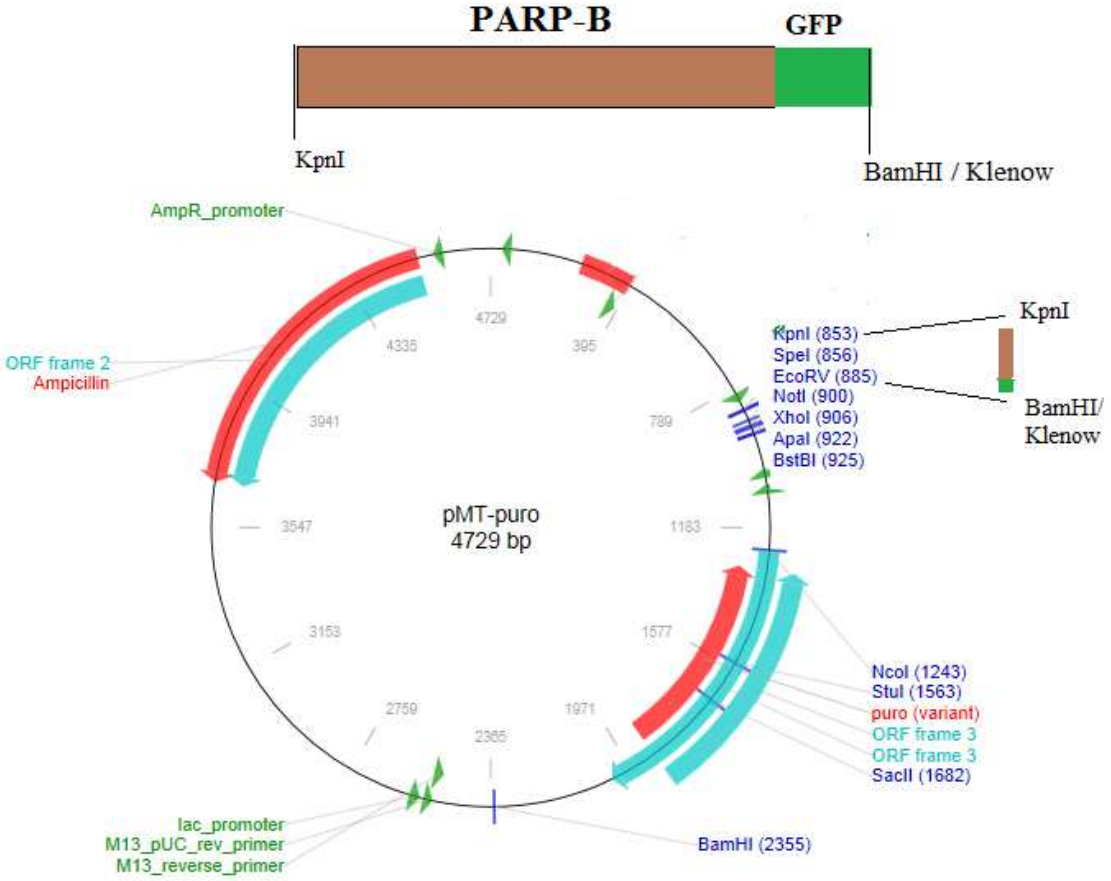

Figure 53: C4 *plasmid: PARP-B-GFP cloned in pMT-puro vector*

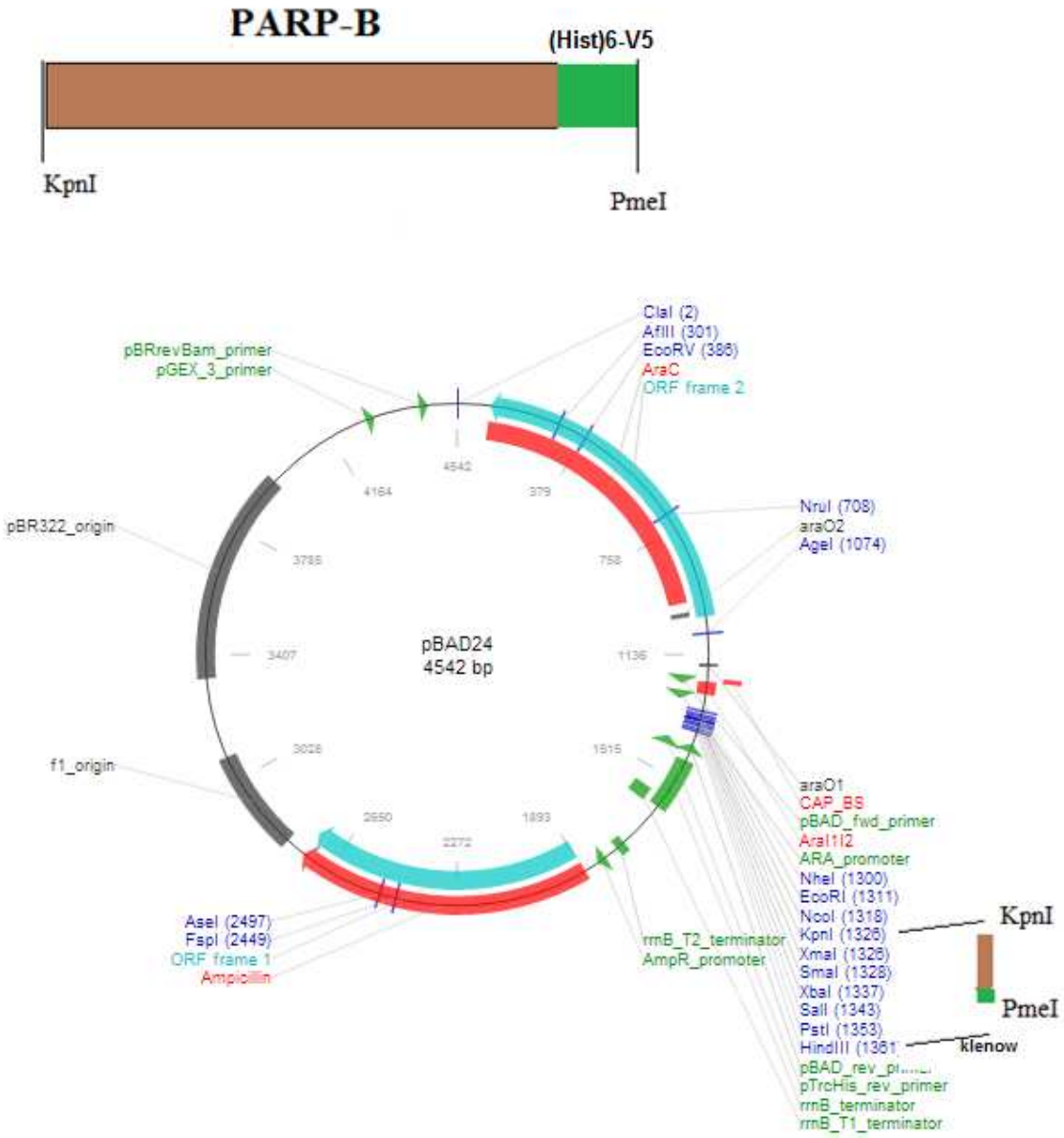

Figure 54: *A8 plasmid: PARP-B-V5 cloned in pBAD24 vector*

IV.4. DNA electrophoresis

The gels were made with different agarose percentage such as 0.8, 1.0 and 2.0%. The agarose was prepared in TAE1X buffer (4 mM Tris, 1 mM EDTA). Ethidium bromide was added 1 drop (50mg/ml) per 50 ml of gel solution at 40°C. Electrophoreses were performed in TAE1X buffer and run at constant voltage (110V).

IV.5. Bacteria transformation

IV.5.1. Competent cells preparation

Competent cells were prepared according to protocol used in our laboratory. A single fresh colony *E. coli DH5*α was inoculated into 3 mL of LB broth and cultured 6 hours at 37°C. Then the LB broth volume was increased to 200 mL and growth was carried out overnight at 37 °C and 200 cycles/min in a rotary shaker. Next, 500 µL of the culture was transferred into 50 mL of LB broth and incubated under the same conditions until culture OD_{600} reaches 0.3-0.4. Growth was stopped by transfer into a 50-mL polypropylene tube stored at 0 °C during 10 min. The tube was centrifuged at 1,700 g for 15 min at 4 °C. Pellet was resuspended in 10 mL of filter-sterilized ice-cold 0.1 M $CaCl_2$ and stored for 5 min on ice. Then suspension was centrifugated at 1,700 g for 15 minutes at 4 °C. After discarding the supernatant the tube was inverted for 1 min to allow the last traces of media to drain away. Finally cell pellet was resuspended in 2 mL of filter-sterilized ice-cold 0.1 M $CaCl_2$ and store for 2-3 hours on ice. The total volume was divided into 200 µL of competent *E. coli DH5* α suspension in sterile microcentrifuge tubes and used immediately. Alternatively cells were stored at –80 °C.

IV.5.2. Transformation

DNA plasmid (80-100ng) was added to competent cells kept on ice-cold and incubated for 1 hour. A 1 min heat shock (42°C) was performed, followed by 2 min on ice. LB medium without ampicillin (500 µL) were added and bacteria were incubated at 37°C with 200 cycles/min in a rotary shaker during 45 min. Bacteria were plated on agar containing 100 µg/mL ampicillin.

IV.5.3. Cloning control

Several clones were selected and numbered. Each of them was split into two tubes. One was inoculated into an empty PCR tubes and PCR mix was added see above). PCR was performed (30 cycles, Tm 60 °C, 3 min at 72 °C, goTaqPol(0.25U)) with specific primers. The other half of the clone was inoculated in 1.5 ml of LB (ampicillin 100ug/ml) incubated at 37°C. Plasmid purification was carried out on positive clones using NucleoBond XtraMidi kit (*MACHEREY NAGEL*). Each plasmid was tested by restriction digests on 1 µg DNA. Clones were subsequently sequenced (*MWG-Biotech, Germany*). All sequences were analyzed by Codon Code Aligner 4.2.4 program (*CodonCode Corporation*).

V.→ In silico analyses

V.1. Mitochondrial targeting analysis

Two softwares (***Figure 55***) were used such as: PSORTII, (http://psort.hgc.jp/form2.html) focused in subcellular localization prediction. (**Horton P, Nakai K., 1997**) and MitoProtII Computational method to predict mitochondrially imported proteins and their targeting sequences (**Claros MG, Vincens P., 1996**). The Mitoprot software is available by: (http://ihg.gsf.de/ihg/mitoprot.html)

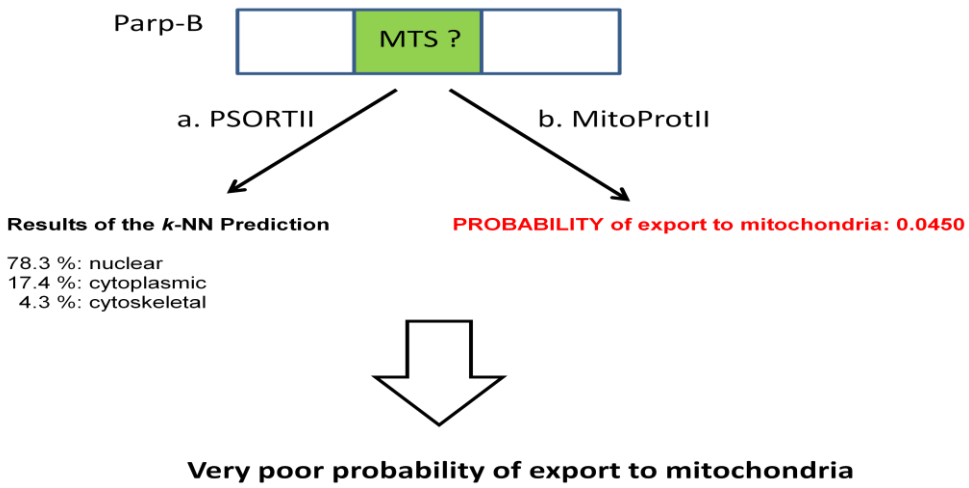

***Figure 55**: Schematic representation of results obtained with these two softwares.*

V.2. Protein sequences homology

The protein Align Sequences analysis was made using BLAST:

http://blast.ncbi.nlm.nih.gov/Blast.cgi?PROGRAM=blastp&PAGE_TYPE=BlastSearch&BLAST_SPEC=blast2seq&LINK_LOC=blasttab&LAST_PAGE=blastn&BLAST_INIT=blast2seq

V.3. Caspase cleavage sites determination

The caspase cleavage site determination was carried using the program PeptideCutter (ExPASy) http://web.expasy.org/peptide_cutter/ In natural substrates, he prediction and characterization of proteolytic cleavage sites can lead to understand these structural relationships. (**Garay-Malpartida HM, et al., 2005**)

V.4. Physico-chemical properties

Molecular Weight (MW) and isoelectric point (pI) were determined using the program: Compute pI/MW (ExPASy) http://web.expasy.org/compute_pi/

VI.→.PARP sub-cellular localization

VI.1. S2 cells culture

According to the manufacturer's protocol (modified) S2 cells were incubated in complete Schneider medium (Invitogen) containing Fetal Calf Serum (10%) antibiotics (Penicillin and Streptomycin 1%) at 24˚C until density reaches 6 to 20 x 10^6 cells/mL.

VI.2. Cells transfection

Cells transfection was carried out on confluent cells using Cellfectin Reagent (Invitrogen)

Day 1: Cell preparation: 3 mL of S2 cells (2 x 10^6 cells/mL) were plated in a 35 mm well with complete Schneider's Drosophila Medium (SDM).

Day 2: Transfection: Solution A (1 µg plasmid in 100 µl of incomplete SDM) was slowly added to 8% Cellfectin in incomplete SDM and gently vortexed. The mix was incubated 20 min at room temperature. It was added to S2 cell culture where SDM complete medium was previously replaced by incomplete one. Incubation was performed during 5 hours at 24 °C.

Then medium was changed to complete SDM. For stable transfected cells lines, a selection was performed using puromycin antibiotic (5 µg/mL) during 6 weeks.

Day 3: Expression of protein of interest: Cells were incubated in presence of 0.7 mM Cu_2SO_4 during 24 hours at 24°C to induce the expression of the specific protein.

VI.3. Validation of stable cells lines

All PCR conditions were shown on ***Table 10***. GoTaqPol (0.5 U) polymerase (Promega) was used with the following conditions: Tm 60°C, 72°C for 3 min, 30 cycles.

Sample	Primers	Sequence 5'-3'	Product size (pb)
S2 genomic DNA	Fw: Parp-B	TTGCTGTCATGGTTCAATCTG	2888
	Rv: Parp-B	ggCCCGGGATAAGAATACTTGAA TTCCATAC	
J2 genomic DNA	Fw: pMT puro	CCCAGTCACGACGTTGTAAAACG	3225
	Rv: V5	TAGAAGGCACAGTCGAGG	
C4 genomic DNA	Fw: pMT puro	Fw: pMT puro	3810
	Rv: GFP	ggggatccgatatcTTACTTGTATAGTTC ATCCATGC	

Table 10*: PARP-B-target amplification: Representation of each primers used in Parp-B, GFP and (Hist)6-V5 PCR amplification. Parp-B and GFP primers were made with restriction site. The targ (Hist)6-V5 was amplified without restriction site.*

The genomic integration of cDNA construct in S2 cells was validated by PCR experiment on whole genomic DNA. Briefly, 100 flies were lysed in buffer (10 mM Tris HCl pH 8; 60 mM NaCl, 10 mM EDTA) and proteinase K (20µg/µL) and incubated for 1 hour at 65°C. After addition of 0.8 M potassium acetate, the suspension was incubated for 15 min at 4°C, and then centrifuged (12000 g, 15 min) at room temperature.

Upper phase was kept and treated by RNAse (4µg/µL) at 37°C during 30 min. A volume of phenol/chloroforme (24/1) was added the solution and it was thoroughly mixed and centrifuged at 4°C, (12000 g, 15 min). The upper phase containing DNA was precipitated for 1 hour with isopropanol at -20°C. The resulting DNA was washed with 70% ethanol,

centrifuged at 4°C, (12000 g, 15 min) and finally diluted in sterile water. DNA quantification was in *Nanodrop 1000 spectrophotometer*. The aliquots were stored at -80°C.

VI.4. Stress conditions

VI.4.1. Copper stress

In order to induce the similar cellular stress that in protein induction mechanism, S2 cells were incubated with Cu_2SO_4 (0.7mM) during 24 hours.

VI.4.2. Oxidative stress

In order to induce a cellular stress and to promote DNA alterations, oxidative stress conditions were created using various [H_2O_2] (***Table 11***).

VI.4.3. Copper /oxidative stress

The stress combination was performed as follow. Cells were incubated during 24h with 0.7mM $CuSO_4$ then 40 mM H_2O_2 was added during 30 min.

H_2O_2 final concentration (mM)	**Incubation time at 24°C (min)**
5	5, 15 and 30
20	5, 15 and 30
40	5, 15 and 30

***Table 11**: Incubation conditions for oxidative stress induction in S2 cells using different H_2O_2 concentrations.*

VII.→.Microscopy

Forty picomoles of Mitotracker CMXRos (Molecular Probes) were added to 5 ml of S2 cells suspension (collected at confluency) and incubated for 30 min at 24°C. The fluorochrome was eliminated by warm PBS 1X (24°C) with 3 quick washes.

Cells fixation was performed using paraformaldehyde (PFA) 4% at 4°C during 30 min. 50 µl of cells lines (GFP tagged) were directly layered with coverslip.

Triton100X (0.2%) was added to J2 line on slides. Protein detection was made using different primaries antibodies such as anti-V5 or anti-PARP (Santa Cruz). Both were diluted 1/500 and 1/200 respectively and incubated for 1 hours at room temperature and washed with PBS1X, 3 times. After BSA (3%) blocking during 30 min at room temperature, 3 other washes with PBS1X were performed.

Both secondary antibodies, anti-rabbit alexa488 (for anti-V5) and anti-goat alexa488 (for anti-PARP) were diluted 1/320 and incubated for 1 hour. Cells were observed with Axioplan-2 microscope (Zeiss) about ten images per slide were captured using Axiovision software (Zeiss) at the following wavelengths: MitoTracker: the excitation Band was 550-700 nm; DAPI: Violet Excitation Band was 401-418nm and FITC: Blue Excitation Band was 480 - 500nm.

VIII.→.Proteins analyses from Drosophila

VIII.1. Protein extraction

After 24 hours induction with 0.7mM Cu_2SO_4, The S2 cells were washed 3 times with PBS1X. Washed cells were diluted in extraction buffer. Cell lysis was performed with ultrasound (*Vibracell; BIOBLOCK SCIENTIFIC*) on ice with 15 cycles of 30 sec pulse and 1 min.

VIII.2. Electrophoresis and blotting

Laemmli 1X (10% glycerol, 5% β-mercaptoethanol, 1% SDS, 0.02% bromophenol blue) was added to 20 µg protein as determined by Bradford assay (*BioRad*) and heated at 95°C during 5 min. Proteins samples run was made in 10% SDS-PAGE (***Table 12***) at constant voltage (80V) during 3 hours.

Protein staining was directly performed in gel using 0.1% Coomassie Brilliant Blue (triphenylmethane) solution.

Protein blotting was performed after SDS-PAGE on nitrocellulose blotting membrane (*Millipore*) at 200mA during 1 hour. Proteins on membrane were stained with 2% ponceau red.

Gels	
Running gel 10%	**Stacking gel 3.2%**
0.375M Tris HCl pH 8.8 Acrylamide 10% (19/1)	0.124M Tris HCl pH 6.8 3.2% Acrylamide (19/1)
0.1% SDS	0.1% SDS
0.05% ammonium persulfate	0.025% ammonium persulfate
0.5% TEMED	0.10% TEMED

***Table 12**: Gels composition.*

VIII.3. Parp-B protein detection

This was made using anti-V5 (*PROMEGA*) and anti-PARP (Santa Cruz) antibodies diluted at 1/200 and the respectively secondary antibodies anti-rabbit and anti-goat both diluted 1/10000. Parp-B-$Hist_6$ detection was made according to manufacturer's protocol using anti-$Hist_6$ diluted 1/20000 and anti-mouse diluted 1/10000 both antibodies.

Incubation times were: 2 hours for primary antibodies and 1 hour for secondary antibodies and all incubations were made at room temperature. *Luminata*^{TM} *crescendo* kit (*Millipore*) was used as a substrate for peroxidase labeled-antibodies.

VIII.4. Mass spectrometry

According to Dr. BONHOMME protocol (personal communication), bands were excised from gel using cutting blade and forceps. Each band cut were about into 1 x 1 mm pieces and place in 1.5mL LoBind tube (Eppendorf). All reagents were HPLC grade. The gel pieces were rinsed with 300 μ L water for 15 min at room temperature on shaker. Acetonitrile (300 μ L) was added and washed for 15 min at room temperature on shaker.

Supernatant was discarded. Gel pieces were washed with 100mM ammonium bicarbonate (300 μ L) for 15 min at room temperature on shaker. The supernatant was discarded. One hundred millimolar ammonium bicarbonate in 50% acetonitrile (300 μ L) was added and incubated at for 15 min at room temperature on shaker, supernatant was discarded and 100 μ L acetonitrile was added to the pellet for 5 min at room temperature on shaker. The supernatant was discarded.

The gel pieces were dried in a Speedvac for 5 min. Ten millimolar DTT (50 μ L) was added and incubated for 1 hour at 60°C. Supernatant was discarded. 50 μ L were added to 50mM IAA and incubated for 30 min in dark at room temperature. Supernatant was discarded. Washing gel pieces were with 300 μ L 100mM Ammonium Bicarbonate for 15 min at room temperature on shaker. Supernatant was discarded. Washing gel pieces were with 300 μ L 20mM Ammonium Bicarbonate in 50% Acetonitrile for 15 min at room temperature on shaker. Supernatant was discarded. It was adding 100 μ L HPLC Acetonitrile for 5 min at room temperature on shaker. Supernatant was discarded. Drying of gel pieces was in a Speedvac for 5 min. It was adding 20 μ L of Trypsin solution and incubated for 1 hour at room temperature.

Finally, enough Ammonium Bicarbonate at 40mM was added in 10% Acetonitrile to completely cover the gel pieces and incubate overnight at 37°C. It was added 150 μ L HPLC water to pieces for 10 minutes at room temperature on shaker. Removed supernatant and placed in a 0.5mL LoBind tube (*Eppendorf*). It was extract the gel pieces twice with 50 μ L of 50% Acetonitrile/5% TFA for 60 min each time at room temperature. It was pooled all extracts and dried in a Speedvac.

The purification and concentration of peptides for *in silico* analysis were carried out using ZipTips (**Tiss A et al., 2007**).

The mass spectrometry was performed on the local Metabolomics platform facility (*INRA, Theix Clermont*)

IX. Recombinant protein production

IX.1. Protein expression

E. coli DH5 α were transfected with plasmid A8 (pBAD24-PARP-B(Hist)$_6$). According to Karin Andersson protocol's, (Amersham Pharmacia Biotech, Uppsala, Sweden) a single fresh colony A8 was inoculated into LB ampicillin (100ng/ml) and cultured overnight at 37 °C with 200 cycles/minutes in a rotary shaker. Next, 500 μL of the culture was transferred into 50 ml of LB broth and it was incubated at the same conditions. When culture OD_{600} reached 0.5-0.6, expression induction was performed using L-Arabinose (with various concentrations ranging from 0.002% to 0.02%) during 3 hours. Bacteria were centrifuged at 1,700 g for 15 min at 4 °C and the cell pellets was recovered.

The pellets were resuspended in 10 ml of appropriate buffer (0.16 M phosphate buffer 4 M NaCl, 25 mM imidazole pH 7.4). Bacterial lysis was performed at ice-cold using ultrasound ten times 0.5 minutes pulses. Centrifugation at 1,700 g for 15 minutes at 4 °C. Recombinant protein was purified on a 0.2 μm filter (*Millipore*).

IX.2. Protein purification

The poly-histidine tagged recombinant protein was purified manually using a column HisTrap Chelating, 1mL (amersham pharmacia biotech). Firstly the column was equilibrated with 3 volume of binding buffer (0.16 M phosphate buffer, 4 M NaCl, 25 mM Imidazole pH 7.4),

The *E.coli* extracts (10mL) was charged into the column and was washed with 10 ml of binding buffer and subsequently a second wash with 10 mL of biding buffer containing 100mM Imidazole.

The protein was recovered with 1mL of eluting buffer (0.16 M phosphate buffer, 4 M NaCl 250 mM Imidazole pH 7.4). The first mL collected corresponds to wash buffer that remained in column. Two fractions about 500 μL were collected and stored at -80C.

RESULTS

I.→ Global analysis of BER system in Drosophila melanogaster

I.1. BER activities

I.1.1. Validation of mitochondrial fractions

I.1.1.1. Purity analysis

As a first step prior to any repair measurement in mitochondria, we sought to obtain purified functional mitochondrial fractions with no contaminants from cytosol or nuclear compartments, in order to ensure that tested repair activities came solely from the expected compartment.

Mitochondrial and nuclear purity was estimated using Western blot analyses with specific antibodies: anti-PDH (mitochondrial matrix), anti-Rieske (mitochondrial inner membrane, component of the respiratory complex III), anti-lamin (Dm0, nuclear envelope), and anti-histone H3 (nucleoplasm).

The crude mitochondrial fraction obtained by differential centrifugation showed, by Western blot analysis, a persistency of nuclear proteins such as lamin and histone H3, suggesting a partial nuclear contamination of this fraction, independent of fruitfly age (***Figure 56***, lane CM). The incubation of these fractions with low digitonin concentration in order to eliminate mitochondria outer membrane did not get rid of these contaminations (data not shown).

A subsequent purification step from crude mitochondrial fractions on Percoll gradient (***Figure 56***, lanes PM) not only preserved the fraction integrity as shown by the presence of mitochondrial matrix protein PDH, but was also sufficient to eliminate residual traces of nuclear components. An additional treatment of these fractions with digitonin removed all residual contaminants (***Figure 56***, lanes Mpl). All the results confirmed that these fractions (purified mitochondria (PM) and mitoplasts (Mpl)) could be further analyzed for mitochondrial BER activity assays.

In parallel, crude nuclear fractions were prepared and analyzed by Western blot. As observed for mitochondria, these fractions were still contaminated with other compartment

proteins (***Figure 56***, lanes CN) such as PDH and Rieske. Another purification step using a sucrose cushion led to the almost complete disappearance of mitochondrial contaminants in purified nuclear fraction (***Figure 56***, lanes PN). These results prove that BER activities measured in the purified nuclear fractions were exclusively of nuclear origin.

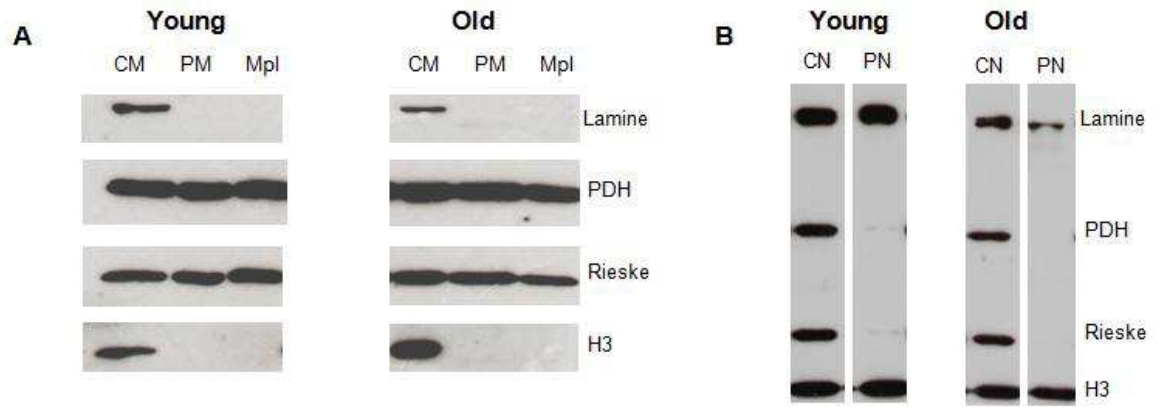

Figure 56*: Western blot analyses of various sub-cellular fractions. Mitochondrial (A) and nuclear (B) protein fractions were analyzed: 15 mg of crude mitochondrial fraction (CM), Percoll gradient purified mitochondria (PM) and purified mitoplast fraction (Mpl) from young (1 week) and old (8 weeks) fruitflies were separated by SDS PAGE, transferred on membrane and analyzed by Western blot. Antibodies directed against complex III Rieske subunit (mitochondrial component) or against lamin and histone H3 (nuclear components) were used.*

I.1.1.2. Functionality analysis

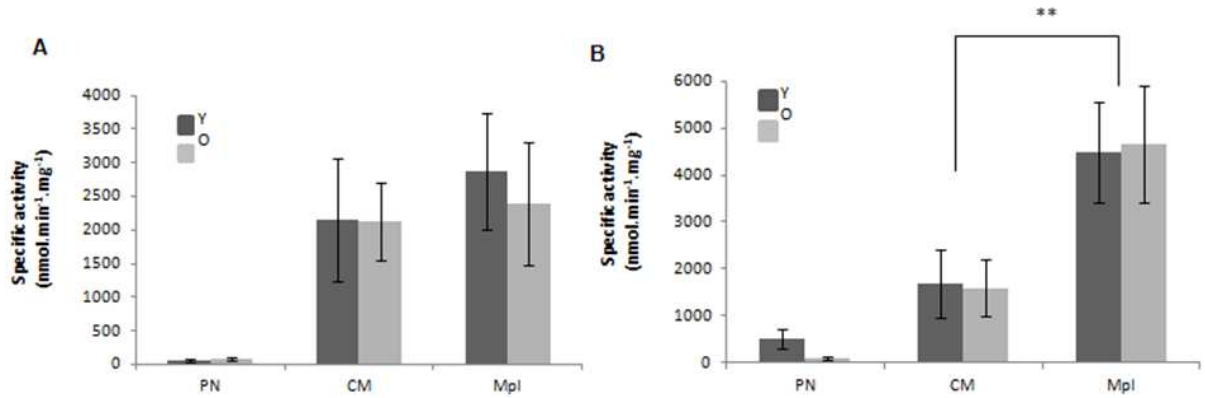

Figure 57*: Enzymatic activity measurements in various sub-cellular fractions. Cytochrome oxidase (A) and citrate synthase (B) activities were measured in various subcellular compartments: purified nuclear fraction (PN), crude mitochondrial fraction (CM) and purified mitoplast fraction (Mpl). Fractions from young (black) and old (gray) fruitflies were analyzed. Error bars represent the SD of independent experiments (n = 12, Student's test: ** p < 0.01).*

After determining the fractions purity, mitochondrial functionality was assessed using enzyme assays. Two enzyme activities were chosen: cytochrome oxidase (complex IV of the respiratory chain, ***Figure 57A***), and citrate synthase (a mitochondrial matrix protein from the Krebs cycle, ***Figure 57B***).Change (2.6-fold) for citrate synthase activity between crude

mitochondria and mitoplasts was significant ($p < 0.05$). By contrast, the increase observed for cytochrome oxidase between these two fractions (1.34-fold) with young fruitflies was not significant. All these results confirmed that mitochondrial fractions were functional for further studies.

I.1.2. Nuclear BER activities

Validation of microarray approach on *Drosophila* model Specific BER glycosylase and endonuclease activities were measured using modified oligonucleotide microarrays designed for the determination of BER capacities in nuclear extracts. As a first step, nuclear BER activities were analyzed to confirm the efficiency of the microarray with fruitfly extracts.

Most of the eight DNA lesions present on the microarray were detected and excised by these extracts, suggesting the presence of the corresponding specific glycosylases/endonuclease in these samples. However, four main activities were observed in nuclear extracts from young individuals (***Figure 58A***).

The endonuclease activity that cleaved THF paired with A with approximately 60% excision rate was predominant. The cleavage rate of Hx, U and A, paired respectively with T, G and 8oxoG was also high (more than 25% excision). Other activities were lower than 10%.

During aging, only Hx-T and A-8oxoG were significantly decreased (68%, $p < 0.05$). Hence, as also for various cell models, these modified oligonucleotide microarrays were efficient in determining BER activities in nuclear extracts from *Drosophila melanogaster*.

I.1.3. Mitochondrial BER activities

Mitochondrial fractions, both crude mitochondria (*Figure 66B*) and pure mitoplasts (***Figure 66C***) from young individuals, were tested in the same conditions. In crude mitochondria samples, four major excision activities were observed with the following efficiency rate order: THF-A (80% excision rate) > U-G>, Tg-A> Eth-A.Other activities were not detectable (Hx-T; 8oxoG-C; A-8oxoG and U-A). Pure mitoplast fraction was analyzed to compare with the crude mitochondria preparation. The global activity profile was quite similar to the one obtained with crude mitochondrial fraction, but provided additional information. The main changes were observed with the excision percentages, which were globally higher in mitoplasts than in crude mitochondria. In particular, excision of U-A was effective in mitoplast fraction whereas it was almost undetectable in crude mitochondria.

An interesting observation was made regarding the effect of aging (***Figures 58B and 58C***). Two tendencies observed with crude mitochondria were significant with the mitoplasts. A marked increase (2.4-fold, $p < 0.05$) of U-G excision was detected, whereas other activities declined. Aging-associated decrease was significant for THF (-18%).

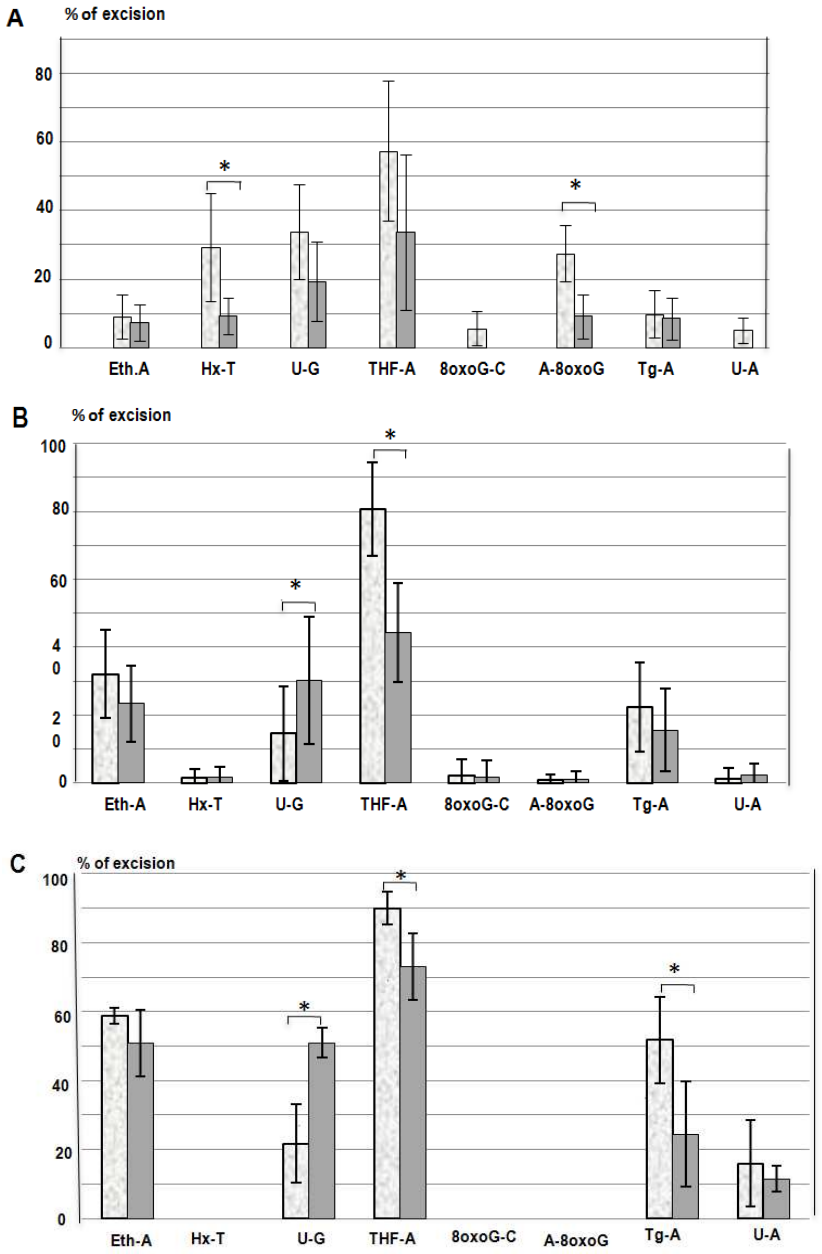

Figure 58*: Cleavage rate measurements using lesion-containing oligonucleotide microarrays. The cleavage rate represents the percentage of loss fluorescence at each lesion spot after incubation with purified nuclear fractions (A), crude mitochondrial fraction (B) and purified mitoplasts (C). The different lesion substrates are indicated: ethenoadenine paired with T (Eth-A), hypoxanthine paired with T (Hx-T), uracil paired with G (U-G), tetrahydrofuran paired with A (THF-A), 8oxoguanine paired with C (8oxoG-C), A paired with 8oxoguanine (A-8oxoG), thymine glycol paired with A (Tg-A), uracil paired with A (U-A). Fractions from young (white) and old (black) fruitflies were analyzed. (n = 3-7, Student's test: * $p < 0.05$). Error bars represent the SD of independent experiments.*

Even though endonuclease activity was high in both nuclear and mitochondrial extracts, these results show that BER activities in mitochondria were different from their nuclear counterpart, and that aging interferes with these capacities.

Most of the observed activities were a consequence of the presence of specific mitochondrial isoforms from various BER glycosylases. *In silico* analyses were performed to investigate the ability of candidates proteins to be involved in such activities. These proteins were described in several organisms mitochondria but were less known for *Drosophila* model.

II.→ Mitochondrial addressing predictions

Two different computer programs were used. In a first step, PsortII was chosen for its ability to give a mitochondrial addressing prediction, but also predictions for other compartments locations. MitoProtII was used as complement software to reinforce the previous results.

A group of 8 proteins from *Drosophila* and one from human was investigated. On one hand, molecules directly involved in BER process were tested such as one glycosylase (Ogg1-PA), two isoforms of a specific endonuclease (Rrp1 PA and PB), the Ligase III partner (XRCC1-PA), two isoforms of poly-(ADP-ribose) polymerase (Parp-PB and PC), poly-(ADP-ribose) glycohydrolase (Parg-PB), and on the other hand a known mitochondrial protein : isocitrate dehydrogenase (idh-PC).

As shown in ***Table13***, two populations of proteins were present. A first group with a high prediction index for nuclear addressing (≥ 75 %) including Rrp1-PA and PB, XRCC1-PA, PARP-PB and PC was observed and a second group (one protein) with a high prediction index for mitochondria (≥75%). Between, these two groups, some proteins were analyzed without any strong predictive index for any locations.

However, we must keep in mind that this predictive approach is based on the presence of consensus sequences in proteins such as NLS (nucleus targeting) or MTS (mitochondria targeting) and that many proteins have been shown to be present in mitochondria without any detectable MTS region.

This first analysis suggested that some of these proteins could be present in *Drosophila* mitochondria. The ***Table 13*** shows PsortII and MitoProtII addressing prediction of certain

protein such as: ogg1, rrp1, xrcc1, parp-B, parp-C, parg-B, Idh-C and RpL32-A from *Drosophila melanogaster* and parp-1 from human. Red color represents very high nuclear addressing prediction and green color very high mitochondrial addressing prediction. ND: non determined.

Name	Addressing prediction		
	Nuclear	Mitochondrial	
FlayBase code	PsortII		MitoProtII
Ogg1-PA	35	22	44
Rrp1-PA	92	ND	19
Rrp1-PB	100	ND	27
XRCC1-	78	9	19
Parp-PB	78	ND	5
Parp-PC	83	ND	2
Parg-PB	61	4	1
Idh-PC	ND	61	90
Human Parp1	67	4	8

***Table 13**: Mitochondrial addressing prediction of some proteins involved in BER mechanism from Drosophila and human species.*

III.→.Base excision repair genes expression in *Drosophila*

III.1 Relative mRNA expression in wild-type context

Using the Flybase database (http://flybase.org/), few BER genes expression (identical to those illustrated in chapter II) was analyzed in young male flies (5 days old). Among the five candidates, Xrcc1 showed the higher level of expression, followed successively by Rrp1, then ParpB/C and PARG and finally Ogg1.

Levels of expression of the same BER candidates were evaluated in 5 days old male flies in order to get a representative pattern of their expression in basal conditions (***Figure 58***). All these values were estimated by RT-q-PCR using Rp49 (Ribosomal protein used as external control of DNA repair systems) as an internal reference. The same expression pattern than that obtained with Flybase data was observed In fact specific gene (glycosylase) displays a lower expression level than those encoding crossroads proteins such as Xrcc1 and Rrp1.

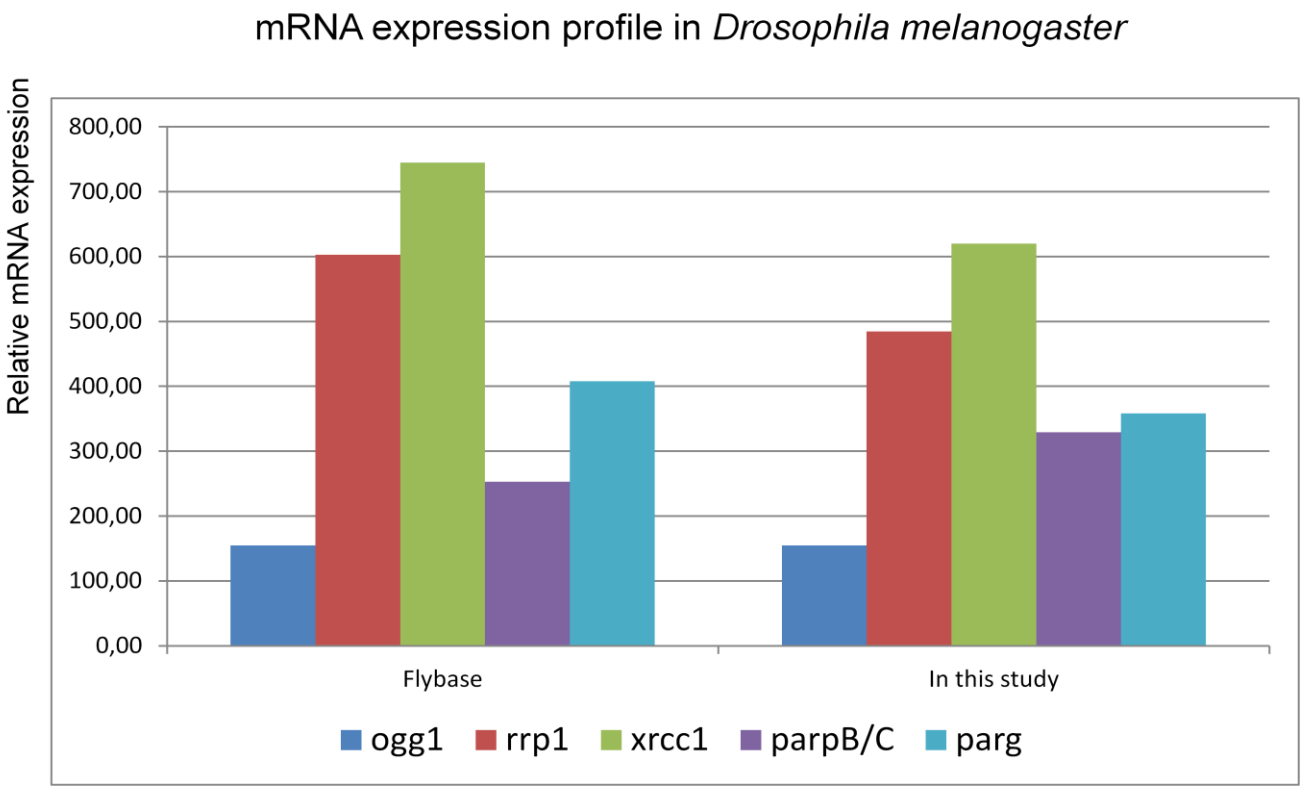

***Figure 58**: Relative mRNA expression of 5 days old male Drosophila melanogaster .from FlyBase Data and in this study RT-q-PCR results (n=3).*

III.2. Relative mRNA expression in ogg1^{-} mutant flies

The ***Figure 59*** shows the relative mRNA expression of ogg1, rrp1, xrcc1, parp and parg in ogg1^{-}(FlyBase code 19122) compared to WT. Ogg1 is very poorly detected with value lower than 5%. This residual expression is not artefactual since the mutant was obtained by an inserted Piggybac transposon element into the *ogg1* gene, resulting into a truncated mRNA and a total disappearance of the protein. rrp1, xrrc1 and parg expressions remain stable compared to levels obtained in wild-type. However Parp expression is almost reduced by 60%.

The DNA glycosylases dOgg1 and RpS3 in *Drosophila* S2 cells are involved in the repair of oxidative damage. Overexpresing of these genes in mitochondria are implicated in apoptosis pathways of S2 cells (**Radyuk SN et al., 2006**).

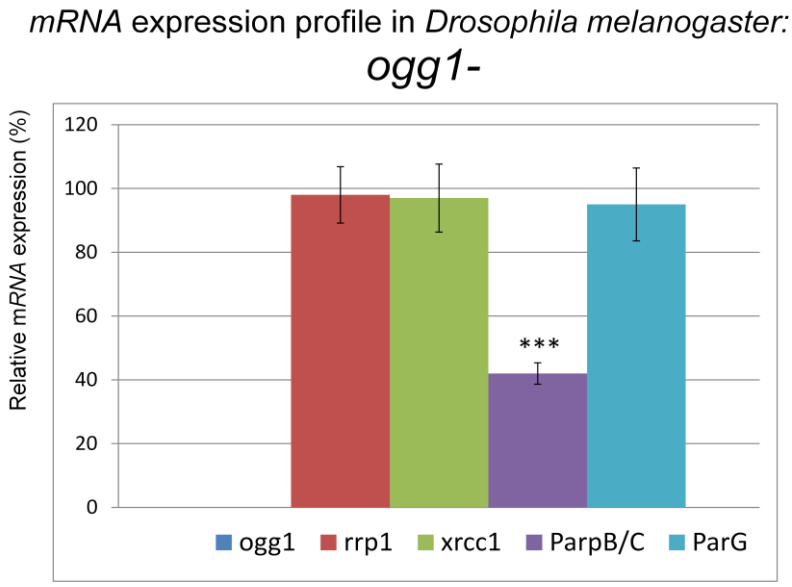

***Figure 59**: Relative mRNA expression of ogg1, rrp1, xrcc1, parp and parg in ogg1⁻ mutants flies compared to WT. The results are the mean ± deviation (Student's test: *** $p < 0.001$). $n = 3$*

III.3. Relative mRNA expression in Rrp1⁻ mutant flies

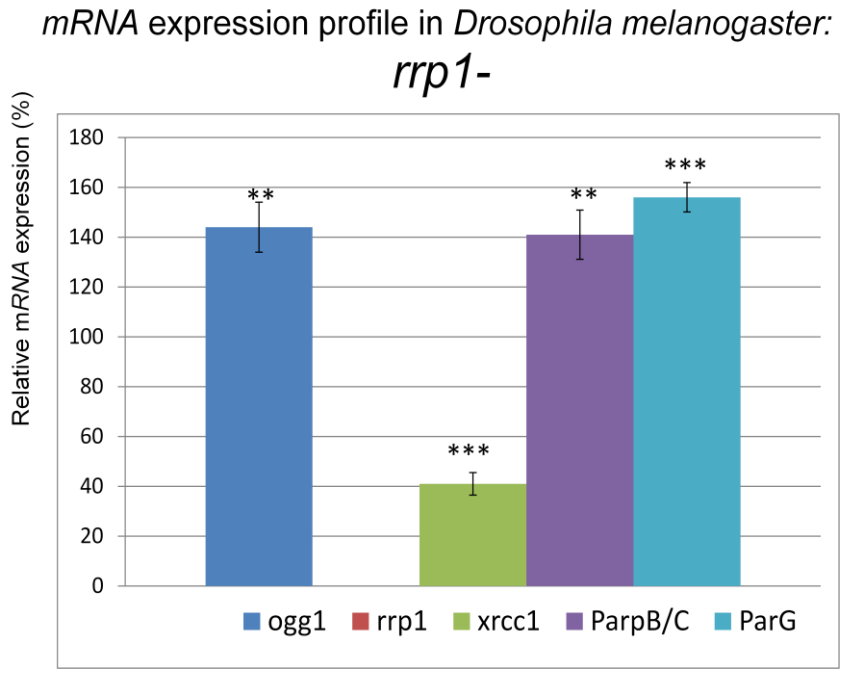

***Figure 60**: Relative mRNA expression of ogg1, rrp1, xrcc1, parp and parg in rrp1⁻ mutants flies compared to WT. The results are the mean ± deviation. Student's test: ***p<0.001, **p<0.01 ,n = 3*

As illustrated in ***Figure 60***, the relative mRNA expression of the six chosen genes in rrp1$^-$ mutants (Flybase code 10213) compared to WT was analyzed. The efficiency of the *Rrp1* knock out was validated by the lack of *Rrp1* mRNA detection. Compared to results obtained with *Ogg1*$^-$ mutant flies, all tested mRNA expressions were increased in the *Rrp1*$^-$ context, by 140 to 160 % except *Xrcc1* that was decreased by 60%. All these changes were highly significant.

III.4. Relative mRNA expression in Xrcc1$^-$ mutant flies

XRCC1 protein is known to be an essential partner for BER processes. This protein presents BRCT domain essential to mediate protein interactions. PARP-1 at sites of DNA strand break facilitates DNA repair by recruiting through BRCT motifs interaction the protein, XRCC1 (**Buelow B et al., 2009 ; El-Khamisy SF. et al., 2003**). Also, Ligase 3 is recruited through BRCT motifs of XRCC1 making strong interactions in the C-termini of these polypeptides during the ligation of newly synthesized strand during the last step of BER processes (**Tomkinson AE, Mackey ZB.,1998**).

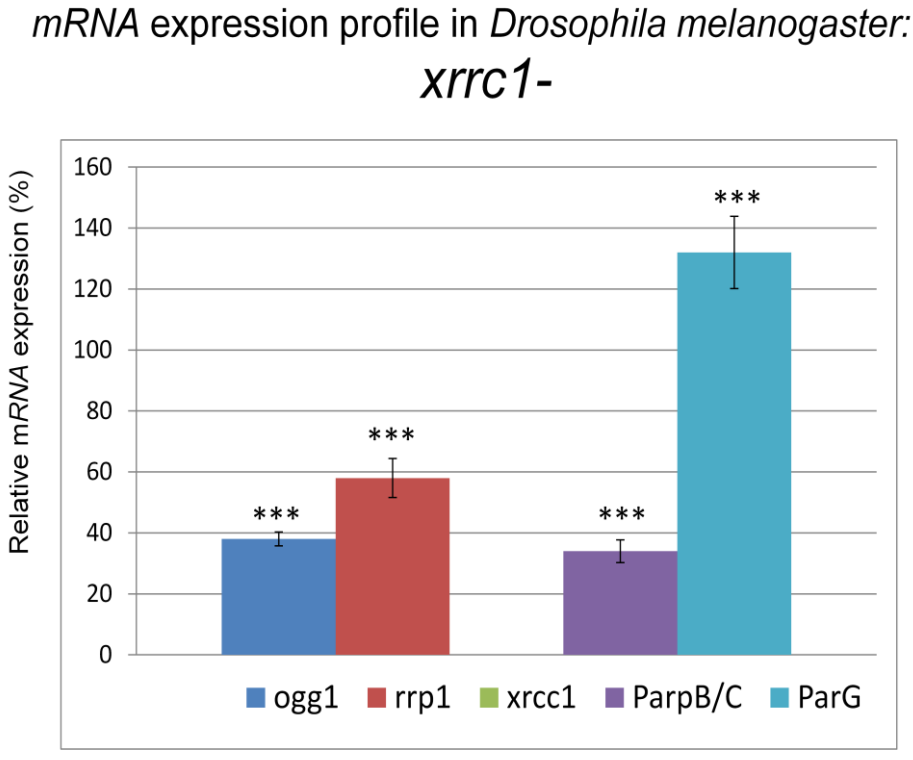

***Figure 61**: Relative mRNA expression of ogg1, rrp1, xrcc1, parp and parg in Xrcc1$^-$ mutants flies compared to WT The results are the mean ± deviation. Student's test: ***p<0.001, n= 3.*

Only *Parg* expression was increased by 130% compared to WT, and all other tested mRNA showed dramatic decreases in their expression levels ranging from 40% (*Rrp1*) to almost 70% (*Parp B/C*). (***Figure 61***)

In order to evaluate interactions between first (glycosylase) and last steps (Xrcc1) processes in the BER pathway and their impact on other partners' regulation, a double knockout was produced.

III.5. ogg1^{-}/xrcc1^{-} double knockout generation

Double knockout (*ogg1*$^{-}$/*xrcc1*$^{-}$) flies were made using as a selection marker the red color eye intensity depending on the PiggyBac copies number present in the genome. Fruitfly parents had pale red color due to Piggybac insertion in a white phenotype background (w^{1118} PBac{WH}Ogg1^{f08013} or w[1118] PBac{w[+mC]=WH}XRCC1[f03685]. Based on eyes color, 3% of total third generation flies were homozygous for *ogg1*$^{-}$/*xrcc1*$^{-}$ mutations

III.6. Relative mRNA expression in ogg1-/xrcc1^{-} double knockout flies

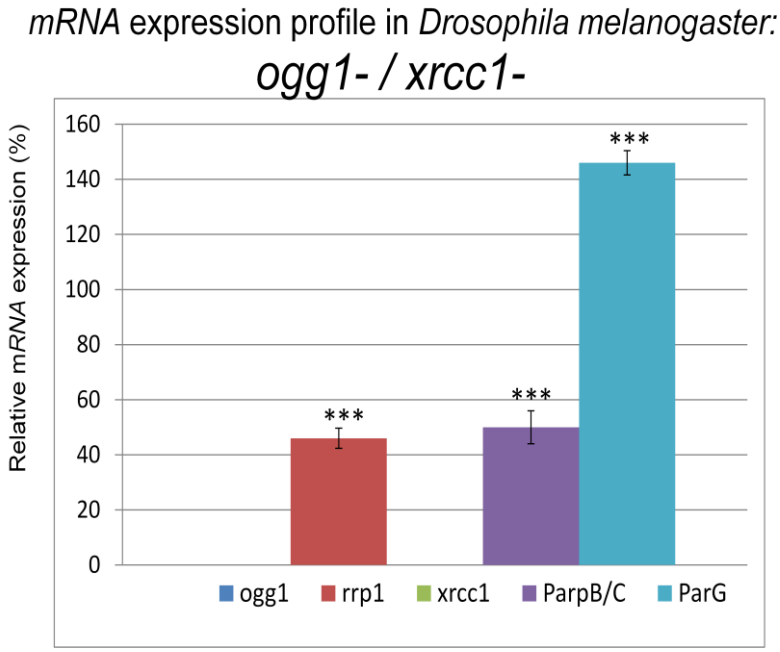

Figure 62: Relative mRNA expression of *ogg1*, *rrp1*, *xrcc1*, *parp* and *parg* in ogg1^{-}/x*rcc1*$^{-}$ mutants flies compared to WT. *The results are the mean ± deviation Student's test:* ***p<0.001 (n = 3).

The reality of the double knockout was confirmed by the lack of *ogg1* and *xrcc1* expression in the tested flies (***Figure 62***). Interestingly, the observed expression pattern was quite similar to that obtained with single xrcc1 knockout strain. A strong decrease in Rrp1 and PARP B/C expression was detected and an increase in PARG expression (+ 145%). Such a behavior suggests that the lack of XRCC1 protein remains a key element in the global regulation process of other BER partners.

IV.→.PARP AS A CANDIDATE FOR MITOCHONDRIAL DNA REPAIR IN DROSOPHILA?

IV.1 PARP isoforms relative expression

In *Drosophila melanogaster*, two different PARP isoforms have been described: PARP B and C. Both of them are transcribed from a single copy gene but PARP-C is a product of an alternative splicing process leading to the removal of exon 5 compared to PARP-B mRNA (**Kawamura T et al., 1998**).

Little information is known regarding either the exact roles for each of these forms or their eventual functional relationships. To help into the understanding of these two PARP isoforms, we started by analyzing the relative expression of both of them in various contexts.

IV.1.1 In whole Drosophila organism

In 5 days old wild type males (***Figure 63***), PARP C expression was 1.5 fold higher than that of PARP B. In the mean time, the expression of PARG mRNA appeared similar to that for PARP B. The same study was performed in *rrp1*$^{-}$(Flybase code 10213) mutant flies. This mutant context was chosen due to the fact that it was the only one displaying an increase in PARP B/C expression.

Our purpose was to investigate the role of PARP B/C or its effects on other BER molecules in *Drosophila*; this is why *rrp1* mutant was chosen with the PARP B/C up-regulation in this genetic background. Interestingly, PARP-C mRNA level remained unchanged compared to PARP-B that was increased by 1.5 fold in mutant flies. In the case of PARG, the observed increase was almost by 170 %.

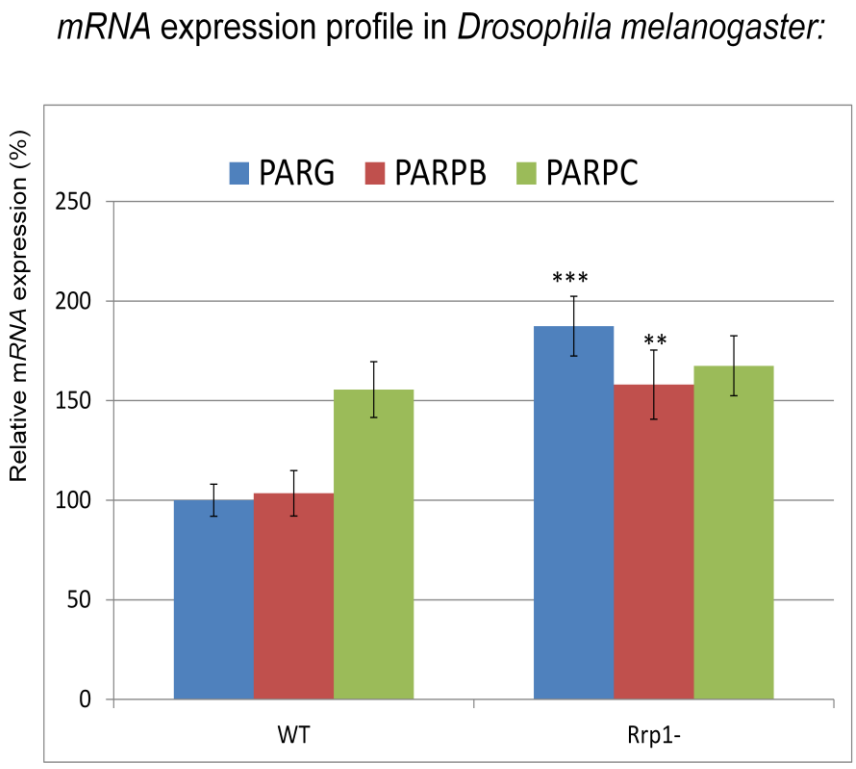

***Figure 63**: Relative mRNA expressions of PARP isoforms and PARG in wild type (WT) or Rrp1⁻ mutant (Rrp1⁻) Drosophila using RT-q-PCR experiments. All values are expressed as percentages using PARG expression level in WT context as a reference. The results are the mean ± deviation Student's test: ***p<0.001, **p<0.01, n = 3.*

IV.1.2. In S2 cells

The same kind of quantification was performed in *Drosophila* derived cell lines: S2 cells in order to get information on a model that could be used further under stress conditions. After RT-q-PCR experiment on mRNA extracted from S2 cells in normal culture conditions, PARP-B and PARP-C level appeared almost identical. PARP-B/PARP-C Expression Ratio (ER) is about 1 (***Figure 64***) compared to ER about 0.7 in WT whole flies.

IV.2. PARP isoforms relative expression in stress conditions

PARP is known in several models to be a key actor during cell responses to various stresses playing roles in DNA repair, apoptosis, and gene transcription (**Shall S. et al., 2000**).

IV.2.1. Copper stress

As a first stress, copper was chosen for its ability to inhibit the repair of some oxidative DNA damages and to interfere with the process of poly-(ADP-ribosyl)ation (**Schwerdtle T et al., 2007**).

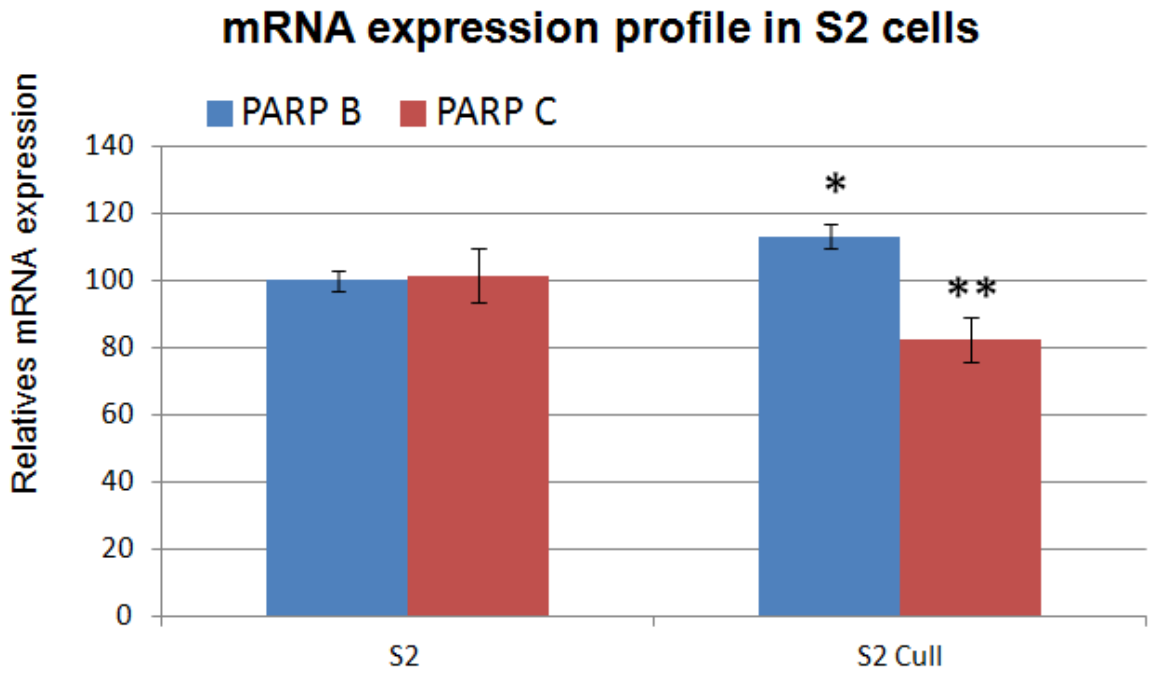

***Figure 64**: Relative mRNA expressions of PARP isoforms in S2 control and S2 under cooper stress using RT-q-PCR experiments. All values are expressed as percentages using PARP B expression level in S2 context as a reference The results are the mean ± deviation. Student's test: *p<0.05, **p<0.01, n = 3.*

In our experiment, after copper incubation (0.7 mM) during 24 hours, PARP-B mRNA levels were increased to 110% and PARP-C mRNA levels depleted by 20%. (***Figure 64***). PARP-B and PARP-C level appeared with ER=1.4 compared with S2 control (ER about 1) with very high significance.

IV.2.2. Oxidative stress

After 40mM H_2O_2 incubation during 30 min, a small increase was noticed for PARP-B and a 40% increase for PARP-C with high significancy. (***Figure 65***) PARP-B/ PARP-C was around 0.8 showing a slight decrease compared to ER in S2 control (approximately 1) without significancy.

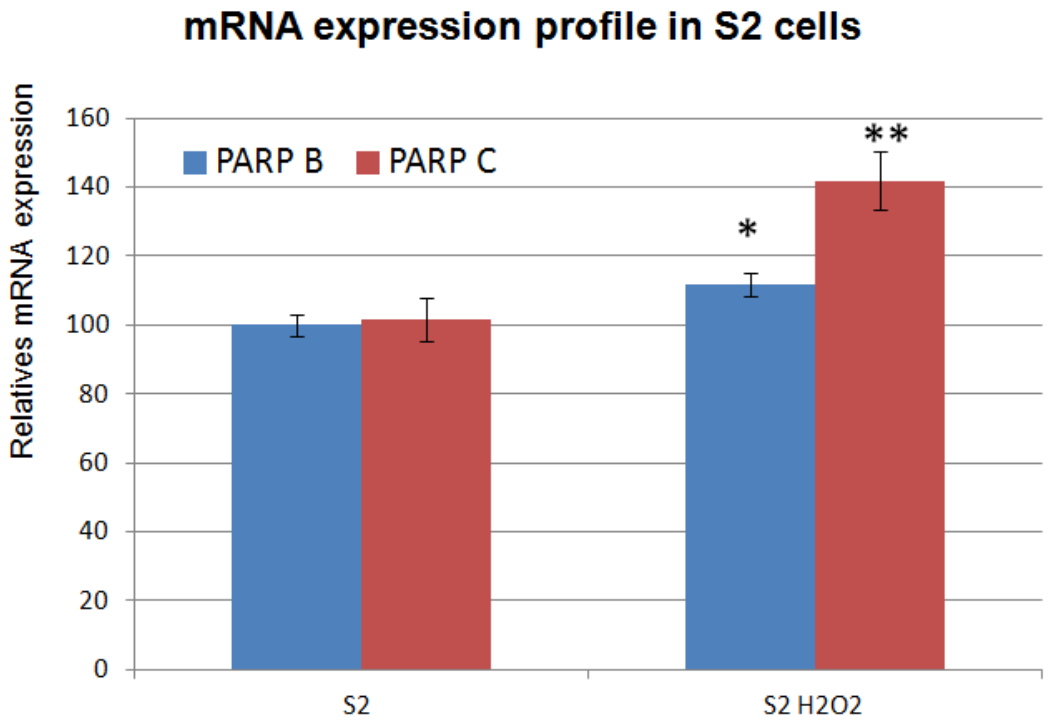

Figure 65*: Relative mRNA expressions of PARP isoforms in S2 control and S2 under H_2O_2 stress. Using RT-q-PCR experiments. The results are the mean ± deviation. Student's test: *p<0.05, **p<0.01 (n = 3).*

IV.2.3 Combination of copper and oxidative stress

Some of the detrimental effects observed with copper are mediated through oxidative stress generation. In the following experiment, incubation was performed with a combination of copper/ H_2O_2.

There is a potentiating effect of both components, illustrated by a 30% increase for PARP-B mRNA levels and by 45% increase for PARP-C with high significance (***Figure 66***).

Nevertheless, PARP-B and PARP-C level were increased but their ER=0.9 was similar to that observed with S2 control (ER about 1).

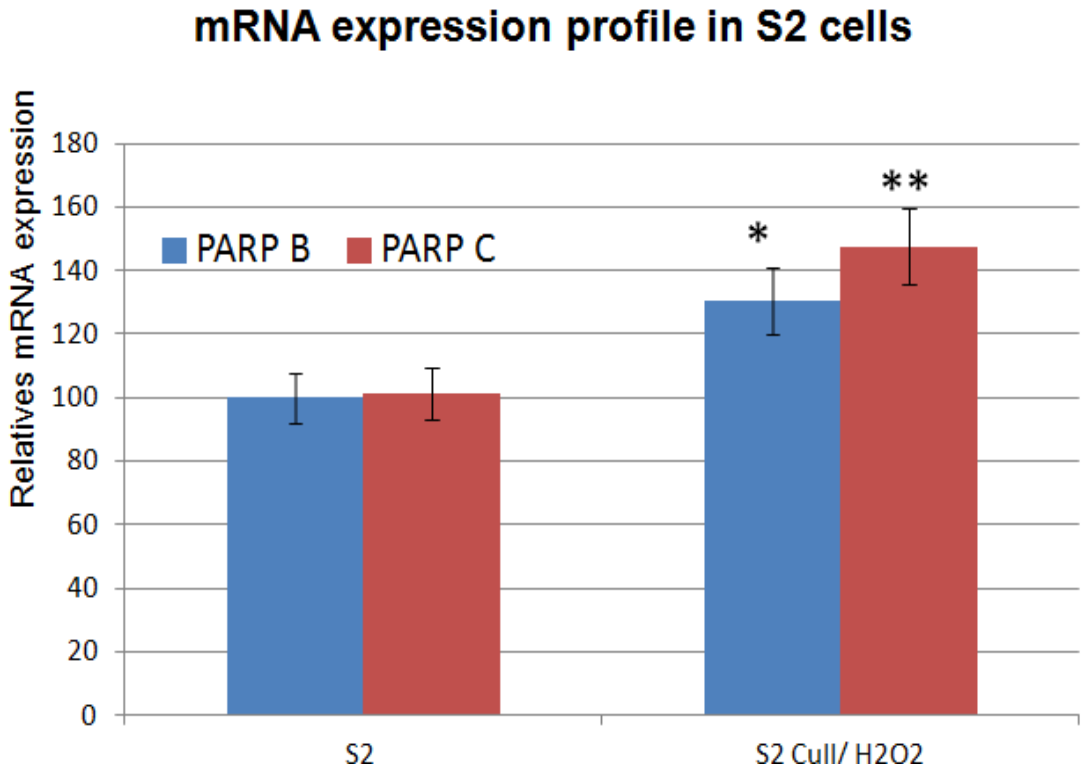

***Figure 66**: Relative mRNA expressions of PARP isoforms in S2 control and S2 under copper/H_2O_2 stress. Using RT-q-PCR experiments. The results are the mean ± deviation. Student's test: *p<0.05, **p<0.01 (n = 3).*

IV.3. PARP isoforms relative expression after stress and recovery

After copper/H_2O_2 stress followed by 30 minutes recovery in normal medium, a decrease was observed for PARP-B (-38%) and for PARP-C (-52%) mRNA levels. However, ER remains unchanged compared to S2 cells in control conditions (***Figure 67***).

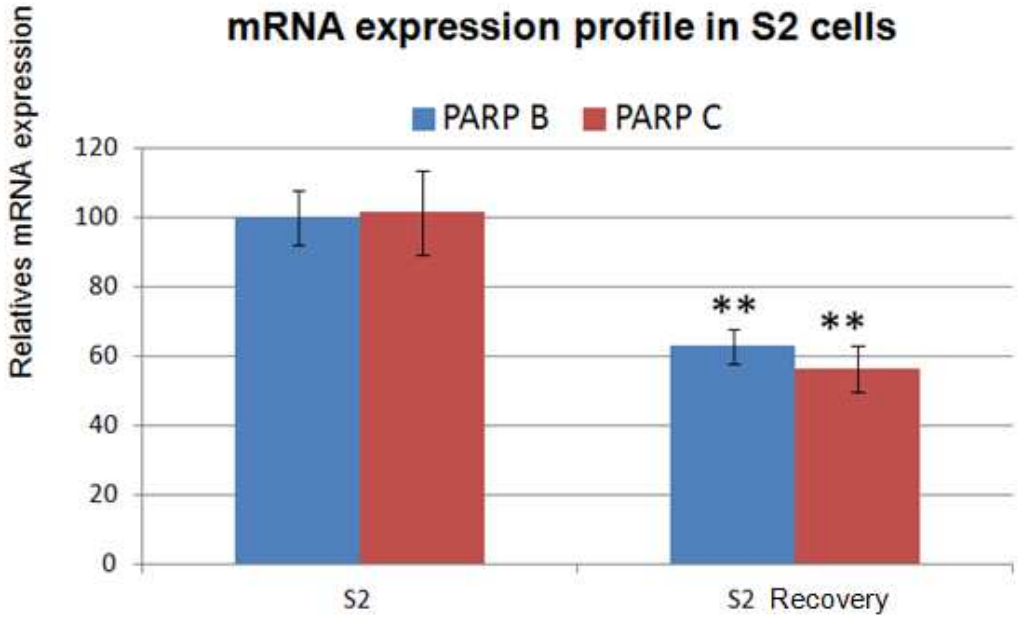

Figure 67*: Relative mRNA expressions of PARP isoforms in S2 control and S2 after copper/H_2O_2 stress S2 DNA repairing). The results are the mean ± deviation. Student's test, **p<0.01 (n = 3)..*

IV.4. Subcellular PARP localization in Drosophila melanogaster model

In order to get a precise view of PARP sub-cellular localization in S2 cells, specific constructs were generated in pMT-puro expression vectors (***Annexes 2***). All the obtained constructs are illustrated in annexes. The cloning procedure was described in the Materials and Methods chapter.

IV.4.1. Expression vectors and transfection in S2 cells

Two constructs were generated in pMT-puro vector. The first one encodes a PARP fusion protein with a V5 tag (***Figure 52***) at the C-terminus end of the protein and will be used for immunodetection in Western blot analysis but also for ¨*in situ*¨ localization of PARP protein. The second construct encodes a PARP-GFP (***Figure 53***) fusion protein to characterize ¨*in situ*¨ the subcellular localization of the PARP protein. Both inserts have been tested through enzymatic digest (***annexes 6***), then fully sequenced (***annexes 7; annexes 8***). They appear conform to the expected sequences. These plasmids were transfected into S2 cells. The stable cell lines obtained after puromicin selection were named J2 and C4 according to the name of transfected plasmids. Genomic integration and mRNA expression of parp-B-V5 and parp-B-GFP were validated by PCR amplification from genomic DNA and from total RNA extraction.

IV.4.2. PARP subcellular localization

IV.4.2.1. PARP PB in basal conditions

The first set of experiments was performed on S2 cells in basal conditions. In ***Figure 68***, using IDH-GFP construct as a positive control, a punctuated signal was observed in the cytosol and co-localized with Mitotracker staining, suggesting a mitochondrial localization.

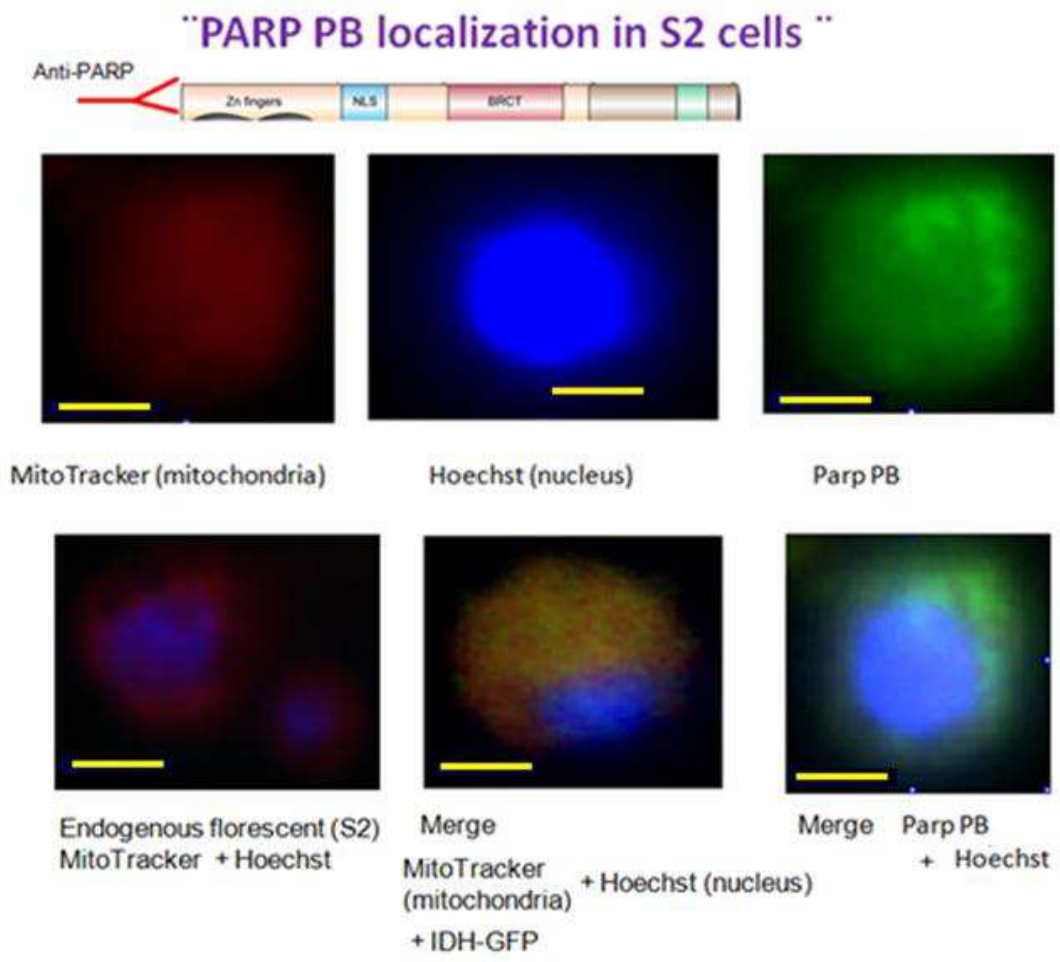

Figure 68*: Mitochondria were identified in red color by MitoTracker detection, nucleus in blue color with Hoechst reactive and parp-B was identified in green color using antibody anti-parp-alexa488. S2 untransfected cells were used as a negative control (Merge MitoTracker + Hoechst). The scale of picture dimension was represented with yellow line of 2.5 µm (n = 3).*

Endogenous PARP molecule was detected through the use of specificic polyclonal anti-PARP antibodies. A strong positive punctuated signal was observed in the cytosol region. However, Mitotracker staining appeared more diffuse within the cell. A very faint signal appeared in the nuclear region in the merge part of the ***Figure 68***.

IV.4.2.2. PARP PB-V5 under copper induction

In a second set of experiments (***Figure 69***) , PARP was overexpressed in S2 cells and detected through the use of antibodies directed against the V5 tag of the fusion protein.

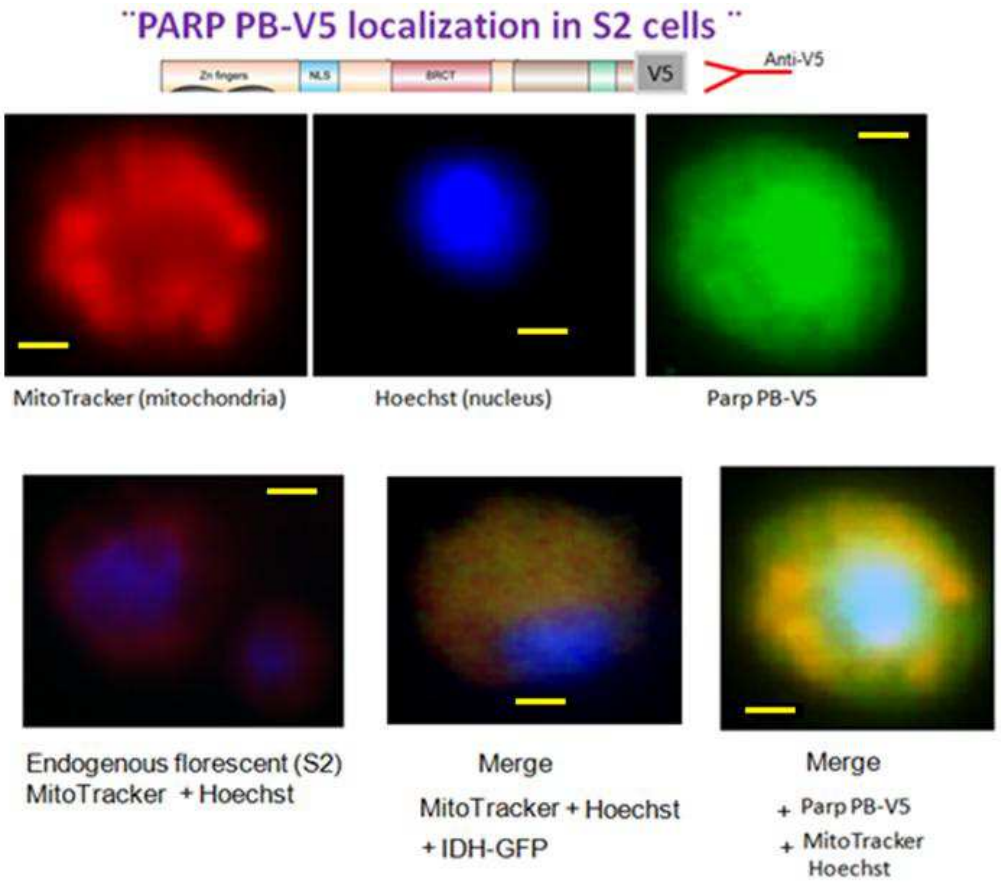

Figure 69*: Mitochondria were identified in red color by MitoTracker detection, nucleus in blue color with Hoechst and parp-B-V5 was identified in green color using antibody alexa488 anti-V5 monoclonal antibody S2 untransfected cells were used as a negative control (Merge MitoTracker + Hoechst). Isocitrate dehydrogenase was used as a positive control for mitochondrial addressing (IDH-GFP). The yellow bar indicates 2.5 µm, n = 3.*

With this procedure, a peripheral MitoTracker detection was observed, but also a co-localisation with ParPB-V5 suggesting at least, a partial mitochondrial presence of PARP. In the mean time, a nuclear signal was also observed for the recombinant protein.

IV.4.2.3. Parp PB-GFP under copper induction

Using the same strategy, but with a PARP-GFP fusion protein (***Figure* 70**), a strong positive GFP signal was observed in the nucleus. However, a green but faint signal was also co-localized with MitoTracker in a diffuse manner in the cytosol, suggesting once again a potential mitochondrial localization.

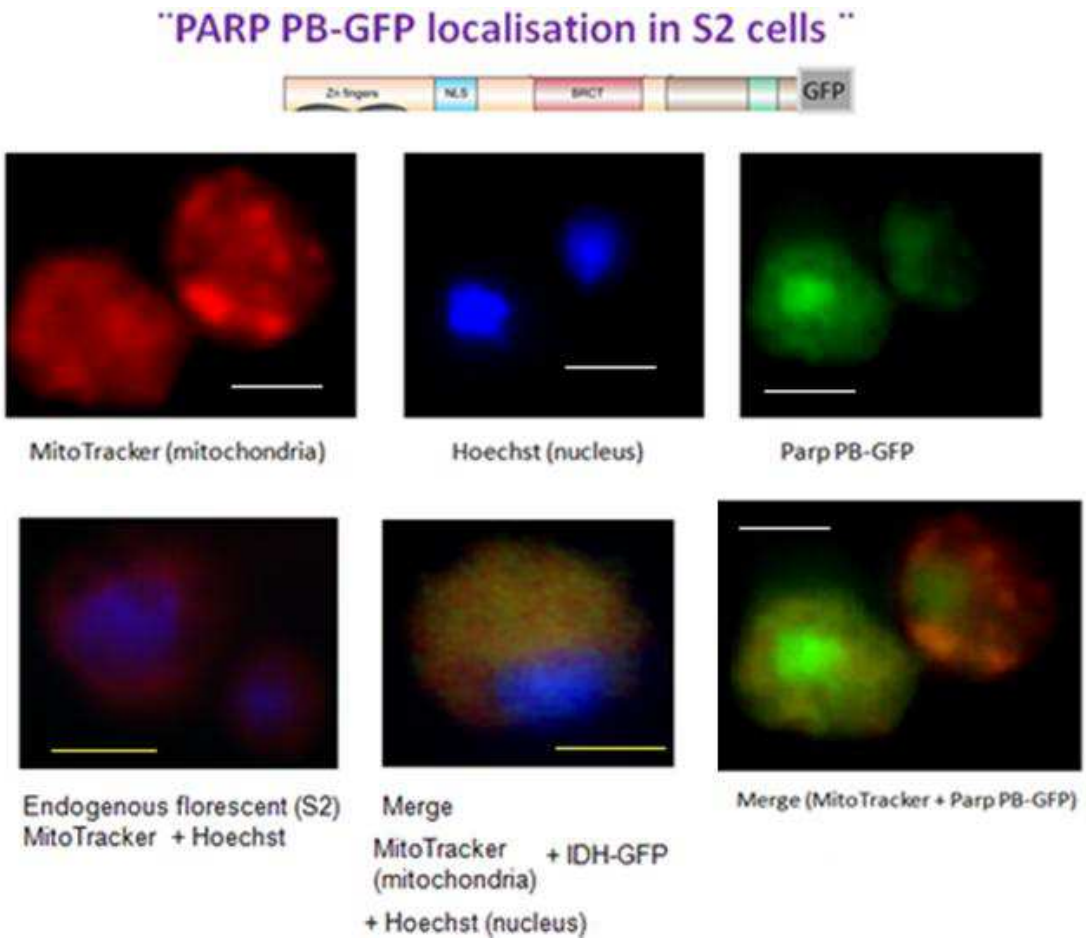

***Figure 70**: Mitochondria were identified in red color by MitoTracker detection, nucleus in blue color with Hoechst reactive and Parp-B-GFP was identified in green color thanks to GFP signal). S2 untransfected cells were used as a negative control (Merge MitoTracker + Hoechst). Isocitrate dehydrogenase was used as a positive control for mitochondrial addressing (IDH-GFP). The yellow bar indicates 3.5 µm. n = 3*

IV.4.3. PARP subcellular localization under oxidative stress

IV.4.3.1. PARP PB

In order to create redox imbalance within the cells but also to induce DNA damage in the mean time, S2 cells were incubated with hydrogen peroxide. This experiment was performed to determine if oxidative stress induces PARP relocalisation within treated cells.

In basal S2 cells, a strong positive signal corresponding to endogenous PARP, was detected in the nuclear region, but also a green faint signal was observed partly co-localized with MitoTracker in a diffuse manner within the cytosol ***(Figure 71)***

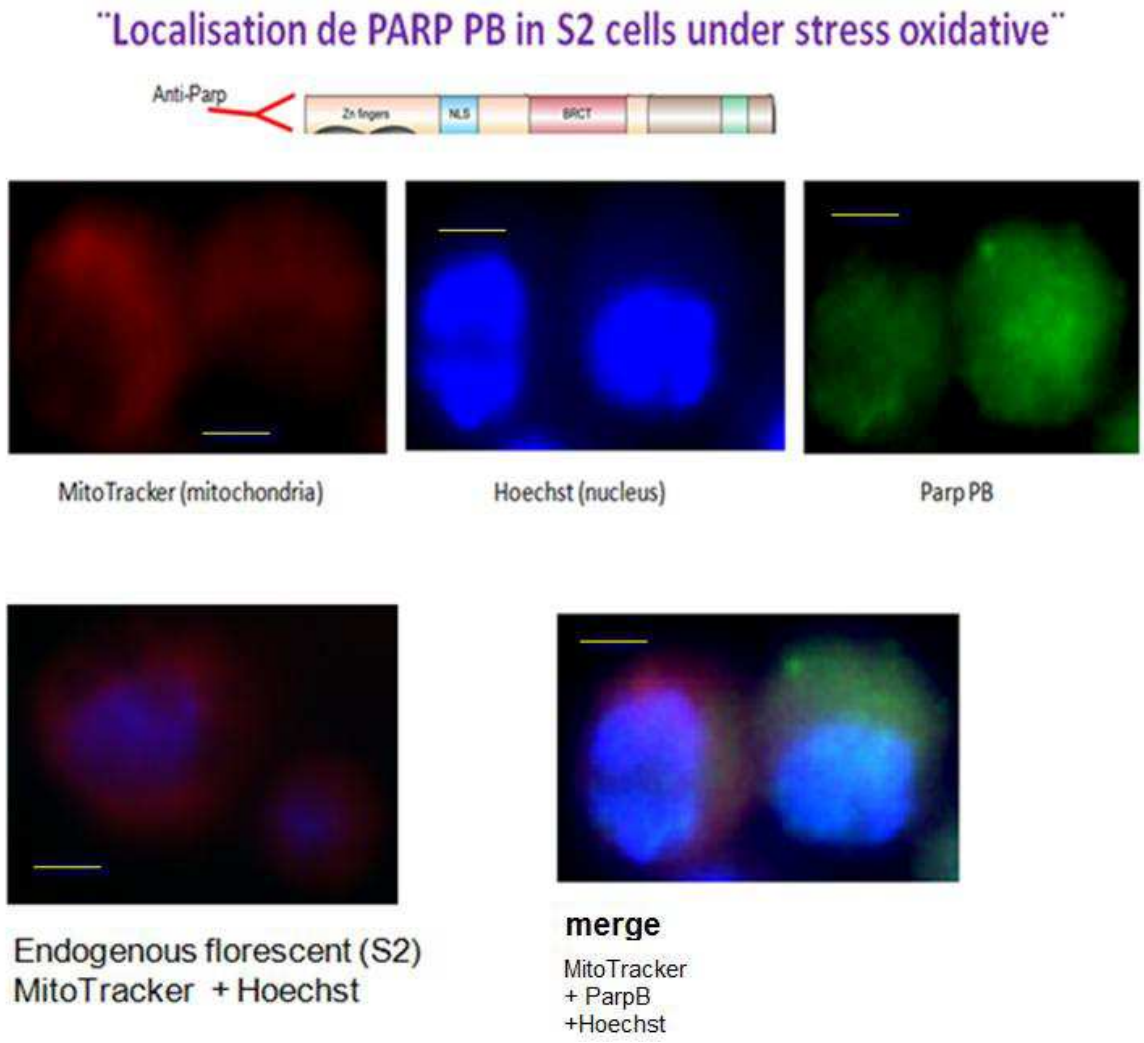

Figure 71*: Mitochondria were identified in red color by MitoTracker detection, nucleus in blue color with Hoechst reactive and Parp-B-GFP was identified in green color thanks to GFP signal). S2 untransfected cells were used as a negative control (Merge MitoTracker + Hoechst). Isocitrate dehydrogenase was used as a positive control for mitochondrial addressing (IDH-GFP). The yellow bar indicates 2.5 µm. (n = 3)*

IV.4.3.2. PARP PB-V5

In PARP overexpressing cells under oxidative stress exposure (***Figure 72***), signals were observed mainly in a diffuse manner within the cytosol, with partial co-localisation with MitoTracker probe.

However, no clear nuclear localization was detected. To summarize all these data, PARP in S2 cells was mainly localized in nuclear compartment, but also present at a lower level in the mitochondrial surroundings. A PARP overexpression led to a higher nuclear targeting, but maintained the signal in "mitochondria".

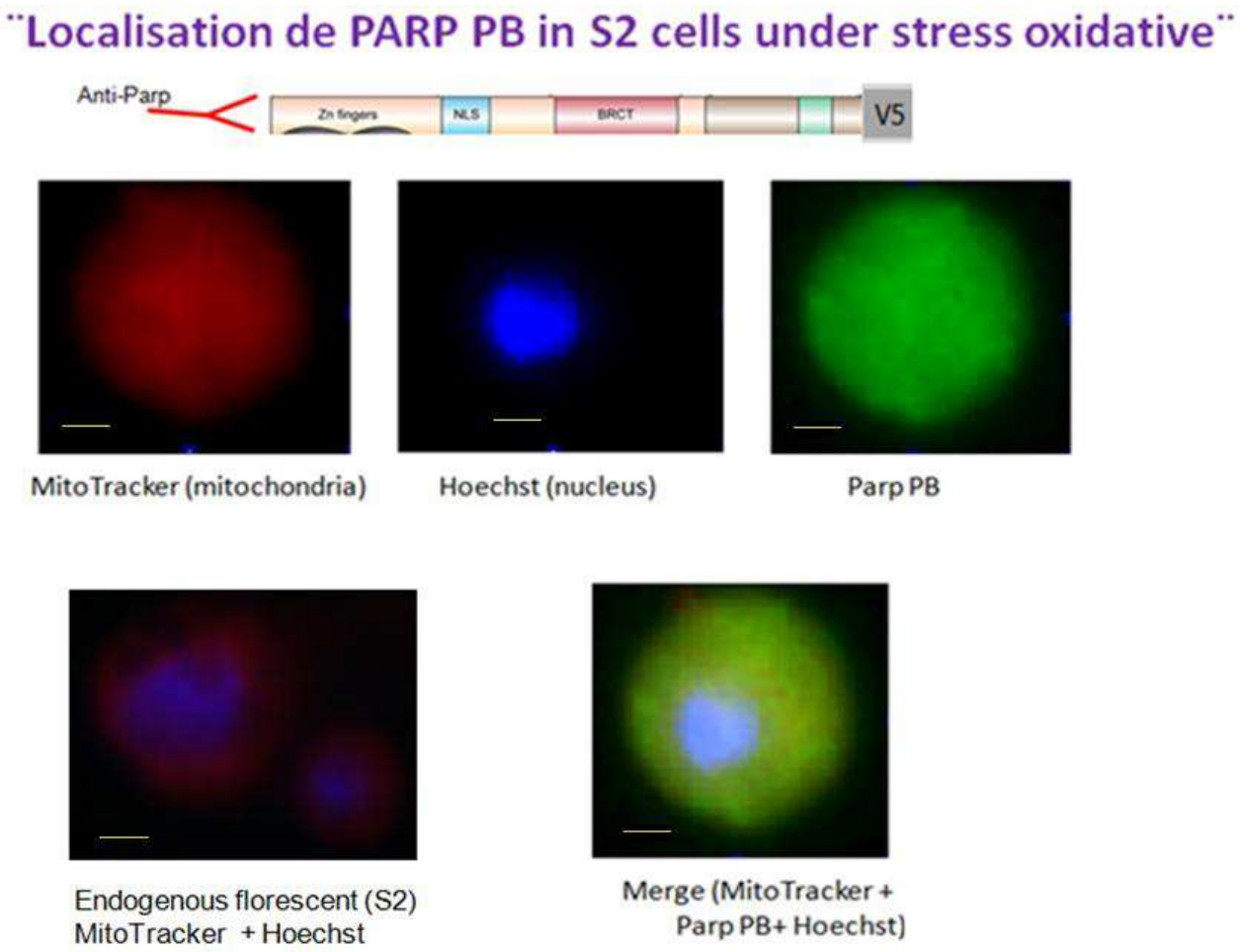

Figure 72*: Mitochondria were identified in red color by MitoTracker detection, nucleus in blue color with Hoechst reactive and Parp-B-GFP was identified in green color thanks to GFP signal). S2 untransfected cells were used as a negative control (Merge MitoTracker + Hoechst). Isocitrate dehydrogenase was used as a positive control for mitochondrial addressing (IDH-GFP). The yellow bar indicates 2.5 µm. n = 3*

Some PARP trafficking occurred in hydrogen peroxide exposure with a decrease in nuclear localization towards more diffuse cytosol localization.

IV.5. Sub-cellular fractionation and PARP detection

In order to confirm the results obtained by microscopy, another approach was performed using sub-cellular fractionation followed by Western-blot analysis on pure fractions.

Two sub-cellular fractions were tested: nuclear and mitochondrial fractions (***Figure 73***). Prior to further analyses, samples were qualified on purity basis. All mitochondrial samples did not show any histone protein suggesting the lack of nuclear contaminants.

On the opposite, nuclear samples still displayed pyruvate dehydrogenase (PDH) signals except for sucrose treated fractions. Using a specific PARP polyclonal antibody, two faint populations were observed in nuclear fractions purified (115 and 80 kDa).

As well, crude nuclear fraction presents very low quantity of PARP. In mitochondrial extracts, only low molecular weights proteins were detected at 70 and 80 kDa. These results were observed either with crude or purified fractions.

These results confirmed those obtained by ¨*in situ*¨ detection on mitochondrial localization but also showed for the first time the presence of different PARP isoforms between nuclear and mitochondrial compartments.

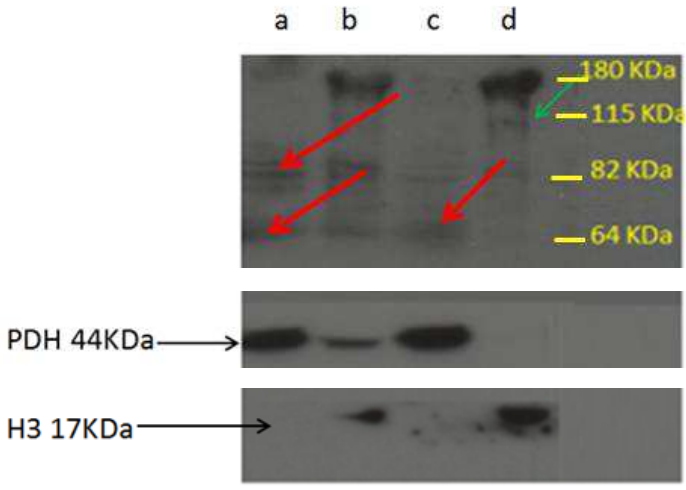

Figure 73*: Western blot analysis of PARP isoforms in subcellular fractions from Drosophila. (a) crude mitochondria, (b) crude nucleus, (c) purified mitochondria, (d) purified nucleus. The red arrows show the main proteins identified in mitochondrial samples and green arrow the protein visualized in nuclear sample.*

Using S2 recombinant cells overexpressing PARP-V5 and PARP-GFP, a new Western blot analysis was performed with either anti-PARP or anti-V5 antibodies.

As shown on ***Figure 74*** on the left, PARP antibodies detected only one faint protein band around 82 kDa in S2 cells, but a strong signal at similar molecular weight was observed for transfected cells (PARP-V5 or GFP). Surprisingly, such a band with identical molecular weight was also seen with anti-V5 antibodies.

Figure 74*: Western blot analysis on S2 cells extracts using either anti-PARP (left) or anti-V5 (right) antibodies. (a) J2 cells (S2 cells transfected with parp-B-V5) after 0.7mM cooper incubated 24 hours, (b) J2 cells after 24h incubation with 0.7mM copper followed by 40mM H_2O_2 during 30 min, (c) C4 cells [S2 cells transfected with parp-B-GFP] after 0.7mM cooper incubated 24 hours, (d) S2 cells in basal conditions. The red band corresponds to the 70KDa band (Prestained Protein Ladder; thermo scientific)*

The molecular weight (MW) of 82 KDa observed in ***Figure 74*** is not according with any PARP isoforms referenced in literature but also their MW of 113 KDa and 92 KDa are not show until nowdays.

IV.6. Mass spectrometry analysis

To confirm, the PARP nature of these various proteins, LC-MS/MS analyze was made where the samples selection was carried out on proteins extracted according to western blot results of ***Figure 73*** from an SDS-PAGE after colloidal blue staining (***Figure 75***).

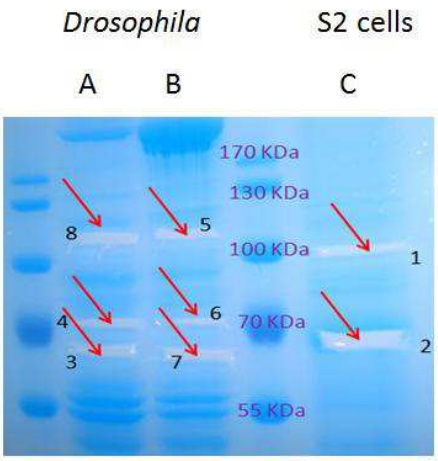

Figure 75*: Protein coloration in gel using coomassie Brilliant Blue (A) Mitochondria fraction from Drosophila, (B) Nuclear fraction from Drosophila, (C) J2 cells extract after 24 hours incubation with 0.7mM copper . Red arrows show the bands (1,2,3,4,5,6,7,8) analyzed by mass spectrometry.*

After mass spectrometry analyses, no PARP detection was observed from derived peptides for all the 8 samples, leading to the question of the exact nature of these bands. The samples analyzed were obtained without anti-proteases in extraction buffer and also any protein purification protocol was adapted to PARP protein.

IV.7. Potential caspase cleavage sites in PARP

In normal cells, PARP behavior is modulated through various post-translational modifications. Among them, poly-(ADP-ribosylation) and inactivation by caspase cleavage are well known (**Boulares AH, et al.,1999**). In this chapter, we investigated Drosophila PARP potential to be cleaved by caspases.

IV.7.1. Human Parp-1

Human Parp1 can be cleaved by caspase 3 and_7 in position 214 and by caspase 1 in position 800 (from N terminus) (***Figure 76***). Both cleavages show identical profile of 24KDa and 89 KDa.

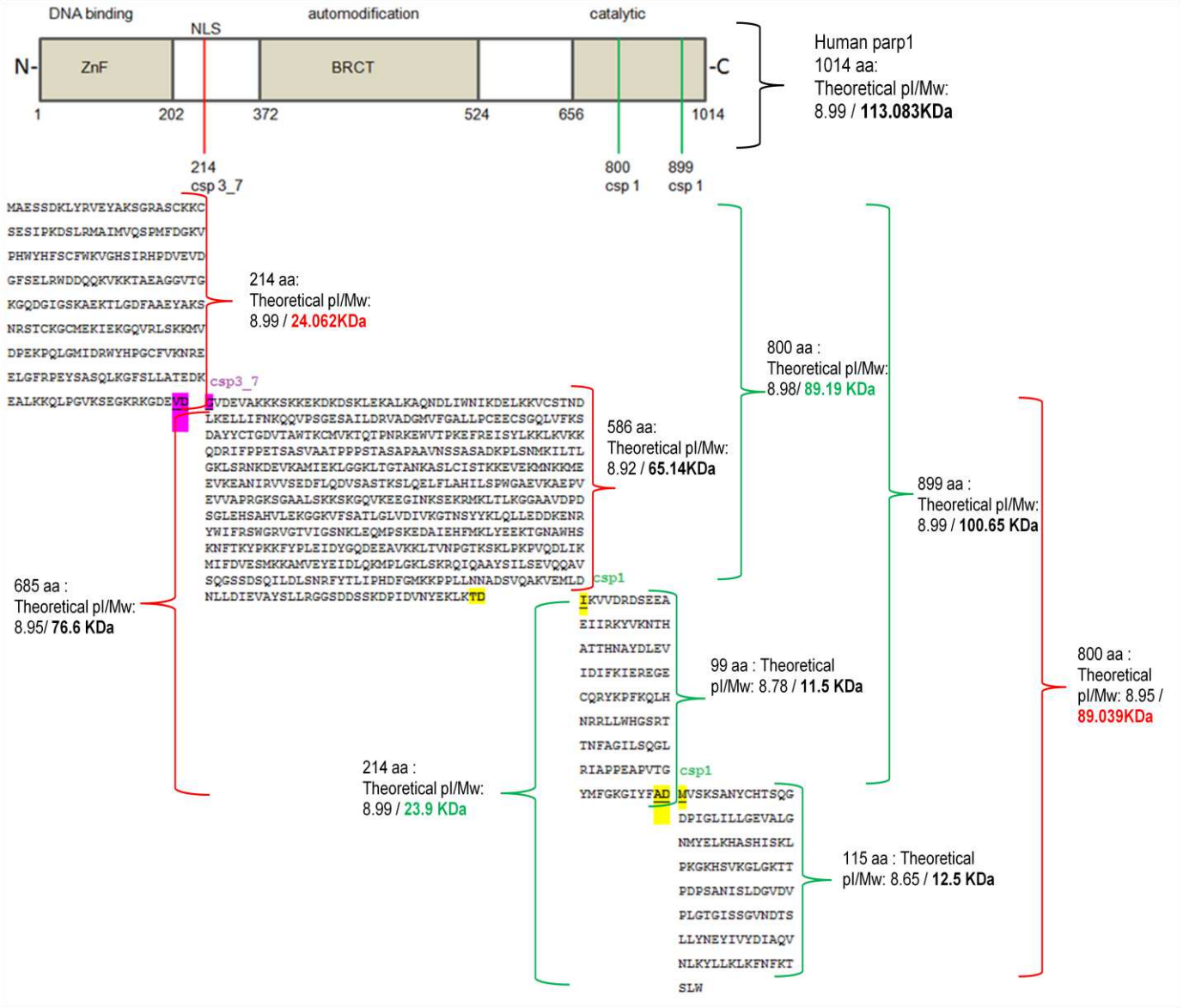

***Figure 76**: Schematic hypothetical hydrolysis of human parp1 by caspases. Red color represents caspase 3 and 7 action and green color caspase 1 action.*

IV.7.2. Recombinant protein Parp-B-V5-(Hist)$_6$

Recombinant protein Parp-B-V5-(Hist)$_6$ from drosophila can be cleaved by caspase 1 in positions 275, 544 and 881 (from N terminus) (***Figure 77***). The caspase 1 digestion profile gave peptides about 32 KDa, 62 KDa, 100 KDa. All of them conserved Parp epitope for the recognition of the protein by Santa Cruz antibody used in our experiments. Other peptides about 16 KDa, 55 KDa, 82 KDa conserved the anti-V5 and anti-Hist6 epitopes.

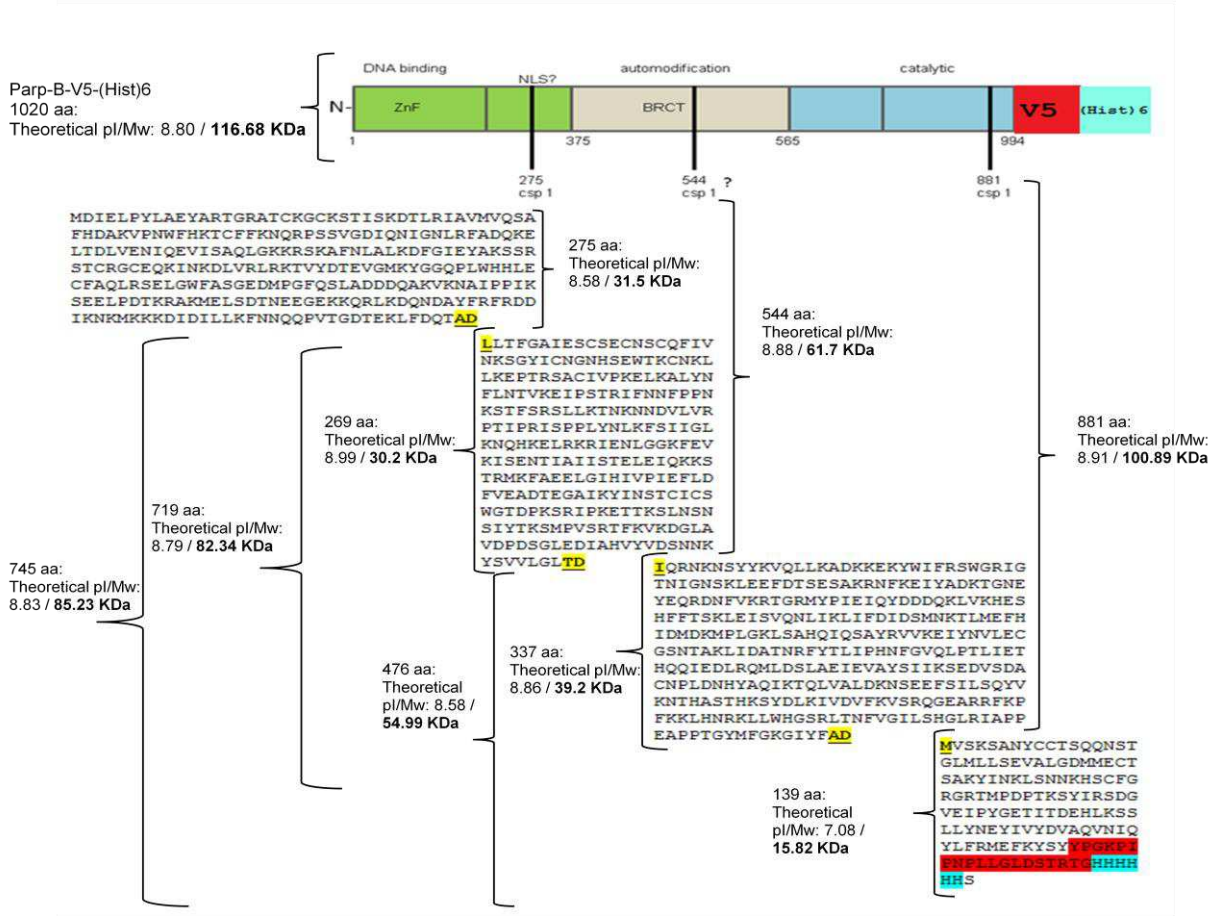

***Figure 77**: Schematic hypothetical parp-B-V5-(Hist)$_6$ hydrolysis by caspase1.*

V.→.Production of recombinant PARP protein

The production of PARP protein was planned to have a tool to:

- Investigate the molecular weight of a standardized PARP protein
- Generate polyclonal antibodies against the whole PARP protein

The pBAD24 expression vector was chosen to produce PARP-B in *E. coli*. The construct used is illustrated (***annexes 3***) and was fully sequenced (***annexes 9***). It appeared conform to the expected PARP sequence After recombinant *E. coli* generation and PARP protein induction through L-arabinose incubation, extract was purified on His-Trap column and subsequent fractions were analyzed by western blot using an anti-His antibody.The ***Figure 78*** represents parp-B-His$_6$ expression in *E. coli*. The western Blot (WB) anti-Histidine was made with bacterial extracts, fraction 1 and fraction 2 following purification on affinity column. In every sample, a single protein with a molecular weight of 85 kDa was detected.

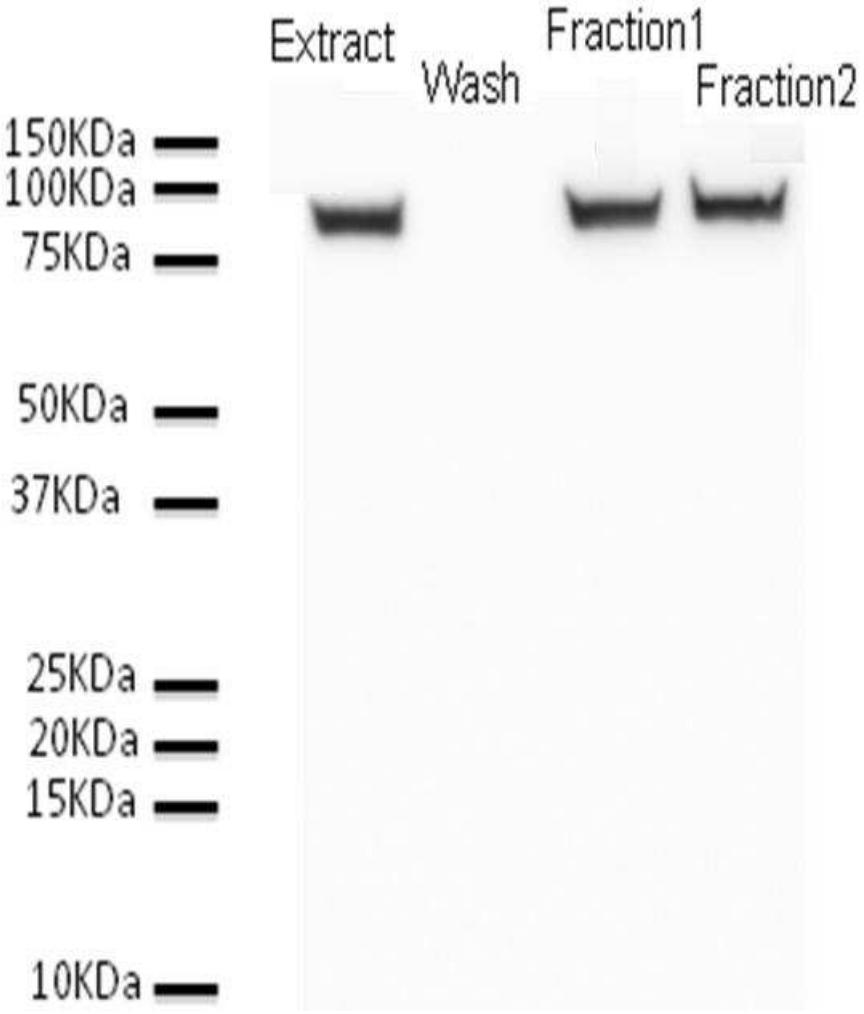

***Figure 78**: Western Blot on various protein fractions from bacteria overexpressing PARP protein (extract) and from purified fractions (fractions 1 and 2). "Wash" fraction represents the washing buffer after passage through the columnn; n=1*

DISCUSION

I.→.BER activities in mitochondria

Research on mtDNA repair mechanisms goes back many years, and numerous studies have characterized mitochondrial BER activities, especially glycosylases (**Dianov GL et al., 2001 ; Maynard S. et al., 2010 ; Boesch P et al., 2011**). The most frequent method used to identify and characterize these activities was based on the excision of a modified oligonucleotide carrying a ^{32}P label, followed by electrophoresis and autoradiography (**Gredilla R. et Stevnsner T.., 2012**). Such an approach appeared less suitable for comparison of BER activities between various samples.

The use of a microarray technology, which has already been tested and validated (**Pons B et al., 2010**) on nuclear BER activities could constitute a powerful analytical tool for another subcellular compartment. However, due to the specificity and sensitivity of this technique, a mitochondrial purification procedure has been developed to remove any nuclear residual contaminant. This protocol has been validated through the detection of specific protein components from each compartment. It has also been chosen due to its ability to preserve inner mitochondrial activities.

We demonstrated that crude mitochondrial fractions displayed strong excision abilities for EthA, Tg, U (paired with G) and THF (abasic sites). However, other base modifications resulting from ROS oxidation were slightly or not recognized by all the mitochondrial fractions. Interestingly, repair activities observed with purified mitoplast fractions were both qualitatively and quantitatively equivalent to those measured with crude mitochondrial fractions, but also revealed more discrete activity (U paired with A).

In purified nuclear fractions, repair activities were partly different from those observed with mitochondria. THF and U (paired with G) were still strongly recognised as already described for human nuclear extracts (**Prasad SC et al., 1992**). Compared with mitochondria samples, Hx and A (paired with 8oxoG) excision activities were high, but EthA and U (paired with A) excision activities were less noteworthy for the mitochondrial counterparts.

High abasic site excision activities in nuclear or mitochondrial fractions were not surprising. This is in fact the middle step of the base excision repair process following specific glycosylase action detecting and removing modified bases. The new phosphate-

deoxyribose bound in the resulting abasic site is then processed by apuric/apyrimidic (AP) endonuclease such as APE1 enzyme in mammals (**Tsuchimoto D et al., 2001**), which is active not only in nuclei, but also in mitochondria. A heterologous protein RRP1 has been characterized in the fruitfly in the nucleus (**Sander M, et al., 1991**), but its mitochondrial location was still unknown.

EthA and Tg alterations were also strongly recognised with both compartments extracts. They arise from ROS attack on adenine and thymine residues, which are both highly abundant in mtDNA particularly in the AT-rich sequence (**Anderson S, et al., 1981**). EthA results from lipid peroxidation (**Speina E, et al., 2003**). These etheno adducts are recognized by MPG (methyl-purine glycosylase) (**Asaeda A et al., 2000**). Neil 1, 2 and 3 glycosylases could also metabolize modified adenine and guanine. They have been identified in nuclei and also detected in mitochondria (**Hu J et al., 2005 ; van Loon B et Samson LD., 2013**). Tg is the main thymine oxidative product of ROS exposure (**Dianov GL et al., 2000**).

We found in our present study that the thymine glycol removal was quantitatively strong in purified mitochondria and higher than that observed in purified nuclei. Some reports have shown that the bifunctional glycosylase NTH1 may be responsible for Tg recognition and excision in mice (**Karahalil B et al., 2003**).

Uracil (paired with A), often encountered in DNA may result from incorporation of dUMP during replication, or be the consequence of cytosine oxidative deamination by ROS, resulting in U:A pairs or U:G mismatch. This DNA damage is controlled by different UNG glycosylases. In humans, two UNG transcripts produced by differential splicing give rise to a nuclear and a mitochondrial (**Nilsen H et al., 1997**). This glycosylase may be the only one able to process uracil residue in mitochondria. In fruitflies, mitochondrial location of this protein was still unknown.

In our experimental conditions, on one side no A removal paired with 8oxoG was detected with crude mitochondrial fractions or pure mitoplast fractions. Also, this activity was quite high in nuclear fractions (27% excision rate in young fruitfly nuclear fractions). In mammals, MYH enzyme catalyzed this activity and has been detected in both nuclear and mitochondrial extracts (**Karahalil B et al., 2003**). To our knowledge, this activity has never been described in fruitfly mitochondria.

On the other side, 8oxoG removal was not observed in our study in mitochondrial compartments, despite the fact that many studies have pointed out high 8oxoG excision activity in mitochondria (ie from mouse liver (**Sander M et al., 1991**). The lack of this activity in mitochondria in our study could be the result of a low recognition in our conditions of the modified oligonucleotide attached on the microarray or a low activity in *Drosophila* mitochondria.

In a previous study, we described the process of aging in *Drosophila melanogaster* 8 weeks after emerging (**Dubessay P. et al., 2007**). mtDNA mutations frequently increased during aging (**de Souza-Pinto NC et al., 2001**). This could be correlated with an increase in ROS production (**Lee HC. et al., 2012**) but also, repair mechanisms involved in DNA maintenance might be concerned.

Our results effectively showed changes in repair activities in both nuclear and mitochondrial fractions during aging. AP site cleavage decreased in mitochondrial fractions. By contrast, we observed an increase in U (paired with G) excision.

In nuclear fractions from old fruitflies, excision activities of A, 8oxoG, and Hx declined significantly. The same results were observed for U (paired with G) and 8oxo G-C, but were not significant. Further, no nuclear glycosylase activity was increased during aging in fruitfly. In mouse liver mitochondrial fractions, a high 8oxoG excision activity increase was observed during aging, while a decrease was noted with nuclear extracts (**de Souza-Pinto NC et al., 2001**).

Other measured activities such as U-G glycosylase and endonuclease did not change in either compartment.

Most of the observed activities were a consequence of the presence of specific mitochondrial isoforms from various BER glycosylases. In silico analyses were performed to investigate the ability of candidates proteins to be involved in such activities. These proteins were described in several organisms mitochondria but it was less known for drosophila model.

II.→.Mitochondrial addressing predictions

In *silico* analysis of mitochondrial addressing prediction of certain proteins from *Drosophila melanogaster* involved in BER pathway would help to understand the addressing

footprints in protein that maybe play a role in mtDNA repair in extending Drosophila model until human. According to ***Table 13*** mitochondrial addressing studies were made using PSORT II and MitoProtII predictors. Certain proteins from *Drosophila melanogaster* such as OGG1, RRP1, XRCC1, PARP-B, PARP-C, PARG-B were analyzed.

The 100% of nuclear addressing was reported to Rrp1-PB considered as negative control of mitochondrial addressing. The RpL32-A (named Rp49) was the mitochondrial positive control with 100% of mitochondrial prediction (data not shown).

IDH reported 90% of mitochondrial prediction as was expected for one mitochondrial protein. OGG1 showed by PSORTII, a mitochondrial and nuclear addressing prediction very similar and by MitoProtII, a 44% mitochondrial addressing. The XRCC1, PARP-B, PARP-C, PARG-B mitochondrial addressing prediction was poor about 1-20% by MitoProtII analysis.

The human PARP1 show 8% of mitochondrial addressing. Nevertheless, Rossi and collaborators in 2009 showed that PARP1 was present in human mitochondria, but also that was related to the mitofilin receptor controlling its entry.

In *Drosophila*, mitofilin receptor (Flybase code CG6455) was discovered (2005) before studies of human mitofilin receptor and Parp1 mitochondrial internalization. *In silico* studies guide to possible presence of main BER actors such as OGG1 and PARP-B in *Drosophila* mitochondria: OGG1 with potential MTS and PARP-B with potential receptor in IMM.

III.→.Base excision repair genes expression in Drosophila

The RT-q-PCR analysis results demonstrated that the *parp* mRNA expression profile was susceptible to regulation in the three key parts of BER pathway such as DNA base excision, AP site removal and DNA ligation.

The ***Figure 79*** shows the possible regulation of parp mRNA through the role of OGG1, XRCC1 and RRP1 proteins, the two first having a positive effect and the last one a negative effect. We are not clear if regulatory mechanism of parp expression was carried out directly by OGG1, RRP1 and XRRC1 proteins or through intermediate molecules.

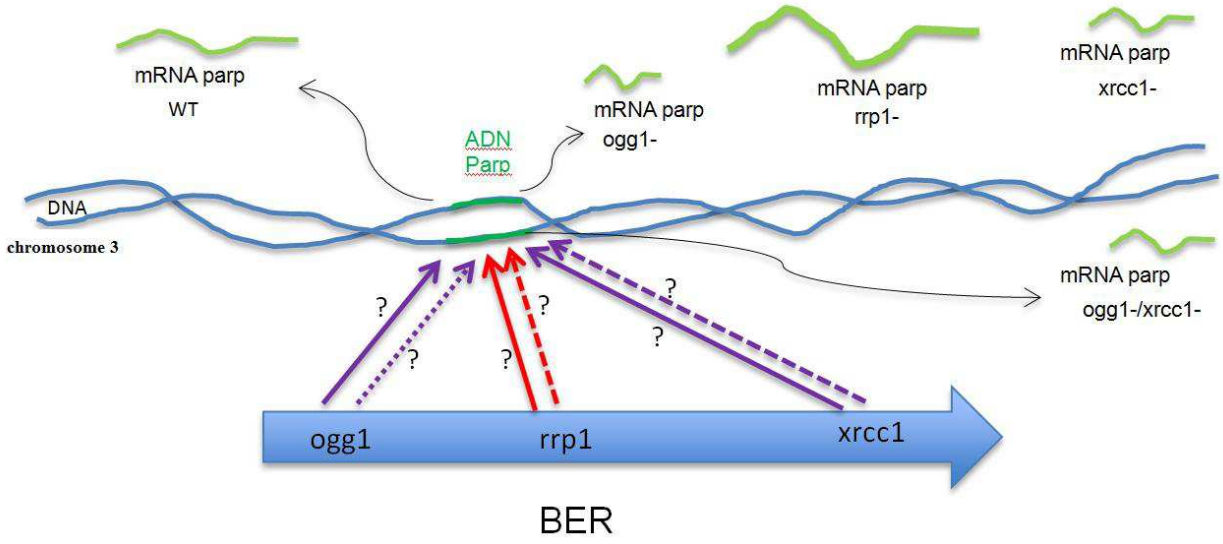

***Figure 79**: Schematic representation of mRNA parp regulation in BER system. The induction of mRNA parp expression was represented in purple and the inhibition in red. Full arrows described a positive action and dotted lines, an indirect action.*

Interesting the parg expression profile (mRNA) increase 40% in mutant context rrp1$^-$, xrcc1$^-$, and ogg1$^-$/xrcc1$^-$; however in ogg1$^-$ context parg expression profile was similar to WT. This results guides that the lack of OGG1 protein did not interfere with parg mRNA expression, compared to RRP1 and XRCC1 proteins which led to a change for this expression. Role for glycosylases as regulators of other genes expression has already been described with knock-out models. In ogg1- mutant mice, a general metabolic perturbation was observed leading to changes in genes expression such as down-regulation of carnitine palmitoyl transferase-1, and the integral transcriptional co-activator Pgc-1α (**Sampath H et al., 2012**). XRCC1 deficiency was classicaly described as a severe BER deficiency. In fruitfly, this deficiency does not interfere with viability compared to the same deficiency in mouse, but in our study all tested genes expressions in fruitfly were reduced except for *parg*.

IV.→.PARP isoforms relative expression

IV.1 It was illustrated in *Drosophila* rrp1$^-$ (Flybase code 10213) mRNA expression of *parp* and *parg* expressions about 40%. The two parp isoforms were quantified using primers adapted to common region among genes. In order to understand parp isoforms regulation in *rrp1* knockout, parp mRNA variants were quantified using specific primers. The parp-B expression is over-expressing in 50% while parp-C expression was similar WT; also, parg expression was about 70%. Thus, the RRP1 protein can be implicated in *parp-B* and *parg* mRNA depletion (these results were discussed above). Nevertheless, western blot anti-

PARPB/C (addressed to catalytic domain); (PARP S/L (dD-12)) and anti-parpB (addressed to automodification domain); (PARP L (dE-17)) would illustrate the PARP proteins with and without remodeling or the new isoforms. The ***Figure 80*** below shows the different antibodies involved in PARP detection and relative position in PARP isoforms. The PARP-B isoform can be identified with sc-L (dE-17) antibody specifically.

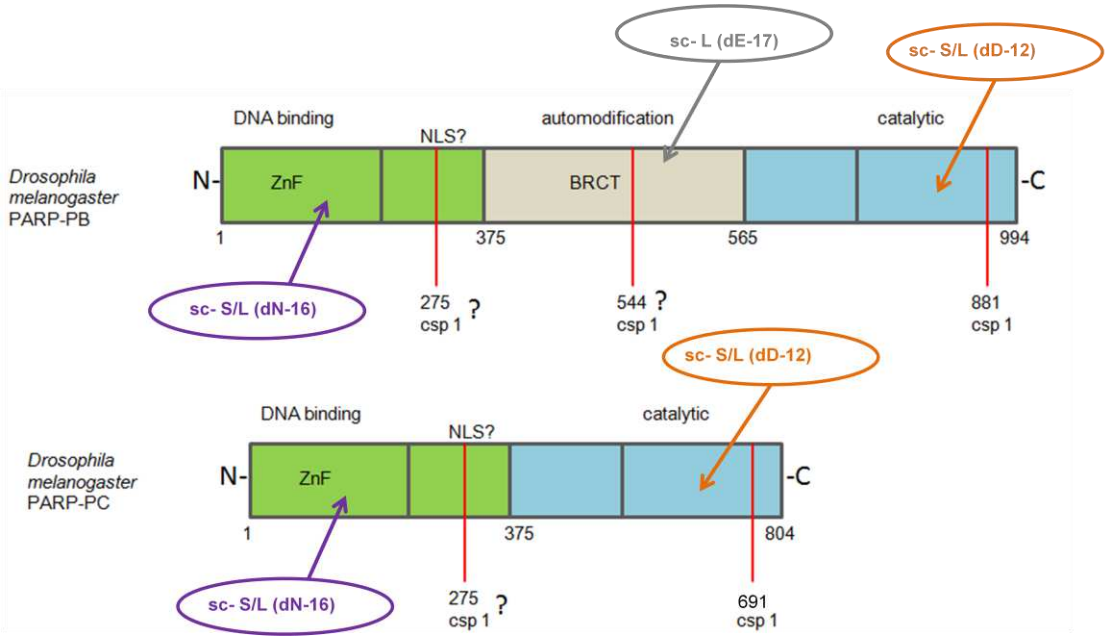

Figure 80: Schematic representation of epitopes localisation in PARP isoforms for various anti-PARP antibodies such as sc-L(dE-17), sc-S/L (dN-16) and sc-S/L (dD-12).

The mRNA expression ratio (ER) of ParpB/ParpC was disrupted under certain condition. After copper incubation ER=1.4 compared with S2 control (ER about 1) with very high significance. Copper is an essential but potentially toxic trace element in *Drosophila* (**Balamurugan K. et al., 2007**).

The S2 cell after copper (0.7mM) incubation of 24 hours at 24°C produces DNA damage because it catalyzes the generation of ROS via the Fenton reaction (**Halliwell B et Gutteridge JM., 1990 ; Puig S et Thiele.DJ, 2002 ; Spencer WA et al., 2009**).

Under copper stress parp-B over-expression was reported about 10%. This result shows the positive effect of cooper on mRNA parp-B expression. Under H_2O_2 incubation the parp-B over-expression was reported about 10% with ER similar to S2 control.

Curiously; the oxidative stress had a positive effect in mRNA as copper stress. Both effects at the same time, Cu^{2+} / H_2O_2 stress: after copper (0.7mM) incubation of 24 hours at 24°C

with addition of H_2O_2 (40mM) incubation 30 min, evidenced that the transcript of parp-B increased over-expression until 30% and ER similar to WT.

This results guides that copper and H_2O_2 are possible synergetic actions. In S2 DNA recovery conditions (after Cu^{2+} / H_2O_2 stress incubation followed by 30 min at 24 °C in normal conditions), we showed depletion in both isoformes about 40% compared to basal S2 cells. As well, over-expression of parp is also associated in apoptotic pathway activation (**Chaitanya GV, et al., 2010**).

It was demonstrated in human cell with severely damaged DNA have amplified PARP-1 activity resulting in high NAD^+ consumption depleting ATP pools and this activity inevitably leads to passive necrotic cell death (due to prolonged ATP depletion) (**Eguchi Y, Shimizu S, et Tsujimoto Y., 1997; Lemaire C et al., 1998**).

In cells expressing caspase-resistant PARP-1 would be more clear the necrosis induction and an increased of apoptosis associate with depletion of NAD^+ and consequently in ATP level (**Herceg Z et Wang ZQ., 1999**).

Interesting recent reports show that caspases are not only involved in apoptosis pathways. They are implicated in forms of cell proliferation in a *Drosophila* model. The caspase Dcp-1 in Drosophila represents caspase-3 in human (**Fan Y et Bergmann A., 2008 ; Kondo S. et al., 2006**).

We show in silico casp1 digestion profile of Parp-B-V5 the peptides about 16 KDa, 55 KDa, 82 KDa, we illustrated by western blot anti-V5 the protein of 82 KDa in J2 cells.

V.2 cells. tion profile of Parp-B-V5 *Drosophila melanogaster*

Human PARP-1 is a nuclear protein identified as an enzyme that performs central roles in the repair of damaged DNA, PARP-1 participates in initiating base excision repair (BER) (**Dantzer F et al., 2000**). Recently, in Human, mitochondrial localization has been shown in HeLa cells (**Rossi et al., 2009**).

We localized by microscopy in S2 cells Parp in nucleus and mitochondria. The oxidative stress increases highly the parp-B presence in nucleus and mitochondria.

The western blot anti-PARP results using polyclonal (PARP S/L (dN-16)) identified proteins about 70KDa and 82KDa in mitochondrial samples and about 113KDa in *culot*

sucrose WT sample fruitsflies. We suppose over-expression of parp-B-targ (V5 or GFP) in S2 cells can activate casp1 in order to modulate parp level. Casp1 site cleavage in Parp-B produces the lost targ and a protein about 82 KDa.

It was demonstrated that PARP-1 over-activation can cause neuroinflammation and apoptosis in human cells (**Turunc Bayrakdar E et al.,2013**). Over-expression and over-activity of PARP-B are involved in apoptotic cellular response in S2 cells?

CONCLUSIONS

The project performed during this PhD thesis was able to give some interesting informations regarding mitochondrial DNA repair in *Drosophila*.

According to the initial first question, we showed that the PARP-B isoform is present both in nuclear fraction. We also showed a possible new isoform about 70 kDa in mitochondria, that still needs to be confirmed.

We focused on PARP proteins under cellular stresses studying both regulation and sub-cellular localization. The oxidative stress lets to modulate the level of each parp isoforms, but also the ratio of these two isoforms. Some data suggested that PARP was for a part a mitochondrial protein. This aspect needs to be confirmed prior going further. Finally we hypothesized that PARP-B over-expression may lead to caspase 1 activation with consequently PARP cleavage.

Regarding PARP regulation in BER mutants, we showed that PARP-B mRNA was modulated in ogg1-/-, rrp1-/-, xrcc1-/- and ogg1-/xrcc1- mutants. Except in rrp1-/- mutant, PARP-B mRNA decreased in every tested mutant. Molecular analyses performed in mutant flies contexts gave some examples of co-regulations, pointing out the functional interactions existing between various glycosylases or adaptator proteins (XRCC1) in the BER process. Such an approach needs to be further analysed, in order to investigate and understand the exact role each protein could have on other BER partners.

The last question regarding BER activities during aging was answered using a comprehensive approach of Base Excision Repair processes in fly mitochondria. This technology could be performed on fly model and was efficient to determine which BER activity were present, but also the level and intensity of this activity. In our study, few activities were high in *Drosophila* mitochondria and directed against THF-A, Eth-A, Tg-A and U-G modifications. These activities were mostly different from those observed in nucleus. Interestingly, aging effects were quantified on mitochondrial BER activities, raising the question of the role of mitochondrial BER mechanisms in aging processes.

PERSPECTIVES

In short term:

I) To understand the exact nature of the protein detected due to difference in molecular weight compare with PARP isoforms. It would be recommendable in first time to study embryos because of high level PARP expression in this state and after, in second time to study PARP function in the mutant casp1^{-} We studied from adult young flies the mRNA profile of certain genes keys of BER system. In order to understand the PARP isoforms mRNA profile it would be useful to associate PARP isoforms mRNA profile with mRNA profile of certain keys genes of BER system. We propose to use a recombinant protein MTS-PARP-B caspase1 cleavage resistant (**Boulares AH et al 1999**) in order to get check if the full length 113 KDa PARP protein could be obtained in nuclear and mitochondrial samples to validate the caspase hypothesis.

II) In order to identify the BRCT domain in nuclear and mitochondrial samples. Firstly, we suggest the production of recombinant *PARP-B* with aim to obtain polyclonal antibodies which will be used in protein immunoprecipitation in nuclear and mitochondrial fractions.

In long term:

I. Analysis of mitochondrial Poly(ADP-ribose)tion in mutants of BER mechanism for key steps. Also using siRNA of mitofilin orthologs it would be possible to validate the role of mitofilin in PARP-B localization.

II. Therapeutic application against cancer. The production of recombinant protein MTS-p24 (that represents PARP-B DNA blinding domain with mitochondrial target). Besides to culture the stable line S2 cells transfected with protein MTS-p24, analysis of S2 sensibility to oxidative stress or irradiation. This model can show various responses with possible application in human cells (WT and prostatic cells cancerous).

REFERENCES AND ANNEXES

Adamietz P. « Poly(ADP-Ribose) Synthase Is the Major Endogenous Nonhistone Acceptor for poly(ADP-Ribose) in Alkylated Rat Hepatoma Cells », *Eur J Biochem.* ***1987*** *Dec 1;169(2):365-72.*

Adams KL, Palmer JD. « Evolution of Mitochondrial Gene Content: Gene Loss and Transfer to the Nucleus », *Mol Phylogenet Evol.* ***2003*** *Dec; 29(3):380-95.*

Aguilar-Quesada R, Muñoz-Gámez JA, Martín-Oliva D, Peralta-Leal A, Quiles-Pérez R, Rodríguez-Vargas JM, Ruiz de Almodóvar M, Conde C, Ruiz-Extremera A, Oliver FJ. « Modulation of Transcription by PARP-1: *Curr Med Chem*. **2007**; 14(11):1179-87.

Ahnesorg P, Smith P, Jackson SP. « XLF Interacts with the XRCC4-DNA Ligase IV Complex to Promote DNA Nonhomologous End-Joining », *Cell.* ***2006*** *Jan 27;124(2):301-13.*

Alziari S, Berthier F, Touraille S, Stepien G, Durand R. « Mitochondrial DNA Expression in Drosophila Melanogaster: Neosynthesized Polypeptides in Isolated Mitochondria », *Biochimie.* ***1985*** *Sep;67(9):1023-34.*

Amé JC, Spenlehauer C, de Murcia G. « The PARP Superfamily », *Bioessays.* ***2004*** *Aug; 26(8):882-93.*

Ames BN, Shigenaga MK, Gold LS. « DNA Lesions, Inducible DNA Repair, and Cell Division: Three Key Factors in Mutagenesis and Carcinogenesis », *Environ Health Perspect.* ***1993*** *Dec;101 Suppl 5:35-44.*

Anderson S, Bankier AT, Barrell BG, de Bruijn MH, Coulson AR, Drouin J, Eperon IC, Nierlich DP, Roe BA, Sanger F, Schreier PH, Smith AJ, Staden R, Young IG. « Sequence and Organization of the Human Mitochondrial Genome », *Nature.* ***1981*** *Apr 9;290(5806):457-65.*

Andres SN, Modesti M, Tsai CJ, Chu G, Junop MS. « Crystal Structure of Human XLF: A Twist in Nonhomologous DNA End-Joining », *Mol Cell.* ***2007*** *Dec 28;28(6):1093-101.*

Antoshechkin I, Bogenhagen DF, Mastrangelo IA. « The HMG-Box Mitochondrial Transcription Factor Xl-mtTFA Binds DNA as a Tetramer to Activate Bidirectional Transcription ». *EMBO J.* **1997** Jun 2; 16(11):3198-206.

Arnold S, Kadenbach B. « Cell Respiration Is Controlled by ATP, an Allosteric Inhibitor of Cytochrome-c Oxidase », *Eur J Biochem.* ***1997*** *Oct 1;249(1):350-4.*

Asaeda A, Ide H, Asagoshi K, Matsuyama S, Tano K, Murakami A, Takamori Y, Kubo K. « Substrate Specificity of Human Methylpurine DNA N-Glycosylase », *Biochemistry*. **2000** Feb 29; 39(8):1959-65.

Augustin A, Spenlehauer C, Dumond H, Ménissier-De Murcia J, Piel M, Schmit AC, Apiou F, Vonesch JL, Kock M, Bornens M, De Murcia G. « PARP-3 Localizes Preferentially to the Daughter Centriole and Interferes with the G1/S Cell Cycle Progression », *J Cell Sci.* **2003** Apr 15; 116(Pt 8):1551-62.

Balamurugan K, Egli D, Hua H, Rajaram R, Seisenbacher G, Georgiev O, Schaffner W. « Copper Homeostasis in Drosophila by Complex Interplay of Import, Storage and Behavioral Avoidance », *EMBO J.* ***2007*** *Feb 21;26(4):1035-44.*

Barlow C, Hirotsune S, Paylor R, Liyanage M, Eckhaus M, Collins F, Shiloh Y, Crawley JN, Ried T, Tagle D, Wynshaw-Boris A. « Atm-Deficient Mice: A Paradigm of Ataxia Telangiectasia », *Cell.* **1996** Jul 12; 86(1):159-71.

Barnes DE, Lindahl T. « Repair and Genetic Consequences of Endogenous DNA Base Damage in Mammalian Cells », *Annu Rev Genet.* ***2004****; 38:445-76.*

Becker T, Horvath SE, Böttinger L, Gebert N, Daum G, Pfanner N. « Role of phosphatidylethanolamine in the biogenesis of mitochondrial outer membrane proteins. ». *J Biol Chem.* **2013** Jun 7; 288(23):16451-9.

Beckman KB, Ames BN. « Endogenous Oxidative Damage of mtDNA », *Mutat Res.* ***1999*** *Mar 8; 424(1-2):51-8.*

Boamah EK, Kotova E, Garabedian M, Jarnik M, Tulin AV. « Poly(ADP-Ribose) Polymerase 1 (PARP-1) Regulates Ribosomal Biogenesis in Drosophila Nucleoli », *PLoS Genet.* ***2012*** *Jan; 8(1):e1002442.*

Boesch P, Weber-Lotfi F, Ibrahim N, Tarasenko V, Cosset A, Paulus F, Lightowlers RN, Dietrich A.« DNA Repair in Organelles: Pathways, Organization, Regulation, Relevance in Disease and Aging », *Biochim Biophys Acta.* ***2011*** *Jan; 1813(1):186-200.*

Bohnert M, Pfanner N, van der Laan M. « A Dynamic Machinery for Import of Mitochondrial Precursor Proteins », *FEBS Lett.* ***2007*** *Jun 19; 581(15):2802-10.*

Bonicalzi ME, Haince JF, Droit A, Poirier GG. « Regulation of poly(ADP-Ribose) Metabolism by poly(ADP-Ribose) Glycohydrolase: Where and When? », *Cell Mol Life Sci.* ***2005*** *Apr;62(7-8):739-50.*

Boulares AH, Yakovlev AG, Ivanova V, Stoica BA, Wang G, Iyer S, Smulson M. « Role of poly(ADP-Ribose) Polymerase (PARP) Cleavage in Apoptosis. Caspase 3-Resistant PARP Mutant Increases Rates of Apoptosis in Transfected Cells », *J Biol Chem.* **1999** Aug 13; 274(33):22932-40.

Braithwaite EK, Prasad R, Shock DD, Hou EW, Beard WA, Wilson SH. « DNA Polymerase Lambda Mediates a Back-up Base Excision Repair Activity in Extracts of Mouse Embryonic Fibroblasts », *J Biol Chem.* ***2005*** *May 6;280(18):18469-75.*

Bredemeyer AL, Sharma GG, Huang CY, Helmink BA, Walker LM, Khor KC, Nuskey B, Sullivan KE, Pandita TK, Bassing CH, Sleckman BP. « ATM Stabilizes DNA Double-Strand-Break Complexes during V(D)J Recombination », *Nature.* **2006** Jul 27; 442(7101):466-70.

Buck D, Malivert L, de Chasseval R, Barraud A, Fondanèche MC, Sanal O, Plebani A, Stéphan JL, Hufnagel M, le Deist F, Fischer A, Durandy A, de Villartay JP, Revy P. « Cernunnos, a Novel Nonhomologous End-Joining Factor, Is Mutated in Human Immunodeficiency with Microcephaly », *Cell.* **2006** Jan 27; 124(2):287-99.

Buelow B, Uzunparmak B, Paddock M, Scharenberg AM. « Structure/function Analysis of PARP-1 in Oxidative and Nitrosative Stress-Induced Monomeric ADPR Formation », *PLoS One.* **2009** Jul 29; 4(7):e6339.

Bürkle A, Brabeck C, Diefenbach J, Beneke S. « The Emerging Role of poly(ADP-Ribose) Polymerase-1 in Longevity », *Int J Biochem Cell Biol.* **2005** May;37(5):1043-53.

Campbell CT, Kolesar JE, Kaufman BA. « Mitochondrial Transcription Factor A Regulates Mitochondrial Transcription Initiation, DNA Packaging, and Genome Copy Number », *Biochim Biophys Acta.* **2012** Sep-Oct; 1819(9-10):921-9.

Cao Q, Qin C, Meng X, Ju X, Ding Q, Wang M, Zhu J, Wang W, Li P, Chen J, Zhang Z, Yin C. « Genetic Polymorphisms in APE1 Are Associated with Renal Cell Carcinoma Risk in a Chinese Population », *Mol Carcinog.* ***2011*** *Nov; 50(11):863-70.*

Chaitanya GV, Steven AJ, Babu PP. « PARP-1 Cleavage Fragments: Signatures of Cell-Death Proteases in Neurodegeneration », *Cell Commun Signal.* ***2010*** *Dec 22;8:31.*

Chang DD, Clayton DA. « Priming of Human Mitochondrial DNA Replication Occurs at the Light-Strand Promoter », *Proc Natl Acad Sci U S A.* **1985** Jan; 82(2):351-5.

Chang DD, Hauswirth WW. Clayton DA. « Replication Priming and Transcription Initiate from Precisely the Same Site in Mouse Mitochondrial DNA », *EMBO J.* **1985** Jun; 4(6):1559-67.

Chen H, Chan DC. « Mitochondrial Dynamics in Mammals », *Curr Top Dev Biol.* ***2004****; 59:119-44.*

Chen H, Zhou B, Lan X, Wei D, Yuan T, Chen P. « Association between Single-Nucleotide Polymorphisms of OGG1 Gene and Pancreatic Cancer Risk in Chinese Han Population », *Tumour Biol.* ***2013*** *Sep 3.*

Chen XJ. « Mechanism of Homologous Recombination and Implications for Aging-Related Deletions in Mitochondrial DNA », *Microbiol Mol Biol Rev.* ***2013*** *Sep;77(3):476-96.*

Christianson TW, Clayton DA. « A Tridecamer DNA Sequence Supports Human Mitochondrial RNA 3'-End Formation in Vitro », *Mol Cell Biol.* ***1988*** *Oct;8(10):4502-9.*

Christianson TW, Clayton DA. « In Vitro Transcription of Human Mitochondrial DNA: Accurate Termination Requires a Region of DNA Sequence That Can Function Bidirectionally », *Proc Natl Acad Sci U S A.* ***1986*** *Sep; 83(17):6277-81.*

Claros MG, Vincens P. «Computational method to predict mitochondrially imported proteins and their targeting sequences ». *Eur J Biochem.* **1996** Nov 1; 241(3):779-86.

Clayton DA. « Replication and Transcription of Vertebrate Mitochondrial DNA », *Annu Rev Cell Biol*. **1991**; 7:453-78.

Cliften PF, Park JY, Davis BP, Jang SH, Jaehning JA. « Identification of Three Regions Essential for Interaction between a Sigma-like Factor and Core RNA Polymerase », *Genes Dev.* ***1997*** *Nov 1; 11(21):2897-909.*

Collins TJ, Berridge MJ, Lipp P, Bootman MD. « Mitochondria Are Morphologically and Functionally Heterogeneous within Cells », *EMBO J.* ***2002*** *Apr 2; 21(7):1616-27.*

Dairaghi DJ, Shadel GS, Clayton DA. « Addition of a 29 Residue Carboxyl-Terminal Tail Converts a Simple HMG Box-Containing Protein into a Transcriptional Activator », *J Mol Biol.* **1995** May 26; 249(1):11-28.

Dairaghi DJ, Shadel GS, Clayton DA. « Human Mitochondrial Transcription Factor A and Promoter Spacing Integrity Are Required for Transcription Initiation », *Biochim Biophys Acta.* ***1995*** *May 24;1271(1):127-34.*

Dantzer F, de La Rubia G, Ménissier-De Murcia J, Hostomsky Z, de Murcia G, Schreiber V. « Base Excision Repair Is Impaired in Mammalian Cells Lacking Poly(ADP-Ribose) Polymerase-1 », *Biochemistry.* ***2000*** *Jun 27; 39(25):7559-69.*

de Bont R, van Larebeke N. « Endogenous DNA Damage in Humans: A Review of Quantitative Data », *Mutagenesis.* ***2004*** *May; 19(3):169-85*.

de Duve C. « The Origin of Eukaryotes: A Reappraisal », *Nat Rev Genet*. **2007** May; 8(5):395-403.

de Souza-Pinto NC, Eide L, Hogue BA, Thybo T, Stevnsner T, Seeberg E, Klungland A, Bohr VA. « Repair of 8-Oxodeoxyguanosine Lesions in Mitochondrial Dna Depends on the Oxoguanine Dna Glycosylase (OGG1) Gene and 8-Oxoguanine Accumulates in the Mitochondrial Dna of OGG1-Defective Mice ». *Cancer Res.* **2001** Jul 15; 61(14):5378-81.

Dianov GL, Souza-Pinto N, Nyaga SG, Thybo T, Stevnsner T, Bohr VA. « Base Excision Repair in Nuclear and Mitochondrial DNA », *Prog Nucleic Acid Res Mol Biol.* ***2001****; 68:285-97.*

Dianov GL, Thybo T, Dianova II, Lipinski LJ, Bohr VA. « Single Nucleotide Patch Base Excision Repair Is the Major Pathway for Removal of Thymine Glycol from DNA in Human Cell Extracts », J *Biol Chem.* ***2000*** *Apr 21; 275(16):11809-13.*

Diffley JF, Stillman B. « A Close Relative of the Nuclear, Chromosomal High-Mobility Group Protein HMG1 in Yeast Mitochondria », *Proc Natl Acad Sci U S A.* ***1991*** *Sep 1;88(17):7864-8.*

DiMauro S. « Mitochondrial diseases », *Biochim Biophys Acta.* ***2004*** *Jul 23; 1658(1-2):80-8.*

Dimroth P, Kaim G, Matthey U. « Crucial Role of the Membrane Potential for ATP Synthesis by F(1)F(o) ATP Synthases », *J Exp Biol.* ***2000*** *Jan;203(Pt 1):51-9.*

Dubessay P, Garreau-Balandier I, Jarrousse AS, Fleuriet A, Sion B, Debise R, Alziari S. « Aging Impact on Biochemical Activities and Gene Expression of Drosophila Melanogaster Mitochondria », *Biochimie.* ***2007*** *Aug; 89(8):988-1001*..

Eguchi Y, Shimizu S, Tsujimoto Y. « Intracellular ATP Levels Determine Cell Death Fate by Apoptosis or Necrosis », *Cancer Res.* ***1997*** *May 15; 57(10):1835-40.*

El-Khamisy SF, Masutani M, Suzuki H, Caldecott KW. « A Requirement for PARP-1 for the Assembly or Stability of XRCC1 Nuclear Foci at Sites of Oxidative DNA Damage », *Nucleic Acids Res.* ***2003*** *Oct 1; 31(19):5526-33.*

Elkoreh G, Blais V, Béliveau E, Guillemette G, Denault JB. « Type 1 Inositol-1,4,5-Trisphosphate Receptor Is a Late Substrate of Caspases during Apoptosis », *J Cell Biochem.* ***2012*** *Aug;113(8):2775-84.*

Eustermann S, Videler H, Yang JC, Cole PT, Gruszka D, Veprintsev D, Neuhaus D. « The DNA-Binding Domain of Human PARP-1 Interacts with DNA Single-Strand Breaks as a Monomer through Its Second Zinc Finger ». *J Mol Biol.* **2011** Mar 18; 407(1):149-70.

Falkenberg M, Gaspari M, Rantanen A, Trifunovic A, Larsson NG, Gustafsson CM. « Mitochondrial Transcription Factors B1 and B2 Activate Transcription of Human mtDNA ». *Nat Genet.* **2002** Jul; 31(3):289-94.

Fan Y, Bergmann A. « Apoptosis-Induced Compensatory Proliferation. The Cell Is Dead. Long Live the Cell! », *Trends Cell Biol.* ***2008*** *Oct; 18(10):467-73.*

Fernández-Silva P, Enriquez JA, Montoya J.« Replication and Transcription of Mammalian Mitochondrial DNA », *Exp Physiol.* ***2003*** *Jan;88(1):41-56.*

Fernandez-Silva P, Martinez-Azorin F, Micol V, Attardi G. « The Human Mitochondrial Transcription Termination Factor (mTERF) Is a Multizipper Protein but Binds to DNA as a Monomer, with Evidence Pointing to Intramolecular Leucine Zipper Interactions », *EMBO J. **1997** Mar 3;16(5):1066-79.*

Finkel T, Holbrook NJ. « Oxidants, Oxidative Stress and the Biology of Ageing », *Nature. **2000** Nov 9;408(6809):239-47.*

Fisher RP, Lisowsky T, Parisi MA, Clayton DA. « DNA Wrapping and Bending by a Mitochondrial High Mobility Group-like Transcriptional Activator Protein », *J Biol Chem. **1992** Feb 15;267(5):3358-67.*

Fuchs E, Fuchs CM. « In Vitro Synthesis of T3 AND T7 RNA Polymerase at Low Magnesium Concentration », *FEBS Lett. **1971** Dec 1;19(2):159-162.*

Fusté JM, Wanrooij S, Jemt E, Granycome CE, Cluett TJ, Shi Y, Atanassova N, Holt IJ, Gustafsson CM, Falkenberg M. « Mitochondrial RNA Polymerase Is Needed for Activation of the Origin of Light-Strand DNA Replication », *Mol Cell. **2010** Jan 15;37(1):67-78.*

Garay-Malpartida HM, Occhiucci JM, Alves J, Belizário JE. « CaSPredictor: a new computer-based tool for caspase substrate prediction ».Bioinformatics. **2005** Jun;21 Suppl 1:i169-76.

Gelfand R, Attardi G. « Synthesis and Turnover of Mitochondrial Ribonucleic Acid in HeLa Cells: The Mature Ribosomal and Messenger Ribonucleic Acid Species Are Metabolically Unstable », *Mol Cell Biol. **1981** Jun;1(6):497-511*.

Gellerich FN, Trumbeckaite S, Opalka JR, Seppet E, Rasmussen HN, Neuhoff C, Zierz S. « Function of the Mitochondrial Outer Membrane as a Diffusion Barrier in Health and Diseases », *Biochem Soc Trans. **2000** Feb;28(2):164-9.*

Gibson BA, Kraus WL. « New Insights into the Molecular and Cellular Functions of poly(ADP-Ribose) and PARPs », *Nat Rev Mol Cell Biol.* **2012** Jun 20;13(7):411-24.

Gredilla R, Stevnsner T. « Mitochondrial Base Excision Repair Assays », *Methods Mol Biol. **2012**;920:289-304.*

Greenleaf AL, Kelly JL, Lehman IR. « Yeast RPO41 Gene Product Is Required for Transcription and Maintenance of the Mitochondrial Genome », *Proc. Natl Acad Sci U S A.* **1986** May; 83(10):3391-4.

Gryfe R. « Inherited Colorectal Cancer Syndromes », *Clin Colon Rectal Surg.* ***2009*** *Nov;22(4):198-208.*

Hajnóczky G, Csordás G, Yi M. « Old Players in a New Role: Mitochondria-Associated Membranes, VDAC, and Ryanodine Receptors as Contributors to Calcium Signal Propagation from Endoplasmic Reticulum to the Mitochondria », *Cell Calcium.* ***2002*** *Nov-Dec; 32(5-6):363-77.*

Halliwell B, Gutteridge JM. « Role of Free Radicals and Catalytic Metal Ions in Human Disease: An Overview », *Methods Enzymol.* **1990**;186:1-85.

Hanai S, Uchida M, Kobayashi S, Miwa M, Uchida K. « Genomic Organization of Drosophila poly(ADP-Ribose) Polymerase and Distribution of Its mRNA during Development », *J Biol Chem.* ***1998*** *May 8;273(19):11881-6.*

He YJ, Liu RH, Ning CQ, Yu NF. « [Research progresses of the PARP inhibitors for the treatment of cancer] », *Yao Xue Xue Bao.* ***2013*** *May;48(5):655-60.*

Herceg Z, Wang ZQ. « Failure of poly(ADP-Ribose) Polymerase Cleavage by Caspases Leads to Induction of Necrosis and Enhanced Apoptosis », *Mol Cell Biol.* ***1999*** *Jul;19(7):5124-33.*

Herrmann JM, Riemer J. « The Intermembrane Space of Mitochondria », *Antioxid Redox Signal.* ***2010*** *Nov 1;13(9):1341-58.*

Hiom K. « Coping with DNA double strand breaks », *DNA Repair (Amst).* ***2010*** *Dec 10;9(12):1256-63.*

Hoeijmakers JH. « Genome Maintenance Mechanisms for Preventing Cancer », *Nature.* ***2001*** *May 17;411(6835):366-74.*

Horton P, Nakai K. « Better prediction of protein cellular localization sites with the k nearest neighbors classifier ». *Proc Int Conf Intell Syst Mol Biol.* **1997**; 5:147-52.

Horvath SE, Daum G. « Lipids of Mitochondria », *Prog Lipid Res.* ***2013*** *Oct; 52(4):590-614.*

Hottiger MO, Hassa PO, Lüscher B, Schüler H, Koch-Nolte F. « Toward a Unified Nomenclature for Mammalian ADP-Ribosyltransferases », *Trends Biochem Sci.* ***2010*** *Apr; 35(4):208-19.*

Hsiao SJ, Smith S. « Tankyrase Function at Telomeres, Spindle Poles, and beyond », *Biochimie.* ***2008*** *Jan; 90(1):83-92.*

Hu J, de Souza-Pinto NC, Haraguchi K, Hogue BA, Jaruga P, Greenberg MM, Dizdaroglu M, Bohr VA. « Repair of Formamidopyrimidines in DNA Involves Different Glycosylases: Role of the OGG1, NTH1, and NEIL1 Enzymes », *J Biol Chem.* ***2005*** *Dec 9; 280(49):40544-51.*

Hunte C, Koepke J, Lange C, Rossmanith T, Michel H. « Structure at 2.3 A Resolution of the Cytochrome bc(1) Complex from the Yeast Saccharomyces Cerevisiae Co-Crystallized with an Antibody Fv Fragment », *Structure.* **2000** Jun 15; 8(6):669-84.

Iliakis G, Wu W, Wang M. « DNA Double Strand Break Repair Inhibition as a Cause of Heat Radiosensitization: Re-Evaluation Considering Backup Pathways of NHEJ », *Int J Hyperthermia.* ***2008*** *Feb;24(1):17-29.*

Isabelle M, Moreel X, Gagné JP, Rouleau M, Ethier C, Gagné P, Hendzel MJ, Poirier GG. « Investigation of PARP-1, PARP-2, and PARG Interactomes by Affinity-Purification Mass Spectrometry », *Proteome Sci.* ***2010*** *Apr 13; 8:22.*

Jakobs S. « High Resolution Imaging of Live Mitochondria », *Biochim Biophys Acta.* ***2006*** *May-Jun; 1763(5-6):561-75.*

Kanai M, Hanashiro K, Kim SH, Hanai S, Boulares AH, Miwa M, Fukasawa K. « Inhibition of Crm1-p53 Interaction and Nuclear Export of p53 by poly(ADP-Ribosyl)ation », *Nat Cell Biol.* ***2007*** *Oct;9(10):1175-83.*

Kanai M, Tong WM, Sugihara E, Wang ZQ, Fukasawa K, Miwa M. « Involvement of poly(ADP-Ribose) Polymerase 1 and poly(ADP-Ribosyl)ation in Regulation of Centrosome Function », *Mol Cell Biol.* ***2003*** *Apr;23(7):2451-62.*

Kang D, Miyako K, Kai Y, Irie T, Takeshige K. « In Vivo Determination of Replication Origins of Human Mitochondrial DNA by Ligation-Mediated Polymerase Chain Reaction », *J Biol Chem.* ***1997*** *Jun 13;272(24):15275-9.*

Kang H, Dai Z, Ma X, Ma L, Jin Y, Liu X, Wang X. « A Genetic Variant in the Promoter of APE1 Gene (-656 T>G) Is Associated with Breast Cancer Risk and Progression in a Chinese Population », *Gene.* ***2013*** *Nov 15;531(1):97-100.*

Karahalil B, de Souza-Pinto NC, Parsons JL, Elder RH, Bohr VA. « Compromised Incision of Oxidized Pyrimidines in Liver Mitochondria of Mice Deficient in NTH1 and OGG1 Glycosylases », *J Biol Chem.* **2003** Sep 5; 278(36):33701-7.

Katoh M, Katoh M. « Identification and Characterization of Human TIPARP Gene within the CCNL Amplicon at Human Chromosome 3q25.31 », *Int J Oncol.* ***2003*** *Aug;23(2):541-7.*

Kaufman BA, Newman SM, Hallberg RL, Slaughter CA, Perlman PS, Butow RA. « In Organello Formaldehyde Crosslinking of Proteins to mtDNA: Identification of Bifunctional Proteins », *Proc Natl Acad Sci U S A.* ***2000*** *Jul 5; 97(14):7772-7.*

Kawamura T, Hanai S, Yokota T, Hayashi T, Poltronieri P, Miwa M, Uchida K. « An Alternative Form of poly(ADP-Ribose) Polymerase in Drosophila Melanogaster and Its Ectopic Expression in Rat-1 Cells », *Biochem Biophys Res Commun.* ***1998*** *Oct 9;251(1):35-40.*

Kelly JL, Greenleaf AL, Lehman IR. « Isolation of the Nuclear Gene Encoding a Subunit of the Yeast Mitochondrial RNA Polymerase », *J Biol Chem.* ***1986*** *Aug 5;261(22):10348-51.*

Kondo S, Senoo-Matsuda N, Hiromi Y, Miura M. « DRONC Coordinates Cell Death and Compensatory Proliferation », *Mol Cell Biol.* ***2006*** *Oct;26(19):7258-68.*

Kremneva E, Kislin M, Kang X, Khiroug L. « Motility of Astrocytic Mitochondria Is Arrested by Ca2+-Dependent Interaction between Mitochondria and Actin Filaments », *Cell Calcium.* ***2013*** *Feb; 53(2):85-93.*

Krokan HE, Bjørås M. « Base Excision Repair », *Cold Spring Harb Perspect Biol.* ***2013*** *Apr 1;5(4):a012583.*

Krupitza G, Cerutti P. « ADP-Ribosylation of ADPR-Transferase and Topoisomerase I in Intact Mouse Epidermal Cells JB6 », *Biochemistry.* ***1989*** *Mar 7;28(5):2034-40.*

Kruse B, Narasimhan N, Attardi G. « Termination of Transcription in Human Mitochondria: Identification and Purification of a DNA Binding Protein Factor That Promotes Termination », *Cell.* **1989** Jul 28; 58(2):391-7.

Kutschera U, Niklas KJ. « Endosymbiosis, Cell Evolution, and Speciation », *Theory Biosci. 2005 Aug; 124(1):1-24. Epub 2005 Jun 1.*

Langelier MF, Servent KM, Rogers EE, Pascal JM. « A Third Zinc-Binding Domain of Human poly(ADP-Ribose) Polymerase-1 Coordinates DNA-Dependent Enzyme Activation », *J Biol Chem. **2008** Feb 15;283(7):4105-14.*

Leanza L, Biasutto L, Managò A, Gulbins E, Zoratti M, Szabò I. « Intracellular Ion Channels and Cancer », *Front Physiol.* **2013** Sep 3;4:227.

Lee HC, Wei YH. « Mitochondria and Aging », *Adv Exp Med Biol. **2012**; 942:311-27.*

Lee HH, Park C, Jeong JW, Kim MJ, Seo MJ, Kang BW, Park JU, Kim GY, Choi BT, Choi YH, Jeong YK. « Apoptosis Induction of Human Prostate Carcinoma Cells by Cordycepin through Reactive Oxygen Species‑mediated Mitochondrial Death Pathway », *Int J Oncol. **2013** Mar;42(3):1036-44.*

Legros F, Lombès A, Frachon P, Rojo M. « Mitochondrial Fusion in Human Cells Is Efficient, Requires the Inner Membrane Potential, and Is Mediated by Mitofusins », *Mol Biol Cell. **2002** Dec;13(12):4343-54.*

Lemaire C, Andréau K, Souvannavong V, Adam A. « Inhibition of Caspase Activity Induces a Switch from Apoptosis to Necrosis », *FEBS Lett.* **1998** Mar 27; 425(2):266-70.

Li G, Alt FW, Cheng HL, Brush JW, Goff PH, Murphy MM, Franco S, Zhang Y, Zha S. « Lymphocyte-Specific Compensation for XLF/cernunnos End-Joining Functions in V(D)J Recombination », *Mol Cell. **2008** Sep 5; 31(5):631-40.*

Li YH, Wang X, Pan Y, Lee DH, Chowdhury D, Kimmelman AC. « Inhibition of Non-Homologous End Joining Repair Impairs Pancreatic Cancer Growth and Enhances Radiation Response », *PLoS One. **2012**; 7(6):e39588.*

Liang PY, Li HY, Zhou ZY, Jin YX, Wang SX, Peng XH, Ou SJ. « Overexpression of Immunoglobulin G Prompts Cell Proliferation and Inhibits Cell Apoptosis in Human Urothelial Carcinoma ». *Tumour Biol.* **2013** Jun; 34(3):1783-91.

Lieber MR, Lu H, Gu J, Schwarz K. « Flexibility in the Order of Action and in the Enzymology of the Nuclease, Polymerases, and Ligase of Vertebrate Non-Homologous DNA End Joining: Relevance to Cancer, Aging, and the Immune System », *Cell Res.* ***2008*** *Jan; 18(1):125-33.*

Lieber MR. « The Mechanism of Double-Strand DNA Break Repair by the Nonhomologous DNA End-Joining Pathway ». *Annu Rev Biochem.* **2010**; 79:181-211.

Lin Z, Kong H, Nei M, Ma H. « Origins and evolution of the recA/RAD51 gene family: evidence for ancient gene duplication and endosymbiotic gene transfer» *Proc Natl Acad Sci U S A.* **2006** Jul 5; 103(27):10328-33.

Lindahl T, Nyberg B. « Rate of Depurination of Native Deoxyribonucleic Acid », *Biochemistry.* ***1972*** *Sep 12; 11(19):3610-8.*

Liu X, Kim CN, Yang J, Jemmerson R, Wang X. « Induction of Apoptotic Program in Cell-Free Extracts: Requirement for dATP and Cytochrome c », *Cell.* ***1996*** *Jul 12;86(1):147-57.*

Lopez-Contreras AJ, et Fernandez-Capetillo O. « http://www.intechopen.com/books/protein-phosphorylation-in-human-health/signalling-dna-damage ».

Maccecchini ML. « Import of Proteins into Mitochondria », *Methods Cell Biol.* ***1981****; 23:39-50.*

Mangus DA, Jang SH, Jaehning JA. « Release of the Yeast Mitochondrial RNA Polymerase Specificity Factor from Transcription Complexes », *J Biol Chem.* **1994** Oct 21; 269(42):26568-74.

Markkanen E, Dorn J, Hübscher U. « MUTYH DNA Glycosylase: The Rationale for Removing Undamaged Bases from the DNA », *Front Genet.* ***2013*** *Feb 28;4:18.*

Maynard S, de Souza-Pinto NC, Scheibye-Knudsen M, Bohr VA. « Mitochondrial Base Excision Repair Assays », *Methods.* ***2010*** *Aug; 51(4):416-25.*

Mbantenkhu M, Wang X, Nardozzi JD, Wilkens S, Hoffman E, Patel A, Cosgrove MS, Chen XJ. « Mgm101 Is a Rad52-Related Protein Required for Mitochondrial DNA Recombination », *J Biol Chem.* ***2011*** *Dec 9; 286(49):42360-70.*

McKinney EA, Oliveira MT. « Replicating animal mitochondrial DNA ». *Genet Mol Biol.* **2013** Sep; 36(3):308-315.

Memisoglu A et Samson L. « Base Excision Repair in Yeast and Mammals », *Mutat Res.* **2000** Jun 30;451(1-2):39-51.

Metzger MJ, Stoddard BL, Monnat RJ Jr. « PARP-Mediated Repair, Homologous Recombination, and Back-up Non-Homologous End Joining-like Repair of Single-Strand Nicks », *DNA Repair (Amst). **2013** Jul;12(7):529-34.*

Millau JF, Raffin AL, Caillat S, Claudet C, Arras G, Ugolin N, Douki T, Ravanat JL, Breton J, Oddos T, Dumontet C, Sarasin A, Chevillard S, Favier A, Sauvaigo S. « A Microarray to Measure Repair of Damaged Plasmids by Cell Lysates », *Lab Chip. **2008** Oct; 8(10):1713-22.*

Miwa M, Hanai S, Masuda H, Koyama Y, Hayashi T, Yoshida Y, Poltronieri P, Maeshima K, Kobayashi S, Okada M, et al. « Analysis of Biological Function of poly(ADP-Ribosyl)ation in Drosophila Melanogaster », *Biochimie. **1995**;77(6):466-71*.

Mladenov E, Iliakis G. « Induction and repair of DNA double strand breaks: the increasing spectrum of non-homologous end joining pathways. », *Mutat Res.* **2011** Jun 3; 711(1-2):61-72.

Montoya J, Christianson T, Levens D, Rabinowitz M, Attardi G. « Identification of Initiation Sites for Heavy-Strand and Light-Strand Transcription in Human Mitochondrial DNA ». *Proc Natl Acad Sci U S A.* **1982** Dec; 79(23):7195-9.

Montoya J, Gaines GL, Attardi G. « The Pattern of Transcription of the Human Mitochondrial rRNA Genes Reveals Two Overlapping Transcription Units », *Cell. **1983** Aug; 34(1):151-9.*

Morel F, Renoux M, Lachaume P, Alziari S. « Bleomycin-Induced Double-Strand Breaks in Mitochondrial DNA of Drosophila Cells Are Repaired », *Mutat Res. **2008** Jan 1;637(1-2):111-7.*

Mosavi LK, Cammett TJ, Desrosiers DC, Peng ZY. « The Ankyrin Repeat as Molecular Architecture for Protein Recognition », *Protein Sci. **2004** Jun;13(6):1435-48.*

Mozdy AD, Shaw JM. « A Fuzzy Mitochondrial Fusion Apparatus Comes into Focus », *Nat Rev Mol Cell Biol.* **2003** Jun; 4(6):468-78.

Muralidharan S, Mandrekar P. « Cellular Stress Response and Innate Immune Signaling: Integrating Pathways in Host Defense and Inflammation », *J Leukoc Biol.* ***2013*** *Dec; 94(6):1167-84.*

Nilsen H, Otterlei M, Haug T, Solum K, Nagelhus TA, Skorpen F, Krokan HE. « Nuclear and Mitochondrial Uracil-DNA Glycosylases Are Generated by Alternative Splicing and Transcription from Different Positions in the UNG Gene », *Nucleic Acids Res.* ***1997*** *Feb 15; 25(4):750-5.*

Noh YH, Kim KY, Shim MS, Choi SH, Choi S, Ellisman MH, Weinreb RN, Perkins GA, Ju WK. « Inhibition of oxidative stress by coenzyme Q10 increases mitochondrial mass and improves bioenergetic function in optic nerve head astrocytes». *Cell Death Dis*. **2013** Oct 3;4:e820.

Nonaka I. « Mitochondrial Diseases », *Curr Opin Neurol Neurosurg.* ***1992*** *Oct; 5(5):622-32.*

Noren Hooten N, Kompaniez K, Barnes J, Lohani A, Evans MK. « Poly(ADP-ribose) polymerase 1 (PARP-1) binds to 8-oxoguanine-DNA glycosylase (OGG1) », *J Biol Chem.* **2011** Dec 30;286(52):44679-90.

Nunnari J, Marshall WF, Straight A, Murray A, Sedat JW, Walter P. « Mitochondrial Transmission during Mating in Saccharomyces Cerevisiae Is Determined by Mitochondrial Fusion and Fission and the Intramitochondrial Segregation of Mitochondrial DNA », *Mol Biol Cell.* ***1997*** *Jul;8(7):1233-42*.

Okamoto K, Shaw JM. « Mitochondrial Morphology and Dynamics in Yeast and Multicellular Eukaryotes », *Annu Rev Genet.* ***2005****;39:503-36.*

Oliver AW, Amé JC, Roe SM, Good V, de Murcia G, Pearl LH. « Crystal Structure of the Catalytic Fragment of Murine poly(ADP-Ribose) Polymerase-2 », *Nucleic Acids Res.* **2004** Jan 22;32(2):456-64.

Osawa S, Jukes TH, Watanabe K, Muto A. « Recent Evidence for Evolution of the Genetic Code ». *Microbiol Rev.* **1992** Mar; 56(1):229-64.

Otera H, Ishihara N, Mihara K. « New Insights into the Function and Regulation of Mitochondrial Fission », *Biochim Biophys Acta.* ***2013*** *May;1833(5):1256-68.*

Pankotai E, Lacza Z, Murányi M, Szabó C. «Intra-«Mitochondrial poly(ADP-ribosyl)ation » *Mitochondrion*. **2009** Apr;9(2):159-64.

Parisi MA, Xu B, Clayton DA. « A Human Mitochondrial Transcriptional Activator Can Functionally Replace Yeast Mitochondrial HMG-Box Protein Both in Vivo and in Vitro », *Mol Cell Biol.* ***1993*** *Mar; 13(3):1951-61*.

Pham XH, Farge G, Shi Y, Gaspari M, Gustafsson CM, Falkenberg M. « Conserved Sequence Box II Directs Transcription Termination and Primer Formation in Mitochondria », *J Biol Chem.* ***2006*** *Aug 25;281(34):24647-52*.

Poirier GG, de Murcia G, Jongstra-Bilen J, Niedergang C, Mandel P. « Poly(ADP-Ribosyl)ation of Polynucleosomes Causes Relaxation of Chromatin Structure », *Proc Natl Acad Sci U S A.* ***1982*** *Jun;79(11):3423-7.*

Pons B, Belmont AS, Masson-Genteuil G, Chapuis V, Oddos T, Sauvaigo S. « Age-Associated Modifications of Base Excision Repair Activities in Human Skin Fibroblast Extracts », *Mech Ageing Dev*. **2010** Nov-Dec; 131(11-12):661-5.

Popot JL, de Vitry C. « On the Microassembly of Integral Membrane Proteins », *Annu Rev Biophys Biophys Chem.* ***1990****;19:369-403.*

Prasad SC, Dritschilo A. « High-Resolution Two-Dimensional Electrophoresis of Nuclear Proteins ». *Anal Biochem.* **1992** Nov 15; 207(1):121-8.

Preston CR, Flores CC, Engels WR. « Differential Usage of Alternative Pathways of Double-Strand Break Repair in Drosophila », *Genetics.* 2006 Feb; 172(2):1055-68.

Puig S, Thiele DJ. « Molecular Mechanisms of Copper Uptake and Distribution », *Curr Opin Chem Biol.* ***2002*** *Apr;6(2):171-80.*

Radyuk SN, Michalak K, Rebrin I, Sohal RS, Orr WC. « Effects of Ectopic Expression of Drosophila DNA Glycosylases dOgg1 and RpS3 in Mitochondria », *Free Radic Biol Med.* ***2006*** *Sep 1;41(5):757-64.*

Reyes A, Kazak L, Wood SR, Yasukawa T, Jacobs HT, Holt IJ. « Mitochondrial DNA Replication Proceeds via a "Bootlace" Mechanism Involving the Incorporation of Processed Transcripts », *Nucleic Acids Res*. **2013** Jun; 41(11):5837-50.

Rhee HW, Zou P, Udeshi ND, Martell JD, Mootha VK, Carr SA, Ting AY. « Proteomic Mapping of Mitochondria in Living Cells via Spatially Restricted Enzymatic Tagging », *Science. **2013** Mar 15;339(6125):1328-31.*

Rice PA. « Holding Damaged DNA Together », *Nat Struct Biol. **1999** Sep; 6(9):805-6.*

Robin ED, Wong R. « Mitochondrial DNA Molecules and Virtual Number of Mitochondria per Cell in Mammalian Cells », *J Cell Physiol. **1988** Sep;136(3):507-13*.

Rodeheffer MS, Boone BE, Bryan AC, Shadel GS. « Nam1p, a Protein Involved in RNA Processing and Translation, Is Coupled to Transcription through an Interaction with Yeast Mitochondrial RNA Polymerase », *J Biol Chem. **2001** Mar 16;276(11):8616-22.*

Rooney S, Chaudhuri J, Alt FW. « The Role of the Non-Homologous End-Joining Pathway in Lymphocyte Development ». *Immunol Rev*. **2004** Aug; 200:115-31.

Rossi MN, Carbone M, Mostocotto C, Mancone C, Tripodi M, Maione R, Amati P. « Mitochondrial Localization of PARP-1 Requires Interaction with Mitofilin and Is Involved in the Maintenance of Mitochondrial DNA Integrity », *J Biol Chem.* **2009** Nov 13;284(46):31616-24.

Rostovtseva TK. « VDAC Structure, Function, and Regulation of Mitochondrial and Cellular Metabolism », *Biochim Biophys Acta. **2012** Jun;1818(6):1437.*

Sampath H, Vartanian V, Rollins MR, Sakumi K, Nakabeppu Y, Lloyd RS. « 8-Oxoguanine DNA Glycosylase (OGG1) Deficiency Increases Susceptibility to Obesity and Metabolic Dysfunction », *PLoS One. **2012**;7(12):e51697.*

Sander M, Lowenhaupt K, Rich A. « Drosophila Rrp1 Protein: An Apurinic Endonuclease with Homologous Recombination Activities », *Proc Natl Acad Sci U S A. **1991** Aug 1;88(15):6780-4.*

Santel A, Frank S, Gaume B, Herrler M, Youle RJ, Fuller MT. « Mitofusin-1 Protein Is a Generally Expressed Mediator of Mitochondrial Fusion in Mammalian Cells », *J Cell Sci*. **2003** Jul 1; 116(Pt 13):2763-74.

Sanz A, Stefanatos R, McIlroy G. «Production of reactive oxygen species by the mitochondrial electron transport chain in Drosophila melanogaster». *J Bioenerg Biomembr*. **2010** Apr; 42(2):135-42.

Sbodio JI, Chi NW. « Identification of a Tankyrase-Binding Motif Shared by IRAP, TAB182, and Human TRF1 but Not Mouse TRF1. NuMA Contains This RXXPDG Motif and Is a Novel Tankyrase Partner », *J Biol Chem. **2002** Aug 30; 277(35):31887-92.*

Scarpa ES, Fabrizio G, Di Girolamo M. « A Role of Intracellular Mono-ADP-Ribosylation in Cancer Biology », *FEBS J. **2013** Aug; 280(15):3551-62.*.

Schreiber V, Dantzer F, Ame JC, de Murcia G. « Poly(ADP-Ribose): Novel Functions for an Old Molecule », *Nat Rev Mol Cell Biol. **2006** Jul;7(7):517-28.*

Schwerdtle T, Hamann I, Jahnke G, Walter I, Richter C, Parsons JL, Dianov GL, Hartwig A. « Impact of Copper on the Induction and Repair of Oxidative DNA Damage, poly(ADP-Ribosyl)ation and PARP-1 Activity », *Mol Nutr Food Res. **2007** Feb;51(2):201-10.*

Shall S, de Murcia G. « Poly(ADP-Ribose) Polymerase-1: What Have We Learned from the Deficient Mouse Model? », *Mutat Res. **2000** Jun 30;460(1):1-15*.

Shang J, Clayton DA. « Human Mitochondrial Transcription Termination Exhibits RNA Polymerase Independence and Biased Bipolarity in Vitro », *J Biol Chem. **1994** Nov 18; 269(46):29112-20.*

Shieh WM, Amé JC, Wilson MV, Wang ZQ, Koh DW, Jacobson MK, Jacobson EL. « Poly(ADP-Ribose) Polymerase Null Mouse Cells Synthesize ADP-Ribose Polymers », *J Biol Chem. **1998** Nov 13;273(46):30069-72.*

Skulachev VP. « Mitochondrial Filaments and Clusters as Intracellular Power-Transmitting Cables », *Trends Biochem Sci. **2001** Jan;26(1):23-9.*

Smits P, Smeitink J, van den Heuvel L. « Mitochondrial Translation and beyond: Processes Implicated in Combined Oxidative Phosphorylation Deficiencies », *J Biomed Biotechnol. **2010**; 2010:737385.*

Sologub MIu, Kochetkov SN, Temiakov DE. « [Transcription and its regulation in mammalian and human mitochondria] », *Mol Biol (Mosk). **2009** Mar-Apr;43(2):215-29.*

Southan GJ, Szabó C. « Poly(ADP-Ribose) Polymerase Inhibitors », *Curr Med Chem.* ***2003*** *Feb;10(4):321-40.*

Speina E, Kierzek AM, Tudek B. « Chemical Rearrangement and Repair Pathways of 1,N6-Ethenoadenine », *Mutat Res.* ***2003*** *Oct 29;531(1-2):205-17.*

Spencer WA, Lehmler HJ, Robertson LW, Gupta RC. « Oxidative DNA Adducts after Cu(2+)-Mediated Activation of Dihydroxy PCBs: Role of Reactive Oxygen Species », *Free Radic Biol Med.* ***2009*** *May 15;46(10):1346-52.*

Starcevic D, Dalal S, Sweasy JB. et Joann B Sweasy. « Is There a Link between DNA Polymerase Beta and Cancer? », *Cell Cycle.* ***2004*** *Aug;3(8):998-1001.*

Stefan Krauss. « Mitochondria: Structure and Role in Respiration », in *eLS* (John Wiley & Sons, Ltd, 2001), http://onlinelibrary.wiley.com/doi/10.1038/npg.els.0001380/abstract.

Su Y, Xu A, Zhu J. « The Effect of Oxoguanine Glycosylase 1 rs1052133 Polymorphism on Colorectal Cancer Risk in Caucasian Population », *Tumour Biol.* **2013** Aug 23.

Sutovsky P, Moreno RD, Ramalho-Santos J, Dominko T, Simerly C, Schatten G. « Ubiquitinated Sperm Mitochondria, Selective Proteolysis, and the Regulation of Mitochondrial Inheritance in Mammalian Embryos », *Biol Reprod.* ***2000*** *Aug; 63(2):582-90.*

Sykora P, Wilson DM, Bohr VA. « Repair of Persistent Strand Breaks in the Mitochondrial Genome » *Mech Ageing Dev*. **2012** Apr; 133(4):169-75.

Tamura Y, Onguka O, Hobbs AE, Jensen RE, Iijima M, Claypool SM, Sesaki H. « Role for Two Conserved Intermembrane Space Proteins, Ups1p and Ups2p, [corrected] in Intra-Mitochondrial Phospholipid Trafficking », *J Biol Chem*. **2012** May 4; 287(19):15205-18.

Tanuma S, Johnson LD, Johnson GS. « ADP-Ribosylation of Chromosomal Proteins and Mouse Mammary Tumor Virus Gene Expression. Glucocorticoids Rapidly Decrease Endogenous ADP-Ribosylation of Nonhistone High Mobility Group 14 and 17 Proteins », *J Biol Chem.* ***1983*** *Dec 25; 258(24):15371-5.*

Thompson WE, Ramalho-Santos J, Sutovsky P. « Ubiquitination of Prohibitin in Mammalian Sperm Mitochondria: Possible Roles in the Regulation of Mitochondrial Inheritance and Sperm Quality Control », *Biol Reprod.* ***2003*** *Jul;69(1):254-60.*

Thorburn DR, Rahman S. « Mitochondrial DNA-Associated Leigh Syndrome and NARP », Pagon RA, Adam MP, Bird TD, Dolan CR, Fong CT, Stephens K, editors. SourceGeneReviews™ [Internet]. Seattle (WA): University of Washington, Seattle; 1993-2013. **2003** Oct 30 [updated 2011 May 03].

Tine M, Kuhl H, Jastroch M, Reinhardt R. « Genomic Characterization of the European Sea Bass Dicentrarchus Labrax Reveals the Presence of a Novel Uncoupling Protein (UCP) Gene Family Member in the Teleost Fish Lineage », *BMC Evol Biol.* ***2012*** *May 11;12:62.*

Tiranti V, Savoia A, Forti F, D'Apolito MF, Centra M, Rocchi M, Zeviani M. « Identification of the Gene Encoding the Human Mitochondrial RNA Polymerase (h-mtRPOL) by Cyberscreening of the Expressed Sequence Tags Database », *Hum Mol Genet.* ***1997*** *Apr;6(4):615-25.*

Tiss A, Smith C, Camuzeaux S, Kabir M, Gayther S, Menon U, Waterfield M, Timms J, Jacobs I, Cramer R. « Serum Peptide Profiling Using MALDI Mass Spectrometry: Avoiding the Pitfalls of Coated Magnetic Beads Using Well-Established ZipTip Technology », *Proteomics.* ***2007*** *Sep;7 Suppl 1:77-89.*

Tomkinson AE, Mackey ZB. « Structure and Function of Mammalian DNA Ligases », *Mutat Res.* **1998** Feb; 407(1):1-9.

Tonin Y, Heckel AM, Dovydenko I, Meschaninova M, Comte C, Venyaminova A, Pyshnyi D, Tarassov I, Entelis N. « Characterization of Chemically Modified Oligonucleotides Targeting a Pathogenic Mutation in Human Mitochondrial DNA ». *Biochimie.* **2013** Aug 28. pii: S0300-9084(13)00292-7.

Trafton A. « Researchers identify biochemical functions for most of the human genome - MIT News Office », http://web.mit.edu/newsoffice/2012/researchers-identify-biochemical-functions-for-most-of-the-human-genome.html.

Trafton A. « Researchers identify biochemical functions for most of the human genome - MIT News Office », http://web.mit.edu/newsoffice/2012/researchers-identify-biochemical-functions-for-most-of-the-human-genome.html.

Tsuchimoto D, Sakai Y, Sakumi K, Nishioka K, Sasaki M, Fujiwara T, Nakabeppu Y. « Human APE2 Protein Is Mostly Localized in the Nuclei and to Some Extent in the

Mitochondria, While Nuclear APE2 Is Partly Associated with Proliferating Cell Nuclear Antigen », *Nucleic Acids Res.* ***2001*** *Jun 1;29(11):2349-60.*.

Tsuchimoto D, Sakai Y, Sakumi K, Nishioka K, Sasaki M, Fujiwara T, Nakabeppu Y. « Human APE2 Protein Is Mostly Localized in the Nuclei and to Some Extent in the Mitochondria, While Nuclear APE2 Is Partly Associated with Proliferating Cell Nuclear Antigen », *Nucleic Acids Res.* ***2001*** *Jun 1;29(11):2349-60.*.

Turunc Bayrakdar E, Uyanikgil Y, Kanit L, Koylu E, Yalcin A. « Nicotinamide Treatment Reduces the Levels of Oxidative Stress, Apoptosis and PARP-1 Activity in Aβ(1-42) Induced Rat Model of Alzheimer's Disease », *Free Radic Res.* ***2014*** *Feb;48(2):146-58.*

Turunc Bayrakdar E, Uyanikgil Y, Kanit L, Koylu E, Yalcin A. « Nicotinamide Treatment Reduces the Levels of Oxidative Stress, Apoptosis and PARP-1 Activity in Aβ(1-42) Induced Rat Model of Alzheimer's Disease », *Free Radic Res.* ***2014*** *Feb;48(2):146-58.*

Uchida K, Miwa M. « Poly(ADP-Ribose) Polymerase: Structural Conservation among Different Classes of Animals and Its Implications », *Mol Cell Biochem.* ***1994*** *Sep; 138(1-2):25-32.*

Uchida K, Miwa M. « Poly(ADP-Ribose) Polymerase: Structural Conservation among Different Classes of Animals and Its Implications », *Mol Cell Biochem.* ***1994*** *Sep; 138(1-2):25-32.*

Uchida M, Hanai S, Uematsu N, Sawamoto K, Okano H, Miwa M, Uchida K. « Genetic and Functional Analysis of PARP, a DNA Strand Break-Binding Enzyme », *Mutat Res.* ***2001*** *Jun 2;477(1-2):89-96.*

Uchida M, Hanai S, Uematsu N, Sawamoto K, Okano H, Miwa M, Uchida K. « Genetic and Functional Analysis of PARP, a DNA Strand Break-Binding Enzyme », *Mutat Res.* ***2001*** *Jun 2;477(1-2):89-96.*

Uchiumi F, Watanabe T, Ohta R, Abe H, Tanuma S. « PARP1 gene expression is downregulated by knockdown of PARG gene». Oncol Rep. **2013** May;29(5):1683-8.

Uchiumi F, Watanabe T, Ohta R, Abe H, Tanuma S. « PARP1 gene expression is downregulated by knockdown of PARG gene». Oncol Rep. 2013 May;29(5):1683-8.

van der Kemp PA, Thomas D, Barbey R, de Oliveira R, Boiteux S. « Cloning and Expression in Escherichia Coli of the OGG1 Gene of Saccharomyces Cerevisiae, Which Codes for a DNA Glycosylase That Excises 7,8-Dihydro-8-Oxoguanine and 2,6-Diamino-4-Hydroxy-5-N-Methylformamidopyrimidine », *Proc Natl Acad Sci U S A.* ***1996*** *May 28;93(11):5197-202.*

van der Kemp PA, Thomas D, Barbey R, de Oliveira R, Boiteux S. « Cloning and Expression in Escherichia Coli of the OGG1 Gene of Saccharomyces Cerevisiae, Which Codes for a DNA Glycosylase That Excises 7,8-Dihydro-8-Oxoguanine and 2,6-Diamino-4-Hydroxy-5-N-Methylformamidopyrimidine », *Proc Natl Acad Sci U S A.* ***1996*** *May 28;93(11):5197-202.*

van Loon B, Samson LD. « Alkyladenine DNA Glycosylase (AAG) Localizes to Mitochondria and Interacts with Mitochondrial Single-Stranded Binding Protein (mtSSB) », *DNA Repair (Amst).* **2013** Mar 1; 12(3):177-87.

van Loon B, Samson LD. « Alkyladenine DNA Glycosylase (AAG) Localizes to Mitochondria and Interacts with Mitochondrial Single-Stranded Binding Protein (mtSSB) », *DNA Repair (Amst).* **2013** Mar 1; 12(3):177-87.

Wallace DC. « Animal Models for Mitochondrial Disease », *Methods Mol Biol.* ***2002****; 197:3-54.*

Wallace DC. « Animal Models for Mitochondrial Disease », *Methods Mol Biol.* ***2002****; 197:3-54.*

Wang Y, Shadel GS. « Stability of the Mitochondrial Genome Requires an Amino-Terminal Domain of Yeast Mitochondrial RNA Polymerase », *Proc Natl Acad Sci U S A.* **1999** Jul 6; 96(14):8046-51.

Wang Y, Shadel GS. « Stability of the Mitochondrial Genome Requires an Amino-Terminal Domain of Yeast Mitochondrial RNA Polymerase », *Proc Natl Acad Sci U S A.* **1999** Jul 6; 96(14):8046-51.

Wang Z, Cai F, Chen X, Luo M, Hu L, Lu Y. « The Role of Mitochondria-Derived Reactive Oxygen Species in Hyperthermia-Induced Platelet Apoptosis », *PLoS One.* ***2013*** *Sep 4; 8(9):e75044.*

Wang Z, Cai F, Chen X, Luo M, Hu L, Lu Y. « The Role of Mitochondria-Derived Reactive Oxygen Species in Hyperthermia-Induced Platelet Apoptosis », *PLoS One.* ***2013*** *Sep 4; 8(9):e75044.*

Wanrooij S, Falkenberg M. « The human mitochondrial replication fork in health and disease », *Biochim Biophys Acta.* ***2010*** *Aug; 1797(8):1378-88.*

Wanrooij S, Falkenberg M. « The human mitochondrial replication fork in health and disease ». *Biochim Biophys Acta.* **2010** Aug; 1797(8):1378-88.

Wanrooij S, Falkenberg M. « The human mitochondrial replication fork in health and disease », *Biochim Biophys Acta.* ***2010*** *Aug; 1797(8):1378-88.*

Wanrooij S, Falkenberg M. « The human mitochondrial replication fork in health and disease ». *Biochim Biophys Acta.* **2010** Aug; 1797(8):1378-88.

Wanrooij S, Fusté JM, Farge G, Shi Y, Gustafsson CM, Falkenberg M. « Human Mitochondrial RNA Polymerase Primes Lagging-Strand DNA Synthesis in Vitro », *Proc Natl Acad Sci U S A.* ***2008*** *Aug 12;105(32):11122-7.*

Wanrooij S, Fusté JM, Farge G, Shi Y, Gustafsson CM, Falkenberg M. « Human Mitochondrial RNA Polymerase Primes Lagging-Strand DNA Synthesis in Vitro », *Proc Natl Acad Sci U S A.* ***2008*** *Aug 12;105(32):11122-7.*

Wei YH, Lu CY, Lee HC, Pang CY, Ma YS. « Oxidative Damage and Mutation to Mitochondrial DNA and Age-Dependent Decline of Mitochondrial Respiratory Function », *Ann N Y Acad Sci.* ***1998*** *Nov 20; 854:155-70.*

Wei YH, Lu CY, Lee HC, Pang CY, Ma YS. « Oxidative Damage and Mutation to Mitochondrial DNA and Age-Dependent Decline of Mitochondrial Respiratory Function », *Ann N Y Acad Sci.* ***1998*** *Nov 20; 854:155-70.*

Weterings E, van Gent DC. « The Mechanism of Non-Homologous End-Joining: A Synopsis of Synapsis », *DNA Repair (Amst).* ***2004*** *Nov 2; 3(11):1425-35.*

Weterings E, van Gent DC. « The Mechanism of Non-Homologous End-Joining: A Synopsis of Synapsis », *DNA Repair (Amst).* ***2004*** *Nov 2; 3(11):1425-35.*

Wong TW, Clayton DA « DNA Primase of Human Mitochondria Is Associated with Structural RNA That Is Essential for Enzymatic Activity », *Cell. **1986** Jun 20;45(6):817-25.*

Wong TW, Clayton DA « DNA Primase of Human Mitochondria Is Associated with Structural RNA That Is Essential for Enzymatic Activity », *Cell. **1986** Jun 20;45(6):817-25.*

Wong TW, Clayton DA. « In Vitro Replication of Human Mitochondrial DNA: Accurate Initiation at the Origin of Light-Strand Synthesis », *Cell. **1985B** Oct; 42(3):951-8.*

Wong TW, Clayton DA. « In Vitro Replication of Human Mitochondrial DNA: Accurate Initiation at the Origin of Light-Strand Synthesis », *Cell. **1985B** Oct; 42(3):951-8.*

Wong TW, Clayton DA. « Isolation and Characterization of a DNA Primase from Human Mitochondria », *J Biol Chem. **1985A** Sep 25; 260(21):11530-5.*

Wong TW, Clayton DA. « Isolation and Characterization of a DNA Primase from Human Mitochondria », *J Biol Chem. **1985A** Sep 25; 260(21):11530-5.*

Woon EC, Threadgill MD. « Poly(ADP-Ribose)polymerase Inhibition - Where Now? », *Curr Med Chem. **2005**;12(20):2373-92.*

Woon EC, Threadgill MD. « Poly(ADP-Ribose)polymerase Inhibition - Where Now? », *Curr Med Chem. **2005**;12(20):2373-92.*

Yang RF, Zhao GW, Liang ST, Zhang Y, Sun LH, Chen HZ, Liu DP. « Mitofilin Regulates Cytochrome c Release during Apoptosis by Controlling Mitochondrial Cristae Remodeling », *Biochem Biophys Res Commun. **2012** Nov 9; 428(1):93-8.*

Yang RF, Zhao GW, Liang ST, Zhang Y, Sun LH, Chen HZ, Liu DP. « Mitofilin Regulates Cytochrome c Release during Apoptosis by Controlling Mitochondrial Cristae Remodeling », *Biochem Biophys Res Commun. **2012** Nov 9; 428(1):93-8.*

Yeh TY, Beiswenger KK, Li P, Bolin KE, Lee RM, Tsao TS, Murphy AN, Hevener AL, Chi NW. « Hypermetabolism, Hyperphagia, and Reduced Adiposity in Tankyrase-Deficient Mice », *Diabetes. **2009** Nov;58(11):2476-85.*

Yeh TY, Beiswenger KK, Li P, Bolin KE, Lee RM, Tsao TS, Murphy AN, Hevener AL, Chi NW. « Hypermetabolism, Hyperphagia, and Reduced Adiposity in Tankyrase-Deficient Mice », *Diabetes. **2009** Nov;58(11):2476-85.*

Yelamos J, Farres J, Llacuna L, Ampurdanes C, Martin-Caballero J. « PARP-1 and PARP-2: New Players in Tumour Development », *Am J Cancer Res.* ***2011****; 1(3):328-346.*

Yelamos J, Farres J, Llacuna L, Ampurdanes C, Martin-Caballero J. « PARP-1 and PARP-2: New Players in Tumour Development », *Am J Cancer Res.* ***2011****; 1(3):328-346.*

Zha S, Guo C, Boboila C, Oksenych V, Cheng HL, Zhang Y, Wesemann DR, Yuen G, Patel H, Goff PH, Dubois RL, Alt FW. « ATM Damage Response and XLF Repair Factor Are Functionally Redundant in Joining DNA Breaks », *Nature.* ***2011*** *Jan 13; 469(7329):250-4.*

Zha S, Guo C, Boboila C, Oksenych V, Cheng HL, Zhang Y, Wesemann DR, Yuen G, Patel H, Goff PH, Dubois RL, Alt FW. « ATM Damage Response and XLF Repair Factor Are Functionally Redundant in Joining DNA Breaks », *Nature.* ***2011*** *Jan 13; 469(7329):250-4.*

ANNEXES

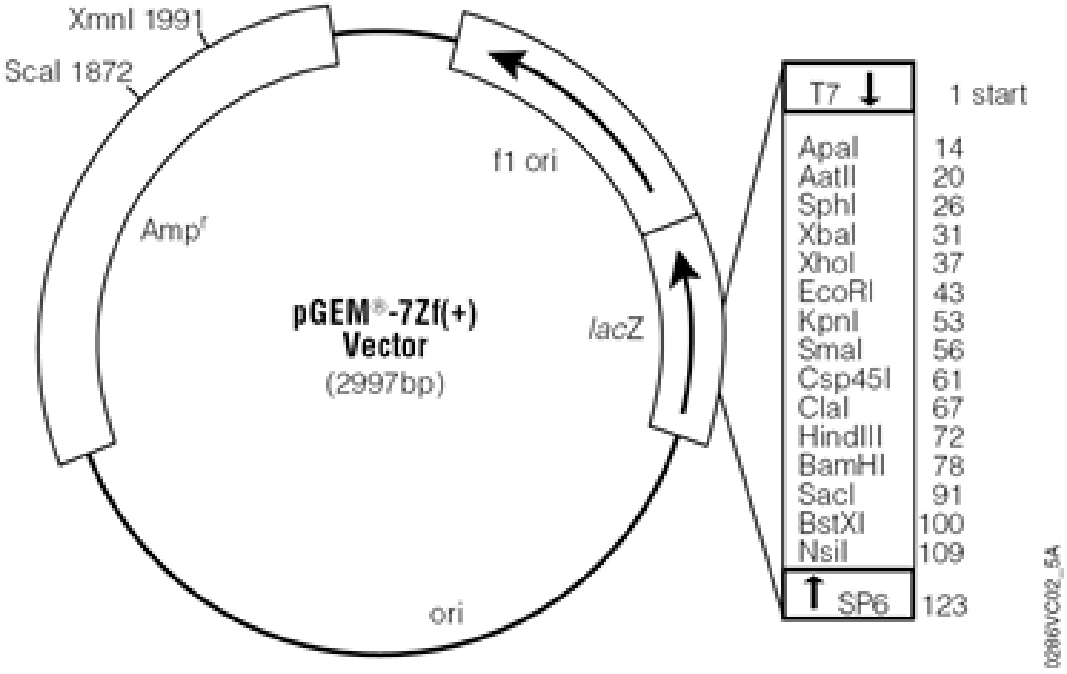

Annexe 1: pGEM7z(+) vector

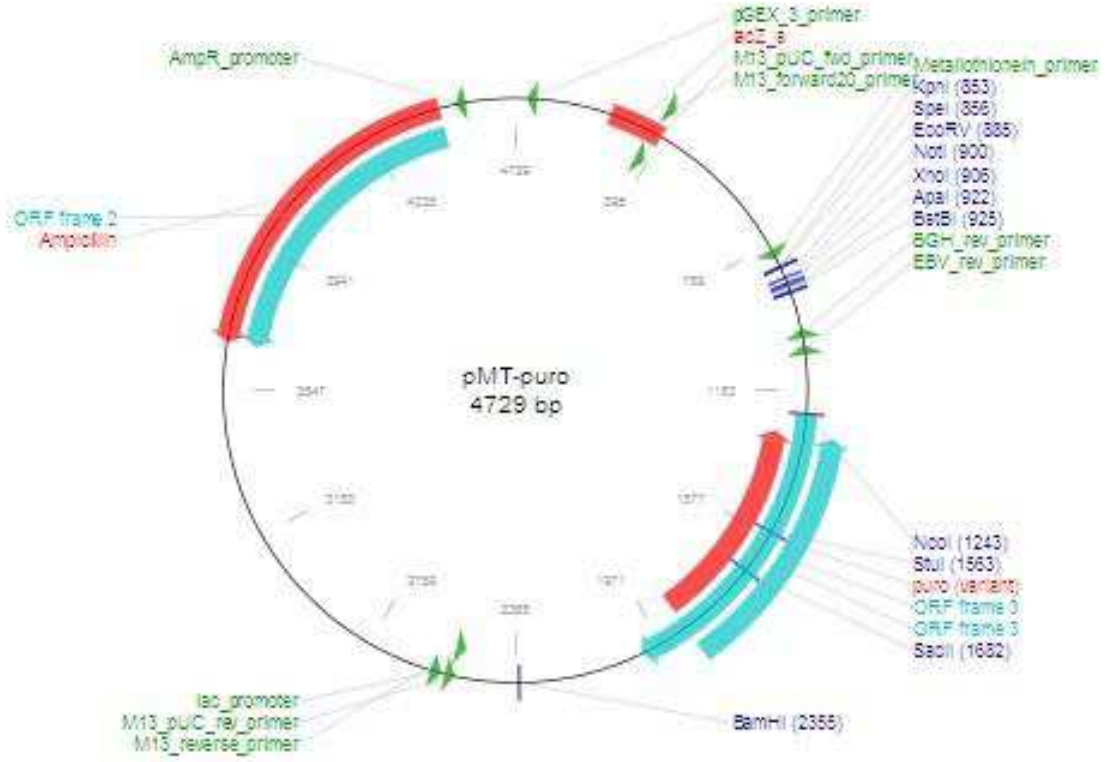

Annexes 2 : pMT puro vector

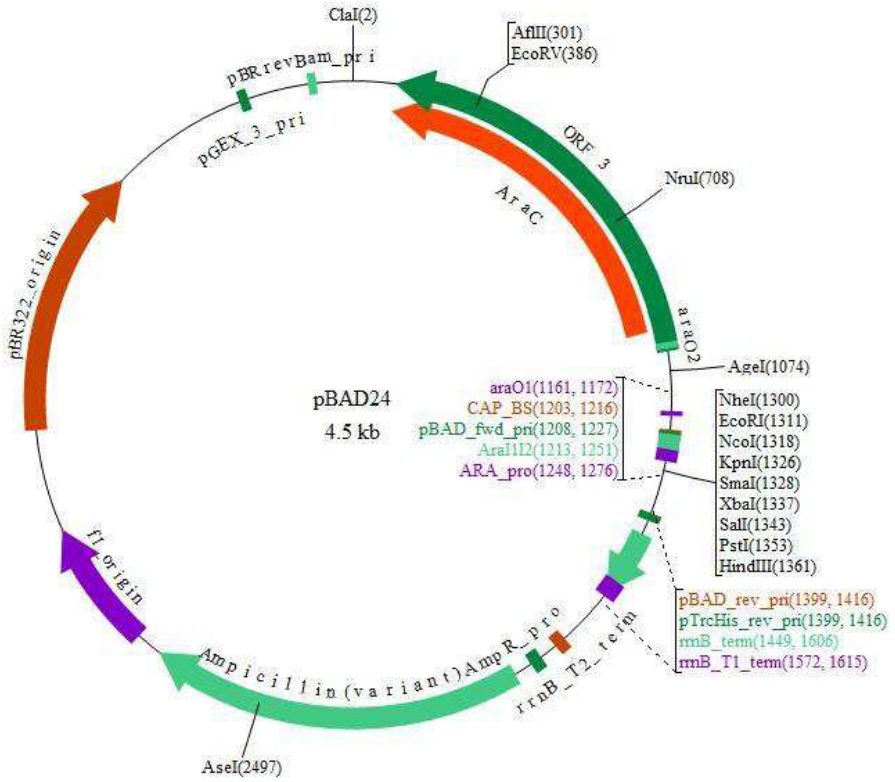

Annexe 3: pBAD24 vector

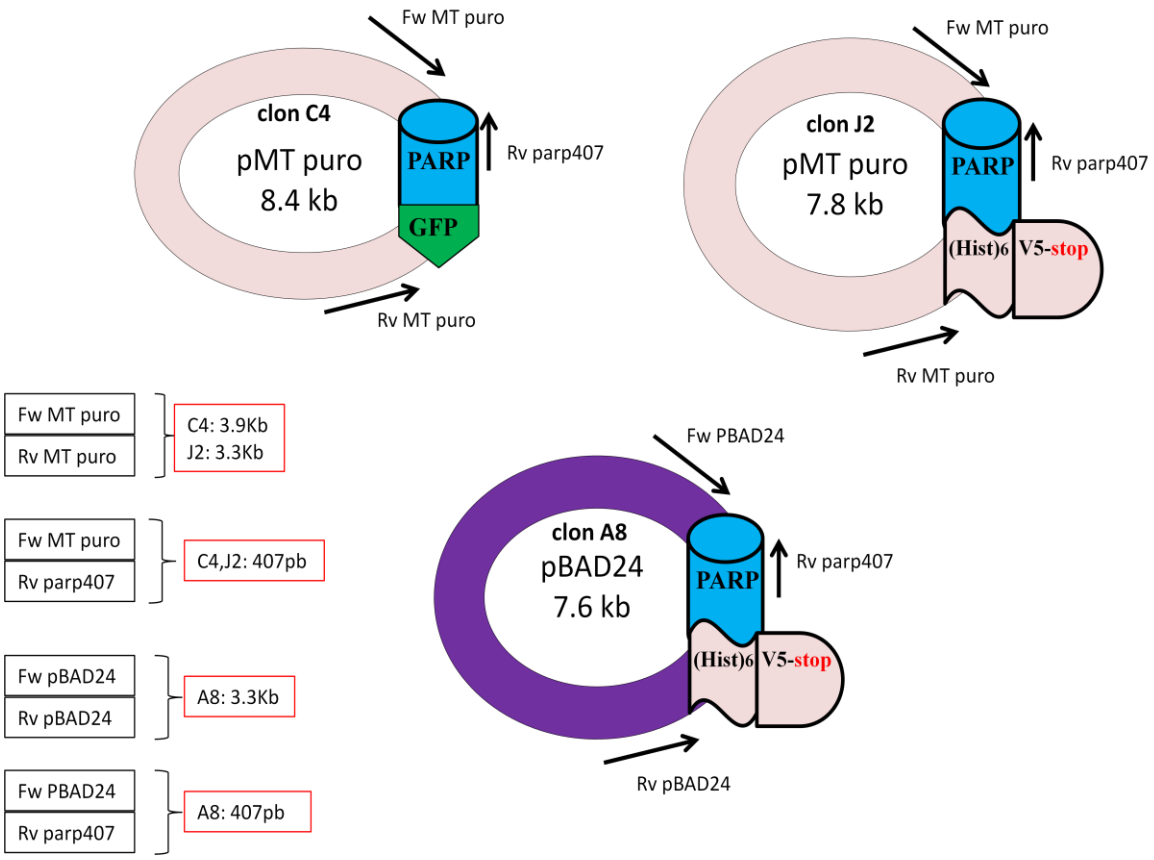

***Annexe 4**: Relative positions of primers in the plasmids J2, C4 and A8. Amplification product sizes.*

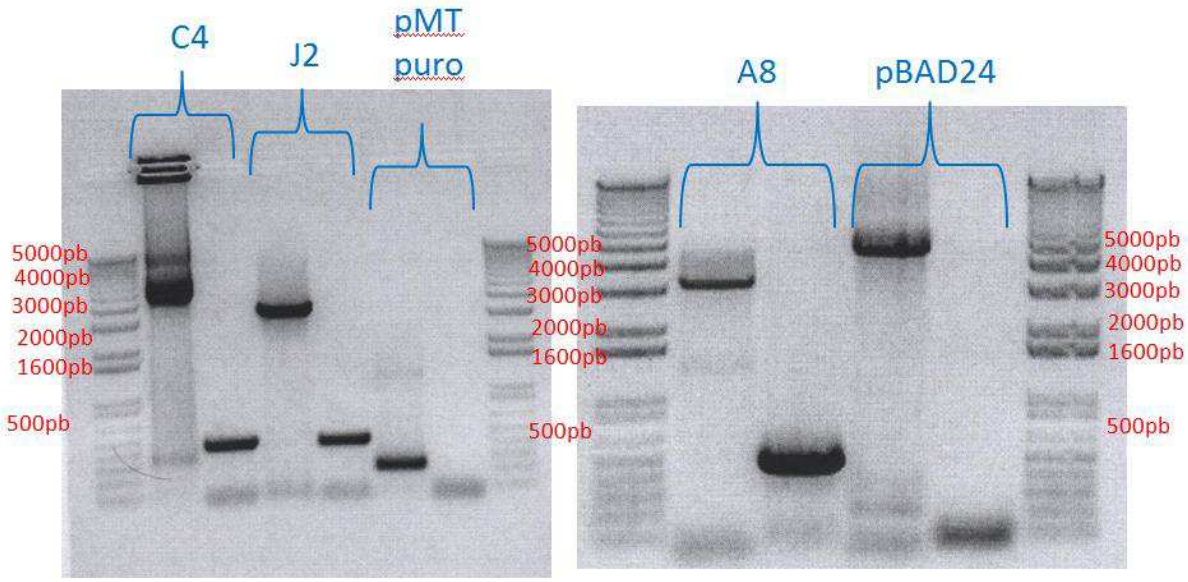

***Annexe 5**: PCR amplifications of plasmids C4, J2, A8 and the vectors pMT puro and pBAD24 using specific primers (annexe 4).*

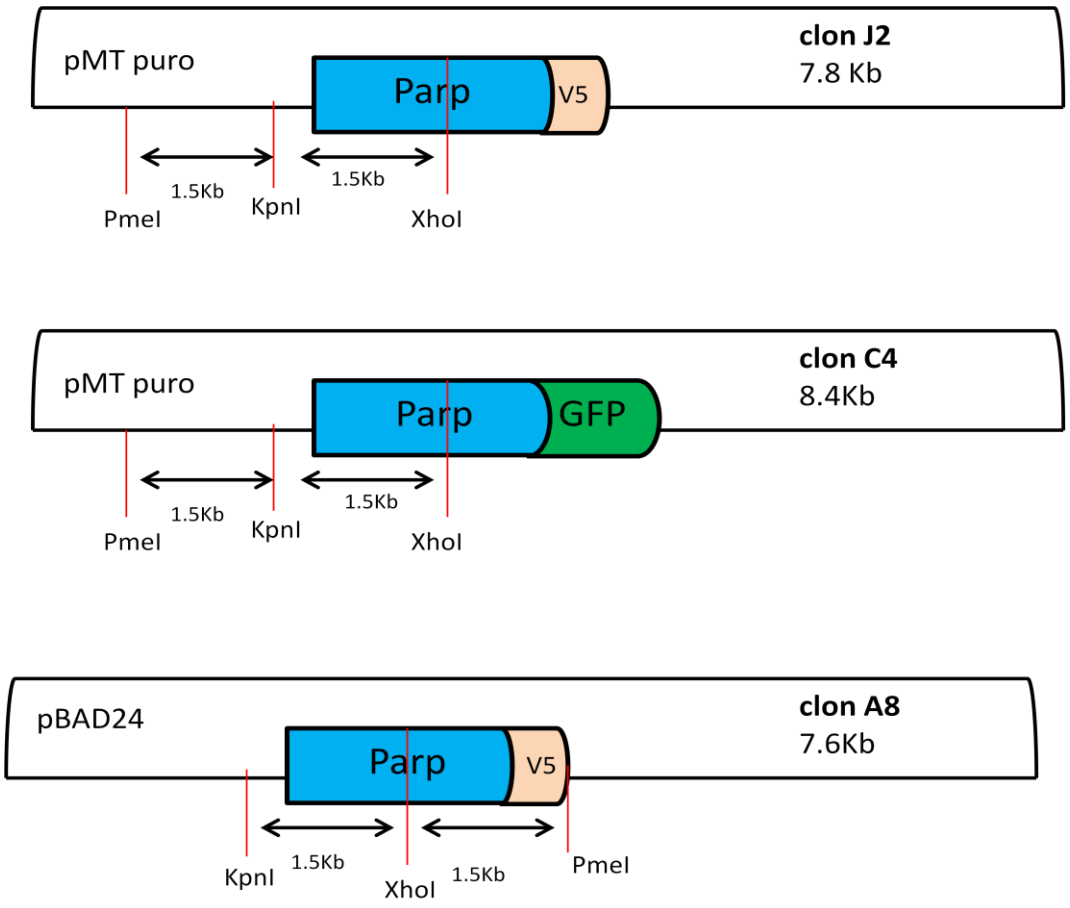

***Annexe 6** : Relative positions of KpnI, XhoI and PmeI in the plasmids J2, C4 and A8.*

ggggatatcGTGTAATATGGATATTGAATTACCTTATCTTGCTGAGTATGCAAGAACTGGACGAGCCACT
TGCAAAGGATGTAAAAGTACTATATCTAAAGATACTCTTCGGATTGCTGTCATGGTTCAATCTGCATTTC
ATGATGCCAAAGTTCCGAATTGGTTTCATAAAACCTGCTTTTTTAAAAACCAGCGTCCCAGCTCAGTAGG
AGACATACAAAACATTGGAAATCTCCGATTTGCCGATCAAAAGGAATTAACGGATCTTGTGGAAAATATA
CAAGAAGTTATAAGCGCACAATTAGGAAAAAAGCGATCGAAGGCTTTTAACTTAGCATTAAAAGACTTTG
GGATTGAATATGCAAAATCTAGTCGATCGACGTGTCGTGGATGTGAACAAAAAATAAACAAGGATCTAGT
TCGCTTACGTAAAACTGTTTATGATACTGAAGTTGGTATGAAGTACGGAGGCCAACCTTTGTGGCATCAT
TTGGAATGCTTCGCCCAATTGCGCTCTGAGCTTGGCTGGTTTGCGTCAGGTGAAGATATGCCAGGATTTC
AGAGCTTAGCAGATGATGATCAAGCGAAAGTTAAAAACGCCATACCACCAATAAAATCTGAAGAACTACC
AGATACAAAAAGAGCTAAGATGGAATTATCAGATACAAATGAAGAAGGAGAAAAGAAACAACGCTTAAAA
GATCAAAATGATGCCTACTTCAGGTTTCGCGATGACATTAAAAATAAAATGAAGAAGAAAGACATTGATA
TACTTCTAAAGTTTAATAATCAACAACCTGTAACTGGTGACACAGAAAAGTTATTTGATCAAACTGCCGA
TTTACTGACATTCGGAGCTATTGAATCATGTTCTGAATGCAACAGCTGTCAGTTTATTGTTAATAAATCT
GGATATATATGTAATGGAAATCATTCTGAGTGGACCAAATGTAACAAGCTGCTAAAAGAGCCAACAAGAT
CGGCATGCATAGTGCCAAAAGAACTTAAAGCATTATATAATTTTTTGAATACCGTGAAAGAAATTCCATC
TACACGGATCTTTAATAACTTTCCTCCCAATAAAAGTACCTTTTCTAGAAGTCTTTTGAAAACGAATAAA
AACAATGATGTTTTGGTTAGGCCAACAATACCTCGTATAAGTCCGCCATTATACAATTTAAAGTTTTCAA
TTATAGGCTTAAAGAACCAGCATAAAGAGCTAAGAAAGCGAATAGAAAATTTGGGCGGTAAATTTGAAGT
TAAAATATCGGAAAACACGATAGCAATAATATCAACAGAATTAGAAATACAAAAAAAATCCACCCGTATG
AAGTTTGCAGAAGAGCTCGGAATTCATATTGTGCCCATTGAATTTTTAGATTTTGTTGAAGCCGATACAG
AAGGAGCTATTAAATATATAAATAGCACATGTATTTGTAGTTGGGGAACAGATCCAAAATCCAGAATTCC
AAAGGAAACAACAAAAAGTTTAAATTCGAACAGTATATATACAAAATCCATGCCAGTATCACGGACATTT
AAAGTAAAAGATGGCCTAGCTGTTGATCCGGACAGTGGGCTCGAGGACATCGCCCATGTTTACGTGGACA
GTAACAATAAATACAGTGTTGTTCTTGGCTTAACTGACATTCAGAGAAATAAGAACTCCTACTACAAAGT
TCAGCTTTTAAAAGCGGATAAAAAGGAGAAATATTGGATTTTTCGTTCATGGGGTCGAATTGGAACAAAT
ATTGGAAACTCAAAACTTGAAGAGTTCGACACGAGCGAGTCTGCAAAAAGAAATTTTAAAGAAATATATG
CAGATAAAACTGGAAATGAATACGAGCAACGAGATAACTTTGTTAAAAGAACAGGTCGAATGTACCCAAT
CGAAATTCAATATGATGATGACCAAAAGTTGGTAAAACACGAAAGCCATTTCTTTACTTCCAAATTAGAG
ATTTCTGTGCAAAATTTAATAAAGCTGATTTTTGATATTGACTCAATGAATAAAACATTGATGGAATTCC
ATATCGACATGGATAAAATGCCGCTGGGCAAGCTCAGTGCTCATCAAATCCAATCTGCTTACAGAGTAGT
GAAGGAAATTTATAATGTACTAGAATGTGGTTCCAATACTGCAAAACTTATTGATGCAACAAATAGGTTT
TATACGTTAATTCCTCATAATTTTGGAGTTCAATTACCAACATTAATTGAAACACATCAACAAATTGAAG
ATTTGCGACAAATGCTTGATTCATTAGCTGAGATAGAGGTTGCGTACAGTATAATCAAAAGCGAAGATGT
ATCTGATGCTTGTAATCCTTTAGATAATCATTACGCACAGATTAAAACTCAGTTGGTGGCATTAGACAAA
AATAGTGAAGAATTTTCGATTCTTAGCCAGTACGTAAAAAACACTCATGCATCTACCCACAAATCTTATG
ATTTAAAAATTGTTGATGTATTTAAAGTATCTCGCCAAGGAGAAGCAAGGCGCTTTAAACCATTTAAGAA
GCTACATAACAGAAAATTATTATGGCACGGATCACGTTTAACTAATTTTGTTGGTATATTATCGCATGGT
TTAAGAATTGCTCCCCCAGAAGCGCCACCAACAGGTTATATGTTCGGAAAAGGCATTTATTTTGCGGATA
TGGTTTCAAAATCCGCAAATTATTGTTGCACAAGTCAACAAAACTCTACTGGATTAATGCTTCTATCTGA
AGTTGCTTTGGGCGATATGATGGAATGCACTTCAGCGAAATACATTAATAAACTATCAAATAATAAACAT
AGTTGTTTCGGTCGTGGTCGCACCATGCCAGATCCTACTAAGAGCTATATAAGAAGTGATGGGGTTGAAA
TTCCTTACGGAGAAACCATTACTGACGAACATTTAAAGTCATCGTTATTATATAACGAGTATATAGTATA
TGATGTTGCGCAGGTCAATATTCAATATTTGTTTCGTATGGAATTCAAGTATTCTTATcccatgAGTAAA
GGAGAAGAACTTTTCACTGGAGTTGTTCCAATTCTTGTTGAATTAGATGGTGATGTTAATGGGCACAAAT
TTTCTGTCAGTGGAGAGGGTGAAGGTGATGCAACATACGGAAAACTTACCCTTAAATTTATTTGCACTAC
TGGAAAACTACCTGTTCCATGGCCAACACTTGTCACTACTTTCGCCTATGGTGTTCAATGCTTTTCAAGA
TACCCAGATCATATGAAACGGCATGACTTTTTCAAGAGTGCCATGCCCGAAGGTTATGTACAGGAAAGAA
CTATATTTTTCAAAGATGACGGGAACTACAAGACACGTGCTGAAGTCAAGTTTGAAGGTGATACCCTTGT
TAATAGAATCGAGTTAAAAGGTATTGATTTTAAAGAAGATGGAAACATTCTTGGACACAAATTGGAATAC
AACTATAACTCACACAATGTATACATCATGGCAGACAAACAAAAGAATGGAATCAAAGTTAACTTCAAAA
TTAGACACAACATTGAAGATGGAAGCGTTCAACTAGCAGACCATTATCAACAAAATACTCCAATTGGCGA
TGGCCCTGTCCTTCTACCAGACAACCATTACCTGTCCACACAATCTGTCCTTTCGAAAGACCCCAACGAA
AAGAGAGACCACATGGTCCTTCTTGAGTTTGTAACAGCTGCTGGGATTACACATGGCATGGATGAACTAT
ACAAATAG

***Annexe 7**: DNA sequence (3718 pb) of parpB-GFP from the C4 plasmid. The ATG (start codon) was represented in green and TGA (stop codon) in red colors. The ccc in violet color represents SmaI remaining site following digest and the tag GFP was illustrated in blue color.*

ggggatatcGTGTAATATGGATATTGAATTACCTTATCTTGCTGAGTATGCAAGAACTGGACGAGCCACTTGCAAAGGATGTAAAAG
TACTATATCTAAAGATACTCTTCGGATTGCTGTCATGGTTCAATCTGCATTTCATGATGCCAAAGTTCCGAATTGGTTTCATAAAA
CCTGCTTTTTTAAAAACCAGCGTCCCAGCTCAGTAGGAGACATACAAAACATTGGAAATCTCCGATTTGCCGATCAAAAGGAATT
AACGGATCTTGTGGAAAATATACAAGAAGTTATAAGCGCACAATTAGGAAAAAAGCGATCGAAGGCTTTTAACTTAGCATTAAAA
GACTTTGGGATTGAATATGCAAAATCTAGTCGATCGACGTGTCGTGGATGTGAACAAAAAATAAACAAGGATCTAGTTCGCTTAC
GTAAAACTGTTTATGATACTGAAGTTGGTATGAAGTACGGAGGCCAACCTTTGTGGCATCATTTGGAATGCTTCGCCCAATTGC
GCTCTGAGCTTGGCTGGTTTGCGTCAGGTGAAGATATGCCAGGATTTCAGAGCTTAGCAGATGATGATCAAGCGAAAGTTAAAA
ACGCCATACCACCAATAAAATCTGAAGAACTACCAGATACAAAAAGAGCTAAGATGGAATTATCAGATACAAATGAAGAAGGAGA
AAAGAAACAACGCTTAAAAGATCAAAATGATGCCTACTTCAGGTTTCGCGATGACATTAAAAATAAAATGAAGAAGAAAGACATT
GATATACTTCTAAAGTTTAATAATCAACAACCTGTAACTGGTGACACAGAAAAGTTATTTGATCAAACTGCCGATTTACTGACATT
CGGAGCTATTGAATCATGTTCTGAATGCAACAGCTGTCAGTTTATTGTTAATAAATCTGGATATATATGTAATGGAAATCATTCTG
AGTGGACCAAATGTAACAAGCTGCTAAAAGAGCCAACAAGATCGGCATGCATAGTGCCAAAAGAACTTAAAGCATTATATAATTT
TTTGAATACCGTGAAAGAAATTCCATCTACACGGATCTTTAATAACTTTCCTCCCAATAAAAGTACCTTTTCTAGAAGTCTTTTGAA
AACGAATAAAAACAATGATGTTTTGGTTAGGCCAACAATACCTCGTATAAGTCCGCCATTATACAATTTAAAGTTTTCAATTATAG
GCTTAAAGAACCAGCATAAAGAGCTAAGAAAGCGAATAGAAAATTTGGGCGGTAAATTTGAAGTTAAAATATCGGAAAACACGAT
AGCAATAATATCAACAGAATTAGAAATACAAAAAAAATCCACCCGTATGAAGTTTGCAGAAGAGCTCGGAATTCATATTGTGCCC
ATTGAATTTTTAGATTTTGTTGAAGCCGATACAGAAGGAGCTATTAAATATATAAATAGCACATGTATTTGTAGTTGGGGAACAGA
TCCAAAATCCAGAATTCCAAAGGAAACAACAAAAAGTTTAAATTCGAACAGTATATATACAAAATCCATGCCAGTATCACGGACAT
TTAAAGTAAAAGATGGCCTAGCTGTTGATCCGGACAGTGGGCTCGAGGACATCGCCCATGTTTACGTGGACAGTAACAATAAAT
ACAGTGTTGTTCTTGGCTTAACTGACATTCAGAGAAATAAGAACTCCTACTACAAAGTTCAGCTTTTAAAAGCGGATAAAAAGGA
GAAATATTGGATTTTTCGTTCATGGGGTCGAATTGGAACAAATATTGGAAACTCAAAACTTGAAGAGTTCGACACGAGCGAGTCT
GCAAAAAGAAATTTTAAAGAAATATATGCAGATAAAACTGGAAATGAATACGAGCAACGAGATAACTTTGTTAAAAGAACAGGTC
GAATGTACCCAATCGAAATTCAATATGATGATGACCAAAAGTTGGTAAAACACGAAAGCCATTTCTTTACTTCCAAATTAGAGATT
TCTGTGCAAAATTTAATAAAGCTGATTTTTGATATTGACTCAATGAATAAAACATTGATGGAATTCCATATCGACATGGATAAAAT
GCCGCTGGGCAAGCTCAGTGCTCATCAAATCCAATCTGCTTACAGAGTAGTGAAGGAAATTTATAATGTACTAGAATGTGGTTC
CAATACTGCAAAACTTATTGATGCAACAAATAGGTTTTATACGTTAATTCCTCATAATTTTGGAGTTCAATTACCAACATTAATTGA
AACACATCAACAAATTGAAGATTTGCGACAAATGCTTGATTCATTAGCTGAGATAGAGGTTGCGTACAGTATAATCAAAAGCGAA
GATGTATCTGATGCTTGTAATCCTTTAGATAATCATTACGCACAGATTAAAACTCAGTTGGTGGCATTAGACAAAAATAGTGAAGA
ATTTTCGATTCTTAGCCAGTACGTAAAAAACACTCATGCATCTACCCACAAATCTTATGATTTAAAAATTGTTGATGTATTTAAAGT
ATCTCGCCAAGGAGAAGCAAGGCGCTTTAAACCATTTAAGAAGCTACATAACAGAAAATTATTATGGCACGGATCACGTTTAACT
AATTTTGTTGGTATATTATCGCATGGTTTAAGAATTGCTCCCCCAGAAGCGCCACCAACAGGTTATATGTTCGGAAAAGGCATTT
ATTTTGCGGATATGGTTTCAAAATCCGCAAATTATTGTTGCACAAGTCAACAAAACTCTACTGGATTAATGCTTCTATCTGAAGTT
GCTTTGGGCGATATGATGGAATGCACTTCAGCGAAATACATTAATAAACTATCAAATAATAAACATAGTTGTTTCGGTCGTGGTC
GCACCATGCCAGATCCTACTAAGAGCTATATAAGAAGTGATGGGGTTGAAATTCCTTACGGAGAAACCATTACTGACGAACATTT
AAAGTCATCGTTATTATATAACGAGTATATAGTATATGATGTTGCGCAGGTCAATATTCAATATTTGTTTCGTATGGAATTCAAGTA
TTCTTATcccGGTAAGCCTATCCCTAACCCTCTCCTCGGTCTCGATTCTACGCGTACCGGTCATCATCACCATCACCATTGAGT
TTAAACCCGCTGATCAGCCTCGACTGTGCCTTCTAAGATCC

***Annexe 8**: DNA sequence (3116 pb) of parpB-V5 from the J2 plasmid. The ATG (start codon) was represented in green and TGA (stop codon) in red colors. The ccc in violet color represents SmaI remaining site following digest and the tag V5 was illustrated in blue color.*

GTGTAATATGGATATTGAATTACCTTATCTTGCTGAGTATGCAAGAACTGGACGAGCCACTTGCAAAGGA
TGTAAAAGTACTATATCTAAAGATACTCTTCGGATTGCTGTCATGGTTCAATCTGCATTTCATGATGCCA
AAGTTCCGAATTGGTTTCATAAAACCTGCTTTTTTAAAAACCAGCGTCCCAGCTCAGTAGGAGACATACA
AAACATTGGAAATCTCCGATTTGCCGATCAAAAGGAATTAACGGATCTTGTGGAAAATATACAAGAAGTT
ATAAGCGCACAATTAGGAAAAAAGCGATCGAAGGCTTTTAACTTAGCATTAAAAGACTTTGGGATTGAAT
ATGCAAAATCTAGTCGATCGACGTGTCGTGGATGTGAACAAAAAATAAACAAGGATCTAGTTCGCTTACG
TAAAACTGTTTATGATACTGAAGTTGGTATGAAGTACGGAGGCCAACCTTTGTGGCATCATTTGGAATGC
TTCGCCCAATTGCGCTCTGAGCTTGGCTGGTTTGCGTCAGGTGAAGATATGCCAGGATTTCAGAGCTTAG
CAGATGATGATCAAGCGAAAGTTAAAAACGCCATACCACCAATAAAATCTGAAGAACTACCAGATACAAA
AAGAGCTAAGATGGAATTATCAGATACAAATGAAGAAGGAGAAAAGAAACAACGCTTAAAAGATCAAAAT
GATGCCTACTTCAGGTTTCGCGATGACATTAAAAATAAAATGAAGAAGAAAGACATTGATATACTTCTAA
AGTTTAATAATCAACAACCTGTAACTGGTGACACAGAAAAGTTATTTGATCAAACTGCCGATTTACTGAC
ATTCGGAGCTATTGAATCATGTTCTGAATGCAACAGCTGTCAGTTTATTGTTAATAAATCTGGATATATA
TGTAATGGAAATCATTCTGAGTGGACCAAATGTAACAAGCTGCTAAAAGAGCCAACAAGATCGGCATGCA
TAGTGCCAAAAGAACTTAAAGCATTATATAATTTTTTGAATACCGTGAAAGAAATTCCATCTACACGGAT
CTTTAATAACTTTCCTCCCAATAAAAGTACCTTTTCTAGAAGTCTTTTGAAAACGAATAAAAACAATGAT
GTTTTGGTTAGGCCAACAATACCTCGTATAAGTCCGCCATTATACAATTTAAAGTTTTCAATTATAGGCT
TAAAGAACCAGCATAAAGAGCTAAGAAAGCGAATAGAAAATTTGGGCGGTAAATTTGAAGTTAAAATATC
GGAAAACACGATAGCAATAATATCAACAGAATTAGAAATACAAAAAAAATCCACCCGTATGAAGTTTGCA
GAAGAGCTCGGAATTCATATTGTGCCCATTGAATTTTTAGATTTTGTTGAAGCCGATACAGAAGGAGCTA
TTAAATATATAAATAGCACATGTATTTGTAGTTGGGGAACAGATCCAAAATCCAGAATTCCAAAGGAAAC
AACAAAAAGTTTAAATTCGAACAGTATATATACAAAATCCATGCCAGTATCACGGACATTTAAAGTAAAA
GATGGCCTAGCTGTTGATCCGGACAGTGGGCTCGAGGACATCGCCCATGTTTACGTGGACAGTAACAATA
AATACAGTGTTGTTCTTGGCTTAACTGACATTCAGAGAAATAAGAACTCCTACTACAAAGTTCAGCTTTT
AAAAGCGGATAAAAAGGAGAAATATTGGATTTTTCGTTCATGGGGTCGAATTGGAACAAATATTGGAAAC
TCAAAACTTGAAGAGTTCGACACGAGCGAGTCTGCAAAAAGAAATTTTAAAGAAATATATGCAGATAAAA
CTGGAAATGAATACGAGCAACGAGATAACTTTGTTAAAAGAACAGGTCGAATGTACCCAATCGAAATTCA
ATATGATGATGACCAAAAGTTGGTAAAACACGAAAGCCATTTCTTTACTTCCAAATTAGAGATTTCTGTG
CAAAATTTAATAAAGCTGATTTTTGATATTGACTCAATGAATAAAACATTGATGGAATTCCATATCGACA
TGGATAAAATGCCGCTGGGCAAGCTCAGTGCTCATCAAATCCAATCTGCTTACAGAGTAGTGAAGGAAAT
TTATAATGTACTAGAATGTGGTTCCAATACTGCAAAACTTATTGATGCAACAAATAGGTTTTATACGTTA
ATTCCTCATAATTTTGGAGTTCAATTACCAACATTAATTGAAACACATCAACAAATTGAAGATTTGCGAC
AAATGCTTGATTCATTAGCTGAGATAGAGGTTGCGTACAGTATAATCAAAAGCGAAGATGTATCTGATGC
TTGTAATCCTTTAGATAATCATTACGCACAGATTAAAACTCAGTTGGTGGCATTAGACAAAAATAGTGAA
GAATTTTCGATTCTTAGCCAGTACGTAAAAAACACTCATGCATCTACCCACAAATCTTATGATTTAAAAA
TTGTTGATGTATTTAAAGTATCTCGCCAAGGAGAAGCAAGGCGCTTTAAACCATTTAAGAAGCTACATAA
CAGAAAATTATTATGGCACGGATCACGTTTAACTAATTTTGTTGGTATATTATCGCATGGTTTAAGAATT
GCTCCCCCAGAAGCGCCACCAACAGGTTATATGTTCGGAAAAGGCATTTATTTTGCGGATATGGTTTCAA
AATCCGCAAATTATTGTTGCACAAGTCAACAAAACTCTACTGGATTAATGCTTCTATCTGAAGTTGCTTT
GGGCGATATGATGGAATGCACTTCAGCGAAATACATTAATAAACTATCAAATAATAAACATAGTTGTTTC
GGTCGTGGTCGCACCATGCCAGATCCTACTAAGAGCTATATAAGAAGTGATGGGGTTGAAATTCCTTACG
GAGAAACCATTACTGACGAACATTTAAAGTCATCGTTATTATATAACGAGTATATAGTATATGATGTTGC
GCAGGTCAATATTCAATATTTGTTTCGTATGGAATTCAAGTATTCTTATcccGGTAAGCCTATCCCTAAC
CCTCTCCTCGGTCTCGATTCTACGCGTACCGGTCATCATCACCATCACCATTGAGTTT

***Annexe 9**: DNA sequence (3068 pb) of parpB-V5-(Hist)$_6$ from the A8 plasmid. The ATG (start codon) was represented in green and TGA (stop codon) in red colors. The ccc in violet color represents the SmaI remaining site following digest and the targ V5 was illustrated in blue color and histidine tag was represented in brown color.*